Synthesis of FITC-PAMAM Conjugates for *in Vitro* Cell Studies

MASTER DISSERTATION

João Tiago Moniz Fernandes
MASTER IN NANOCHEMISTRY AND NANOMATERIALS

UNIVERSIDADE da MADEIRA
A Nossa Universidade
www.uma.pt

December | 2014

Synthesis of FITC-PAMAM Conjugates for *in Vitro* Cell Studies

MASTER DISSERTATION

João Tiago Moniz Fernandes
MASTER IN NANOCHEMISTRY AND NANOMATERIALS

SUPERVISOR
João Manuel Cunha Rodrigues

CO-SUPERVISOR
Helena Maria Pires Gaspar Tomás

Synthesis of FITC-PAMAM conjugates for *in vitro* cell studies

Dissertation submitted to the University of Madeira in fulfillment of the requirements for the degree of Master in Nanochemistry and Nanomaterials

by João Tiago Moniz Fernandes

Work developed under the supervision of
Professor Dr. João Manuel Cunha Rodrigues and
co-supervised by Professor Dr. Helena Maria Pires Gaspar Tomás

Centro de Competência de Ciências Exatas e de Engenharia,
Centro de Química da Madeira,
Campus Universitário da Penteada,

Funchal – Portugal
December 2014

“Somewhere, something incredible is waiting to be known.”

- **Carl Sagan.**

Declaration

I hereby declare that this thesis is the result of my own work, is original and was written by me. I also declare that its reproduction and publication by Madeira University will not break any third party rights and that I have not previously (in its entirety or in part) submitted it elsewhere for obtaining any qualification or degree. Furthermore, I certify that all the sources of information used in the thesis were properly cited.

Funchal, 30th of December 2014

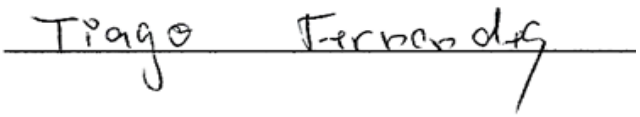

Dedication

To Marisol, my Parents and my Sister for their unconditional love and support.

Conference Contributions

January/February 2014 – Oral Presentation:

Tiago Fernandes, João Rodrigues, Helena Tomás, *Endocytosis Mechanisms of Dendrimers in Mesenchymal Stem Cells*, presented at the 1st CQM Annual Meeting/9th Materials Group Meeting – 31st of January to 1st of February 2014 - University of Madeira, Portugal.

Acknowledgements

First of all, this thesis was only possible thanks to the support of several persons and institutions. For this reason, I express my deepest gratitude to them.

Additionally, I want to thank my supervisors Prof. Helena Tomás and Prof. João Rodrigues for all the help, patience and encouragement provided along this one year master project. Also, in the past 5 years I have acquired immeasurable knowledge and guidance from them. For these reasons, I am highly grateful.

I also want to thank for all the efforts taken by the Professors and Researchers from the institutions involved in the construction of this Master in Nanochemistry and Nanomaterials. Without their dedication and contribution this reality could not be accomplished in Madeira Island.

Despite this difficult economic period, I want to thank the University of Madeira and all the persons associated with this institution for providing the best conditions and infrastructures for the elaboration of this thesis.

The Madeira Chemistry Research Centre (CQM) is also gratefully acknowledged for accepting me in is team and for providing all the chemicals and materials needed to develop the experimental work. I want to express my gratitude to Prof. Pedro Pires and Prof. José Câmara for all the knowledge and critical perspective provided during my master degree and research work. I also thank the patience and the professionalism transmitted by the former CQM senior researcher Dr. Yulin Li. Prof. Paula Castilho is also gratefully acknowledged for providing the ATR during the FTIR characterization.

The *Instituto do Emprego da Madeira* (IEM) is also highly acknowledged for their financial support regarding my professional internship during my stay in CQM. The support of the *Fundação para a Ciência e a Tecnologia* (FCT) was fundamental for this work through the Projects PTDC/CTM-NAN/112428/2009, the NMR Portuguese Network (PTNMR-2014) and the CQM strategic project (Ref. PEst-OE/QUI/UI0674/2013-2014).

A big thanks to all CQM members, both past and present, for providing countless knowledge and support during my stay there in the last 5 years. An especial thanks, to the former researchers Dr. José Luís dos Santos and Dr. Alireza Nouri for their transmitted knowledge, wisdom and help during my first steps as a scientist. Thanks also to Dr. João Figueira and Nilsa Oliveira for helping me in the NMR equipment operation. Similarly, I would like to thank the help and tips provided by Dina Maciel and Rita Castro during the cell studies. I am also grateful to Dr. Carla Alves for the help

provided to lyophilize my samples. I want also to show my gratitude to the laboratory technician Ana Paula Andrade for her support at any moment and any time in order to provide me with all the tools that I needed to accomplish my work. Additionally, I am thankful for the support and friendship of Carla Miguel during my stay in CQM.

I want to thank the friendship and the novel cultural perspectives provided by my colleagues from the master degree in Nanochemistry and Nanomaterials. By this way, I am grateful to Kirthiga Ramalingam, Xuedan He and Raja Shekar Akudari for participating in this professional journey along with me.

I also want to express my deepest gratitude to my father and my sister. For all the unconditional love, support and extreme patience provided during my life. Also, to my unforgettable mother, that will be always in my heart no matter what. I love you all.

The last and most important thanks goes to the love of my life, Marisol Gouveia. With love, I dedicate this thesis to you. I am endlessly grateful for all the love, support, care and patience given during the darkest times. I am forever in debt for all your wisdom, critical perspective and willpower that made me the person that I am today.

Abstract

The poly(amidoamine) (PAMAM) dendrimers have become one of the most widely explored dendrimer architectures given their commercial availability at high generations and their great possibility of chemical multifunctionality. For these reasons and due to their unique physicochemical properties, the PAMAM dendrimers are currently one of the most prominent synthetic hyperbranched polymer families. PAMAM dendrimers have a multitude of applications in biomedicine through, for example, dendrimer surface functionalization with drugs, genes or fluorescent markers. As a result, it becomes increasingly important to investigate the influence of size and distinct surface functionalities over its biological interactions and intracellular trafficking.

Several methodologies have been proposed to investigate the biological fate of PAMAM dendrimers. One of the most widely used approaches consists on the stochastic fluorescent labeling of the dendrimer surface for colocalization studies during intracellular trafficking.

Herein we explored different types of conjugation chemistry for fluorescent probe surface functionalization of PAMAM dendrimers using two different generations with distinct terminal units (*i.e.* -NH_2; -OH; -COOH). For this goal, the fluorescein isothiocyanate (FITC) was chosen due to the wide use of this fluorescent dye for the surface labelling of PAMAM dendrimers.

By exploring different functionalization methods, we have identified through several characterization techniques (*i.e.* ^{1}H NMR; UV/Vis; FTIR) the successful FITC surface functionalization of G3 and G5 PAMAM dendrimers containing –NH_2 and –OH termini. On the other hand based on the conditions presented herein, we were not certain about the successful functionalization of G2.5 and 4.5 PAMAM-COOH dendrimers. Additionally, based on our optimization attempts, it was not always an easy task to completely purify the final products using the conventional purification techniques.

Furthermore, other physicochemical parameters of the obtained conjugation products were also investigated specifically, the surface charge (at physiological pH) and fluorescent emission (at distinct pH and concentrations). Our results indicate that after functionalization, no deep changes occurred on the PAMAM dendrimer surface charge and that the fluorescent properties of FITC probe are strongly dependent of environmental pH.

The cytotoxicity of the conjugation products was also evaluated through the resazurin reduction assay on the mouse embryonic fibroblast cell line NIH 3T3. Our preliminary results suggest that the prepared conjugation products do not induce deep changes on the cell's metabolic activity at the investigated conditions.

Keywords: PAMAM dendrimers; FITC; Endocytosis; Intracellular trafficking; Stochastic method;

Resumo

Os dendrímeros de poli(amidoamina) (PAMAM) tornaram-se uma das arquiteturas dendriméricas mais estudadas devido à disponibilidade comercial das gerações superiores e à grande variedade de grupos funcionais. Por estas razões e devido às suas propriedades físico-químicas consideradas únicas, os dendrímeros PAMAM são atualmente um dos polímeros hiper-ramificados mais estudados. Os dendrímeros PAMAM possibilitaram uma grande variedade de aplicações em biomedicina, como por exemplo, no transporte de fármacos, genes ou marcadores fluorescentes. Por conseguinte, torna-se cada vez mais importante investigar a influência de diferentes grupos funcionais sobre a interação biológica e o tráfico intracelular.

Têm sido explorados diversos métodos para investigar o destino biológico dos dendrímeros PAMAM. Os métodos atualmente mais comuns, usados nos estudos de colocalização celular durante o tráfico intracelular, consistem na conjugação estocástica da superfície dos dendrímeros com marcadores fluorescentes.

Neste trabalho explorámos diferentes métodos químicos para a funcionalização estocástica dos dendrímeros PAMAM com um marcador fluorescente, usando duas gerações distintas, com diferentes grupos terminais (*i.e.* -NH_2; -OH; -COOH). Para esse fim, o isotiocianato de fluoresceína (FITC) foi selecionado devido à sua grande utilização na funcionalização destes dendrímeros.

Com os métodos químicos explorados neste trabalho identificamos, através de diversas técnicas de caracterização (*i.e.* ^{1}H NMR; UV/Vis; FTIR), a funcionalização bem-sucedida com o FITC das gerações 3 e 5 do dendrímeros PAMAM terminados em –NH_2 e –OH. Por outro lado, tendo por base as condições exploradas ao longo deste trabalho, não foi possível confirmar a funcionalização das gerações 2.5 e 4.5 do dendrímeros PAMAM terminados em –COOH. Para além do mais, apesar nossas tentativas de otimização revelou-se sempre difícil a purificação completa dos produtos finais através das técnicas convencionais de purificação.

Adicionalmente, outras propriedades físico-químicas dos produtos obtidos foram também exploradas incluindo, a carga superficial (a pH fisiológico) e a emissão de fluorescência (a diferentes pH e concentrações). Os nossos resultados indicam que, após a funcionalização, não houveram grandes alterações das cargas superficiais dos dendrímeros PAMAM e que as propriedades fluorescentes do FITC conjugado estão fortemente dependentes do pH do meio.

A citotoxicidade dos produtos obtidos também foi avaliada através do teste da resazurina na linha celular fibroblástica NIH 3T3. Os nossos resultados preliminares sugerem que os conjugados não induzem alterações profundas no funcionamento metabólico das células tendo em conta as condições investigadas.

Palavras-chave: Dendrímeros PAMAM; FITC; Endocitose; Tráfico intracelular; Método estocástico;

Contents

Synthesis of FITC-PAMAM conjugates for in vitro cell studies

Part 1. Introduction – Dendrimers: from synthesis to cellular internalization

Part 2. Materials and methods

List of figures

Part 1. Introduction - Dendrimers: from synthesis to cellular internalization

Part 2. Materials and methods

Part 3. Results and discussion

Annexes

List of tables

Part 1. Introduction - Dendrimers: from synthesis to cellular internalization

Part 2. Materials and methods

Annexes

List of acronyms, abbreviations and symbols

	Definition
	A
A	Absorbance
A549	Adenocarcinoma human alveolar basal epithelial cell line
AFM	Atomic force microscopy
ALN	Alendronate
APs	Adaptor proteins
Asp	Aspartic acid
ATP	Adenosine triphosphate
ATPase	Class of enzymes that catalyze the decomposition of ATP into ADP
ATR	Attenuated total reflectance
a.u.	Arbitrary units
	B
B16F10	Murine melanoma cell line
BAR	Bin–Amphiphysin–Rvs domains - highly conserved protein domains that occur in many proteins involved in membrane dynamics
BF	Bright field
bis-MPA	Dimethylolpropionic acid
	C
C6	Rat glial tumor cell line
Caco-2	Human epithelial colorectal adenocarcinoma cell line
CavME	Caveolae mediated endocytosis
CCV	Clathrin-coated vesicles
CFTR	Cystic fibrosis transmembrane-conductance regulator
CHDPs	Critical hierarchical design parameters
CIC-7	Chloride proton antiporter
CLIC	Clathrin-independent carriers
CME	Clathrin mediated endocytosis
CNDPs	Critical nanoscale design parameters
Cos-7	Monkey kidney cell line
COSY	Correlation spectroscopy
	D
DAB	Diaminobutane
DAPI	4',6-diamidino-2-phenylindole
DCC	N,n'-dicyclohexylcarbodiimide
DCU	Dicyclohexylurea
DMAP	4-dimethylaminopyridine
DMEM	Dulbecco's modified eagle medium
DMSO	Dimethyl sulfoxide
DNA	Deoxyribonucleic acid
DOSY	Diffusion-ordered spectroscopy (NMR)
DOX	Doxorubicin
DSC	Differential scanning calorimetry
	E
E_0	Ground energy state
E_1	Lowest excited energy state
EC50	Half maximal effective concentration
EDA	Ethylenediamine
EDC	1-Ethyl-3-(3-dimethylaminopropyl)carbodiimide
EDC/NHS	1-Ethyl-3-(3-dimethylaminopropyl)carbodiimide and NHS-based crosslinker

	Definition
EEs	Early endosomes
EGF	Epidermal growth factor
EP	Early phagosome
EPR effect	Enhanced permeability and retention effect
EPS15	Epidermal growth factor receptor protein tyrosine kinase substrate # 15
EM	Early macropinosome
ERS	External reflection spectroscopy
EtOH	Ethanol
	F
FA	Folic acid
FAR	Folic acid receptors
FBS	Fetal bovine serum
FCHO	Proteins that nucleate clathrin-coated pits and generate the initial membrane curvature
FITC	Fluorescein isothiocyanate
FM	Fluorescence mode
FTIR	Fourier transform infrared spectroscopy
	G
G	Generation number
g/mL	Grams per milliliter
GATG	Gallic acid-triethylene glycol
GC	Gas chromatography
GEEC	GPI-enriched early endosomal compartments
GPC	Gel permeation chromatography
GTPase	Family of hydrolase enzymes that can bind and hydrolyze guanosine triphosphate (GTP)
	H
HaCaT	Immortal human keratinocyte cell line
HEK293A	Human embryonic kidney 293 cell line (sub-clone)
HeLa	Human epithelial carcinoma cell line
HepG2	Human hepatocellular liver carcinoma cell line
hMSCs	Human mesenchymal stem cells
HPLC	High-performance liquid chromatography
HT-29	Human colon adenocarcinoma cell line
	I
IC	Half maximal inhibitory concentration
IDS	International dendrimer symposium
Inc.	Incubation times
IR	Infrared
ISI	Institute for scientific information
	J
J774	Murine macrophage cell line
	K
KB	Subline of the tumor cell line HeLa
	L
LC	Liquid chromatography
LDH	Lactate dehydrogenase
LDL	Low density lipoprotein
LE	Late endosomes
LLS	Laser light scattering
LM	Late macropinosome

	Definition
LP	Late phagosome
LYs	Lysosomes
	M
$M^{-1}.cm^{-1}$	Molar per centimeter
MALDI	Matrix-assisted laser desorption/ionization
MeOH	Methanol
MHz	Megahertz, 10^6 hertz
MI	Michigan, United States of America
mL/cm^2	Milliliter per square centimeter
MP	Mobile phase
MPS	Mononuclear phagocytic system
MRI	Magnetic resonance imaging
MS	Mass spectrometry
MW	Molecular weight
MWCO	Molecular weight cut-off
mV	Millivolt
	N
NIH 3T3	Mouse embryo fibroblast cell line
NIR	Near infrared
nm	Nanometer, 1 nm = 10^{-9} meters
NMR	Nuclear magnetic resonance
Non-CME	Non-clathrin mediated endocytosis
	P
PAMAM	Poly(amidoamine)
PBS	Phosphate buffered saline
PC	Phosphatidylcholine
PC-3	Caucasian prostate adenocarcinoma cell line
pDNA	Plasmid DNA
PE	Phosphatidylethanolamine
PEG	Polyethylene glycol
pH	Potential hydrogen
PI	Phosphoinositide
POM	Polarizing optical microscopy
POSS	Polyhedral oligomeric silsesquioxane
PPI	Polypropylenimine
PS	Phosphatidylserine
Purum	A chemical compound that is greater than 95% pure
Py-5	Pyrylium Dye derivative
	Q
QDs	Quantum dots
QY	Quantum yield
	R
Rab5	Member of the Ras superfamily of monomeric G proteins
Rat2	Rat embryo fibroblast cell line
RES	Reticulum endothelial system
RGD	Motif of arginine-glycine-aspartic acid
RNA	Ribonucleic acid
RSD	Relative standard deviation
	S
S-BINOL	(*S*)-(−)-1,1′-Bi(2-naphthol)
SANS	Small-angle neutron scattering

	Definition
SEC	Size-exclusion chromatography
SEM	Scanning electron microscopy
siRNA	Small interfering ribonucleic acid
SKOV-3	Human ovarian carcinoma cell line
SNARE	Soluble NSF attachment protein receptor
SP	Stationary phase
SPR	Surface plasmon resonance
	T
T98G	Human caucasian glioblastoma cell line
TEM	Transmission electron microscopy
TIF	2',4',5',7'-tetraiodofluorescein
TLC	Thin-layer chromatography
TMAH	Tetramethylammonium
TOF	Time of flight
TRPML1	Transient receptor potential-mucolipin
	U
UP	Ultra-pure
UV-Vis	Ultra-violet visible
	V
V-ATPase	Vacuolar-type H^+-ATPase
V79	Chinese hamster lung fibroblast cell line
VD	Volume of dialysate
VS	Volume of sample
	Others
Å	Angstrom, 1 Å = 10^{-10} meters
ε	Molar extinction coefficient
ξ	Zeta potential
λ	Wavelength
v	Wavenumber
[ ]	Concentration
1-D	One-dimensional
2-D	Two-dimensional
3-D	Three-dimensional

Part 1. Introduction

Contents

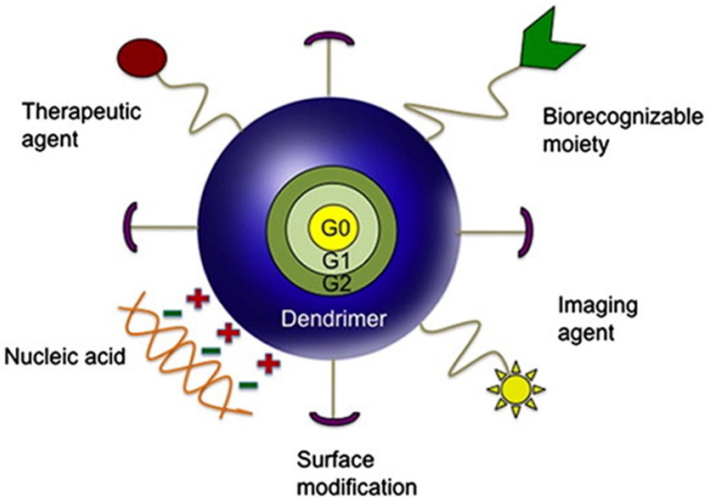

Dendrimers as a multiplatform for cargo delivery. Figure taken from: Sadekar, S.; Ghandehari, H. Transepithelial Transport and Toxicity of PAMAM Dendrimers: Implications for Oral Drug Delivery. *Adv. Drug Deliv. Rev.* **2012**, *64*, 571–588.

1. Introduction – Dendrimers: from synthesis to cellular internalization

1.1. Historical Background

The term dendrimer has its origin from the Greek words *dendron* and *meros.* Both root words emphasize the branching and the treelike shape of this type of molecular structures[1,2].

The dendritic architecture is one of the most common motifs in nature being found at different length scales and ranging from the meter to the nanoscale. Such distinctive architecture is easily found in either abiotic or biotic systems. In abiotic systems, the dendritic shape can be observed in lightning patterns or snow crystals. In the biological realm, the dendritic network of bronchioles and alveoli in the lungs are another well-known examples[1–3]. Remarkably, it is thought that the existence of this type of dendritic structures in nature, occurred as an evolutionary solution, allowing the enhancement and optimization of specific properties[3]. As an example, the dendritic network of tree roots (see Figure 1) facilitate the collection of water from the soil by exposing a large functional surface area[4].

Figure 1 – The dendritic pattern of tree roots (Figure from Ref. 5).

Initially thought only to occur naturally, the dendritic structures emerged in the polymer chemistry at the end of the 70s and early of 80s thanks to the efforts taken by Vögtle[6], Tomalia[7], Newkome[8] and others[9,10]. Indeed, although the first theoretical concepts of dendritic molecules occurred as early as the 40s, by P. Flory[11], the successful attempts to synthesize and completely characterize this type of structures only occurred almost 40 years later[2].

In 1978, Vögtle and coworkers[6] reported a series of repetitive reaction steps for the preparation of the first compounds presenting perpetual branching. Relying on a sequence of synthetic "cascade molecules", the reactions were carried out through an iterative (repetitive) approach alternating between a Michael addition and a reduction step. By starting the reaction with a primary monoamine via a two-fold Michael addition with acrylonitrile (step A, Figure 2), the preparation of a dinitrile could be achieved. Then, the two nitrile groups were subsequently reduced by hydrogenation with sodium borohydride in the presence of cobalt (II) ions giving rise to the terminal diamine (step B, Figure 2). Further repetition of this sequence provided the means for the first successful preparation of regularly branched polypropylenimine (PPI) structures[12]. Due to the limited yields and laborious synthetic approach, the preparation of these PPI dendrimers was limited to what is now referred as 2nd generation dendrimers[13,14].

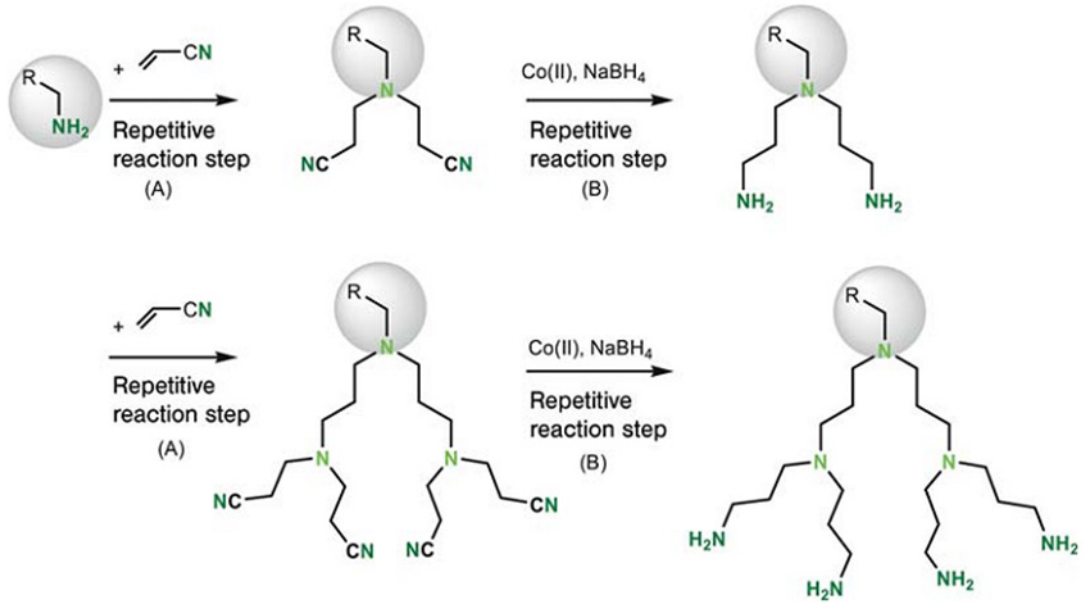

Figure 2 – Schematic representation for the preparation of "cascade molecules" by Vögtle and coworkers. The term "cascade" was initially used in analogy to the repetitive branching of the arms that resembles the water cascade of a fountain (Figure adapted from Ref. 12).

After these initial works, the preparation of new dendritic structures started to show up slowly. Thanks to the development of novel preparation methods along with better analytical capabilities, the introduction of new dendrimer families with unique molecular identities started to appear[12]. These new structures included, the polylysine dendrimers reported by Denkenwalter *et al*. in 1981[15], the hyperbranched poly(amidoamine) (PAMAM) dendrimers presented by Tomalia *et al*. in 1985[7] or the perpetually branched "arborol systems" described by Newkome *et al*. also in 1985[8].

Along with the discovery of the new dendritic structures, important theoretical considerations regarding this type of architectures also emerged. The densest packing concept for these "cascade-like" (core/shell) polymers reported by Maciejewski *et al*. in 1982[9] and the statistical consideration regarding the growth limit for hyperbranched molecules by de Gennes and Hervet in 1983[10], provided important knowledge for further development of these novel well-defined hyperbranched structures. Such considerations revealed to be important later on to understand the limited growth (*i.e.* limiting generation) of the distinct dendrimer families[10].

Tomalia *et al*., coined the term dendrimer for the first time in 1983[7] to describe this type of perpetually hyperbranched polymers, in the case, PAMAM dendrimers. Similarly to the approach presented by Vögtle *et al*., the preparation of these PAMAM dendrimers relied on the iterative Michael addition of methyl acrylate with ammonia (step A, Figure 3). The posterior conversion of the resulting ester to primary amines was then accomplished through the reaction with ethylenediamine (step B, Figure 3). Based on this strategy, Tomalia and coworkers were capable of preparing, for the first time, PAMAM dendrimers as high as the 10th generation. Interestingly, they verified that as the generation increased, the degree of perfection decreased, resulting in a greater number of final defective structures. The term half-generation was also coined by Tomalia *et al*. to describe the individual ester-stages[7]. For the first time, Tomalia and corworkers were able to accurately report a validated method for the design of complete dendrimers of higher generation[7,16].

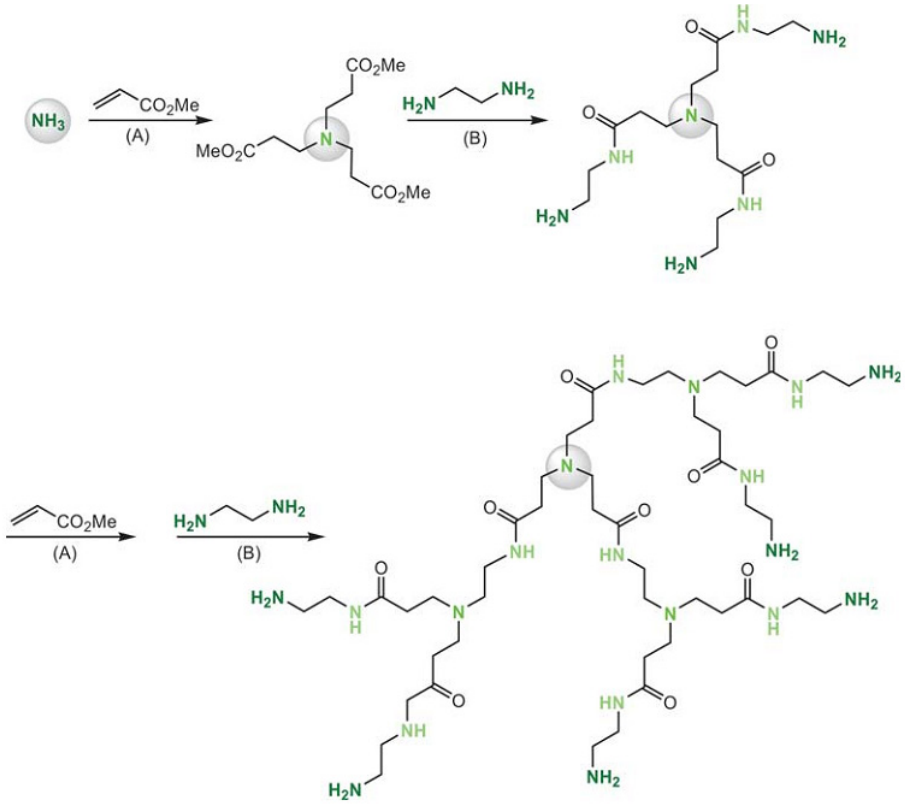

Figure 3 – Schematic representation of the synthesis of PAMAM dendrimer reported by Tomalia *et al*. (Figure adapted from Ref. 7).

Since the initial discovery until the current days, the number of reported dendrimer families surpasses 100, and more than 1000 different surface modifications have been described[13,17]. Several of the aforementioned dendritic structures can now be easily acquired, since that they are commercially available from many different suppliers[13]. Figure 4 provides an insight of some of the commercially available dendrimers as well as the chemical diversity between the different families.

The continuous introduction of such chemical diversity, both organic and inorganic, in this type of dendritic structures, allowed the preparation of new molecular identities with unique physicochemical properties. Moreover, with the further improvement of the synthetic methodologies and analytical characterization techniques, it is now possible to synthesize many dendritic structures that are mainly monodisperse and fine-tuned in terms of size, shape, interior and surface chemistry, flexibility and composition[2,16,18].

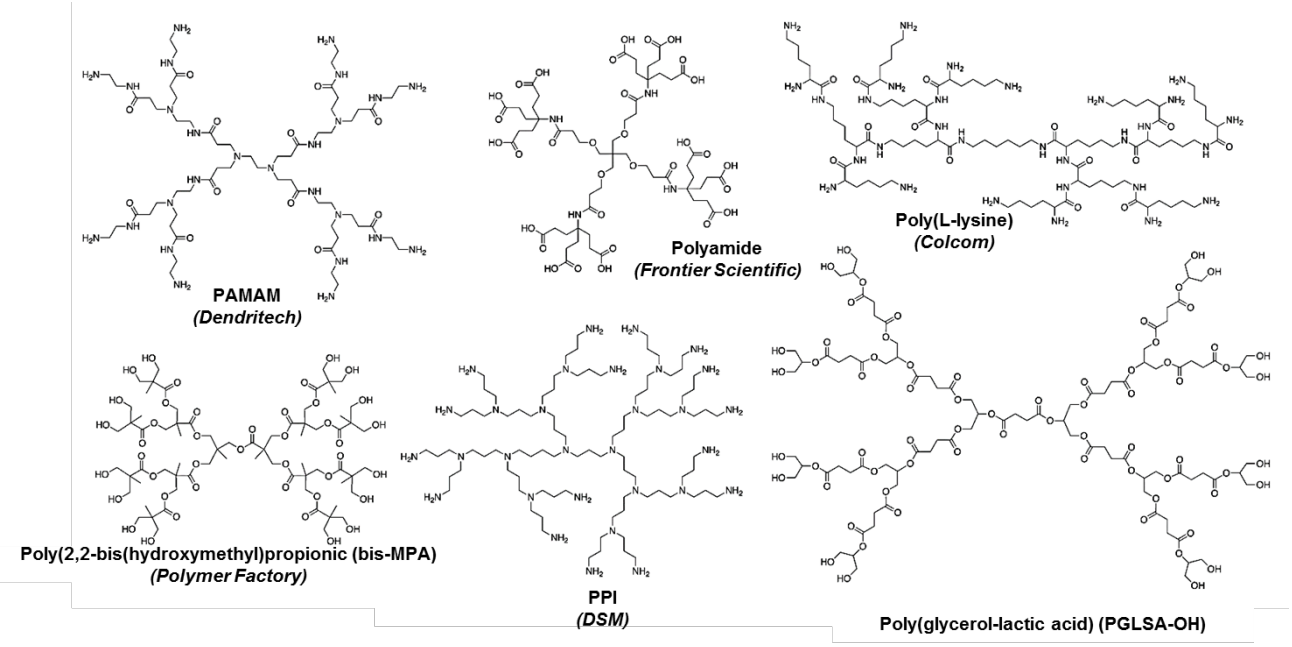

Figure 4 – Chemical structures of some of the commercially available dendrimers (Figure adapted from Ref. 13).

The dendrimers can also be mentioned in the literature as “arboroles”, “arboscent polymers”, “cascade molecules” or “hyperbranched polymers”. However, in reality, due to the well-defined nature of this type of macromolecules, they should be considered as a special subgroup of hyperbranched polymers (see Figure 5). The physicochemical properties of the dendrimers differ from the random hyperbranched polymers, as the latter structures are usually polydisperse and contain a lower degree of structural perfection[4,19].

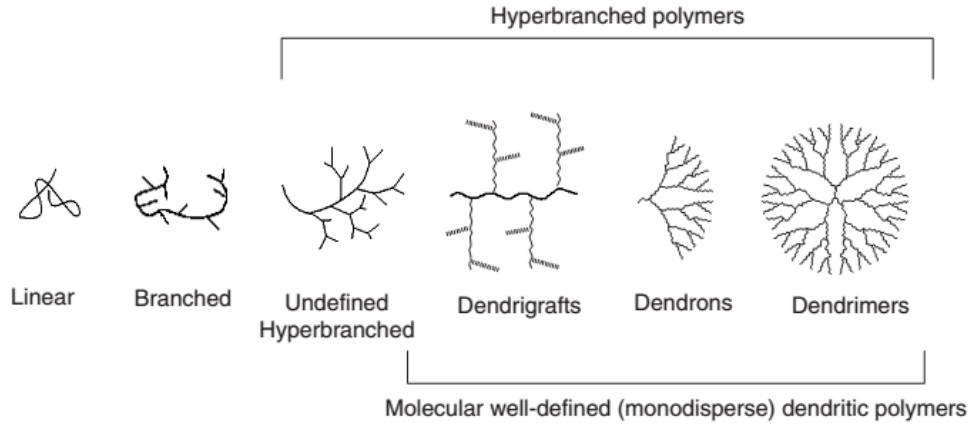

Figure 5 – The different types of polymer architectures and the relationship with dendrimers (Figure adapted from Ref. 4).

Since the initial developments, many research groups have dedicated their work to the synthesis and application (*e.g.* catalysis, nanomedicine, optoelectronics) of dendrimers. Such contributions have supported the continuous growth of the field. As shown in Figure 6, a notorious increase in the number of publications and patents was observed in the last 20 years[20,21].

Furthermore, the existence of the biannual *International Dendrimer Symposium* (IDS) since 1999 (Germany) reflects the constant development of the field. The most recent IDS (8th edition) occurred in 2013, Madrid, Spain, which counted with more than 200 participants[22,23]. The next IDS edition will happen in 2015, Canada[23].

Additionally, due to the rapid development of dendrimer-based nanomedicines, a more specialized international symposium started to happen in the alternate years of the IDS, being known as the Biodendrimer Symposia (its last edition (4th) occurred in June 2014, Switzerland)[24].

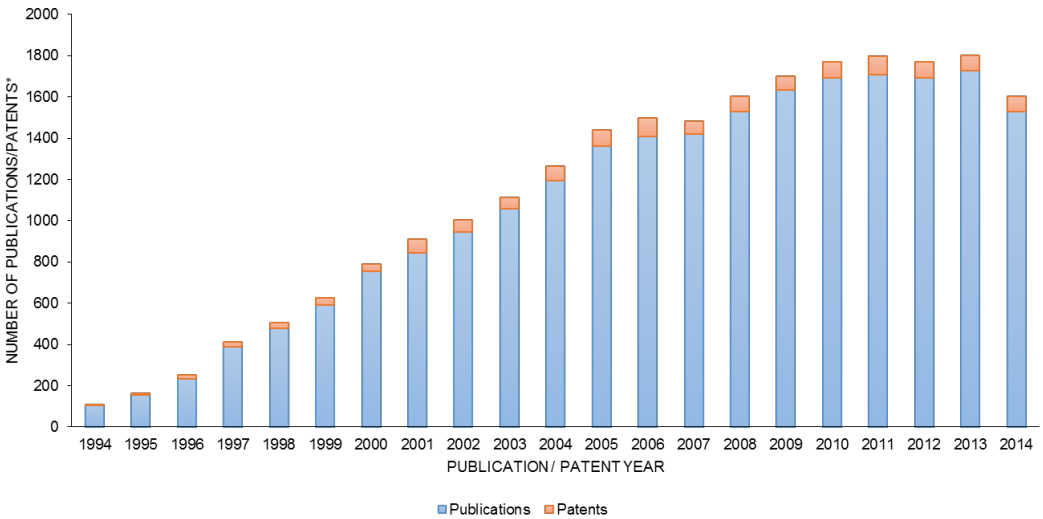

Figure 6 – Number of worldwide publications/patents related with dendrimers and that were published between the years 1994 and 2014 (Data adapted from Refs. 20 and 21).

1.2. The architecture of dendrimers

As described in the previous chapter, dendrimers belong to a special field of the polymer science[19]. Depending on the chemical nature of the dendrimers, they can be prepared with very high molecular weights and exhibit a greater symmetry, purity, water solubility and monodispersity when compared with the linear polymers (see Figure 7)[16,25].

Main advantages of the dendrimers over the linear polymers:

- ✓ Higher degree of symmetry;
- ✓ Controlled synthesis based on a defined number of functionalities;
- ✓ Monodispersity;
- ✓ High density of functional groups that allow further multivalent binding;
- ✓ Higher surface reactivity allowing functionalization through noncovalent or covalent interactions (*e.g.* Fluorochromes, drugs, etc.);
- ✓ Higher water solubility;
- ✓ Lower viscosity;
- ✓ Multifunctionality;
- ✓ Globular shape at higher generations;
- ✓ Increased half-life of loaded drugs;
- ✓ Unique interior chemistry (*e.g.* host of drugs);
- ✓ Fine-tuned size, shape and number of terminal groups.

Figure 7 – Summary of the advantages of dendrimers over the linear polymers (Adapted from Ref. 25).

Dendrimers are known for their nano-sized (10-130 Å) hyperbranched core/shell three-dimensional (3D) architecture (see Figure 8) which is characterized by a (i) multifunctional core and (ii) repeating branched units (known as dendrons) that are attached to this core. The high-density terminal groups of the dendrons give rise to the formal surface of the dendrimer[12,13,16,25].

Dendrimers are characterized by distinct generations (G) depending on the number of branching units that are radially attached to the core. Usually, different generations within a family results in distinct dendrimer sizes where the number of functional end groups doubles within each full-generation increment[25]. For example, in PAMAM dendrimers, each new full generation increases the dendrimer diameter in about 1 nm^2.

Many different types of atoms or multifunctional molecules can be applied as a core for the preparation of dendrimers. Depending on the synthetic route, the core can be used as an initiation point or as a final anchoring site. Some examples of molecules that have been used as a core include

ethylenediamine (EDA), polyethylene glycol (PEG), diaminobutane (DAB), ammonia, carbosilane, fullerene, porphyrin, metals, and many others[2,12,25]. The functionality of the core dictates the structural valence of the dendrimer relatively to the number of dendrons that can form the hyperbranched scaffold (see example, Figure 8). For this reason, the core has a profound influence on the size and 3D shape of the dendrimer[2,12,16,25]. The core may also be used to provide unique physicochemical properties to the dendrimer acting as an electro-, photo- or catalytically-active site[2].

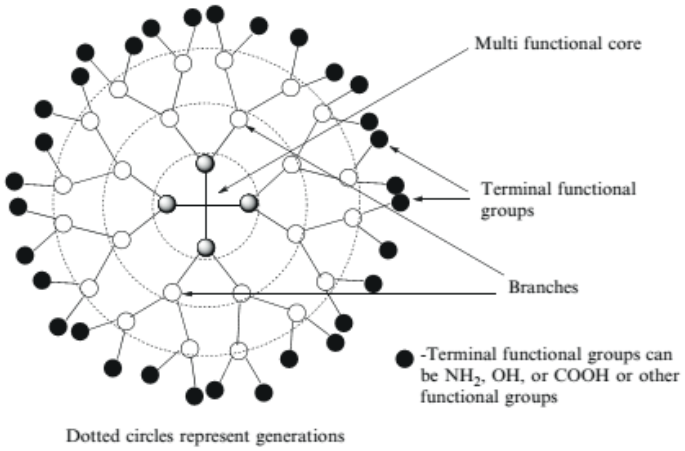

Figure 8 – Representation of the dendrimer architecture. In this case, the functionality of the core 1 → 4 allows the connection with 4 dendrons (Figure adapted from Ref. 25).

As shown in Figure 9, the introduction of cores with different shapes can give rise to dendrimers with very distinct morphologies. The flexibility of the core can also determine the degree of steric crowding caused by the branching units and, as a result, may have an impact over the structural perfection and globular shape of the dendrimer. While most of the cores mentioned in the previous paragraph give rise to spherical dendrimers, other molecules like the linear-poly(oxazoline) produce rod-like dendrimer scaffolds[2,26]. Furthermore, novel strategies based on inorganic nanoparticles or quantum dot cores have also been applied to produce dendronized structures. Some examples include the dendronization of thiol functionalized gold (Au) nanoparticles or cadmium selenide quantum dots (CdSe QDs)[2,27].

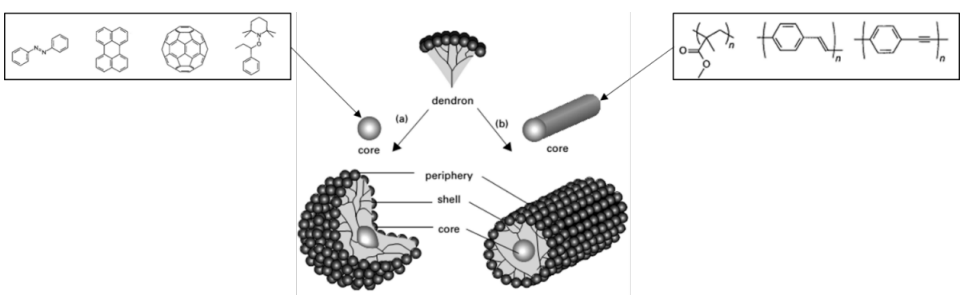

Figure 9 – Possible dendrimer morphologies depending on the core-type (Figure adapted from Refs. 2,26).

Around the core, the interior of the dendrimer is based on the perpetual arrangement of branch cell monomers* that are the structural basic unit of the dendrons. The dendrons are the main components that provide the link between the core and the surface groups in this type of core/shell architectures. The number of these individual dendritic units that are radially attached to the core will define the generation of the dendrimer and consequently the overall molecular size[2,13].

Many different types of branch cell monomers have been reported in the literature (see Figure 10). As a result, depending on the units used to build the interior of the dendrimer, unique physicochemical properties may arise. Moreover, the identity and nature of the dendrimer interior depends on the multiplicity, elemental composition, bonding, architecture, chirality and flexibility of the branch cell monomers[2,12,25].

Despite the huge diversity of dendritic monomers reported in the literature, they can be organized in two major classes depending on their nature. Firstly and the most commonly used are the pure synthetic monomers that comprise alkyl or aromatic moieties. On the other hand, the biological monomers include carbohydrates, nucleotides and amino acids[2,12,13,25,28–34]. Furthermore, the branch cell monomers may also contain elemental compositions derived from phosphorous, silicon, sulfur, nitrogen, metals, among many others[2,13,16,25].

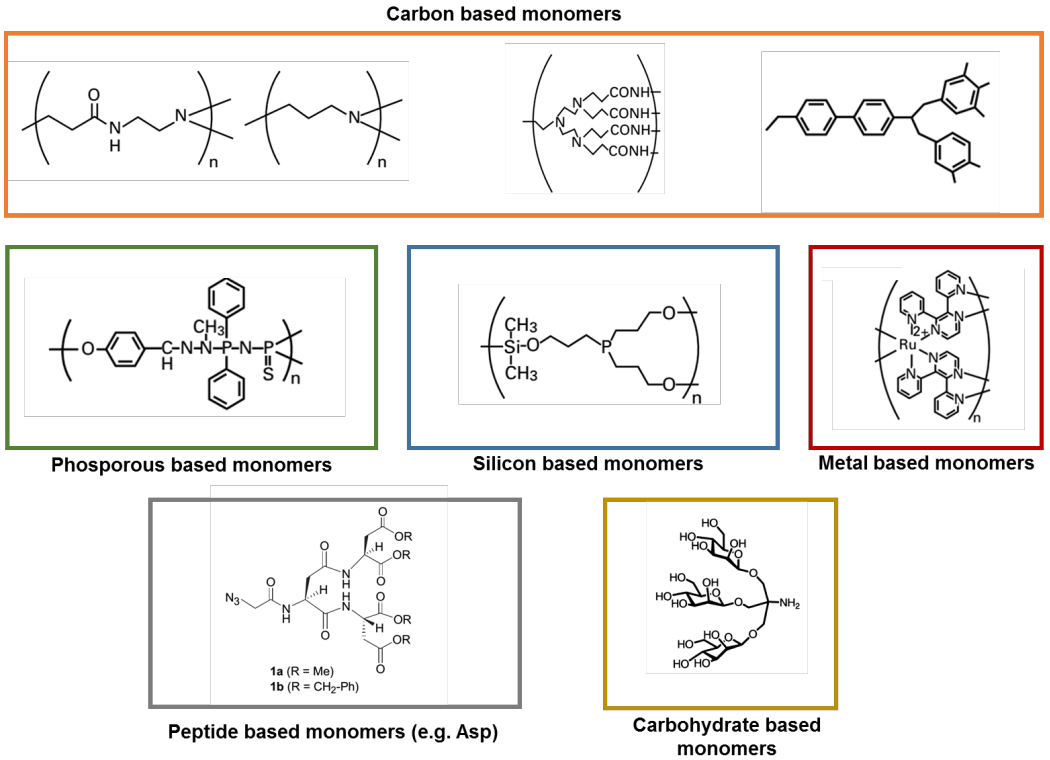

Figure 10 – Examples of branch cell monomers used to build the interior of the dendrimers (Figure adapted from Refs. 2,28,31).

*The term branch cell monomer refers to the molecular building blocks used for the construction of well-defined hyperbranched structures around the dendrimer core.

Some of the aforementioned branching units may provide unique host-guest properties to the dendrimer (see Figure 11), allowing the entrapment of drugs/fluorochromes or promoting a nano-environment for the complexation of metal salts. The posterior reduction of these metal salts, results in the formation of zero-valent dendrimer-metal nanocomposites[2,16].

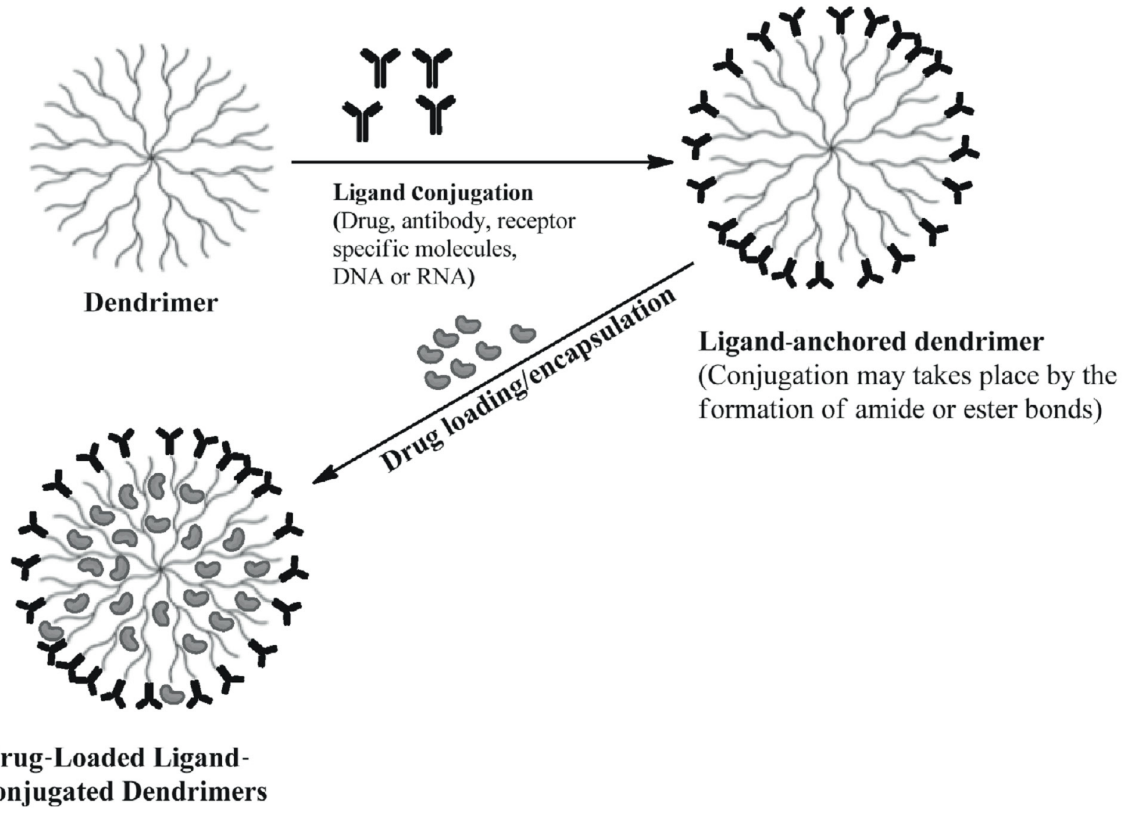

Figure 11 – Ligand conjugation and drug loading of dendrimers (Figure adapted from Ref. 25).

Most of the functional organic or inorganic elements with high multiplicity have been used for the preparation of dendrimers. The bonding between each branch cell monomer can be accomplished based on many different types of chemical reactions. The process usually involves high yield reactions like Michael addition, esterification, amidation, phosphorylation, among many others. More recently, novel reactions have been proposed for a more efficient, greener and less laborious preparation of dendrimers. Some examples include, click chemistry/lego chemistry[2,12,16,25].

As described before, the connectivity between each branch cell monomer can deeply influence the interior chemistry of the dendrimer. Many different types of organic or inorganic elements can be used to build dendrimers with unique connectivity, providing very distinct properties within each dendrimer family. For example, in the case of PAMAM dendrimers, the 1 → 2 N-branched amide connectivity provides a flexible interior, which promotes a random encapsulation of metals or drugs.

In contrast, dendrimers possessing a more rigid connectivity usually promote an organized interior metal/drug filling.

Moreover, the dendrimers that contain highly symmetrical branch cells (*e.g.* PAMAM or PPI) usually exhibit improved host-guest properties when compared with the less symmetrical ones. This behavior is observed due to the reduced packing in the interior of the symmetric dendrimers (see Figure 12)[2].

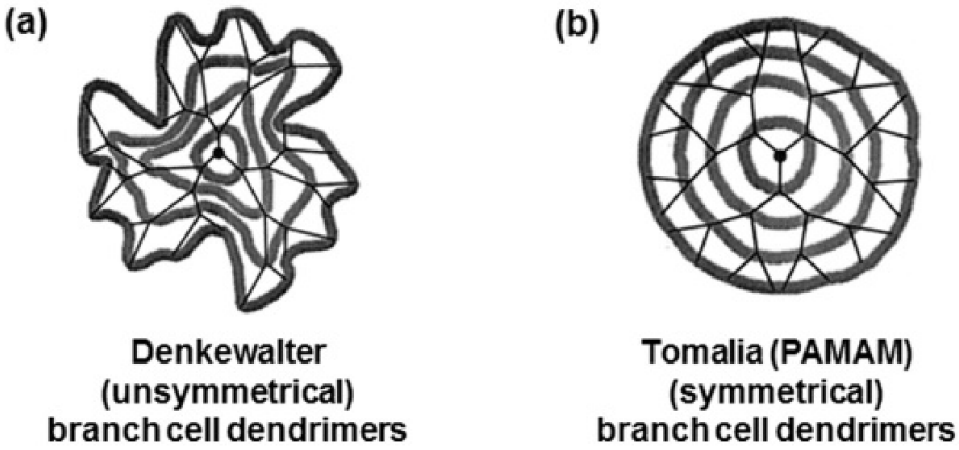

Figure 12 – The structural differences of dendrimers containing (a) unsymmetrical and (b) symmetrical branch cells. It can be seen that the packing of the dendrimer interior is greater for unsymmetrical branch cells resulting in reduced void spaces (Adapted from Ref. 2).

Besides the previously referred monomer units, oligomers may also be used for the preparation of dendrimers[2]. Recently, Royo *et al.* have reported the preparation of co-oligomeric dendrimers based on polyproline-oligo(ethylene glycol)[35]. It is clear that the use of oligomers just expands even more the structural diversity of the dendrimer families.

As shown in Figure 8, the functional end groups compose the third element of the dendrimer architecture. Thanks to the endless chemical diversity of the terminal groups employed until today, novel dendrimer families have emerged. The end groups can bear unique properties, as being reactive or non-reactive and contain variable charge (positive, neutral or negative). The terminal units may also provide special functionalities like fluorescence, thermo-responsiveness, chelating power, catalytic and antimicrobial activity to the dendrimer scaffold[2,13,16,25].

The nature of the dendrimer surface will define the way that the dendrimer interacts with the environment, including when in the biological media. As a result, the terminal end groups can influence the type of intermolecular, intramolecular and supramolecular interactions.

Moreover, the end groups can also change the behavior of the dendrimer at different pH and ionic strength conditions. This increased sensitivity may lead to variable protonation states (see Figure 13) and result in unique dendrimer structural organizations. As shown in Figure 14, the

PAMAM dendrimers tend to exhibit a globular shape at high pH and extended conformations at low pH values (< 5). Such behavior is observed as a result of the electrostatic repulsion of both, the tertiary amines ($pK_a \approx 5$) in the interior and the primary amines ($pK_a \approx 9$-11) at the dendrimer surface. Interestingly, these conformational changes observed at different pH conditions will not only influence the flexibility/rotation of the surface groups (*i.e.* gyration radius) but also the radial density, terminal group distribution, solvent accessibility, surface area and dendrimer volume[2,13,16,25,36].

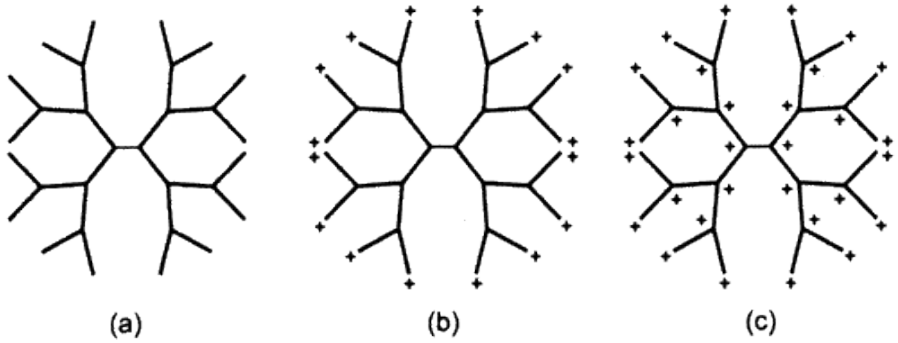

Figure 13 – Charge distribution for the G2 PAMAM-NH_2 dendrimer at (a) high; (b) neutral and (c) low pH (Figure adapted from Ref. 37).

It is worth mentioning that the behavior of the different dendrimer families may be very distinct at the same environmental conditions. Contrasting with the PAMAM dendrimers, the carboxylate PPI dendrimers show an extended conformation at low (< 4) and high (> 11) pH and a more condensed structure at neutral pH (≈ 6). Such structural changes happen because at low/high pH values this type of PPI dendrimers exhibit two kinds of electrostatic repulsions. While at low pH these repulsions are observed among the protonated internal amines, at high pH the repulsions are caused by deprotonated carboxylic acid surface groups. On the other hand, at neutral pH, the structure is more condensed due to the intramolecular hydrogen bonding of this zwitterionic structure[13,38].

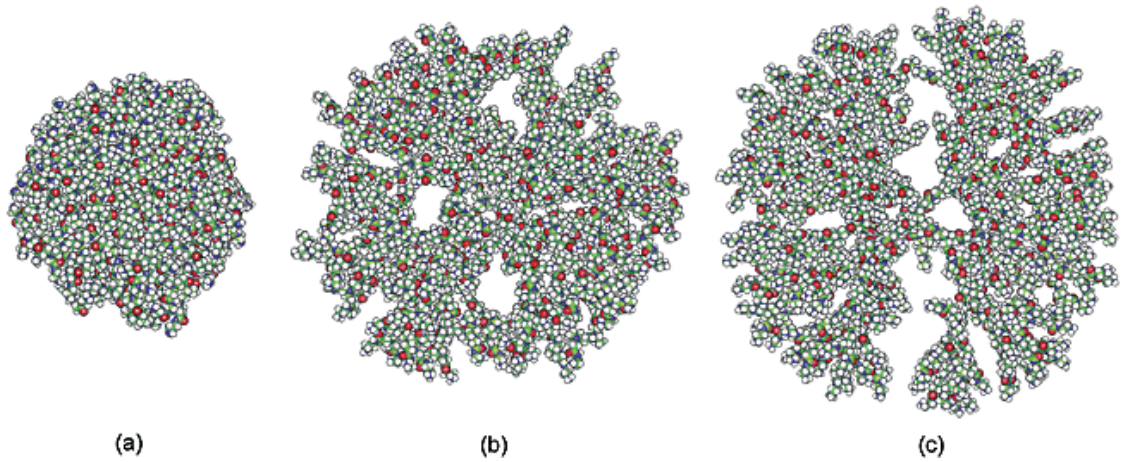

Figure 14 – Molecular dynamic simulation of the structural organization of a G6 PAMAM dendrimer at (a) high; (b) neutral and (c) low pH (Figure adapted from Ref. 37).

It is also known that the surface groups can clearly modulate and selectively control the access of guest molecules to the interior of the dendrimer. This selectivity can be tuned based on several factors, like the molecular size or protonation state of the terminal groups. For example, it is known that in the case of G5 PAMAM dendrimers, 3 to 6 water molecules per tertiary amine can be present in the dendrimer interior depending on the pH conditions[36].

Since the nature of the end groups will influence the interaction of the dendrimer with its surrounding molecules, the terminal groups can be tuned in order to increase the solubility of the dendrimer in a specific medium. By this way, a proper selection of the end groups can be explored in order to improve the solubility of a specific drug that can be encapsulated in the dendrimer interior[13,16,25,39].

Due to the fractal structure that is characteristic of the dendrimers, the number of terminal groups per generation can be predicted based on the (Equation 1).

$$n_G = F_K\,(F_v - 1)^G \qquad \text{(Equation 1)}$$

Where n_G corresponds to the number of terminal groups in the "G" generation; F_K to the multiplicity of the core; F_v to the multiplicity of the branching units; G to the generation.

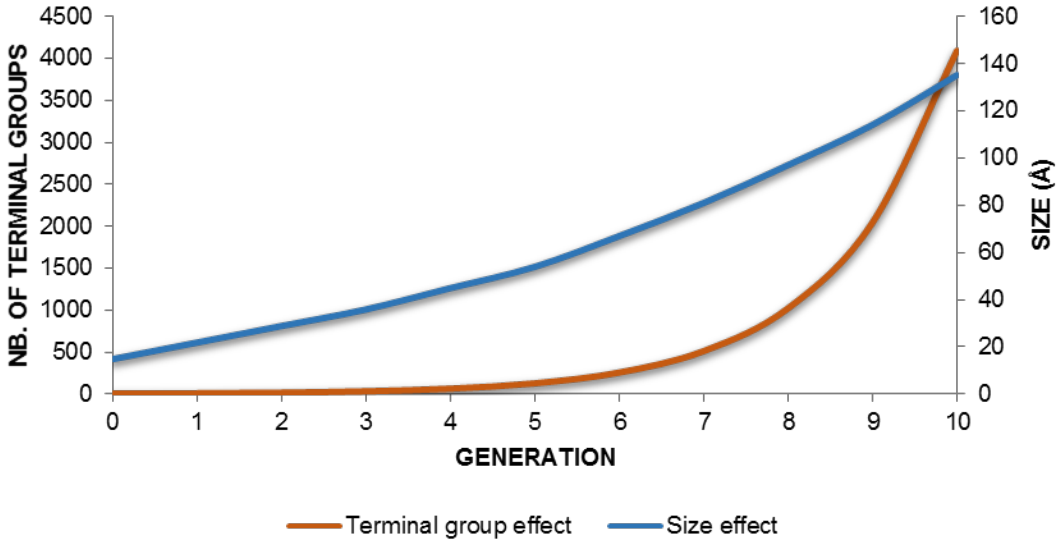

Figure 15 – Representation of the effect of the generation increase on the size and number of terminal groups of PAMAM dendrimers (Figure adapted from Ref. 40).

According to the previous equation and the data shown in Figure 15, it is possible to verify that the number of end groups increases exponentially while the size of the dendrimer increases almost

linearly per generation increment. For this reason, most of the dendrimer families tend to exhibit more flexible/open structures at low generations and dense/globular shapes at higher generations.

Given the great chemical diversity of the dendrimers, the conformational change of the shape along the generation can be variable for distinct dendrimer families. For example, while the PPI dendrimers show more globular shapes in generation 4 and above, in the case of the PAMAM dendrimers, the higher density is only observed over the generation 4.5[10,12,13,16]. For this reason, most of the dendrimers applied in the biomedical field are usually over generation 4, since when they present a globular shape, they tend to show unique solubility and reactivity[13].

As a function of the surrounding conditions, the dendrimers usually contain more dense interiors rather than denser shells due to the possible back-folding of the end groups (see Figure 16). Moreover, it is known that the extent of this back-folding usually increases with the generation number for some of the dendrimer families. Some interesting studies have shown that, for G11, the back-folding level of the PAMAM dendrimer terminal groups can be so high that the outermost sub-generation can gradually penetrate into the core (see Figure 16)[13,16,41].

It is important to note that the "*de Gennes* dense packing principle" can help to predict the surface congestion of the dendrimer after a specific generation[10]. As described above, this "limiting generation" can vary among the dendrimer families.

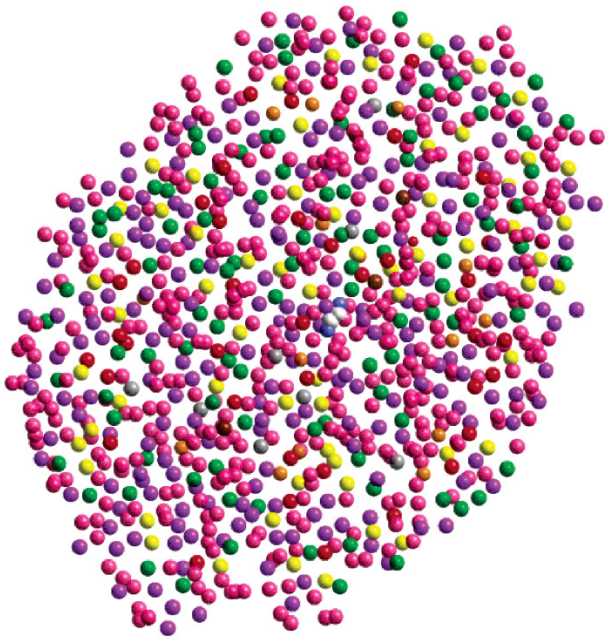

Figure 16 – Instantaneous snapshot of a molecular dynamics simulation for the Generation 11 (G11) PAMAM-NH_2 dendrimer. Notice that the purple spheres representing the primary amines are penetrating the core (white and blue spheres in the middle) (Figure adapted from Ref. 41).

In the case of PAMAM dendrimers, the densest pack generation is reached at G10. Usually, beyond the "limiting generation", a greater degree of defects start to appear in the dendritic structure due to the extreme back-folding of the terminal groups. As a result, over the limiting generation, the construction of the dendrimers proceeds in the interior, that is strongly influenced by slow kinetics[2,42].

It is important to note that many dendrimers families have been prepared much beyond the "limiting generation". By this way, some exceptions may be observed from the *de Gennes* principle depending on the volume of the dendrimer interior or size of the terminal groups. Usually, larger, less flexible terminal groups show reduced back-folding[2,42].

As shown in the equation 2, the "limiting generation" depends on many factors, including the multiplicity of the core and branch cell monomers or on the dendrimer radius and surface area.

As described by the equation 2, A_z decreases as the generation number increases. As a result, the "limiting generation" is reached when A_z reaches the cross-sectional area related with the van der Waals radii[42]. Interestingly, beyond the limiting generation a lower solubility is also observed. Usually, dendrimers containing terminal amino groups or other intermolecular hydrogen bonding functionalities usually follow the "*de Gennes* dense packing principle"[2].

$$A_z = \frac{A_D}{N_z} \propto \left(\frac{r^2}{N_c N_b^G}\right) \qquad \text{(Equation 2)}$$

Where, A_z is the surface area and Z the number of terminal groups; A_D is the total surface area of the dendrimer; r is the radius of the dendrimer; N_z the number of surface groups per generation; N_c the multiplicity of the core; N_b multiplicity of the branches; G the number of generations.

It is also clear that the charge of the surface groups can play an important role in the interaction of the dendrimer with biological identities or the surrounding media.

Currently, it is possible to commercially obtain different dendrimers families containing specific surface charge and functionality. A clear example is the commercial availability of PAMAM dendrimers with different surface groups like primary amines (-NH_2), hydroxyl groups (-OH) or carboxyl groups (-COOH).

The ability to play with the polyvalency of the dendrimer surface, can also allow the non-covalent functionalization with other chemical identities (*e.g.* DNA) or even influence the cytotoxicity and the way that the dendrimer is internalized by cells[16,25]. Although with higher cytotoxicity, positively charged dendrimers tend to show an improved cellular internalization when compared with negatively charged ones due to the reduced electrostatic repulsion with the negatively charged cell membrane. Interestingly, the increased cytotoxicity of positively charged dendrimers can be attenuated by the partial functionalization of the dendrimer surface with other agents like carbohydrates, poly(ethylene glycol), among others[16].

As we shall see later on, along with the charge, the dendrimer concentration and number of surface groups can also lead to distinct cytotoxic consequences. For example, at higher concentrations and generations PAMAM dendrimers tend to be more cytotoxic than the lower generation counterpart[16,43].

Molecular identities with specific functionality can be introduced in any position of the dendrimer and provide, in the same way, unique physicochemical properties wherever the position. For example, the introduction of metals in the dendrimer structure can provide unique biological, catalytic, sensing or optoelectronic properties[42,44–51]. Moreover, the position of the metal in the dendrimer can work as a way to selectively determine the accessibility of the substrate to the catalytic center. As shown in the Figure 17, many different dendrimer families have been reported in the literature containing metals or any other type of functional unit at the core, branch cell junctions or end groups.

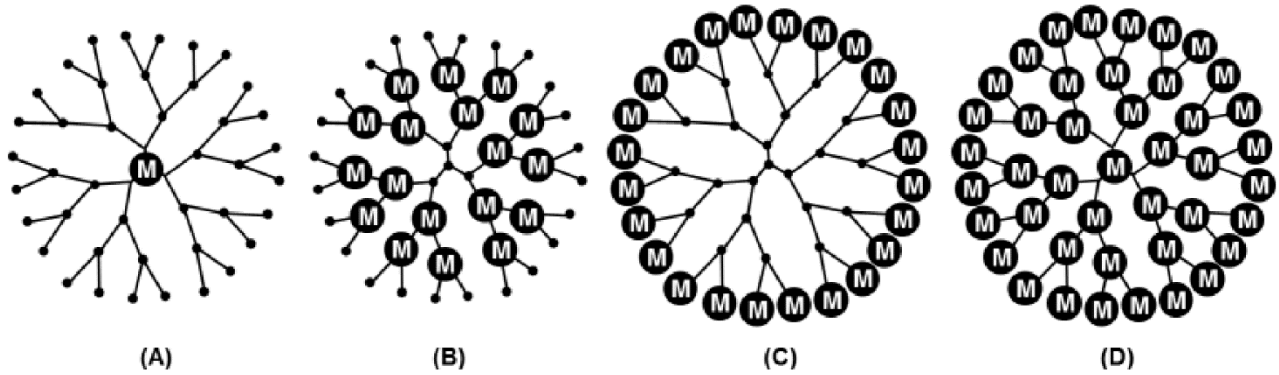

Figure 17 – Schematic representation of possible dendrimers containing metals at (a) core; (b) branch cell junctions; (c) end groups; (d) in the 3 positions (Figure adapted from Ref. 2).

Finally, thanks to the great complexity and variability of the dendrimer architecture, the dendritic scaffold can be tailored or loaded at the preferred position (interior or surface) for specific cell targeting, imaging, or modification of pharmacokinetics (see Figure 18)[16,25,52]. As we shall see later on, many different approaches can be used to proceed with the functionalization of the dendrimer after or during their synthesis.

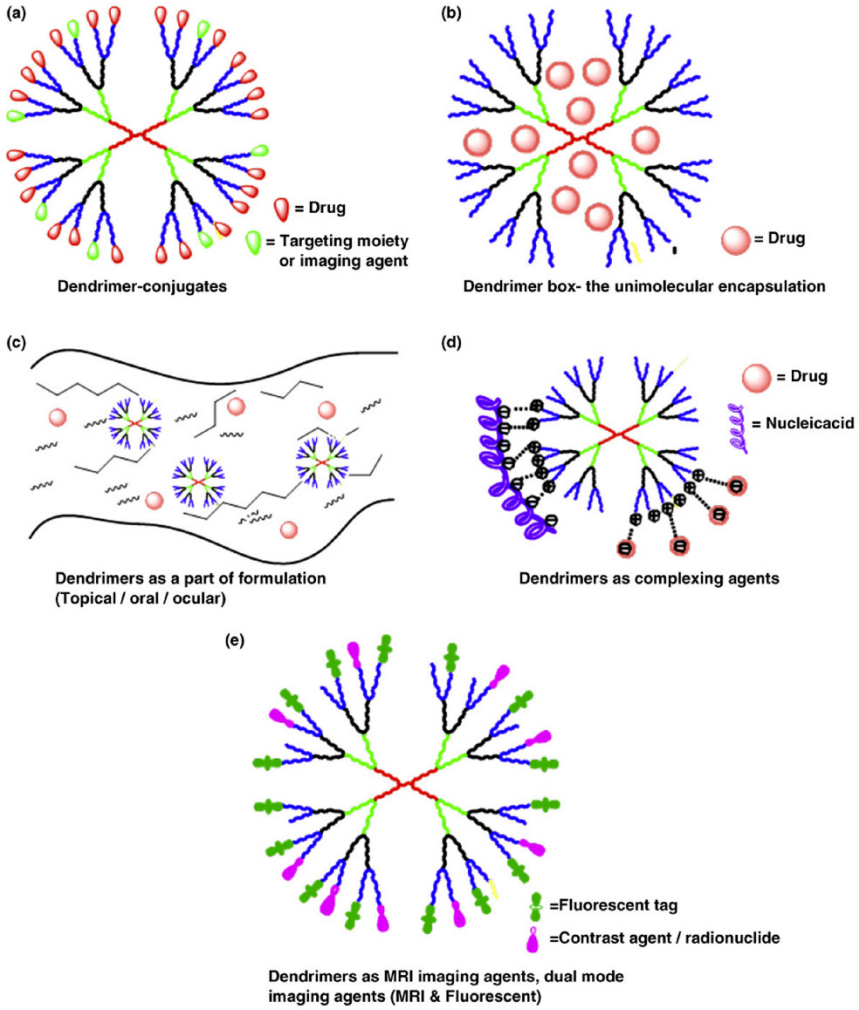

Figure 18 – Scheme representing the potential utility of dendrimers and their functionality as: (a) drug-conjugates linked to imaging agents; (b) drug-loading agents; (c) modification of drug pharmacokinetics; (d) complexing agents; and (e) MRI or fluorescent imaging elements (Figure adapted from Ref. 52).

Table 1 summarizes the major influence of each component over the global physicochemical properties of the dendrimer[12].

Table 1 – The effect of the different dendrimer components over its physicochemical properties (Adapted from Ref. 12).

Core	Branching Unit	End groups
Shape	Shape	Shape
Size	Size	Stability/Reactivity
Multiplicity	Density	Solubility
Functions	Endo-complexation	Viscosity

1.3. Synthetic routes for the preparation of dendrimers - a way to understand the dendrimer diversity

The dendrimer literature is vast, and many synthetic approaches have been reported since their discovery in the 70s[2,42]. As shown in the Figure 19, the dendritic architecture involves a set of five subclasses including the dendrigraft polymers, random hyperbranched polymers, dendritic-linear hybrids, dendrons and dendrimers[2,12,25,53].

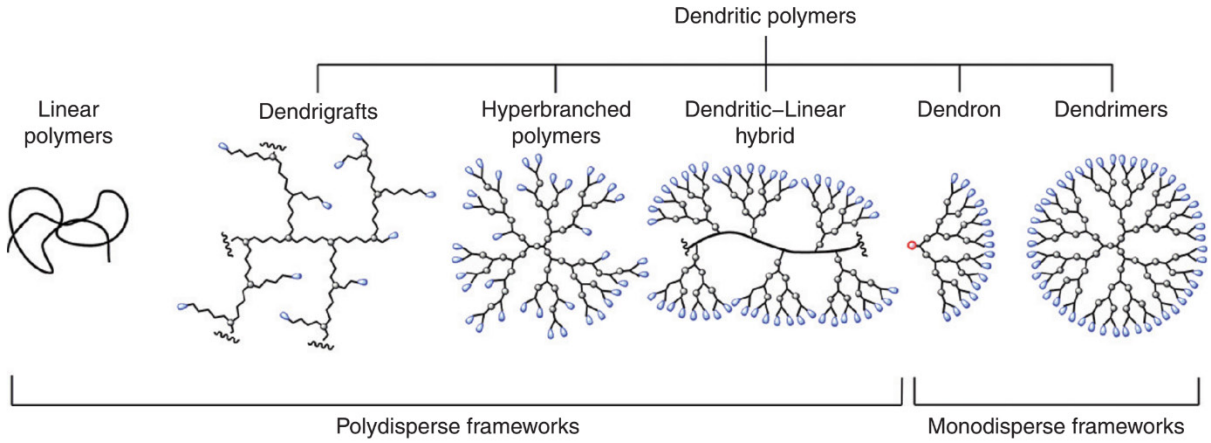

Figure 19 – Representation of the different subclasses associated to the dendritic architecture (Figure adapted from Ref. 53).

Given the diversity of dendritic architectures, each subclass possesses characteristic physicochemical properties that are directly influenced by the synthetic methodologies followed to prepare them. While the polydisperse frameworks are usually prepared based on statistical/semi-controlled approaches, the monodisperse frameworks rely on finely controlled preparation methods. As a result, the strategy followed to proceed with the assembly of the branch cell monomers will clearly define the dispersity and perfection degree of the final dendritic structure[2,12,25,53].

Since that the connectivity of the branch cells is highly defined by their nature, parameters like chemical composition, symmetry, flexibility, multiplicity and rotation of the starting materials will have a deep impact in the final dendritic structure (see Figure 20)[2,12,16,25].

The attachment of the individual branch cells is usually achieved through the traditional covalent bonding of the cell units to the core (see Figure 20). Consequently, while that in the preparation of dendrimers, this connectivity is processed in a controlled manner, a polydisperse/randomized approach is observed in the case of the undefined hyperbranched polymers. Interestingly, novel approaches have been presented more recently involving the extemely controlled preparation of dendrimers or supramolecular dendritic structures through the click type covalent bonding or through the self-assembly (*i.e.* generally non-bonding) of branch cells/dendrons[2,12,16,25,54–57].

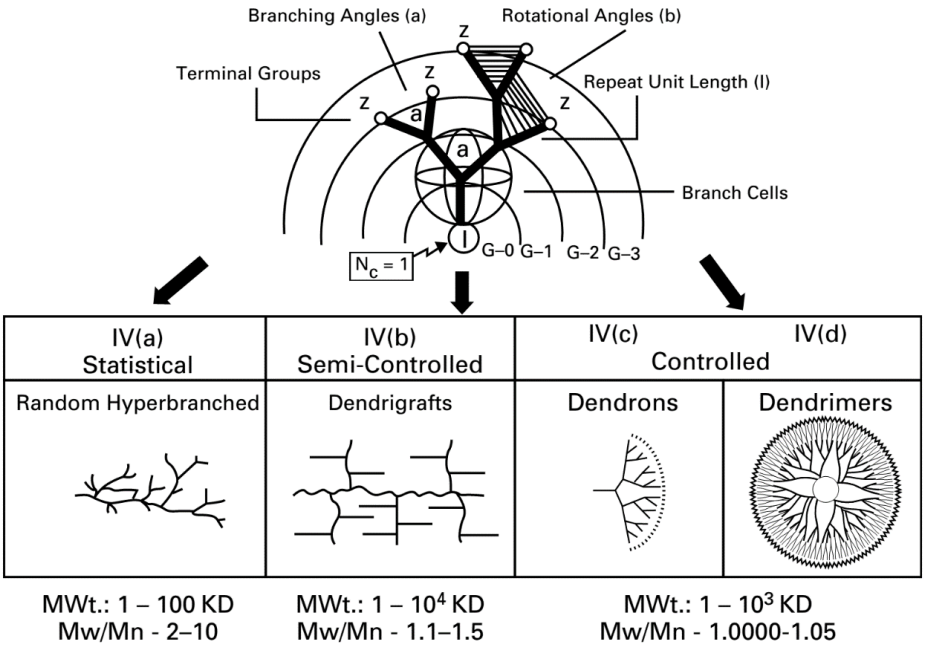

Figure 20 – The nature of the branch cell and its influence on the preparation of the different dendritic architectures (Figure adapted from Ref. 2).

The preparation of dendrimers usually involves the assembly of the individual components referred in the previous section (*i.e.* core, branch cells and functional groups). Despite the great diversity of preparation methods already reported in the literature, they can be mainly classified into divergent or convergent approaches (see Figure 21). As described later on, each method as its advantages and disadvantages. Additionally, many of the novel synthesis rely on adaptations of these two major methodologies in order to deliver dendrimers in less laborious way and with greater purity[2,12,13,16,25,53,58–61].

Nevertheless, much work still needs to be done for a high-yield preparation of some dendrimer families at higher generations, as well as the controlled functionalization (mono- or multi-) of the individual dendrimer molecules. Indeed, the latter limitation was the main issue observed in the current work, where the controlled functionalization of the individual dendrimer molecules was always difficult to achieve. Moreover, new advances are also required for the eco-friendly preparation of some dendrimer types[2,12,13,16,25,53].

In the next section and keeping with the scope of the current thesis, some insights regarding the preparation methods of dendrimers will be given.

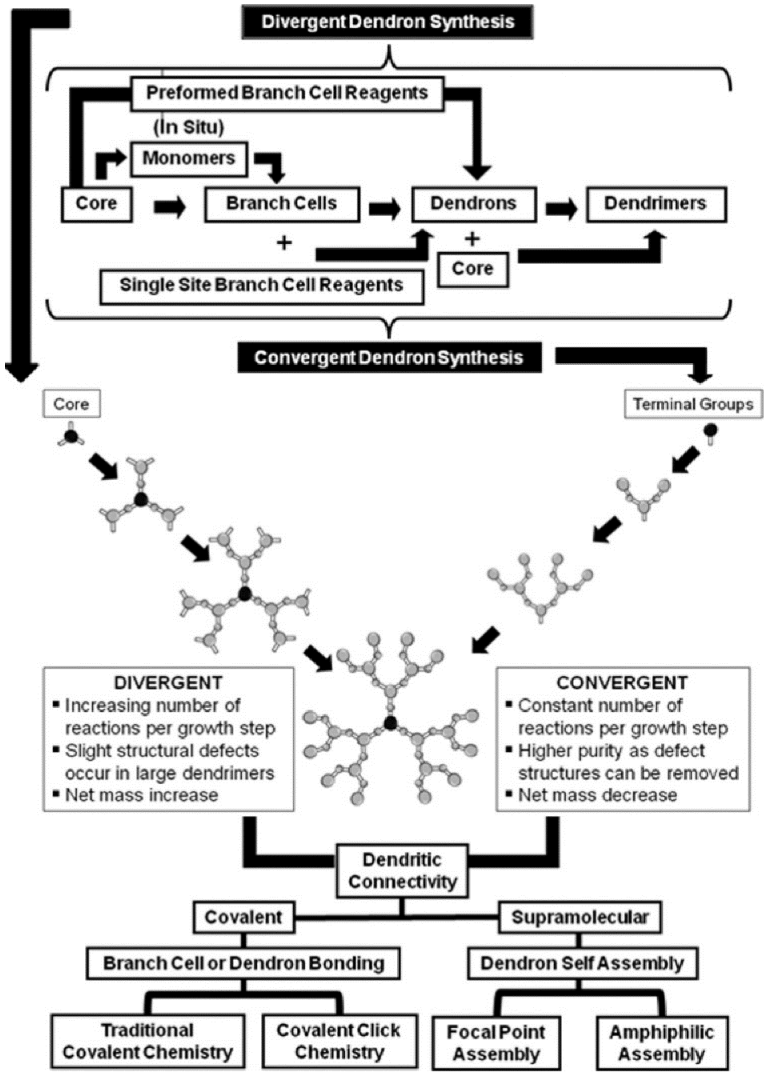

Figure 21 – Main strategies followed for the preparation of dendrimers (Figure adapted from Ref. 2).

1.3.1. Preparation of dendrimers based on the controlled divergent growth

The initial attempts for the preparation of dendritic structures relied on the controlled divergent growth as reported by Vögtle *et al*.[6], Tomalia *et al*.[7] and Newkome *et al*.[8]. In this method the dendrimer growth starts from a multifunctional core that is made to react with branch cells units that have one reactive site and several protected or unreactive groups. Past this initial step, the dendrimer growth proceeds with the activation of the previous protected or unreactive groups that are then ready to react with an excess amount of new branch cell units (see Figure 22). Between each growth and activation step, the purification of residual by-products is accomplished. The continuous repetition of growth/activation stages (iterative) will lead to the preparation of the dendrimer with increasing generations and number of end groups[2,12,13,53,59,62,63].

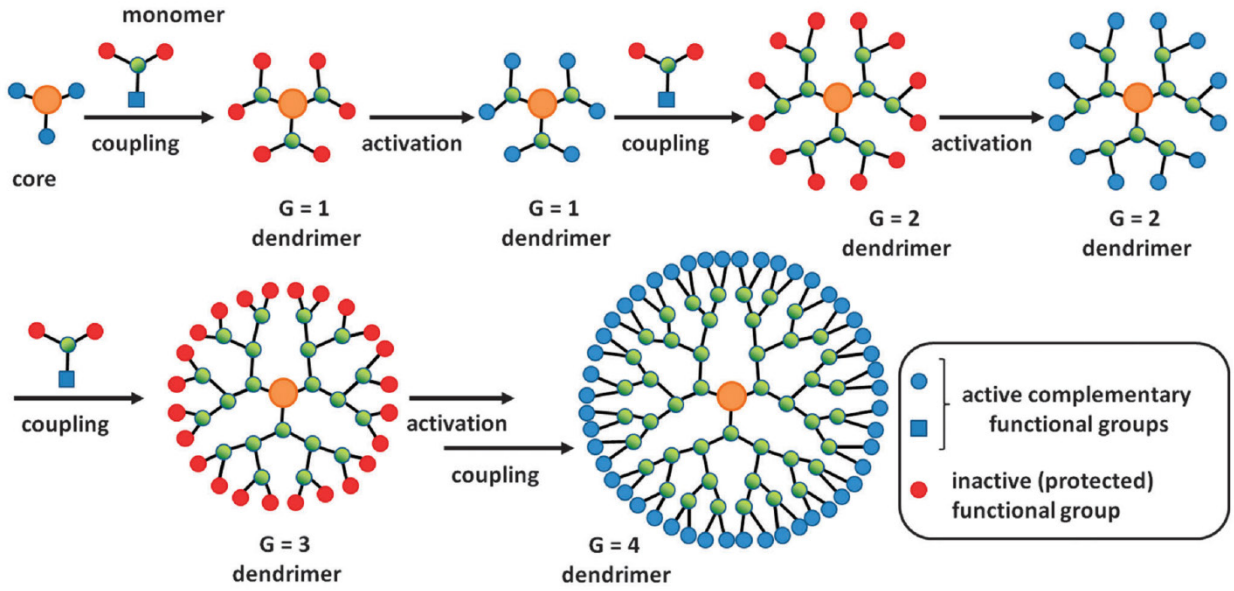

Figure 22 – Schematic representation of the dendrimer synthesis through the controlled divergent growth. The activation can be accomplished by chemically removing the protection groups or through coupling (Figure adapted from Ref. 63).

The most common branch cells units used in the controlled divergent growth are of the type AB_2 or AB_3 (see Figure 23). The connectivity established between the individual branch cells monomers is mainly of (a) traditional covalent or (b) click type covalent[2,12,13,25,53].

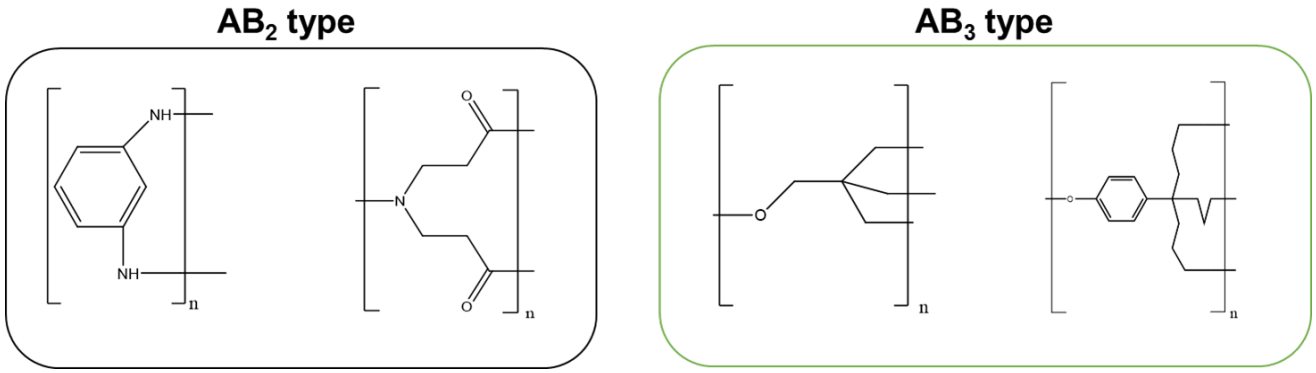

Figure 23 – Examples of branch cell monomers that have been used in the controlled divergent growth. Note that in the divergent strategy "A" means the activated part and "B" the protected functionalities.

For example, the preparation of the Tomalia-type PAMAM dendrimers proceeds through the divergent growth and relies on the traditional covalent bonding between the individual branch cell units. This synthesis involves the two-step iterative (i) Michael-addition of methyl acrylate with a polyamide followed by (ii) amidation based on the excess of 1,2-diaminoethane (see Figure 24). This excess is needed in order to avoid possible inter-dendrimer crosslinking as well as internal macrocyclization. The preparation of the PAMAM dendrimers relies on a wide range of amine or ester

functionalized cores. While the Tomalia-type PAMAM dendrimers start from an ethylenediamine core (EDA, 1→2), the Peng-type PAMAM dendrimers start from triethanolamine core (1→3). Until this date, many variations of this synthetic procedure have been proposed resulting in distinct PAMAM-type dendrimers. In the case of the PAMAM dendrimers almost any identity can be used as a core, where the only requirement relies on the ideal chemical functionality for the favorable iterative growth[2,12,13,25,53].

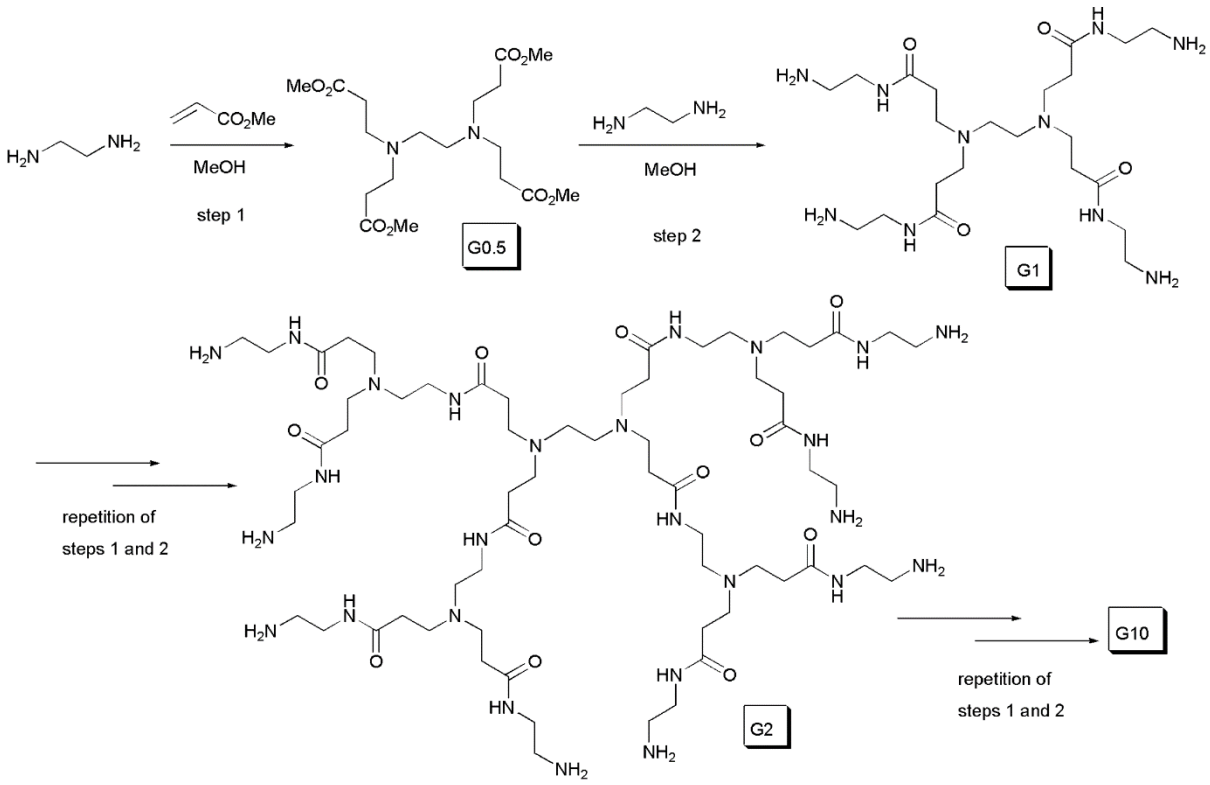

Figure 24 – Preparation of the Tomalia-type PAMAM dendrimer through the divergent approach (Figure adapted from Ref. 63).

Many other dendrimer families can be prepared upon the controlled divergent strategy. Moreover, after reaching the intended generation, the end groups can be further post-functionalized with the desired chemical identity[2,12,13,25,53].

The major advantages of the divergent approach rely on the ability to attain high generation dendrimers, as well as the possible automation of the process. As a result, the divergent method has been the method of choice for the commercial preparation of higher generation PAMAM or PPI dendrimers, among others[63].

On the other hand, due to the exponential growth in the number of end groups after each generation, the degree of steric hindrance becomes higher at the surface as the generation increases. For this reason, through the divergent method, it can be difficult to proceed with the same quantitative reactivity among all the end groups (*i.e.* 100% conversion), which can lead to structural defects. In most of the cases, this issue cannot be surpassed even with excess amounts of reactants.

Additionally, the removal of the defective dendrimer structures from the "perfect" ones can be very difficult to achieve through the conventional purification techniques, since that the resulting compounds are highly similar in terms of chemistry, molecular weight and size. For example, in the case of PAMAM dendrimers, the defects caused by retro-Michael addition and intramolecular cyclization can strongly limit the perfection level past the G4[2,12,13,25,53,63].

Nevertheless, novel approaches have been introduced to surpass some of the previous limitations and deliver the ability to prepare several dendrimer families with less structural defects and in an environmental friendly way. For example, the click type covalent synthesis relies on the use of two different but complementary monomers that react spontaneously under ideal conditions. Through this approach, an improved yield and faster preparation of dendrimers can be achieved. Recently, Bowman *et al*. reported a divergent click reaction for the preparation of dendrimers based on the use A^*A_2 (vinyl) and B^*B_2 (thiol) monomers. By sequentially reacting these monomers (see Figure 25), the authors claimed the preparation of 5th-generation dendrimers with 96 peripheral groups based on the thiol-Michael addition reaction conditions[55].

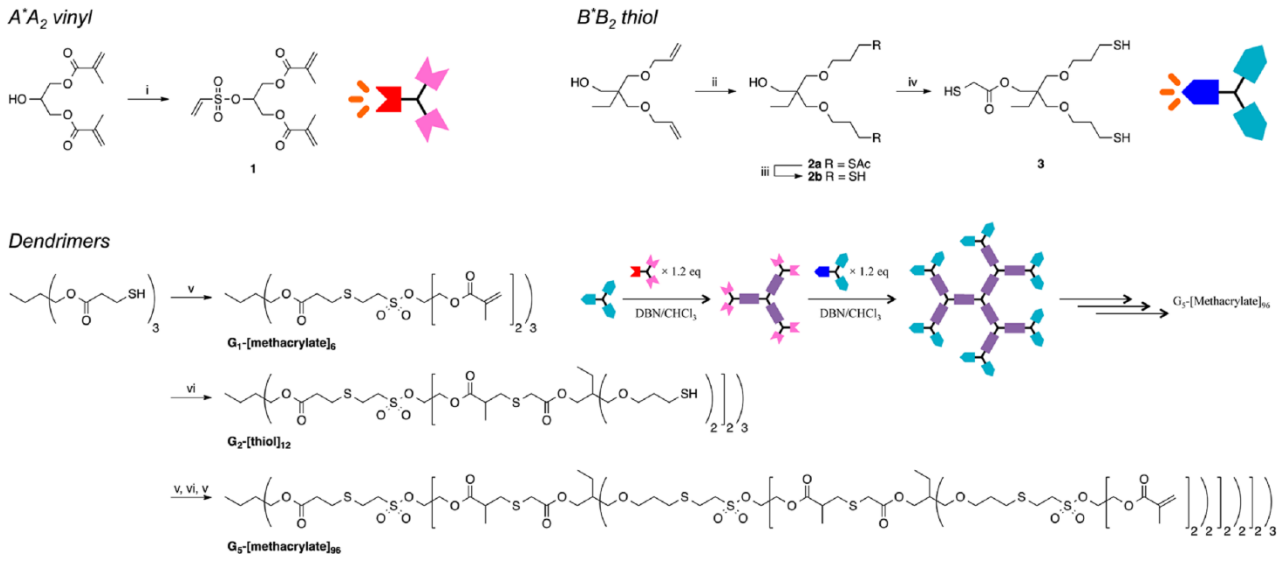

[a]Reagents and conditions: (i) $ClCH_2CH_2SO_2Cl$, TEA, CH_2Cl_2, 0 °C then rt, 10 h, 50%; (ii) CH_3COSH, AIBN, 60−70 °C, 10 h; (iii) concentrated HCl(aq), MeOH, reflux, 3 h; (iv) $CH_2(SH)COOH$, *p*-TSA, toluene, reflux, 3 h, 33% overall; (v) **1** (1.2 equiv to thiol), DBN (0.05 equiv to thiol), $CHCl_3$, 30 min, 98% (G_1), 90% (G_3), 92% (G_5); (vi) **3** (1.2 equiv to methacrylate), DBN (0.05 equiv to methacrylate), $CHCl_3$, 2 h, 97% (G_2), 90% (G_4).

Figure 25 – Divergent click reaction reported by Bowman *et al.* (Figure adapted from Ref. 55).

Many other examples of orthogonal "click" chemistry pairs have been reported until date for the divergent preparation of dendrimers (*e.g.* thiol-ene/esterification)[64,65]. Usually, these methods do not require any protection/deprotection steps and allow further functional group conversion without any side reactions. Consequently, this approach provides many useful advantages taking into consideration the ever increasing diversity and complexity of the emerging dendrimer families (see Figure 26)[55,63].

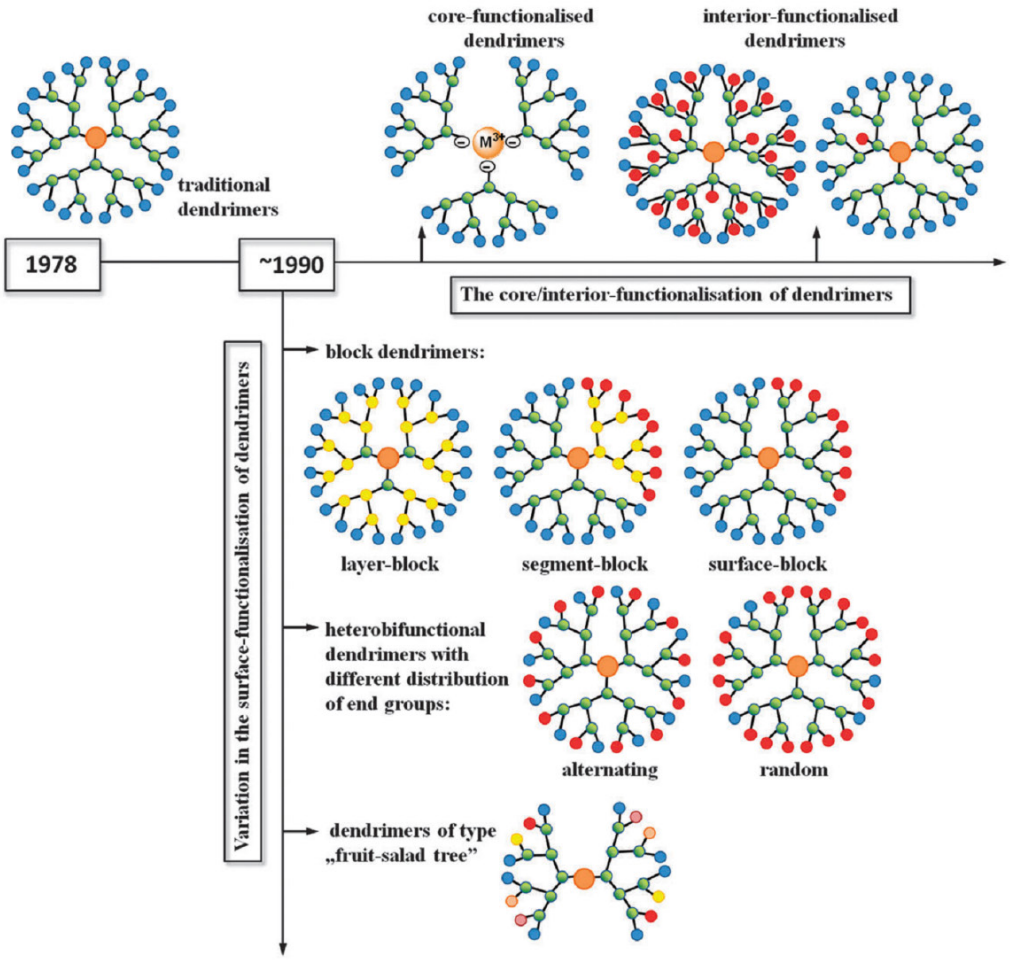

Figure 26 – The continuous increase in diversity and complexity of dendrimer families and functionalities requires the development of faster and more efficient preparation methods (Figure adapted from Ref. 63).

1.3.2. Preparation of dendrimers based on the controlled convergent growth

Hawker and Fréchet firstly described the controlled convergent approach in the early 1990s. By that time, the authors were capable of preparing poly(aryl ether) dendrimers through the convergent synthesis[66].

Simply explained, this strategy relies on the early preparation of the dendrons that are then coupled to a multifunctional core (see Figure 27). The dendrons are usually constructed based on the AB_2 type branch cell monomers and upon the same activation/deactivation conditions observed in the divergent method. Note that in the convergent approach, the "A" refers to the inactive functional group and "B" to the active moieties.

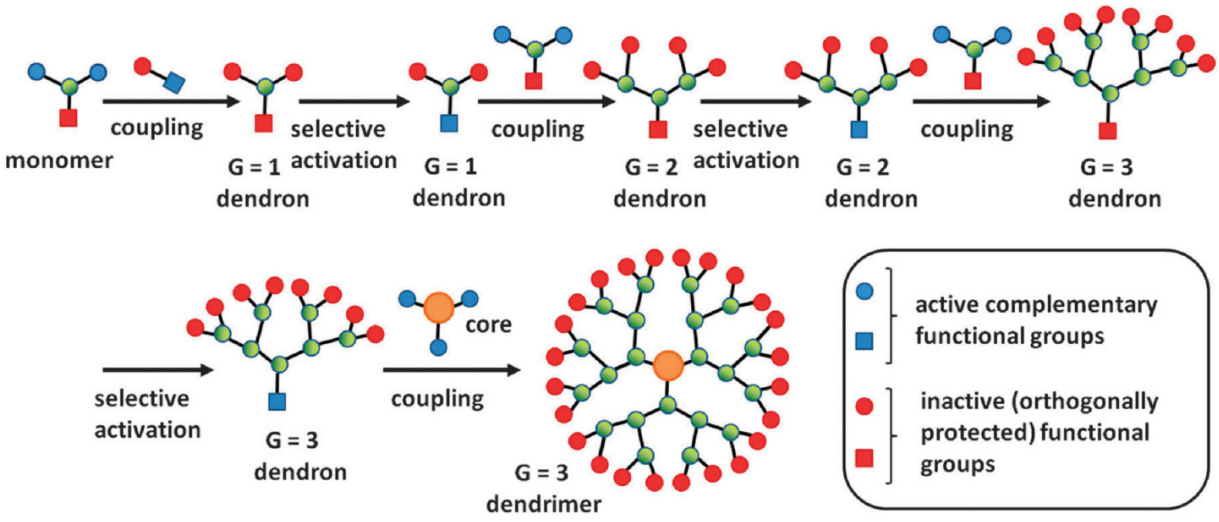

Figure 27 - Schematic representation of the dendrimer synthesis through the controlled convergent growth. As shown, the sequential reaction of an AB_2 monomer with the desired terminal functionality will give rise to the 1st generation dendron. By repeating this strategy, the anticipated generation is obtained. The resulting dendrons are then attached to a multifunctional core (Figure adapted from Ref. 63).

After reaching the desired generation, the dendrons are then coupled to the multifunctional core, resulting in a structure that is built from the exterior to the interior. At the end, since the resulting dendrimer contains terminal groups that are deactivated, a prior activation is needed in order to proceed with any further reaction on the dendrimer surface[2,12,13,25,53,63,66].

The poly(aryl ether) dendrimers initially prepared by Hawker and Fréchet, relied on the preparation of the peripheral units through the Williamson etherification between benzyl bromide and 3,5-dihydroxybenzyl alcohol (see Figure 28). This freshly prepared dendron (G1) was then activated by substitution of the hydroxyl group with a bromide and coupled with the next branch cell unit. The further repetition of this steps could lend dendrons as high as the 4th generation, being then coupled to a trifunctional core[13,63,66].

Similarly to the divergent approach, the connectivity between the individual branch cell monomers can be mainly accomplished through the traditional covalent or click type covalent[2,67]. For example, phenyl functionalized PAMAM dendrimers (Christensen-type PAMAM, see Figure 29) have been prepared by the convergent approach based on the traditional covalent connectivity. The reaction relied on the preparation of dendrons with the partially protected 1,2-propenediamine branch cells, followed by the reaction with alkyl phenyl carbonates. The anchoring of the resulting dendrons with the core containing carboxylic acid moieties allowed the preparation of PAMAM dendrimers ranging from 4 to 32 end groups[68].

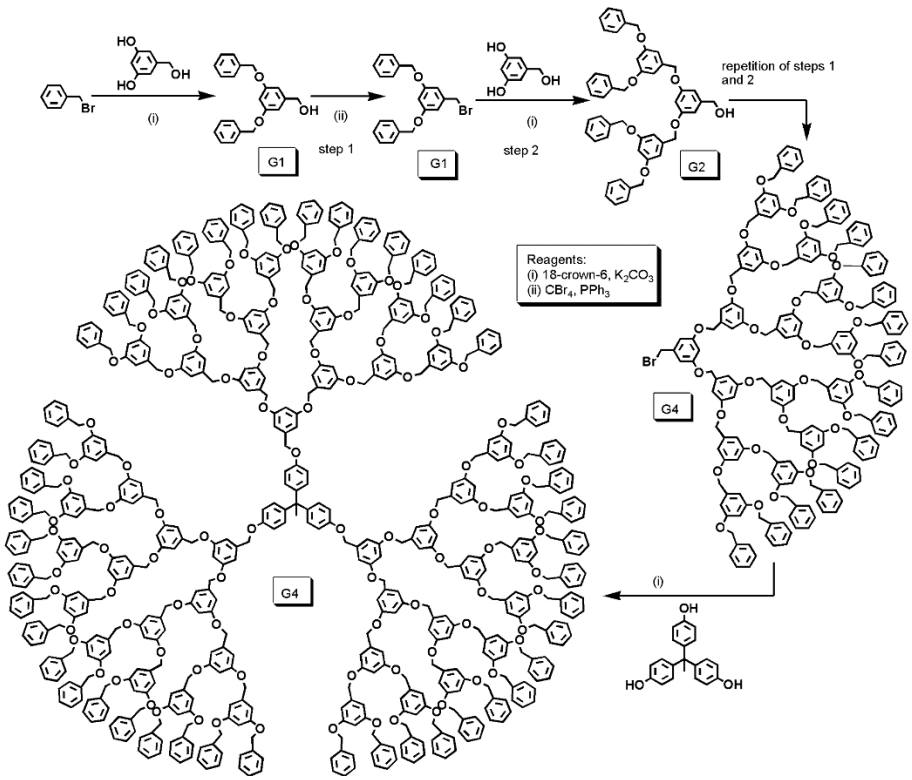

Figure 28 – Synthesis of the G4 poly(aryl ether) dendrimers through the convergent approach (Figure adapted from Ref. 63).

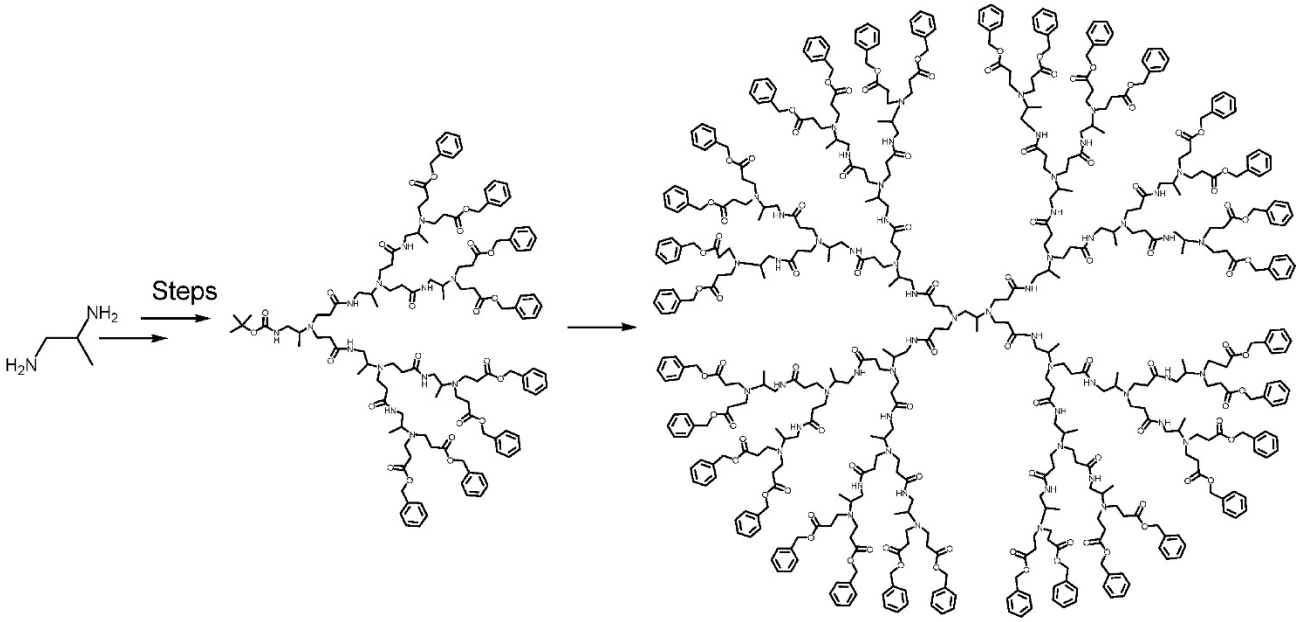

Figure 29 – The Christensen-type PAMAM dendrimers (Figure adapted from Ref. 68).

Recently, Simanek *et al*. reported the preparation of G3 triazine dendrimers based on a microwave assisted iterative convergent approach. By performing aromatic nucleophilic substitutions on cyanuric chloride with primary amines, the authors were capable of producing monochlorotriazine

dendrons. These dendrons were then made to react with an excess amount of diamine yielding amine dendrons. After purification, the diamine dendrons were dimerized giving rise to the next sub-generation (see Figure 30)[69].

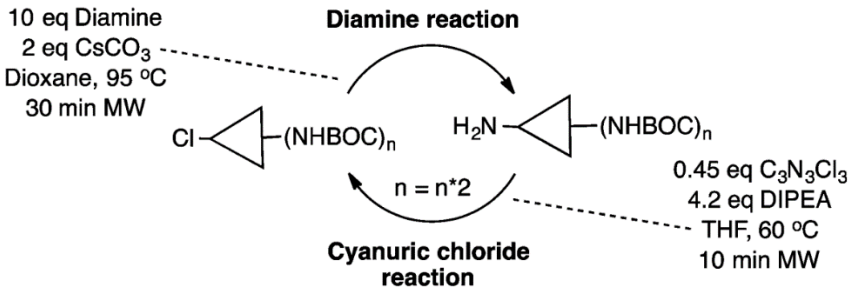

Figure 30 – Iterative convergent synthesis of G3 triazine dendrimers (Figure adapted from Ref. 69).

Moreover, Rajakumar *et al*. have recently described the preparation of triazole dendrimers with m-terphenyl surface units based on the convergent synthetic strategy and through the click chemistry approach (see Figure 31). By following propargylation, azidation and click chemistry conditions the authors were capable of synthesizing triazole dendrimers containing the chiral S-BINOL core. Interestingly, the authors also observed that these type of dendrimers presented antibacterial activity against *Shigella dysenteriae*, *Staphylococcus aureus* and *Serratia marcescens*[70].

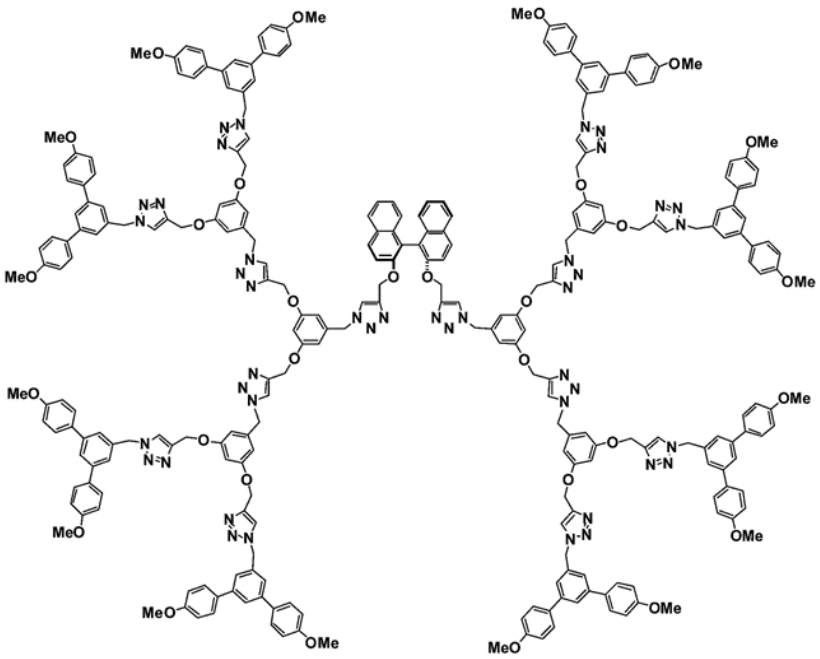

Figure 31 - The chiral triazole dendrimers prepared by Rajakumar *et al.* (Figure adapted from Ref. 70).

Several advantages are associated with the convergent preparation of dendrimers or other dendritic structures. Firstly, due to the reduced number of reaction steps involved during each generation increment, it is possible to produce dendrimers with less structural defects. As shown in Figure 27, the propagation step requires a single reactive functional group. Moreover, at each coupling phase two dendrons react with a single monomer where the activation step compromises only one reaction per molecule independently of the generation. Based on this methodology, it is possible to have a fine control over the synthetic process and prepare dendrimer with greater purity and less structural effects when compared with the divergent approach[2,12,13,58,63].

Additionally, since that the convergent synthesis usually requires equimolar quantities of reagents, an easier preparative work-up is achieved along a less expensive application of reagents[53].

Contrary to the divergent synthesis, the purification process can be simply achieved through the traditional methods due to the greater differences in the molar mass and polarity between the final dendrimers and the by-products. Usually, after each coupling phase, the desired product is two times heavier than the starting dendron[2,12,13,58,63].

Another favorable aspect of the convergent method relies on the ability to create almost limitless dendrimer families based on the use of the same dendrons that only differ by the core (*i.e.* organic or inorganic). For this reason, many of the dendrimers that contain unique functional cores are usually synthesized by the convergent method. In addition, since that the coupling of the dendrons to the core only occurs in the last reaction step, the application of more sensitive functional cores can be accomplished. By this way, based on the convergent approach, many supramolecular dendrimers can be obtained through the self-assembly of dendrons around the functional core (see Figure 32)[53].

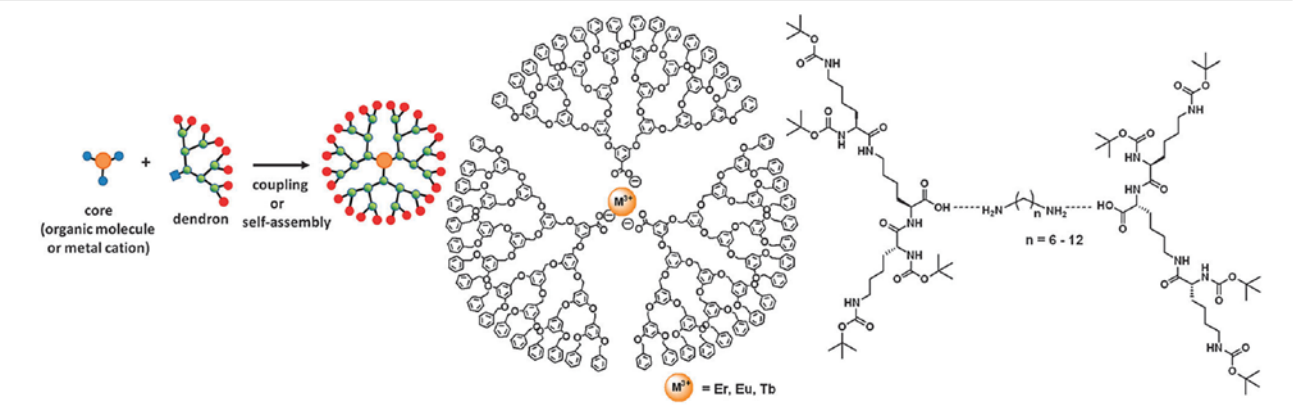

Figure 32 – The convergent synthesis and the ability to create unique dendrimer families containing distinct functional cores (Figure adapted from Ref. 53).

The convergent synthesis can also facilitate the preparation of dendritic structures containing variable compositions and functionalities (see Figure 33). For example, dendrons containing different

end groups or generations can be coupled with each other or to the same core. The major class of dendrimers built from two dendrons with a distinct nature are the so-called “Janus dendrimers”[63,71]. The “Janus dendrimers” usually contain “two sides”, a hydrophilic part in one side and a hydrophobic part in another, giving rise to an amphiphilic molecule (see Figure 34)[72]. Other types of dendritic structures can also be prepared by the convergent approach including the dendritic-linear polymer hybrids[53].

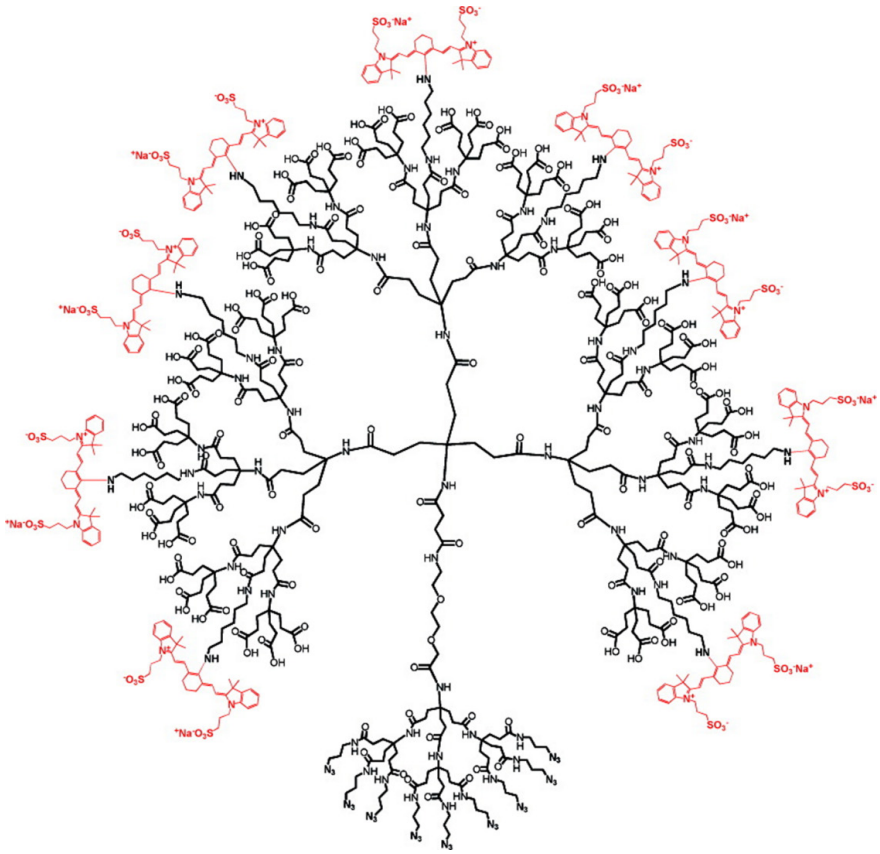

Figure 33 – As reported by Weck *et al.*, this dendrimer contains 9 azide termini, 9 amine termini and 54 carboxylic acid groups (Figure adapted from Ref. 71).

The major restriction of the convergent approach is the limited dendrimer growth that is influenced by chemical and stereochemical factors. As the generation of the dendron increases, the reactivity and availability of the focal points for further coupling are reduced. Consequently, the preparation of high generation dendrimers is very difficult to achieve. Moreover, the coupling of high-density dendrons can limit the accessibility of other dendritic structures to the core, leading to incomplete substitutions. As a result, only the dendrimers below the 6th generation can be prepared by the convergent synthesis[12,53].

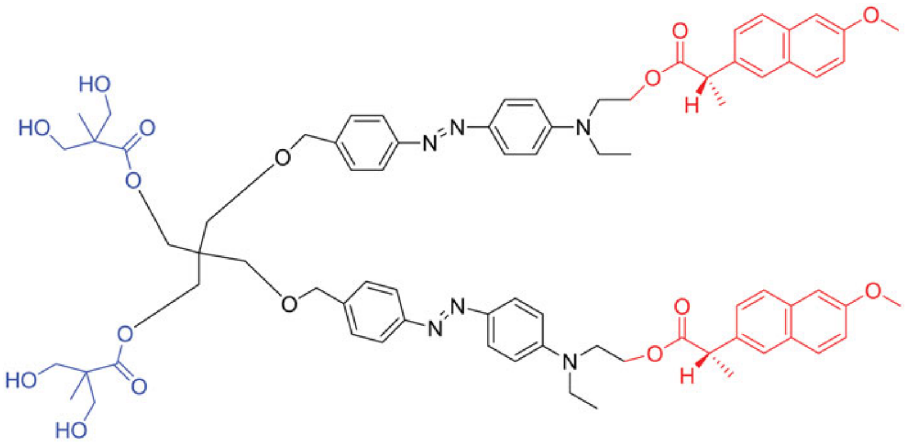

Figure 34 – Example of a G1 Janus dendrimer containing a polar (blue) and non-polar (red) sides (Figure adapted from Ref. 73).

1.3.3. Other methods for the preparation of dendrimers

With the development of highly complex dendritic structures, there was a need to redesign the traditional synthetic methods in order to surpass some of the existing limitations. The main goals of the novel synthetic methods rely on the ability to create high generation multifunctional dendritic structures in less time, following an environmental and economic friendly way (*e.g.* solvent- and metal catalyst-free reactions)[13,53,54,63,64,74].

If an accelerated and more efficient synthetic approach is desired, three major parameters should be taken into consideration. Firstly, the selection of commercially available/easily synthesized branch cell units should be ideally used. The application of more complex/difficult to obtain branch cells may limit the idea of an accelerated approach and the future research of the resulting dendrimers. Secondly, the number of reaction steps required for each generation increment should also be taken into consideration. For example, the synthesis of dendrimers without the need of activation steps may reduce the time required for their preparation. Third, the synthesis of dendrimers in one-pot chemistries can fairly reduce the time needed for purification of the final products[13,53,63,64].

Some of the novel accelerated and more efficient methods applied in the preparation of dendrimers are shortly discussed below. The further reading of the reviews published by Lipkowska *et al.*[63] and Malkoch *et al.*[64] is advised in order to understand in greater detail the recent accelerated approaches for the synthesis of dendrimers.

The double-stage convergent method (or hypercore approach) relies on the initial preparation of low generation dendrons (with protected end groups) that are then coupled to a multifunctional core through their focal points. The resulting framework, called hypercore, is then made to react with a new set of dendrons (identical or not to the initial ones) resulting in dendrimers of high generation (see Figure 35). Through this method, the main limitation of the traditional convergent method can be surpassed thanks to the reduced steric crowding and the ability to rapidly create high generation

monodisperse dendrimers. Additionally, this method can also be used to prepare layer-block dendrimers, by producing architectures with distinct internal and external branches[16,53,63]. The double-stage convergent concept was initially introduced in 1991 by Fréchet *et al*. for the preparation of G7 dendrimers[75].

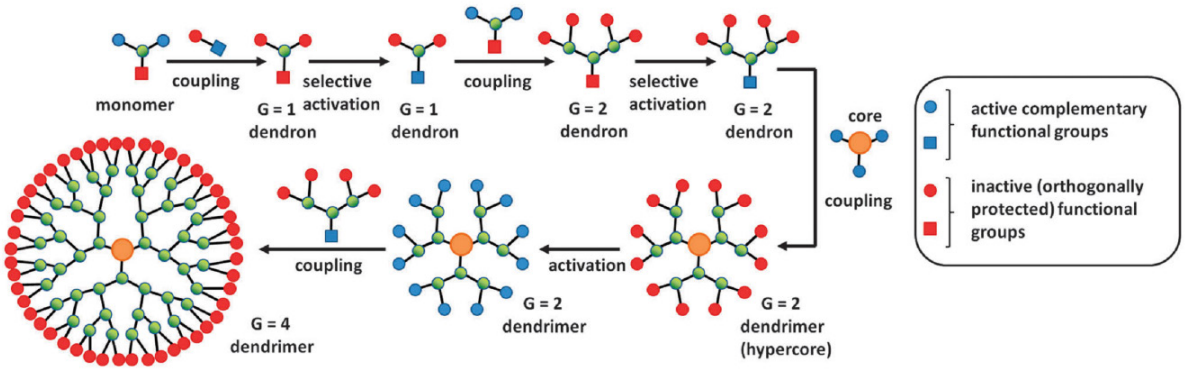

Figure 35 – Schematic representation of the double-stage convergent method (Figure adapted from reference 63).

Nevertheless, the main limitation of the double-stage convergent method comes from the time-consuming preparation of the hypercore/dendrons, since that in most cases, it follows the traditional routes that are characteristic of the convergent synthesis. For this reason, hybridized methods started to emerge[13,53,63,64]. More recently, López *et al*. have reported the preparation of hybrid, layer-block dendrimers based on the alternate coupling of thienylenevinylene and phenylenevinylene units (see Figure 36). As described by the authors, the preparation of these dendrimers was accomplished by the combination of an orthogonal and convergent methodology[76].

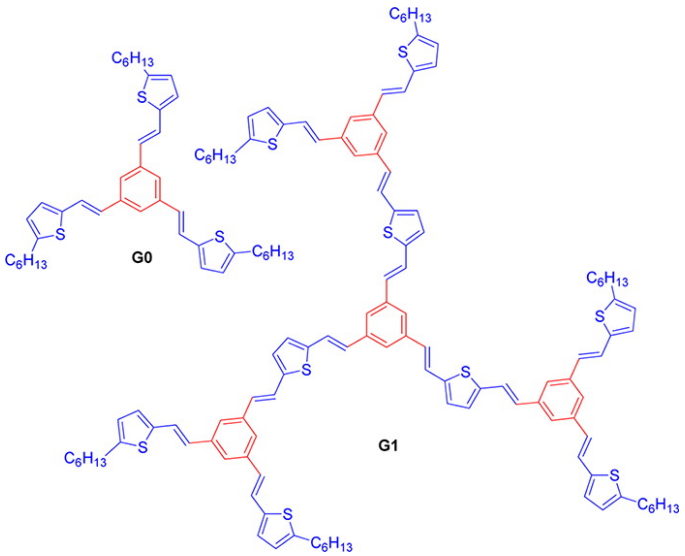

Figure 36 – The layer-block dendrimers prepared by López *et al.* based on a hybridized approach (Figure adapted from Ref. 76).

Many other approaches have been recently reported for the facile and accelerated synthesis of dendrimers including: (a) hypermonomer method, (b) double-exponential method; (c) orthogonal coupling methods; (d) solid-phase routes; (e) supramolecular chemistry; (f) lego chemistry[16,53,63]. In order to have an idea of the great diversity of dendrimer families, simple concepts regarding some of these methods will be discussed below.

The hypermonomer method explores the use of monomers containing higher functionality levels. Instead of the traditional AB_2 or AB_3 type branch cells monomers, typically in this method, AB_4 or higher type monomers are employed. Through this approach, dendrimers containing a high number of functional groups can be obtained in fewer steps. Recently, Wu *et al*. have reported the preparation of G2 polyhedral oligomeric silsesquioxane (POSS) dendrimers containing 392 terminal vinyl groups based on AB_7 type POSS branch cell monomers and in less than 3 reaction steps (see Figure 37)[77].

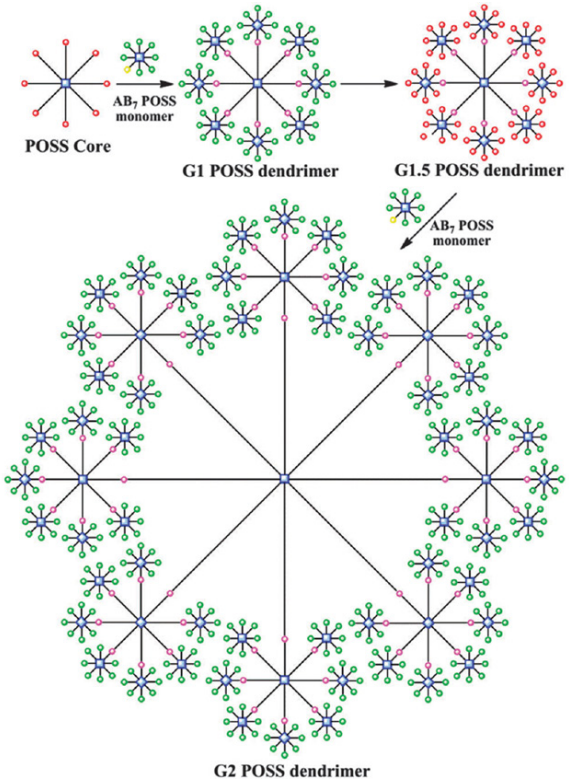

Figure 37 – Schematic representation of the POSS dendrimers prepared by Wu *et al.* based on the use of a hypermonomer (Figure adapted from Ref. 77).

In the double-exponential synthesis, fully protected low generation dendrons are firstly synthesized. These dendrons are then selectively split into two complementary groups: (a) one set of dendrons deprotected at the focal point and (b) another set of dendrons deprotected at the end groups. By orthogonally coupling the dendrons from the group (a) with the ones of the group (b), higher generation dendrons can be obtained. After achieving the desired generation through the iteration of the previous steps, the final dendrons are then convergently coupled to a multifunctional

core (see Figure 38). Through this method, the generation of the dendrons can be doubled in three steps: two activation sequences and one coupling phase. Interestingly, based on this approach, the preparation of G8 dendrons can be shortened in nine steps when compared to the traditional convergent method[12,53,63,72,78].

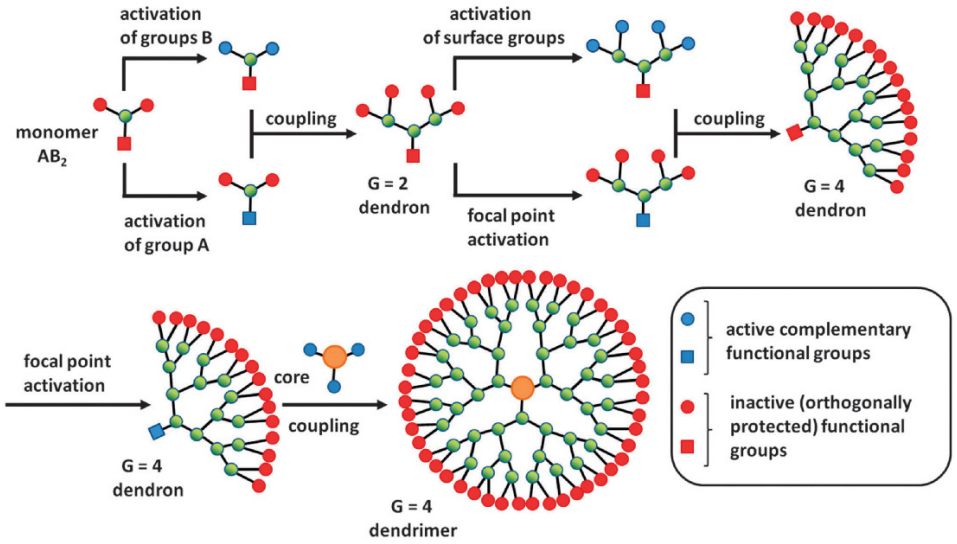

Figure 38 – Schematic representation for the preparation of dendrimers based on the double-exponential method (Figure adapted from Ref. 63).

Several dendrimer families have been successfully prepared through the double-exponential synthesis, including some poly(amide) and poly(ester) dendrimers[63,79]. For example, the commercially available aliphatic polyester dendrimers based on 2,2-bis(hydroxymethyl)propionic acid (bis-MPA) (see Figure 39) can be prepared by the double-exponential method as firstly reported by Gitsov *et al.*[80].

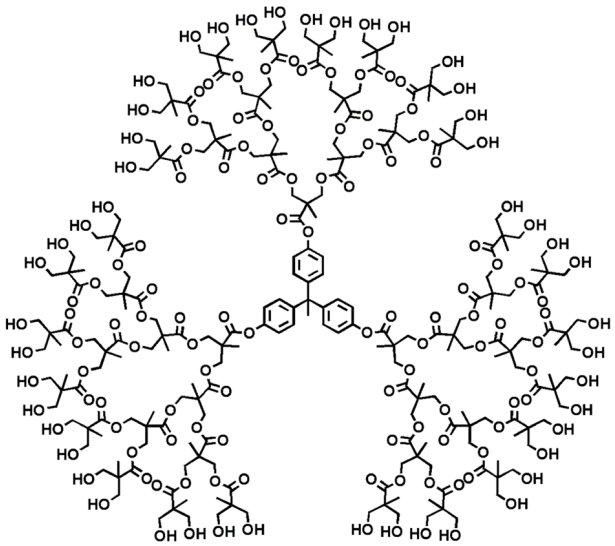

Figure 39 – The G4 bis-MPA dendrimer that can be prepared by the double-exponential method (Figure adapted from Ref. 63).

The orthogonal approach exploits the use of two distinct sets of branch cell monomers that contain chemoselective groups. As a result, monomers of the type AB_n and CD_n are coupled in divergent or convergent approach. Thanks to their chemoselective functional units, specific groups of the AB_n monomers will react at particular sites of the CD_n monomers and vice-versa. As shown in the Figure 40, the A and B groups are selectively designed to react with the D and C groups respectively. Thanks to this chemoselectivity, there is no need to proceed with activation steps, resulting in reduced preparation times[53,63,78].

Although this method may provide an accelerated way for the preparation of some dendrimer families, a limited number of functionalities can be introduced into the dendritic structure. These limitations arises due the requirment of highly efficient orthogonal pairs that must not interfere with the reaction cycle[53].

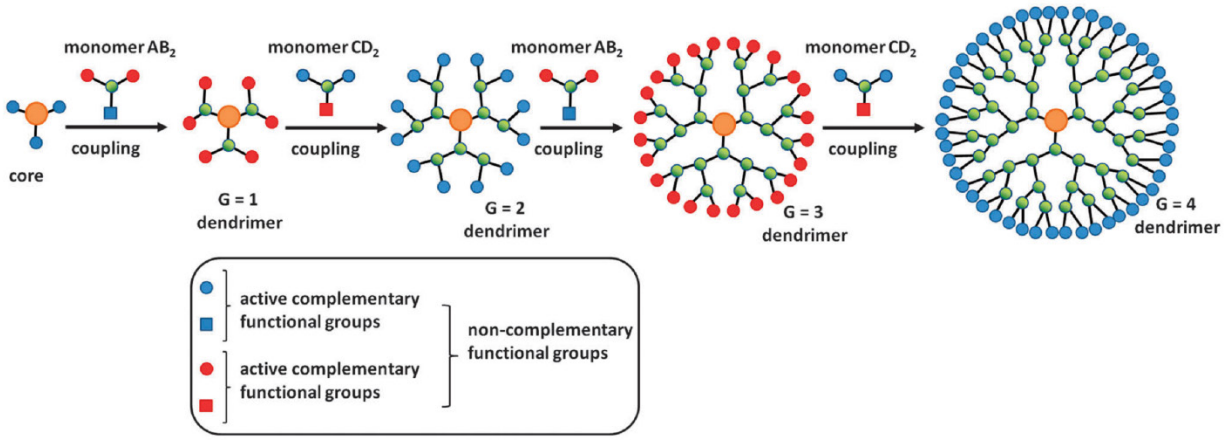

Figure 40 – Orthogonal synthesis of dendrimers through the divergent approach (Figure adapted from Ref. 63).

In the last years, a large number of novel dendrimer families have been prepared through the orthogonal approach. Initially described by Splinder and Fréchet for the preparation of G3 poly(ether urethane) dendrons, this method was then tuned by Zimmerman *et al*. for the high yield preparation of G4 poly(alkyne ester) dendrons[63,78,81,82]. The advantage of this method is the ability to prepare dendrimers that contain alternating functionalities in the interior. For example, Recently, Roy *et al*. have reported the preparation of multifunctional carbohydrate-based dendrimers through the orthogonal coupling strategy (see Figure 41)[60].

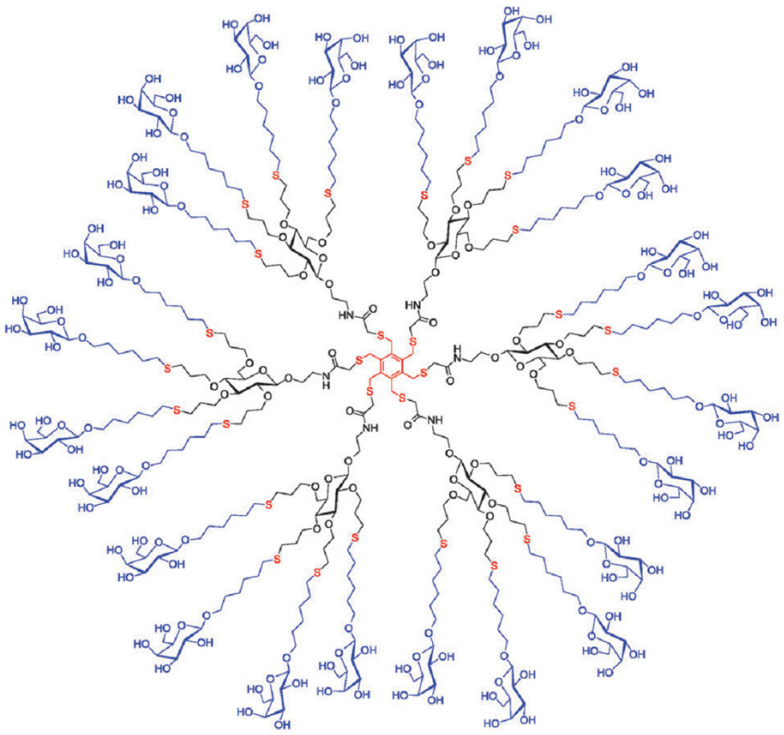

Figure 41 – The carbohydrate-based dendrimer prepared by Roy *et al.* based on the orthogonal approach (Figure adapted from Ref. 60).

In the solid phase synthesis, the preparation of the dendritic structures occurs in a step-wise approach. This method depends on the use of polymeric units that are employed to a solid support and then functionalized with the intended functional groups (see Figure 42)[53].

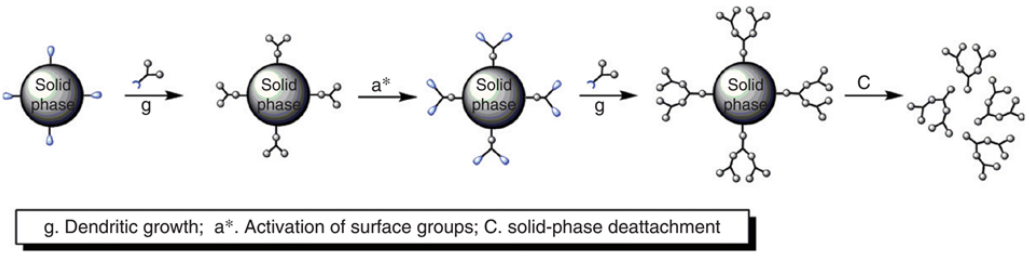

Figure 42 – Solid phase synthesis of dendritic structures (Figure adapted from Ref. 53).

On the other hand, in the supramolecular self-assembly synthesis, the dendritic structures are mainly built upon the noncovalent interactions between complementary branch cells monomers that self-assemble into more complex structures. Many different interactions can contribute for the supramolecular synthesis of dendrimers including hydrogen-bonding, hydrophobic, among others (see Figure 43)[53].

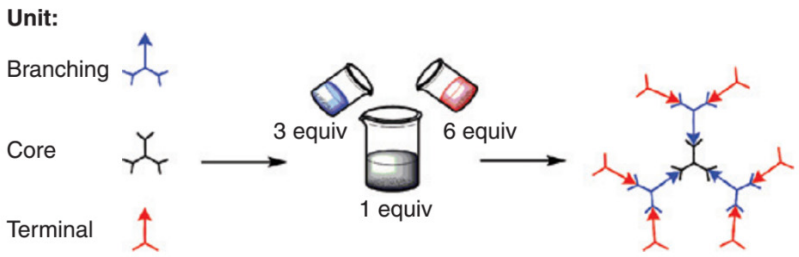

Figure 43 – Preparation of dendrimers based on self-assembly of individual components (Figure adapted from Ref. 53).

Moreover, highly complex architectures can be prepared by the supramolecular self-assembly of distinct dendritic structures. Recently, Gu *et al*. reported the preparation of multifunctional supramolecular hybrid dendrimers based on low generation peptide dendrons (see Figure 44). As reported by the authors, these hybrid dendritic structures exhibited fluorescent signaling properties along with an interesting gene transfection efficiency[83].

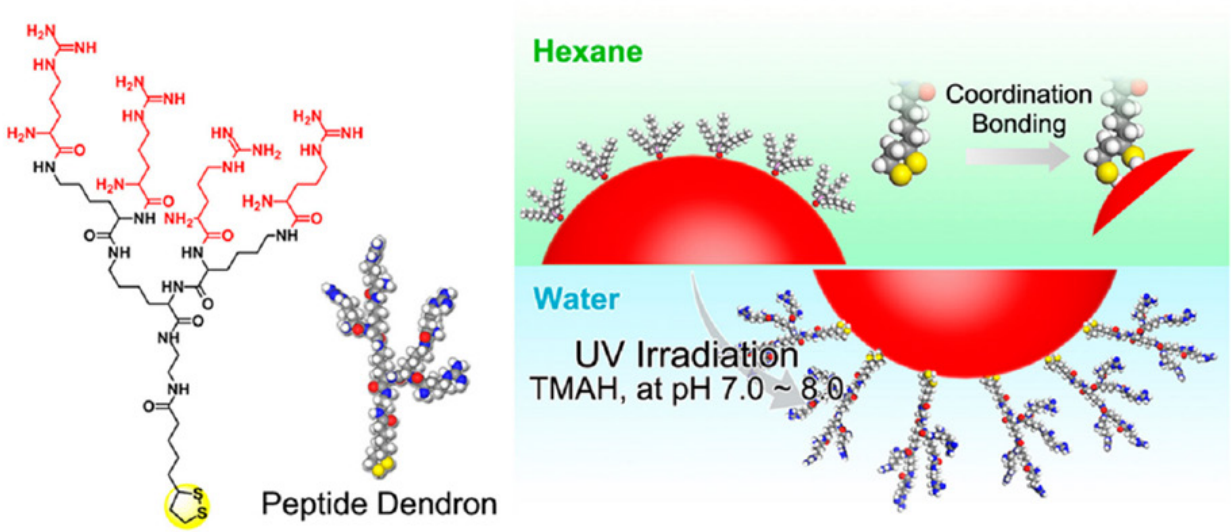

Figure 44 – Schematic representation of the peptide dendrons and the conditions used for the preparation of multifunctional supramolecular hybrid dendrimers as reported by Gu *et al.* (TMAH = tetramethylammonium) (Figure adapted from Ref. 83).

Finally, based on the lego chemistry concept and reassembling the same idea of the well-known child's toys, the synthesis starts with a limited number of small building blocks that are then used to build extremely complex dendritic structures. This approach is usually applied to build dendrimers that contain highly functionalized cores and branching units. In some cases, the lego synthesis is designed in such a way that a great amplification of the terminal groups can be achieved in just a single reaction step. Another advantage of this method is the ability to proceed with the reactions using minimal quantities of solvent along with facile purification methods and environmental friendly by-products[16,84]. This method is usually applied for the preparation of phosphorous-based dendrimers[85].

1.4. Main purification and characterization methods of dendrimers and their conjugates

Thanks to the great diversity of dendrimer families, unique properties can be exploited for many different applications. However, the potential use of dendrimers in several fields depends on their rigorous and methodic characterization. Unfortunately, due to the complexity of the dendrimer architecture, their unequivocal analytical characterization can be very difficult to achieve. It is, therefore, essential that a conjugated set of characterization techniques is used in order to provide the most reliable information regarding this type of structures[12,16,25,62,86,87].

Taking into consideration that the dendrimer "kingdom" lies between the small molecular and macromolecular worlds, the dendritic structures may benefit from characterization techniques that are traditionally used in both cases (see Figure 45)[2,62].

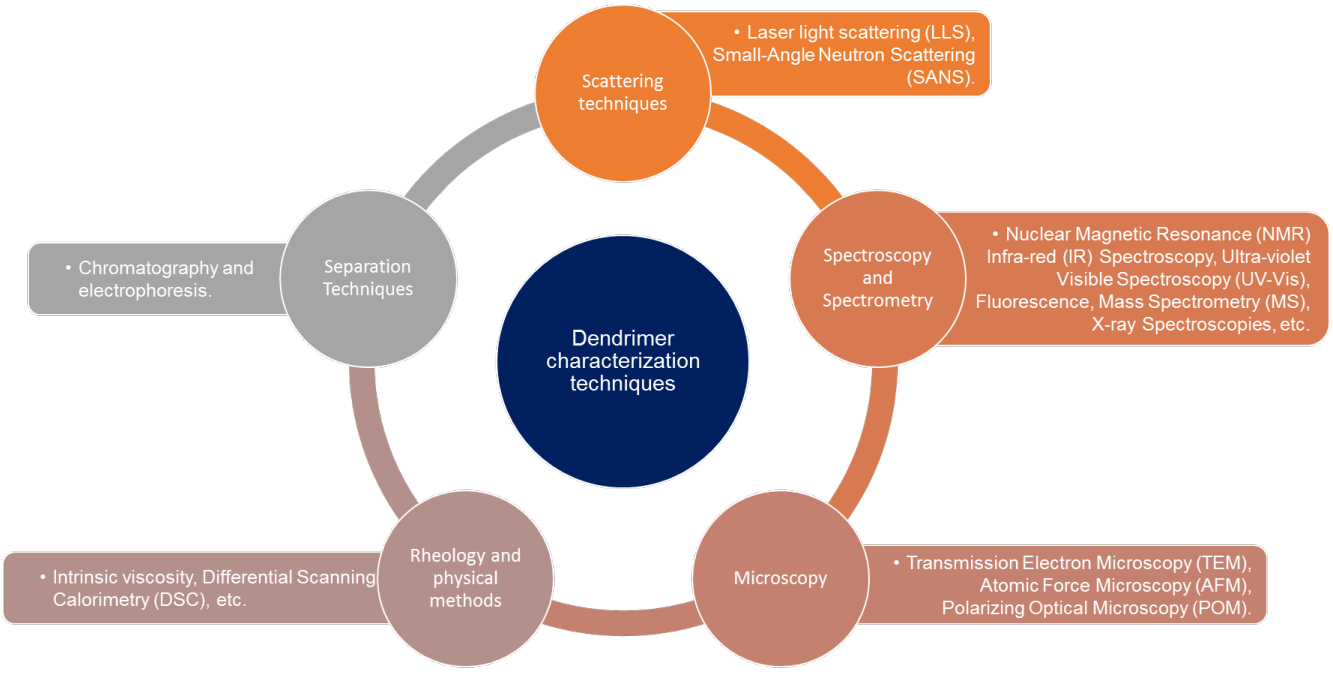

Figure 45 – The most common characterization methods of dendrimers.

Many different analytical techniques have been reported in the literature for the proper characterization of dendrimers and their conjugates. The determination of several parameters like, chemical composition, degree of functionalization, morphology, size, shape, purity or homogeneity depends on the simultaneous use of several techniques (see Figures 45 and 46). Moreover, the use of such analytical techniques is of outmost importance for the fine controlled synthesis and functionalization of dendrimers allowing by this way a better control of the reaction progress between each step[2,12,16,25,62,86,87].

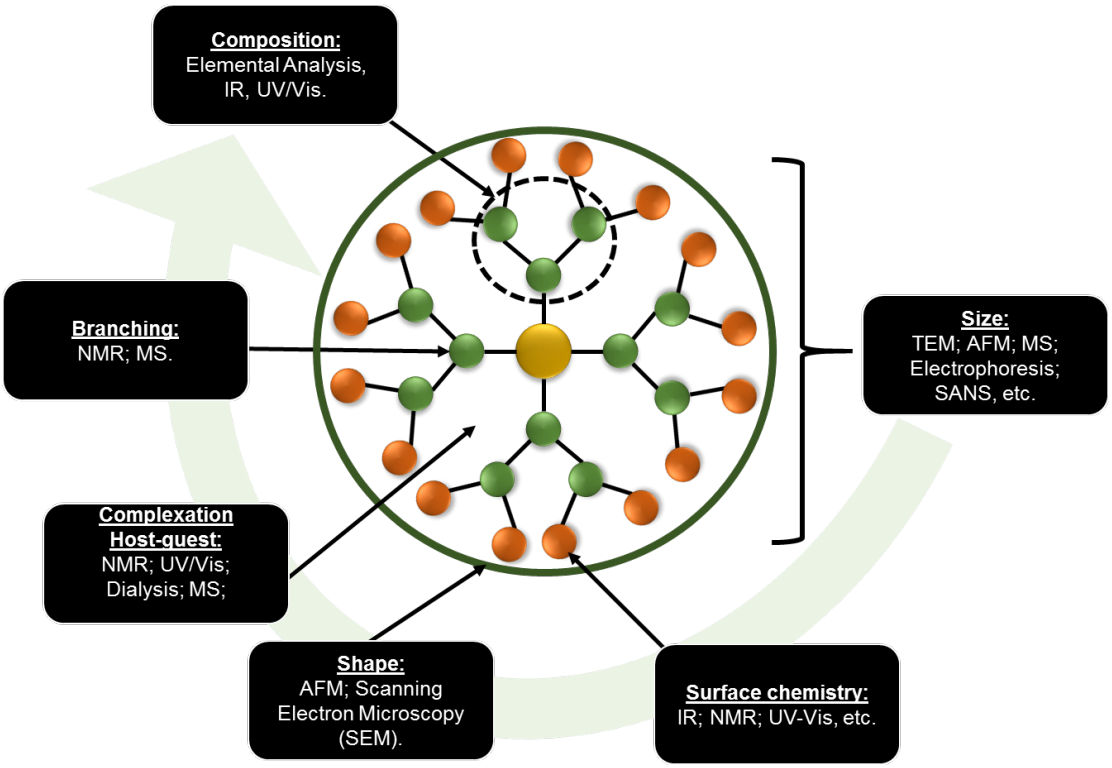

Figure 46 – Examples of characterization techniques used for the analysis of the individual dendrimer components.

Given the great diversity of analytical techniques that can be employed for the analysis of dendrimers (see Figure 46), herein we will only discuss the characterization methods that were used in the current thesis. Additionally, in order to emphasize the importance of these characterization techniques in the dendrimer chemistry, an overview of their application for the analysis these structures is discussed in the next sections.

For a more detailed information regarding the characterization of dendrimers and dendritic structures, the further reading of the following reviews is recommended[2,12,16,25,62,86–88]. Despite the great number of reference works related with the dendrimer characterization, a more generalized recent review regarding this topic is still required.

1.4.1. Nuclear Magnetic Resonance (NMR) spectroscopy

The NMR spectroscopy is a powerful and one of the most widely used techniques that have been applied to identify innumerous properties of dendrimers and other dendritic structures. In the last 20 years, many papers have been published based on 1-D and 2-D NMR experiments for the analysis of dendrimer-specific properties. Additionally, depending on the dendrimer family being studied, these structures are mainly analyzed by ^{1}H and ^{13}C NMR but can also be characterized by ^{19}F, ^{31}P, ^{29}Si, ^{57}Fe, ^{119}Sn or ^{195}Pt, if these heteroatoms are present in the dendrimer scaffold[2,12].

In a simple way, the NMR spectroscopy relies on the radio waves for the acquisition of a spectrum based on the resonance frequency of an atomic nucleus (nuclear spin). The signals obtained in the spectrum do not only depend on the external magnetic field but also on the electronic microenvironment of the nucleus being studied. That influence is measured in terms of chemical shift (δ) where each specific microenvironment results in a well-known and reported δ value. As a result, the existence of distinct nuclei/neighborhood moieties in a molecule, results in a fine NMR spectrum of that molecule dissolved in a solvent (*i.e.* deuterated solvent). Moreover, characteristic covalent linkages between atoms can be identified based on the scalar (*J*) coupling. Note that solid-phase NMR can also be applied for dendrimer characterization however it is less used than the liquid NMR[12].

Given the main concept behind the NMR spectroscopy, this technique is used to analyze transformations on the dendrimer surface as well as to control and confirm generational growth during their synthesis. As a result, the 1-D NMR characterization of dendrimers in solution is one of the most widely used methods to obtain valuable information about the dendrimer architecture. As shown in the Figure 46, thanks to the differences in the chemical environment between the atoms in the inner layers and the ones in the outer layer, the 1-D NMR can be used for the analysis of the surface atoms. However, these studies are more simplified for dendrimers at low generations (< 4^{th}) or for dendrimers containing other heteroatoms (*e.g.* P, F, Si) in the dendritic scaffold[2,12,16,25,62,86,87].

Furthermore, the problem that may arise during the NMR characterization of high generation dendrimers is the possible overlapping of peaks. This behavior is usually observed due to the broad signals generated by chemically similar groups distributed at distinct microenvironments along the dendrimer scaffold. Moreover, the existence of defects (*e.g.* missing branches) is usually very difficult to detect solely based on the 1-D NMR characterization[2,16,25,62,86,87].

The multidimensional NMR spectroscopy (*e.g.* 2-D; 3-D) relies on the acquisition and plotting of additional data components into the NMR spectrum (*e.g.* resonance frequencies versus the spin/spin coupling, COSY). By this way, supplementary information can be obtained for further analysis of the dendrimer structure including, (a) the conformation of the dendrimer scaffold components; (b) the identification of stable host-guest complexes (*e.g.* drugs/fluorochromes); (c) the investigation of intermolecular interactions in solution; or (d) determination of the internuclear distances of the nuclei at different positions in the dendrimer scaffold[12].

Moreover, other NMR-based analysis including diffusion (DOSY) or dynamic NMR spectroscopies, have been recently used to study the influence of different environmental conditions (*e.g.* pH or temperature) over dendrimer scaffold. For example, in the diffusion NMR spectroscopy, through the determination of the self-diffusion coefficient, it is possible to accurately measure the hydrodynamic size of the dissolved dendrimer and the effect of the pH over this parameter[89]. On the other hand, the dynamic NMR spectroscopy has also been used to study the behavior of some dendrimer families in specific solvents (*e.g.* differences in the interior density). It is clear that the study

of such parameters is of utmost importance in order to understand and predict the influence of the biological medium over the dendrimer physicochemical properties[12,90].

1.4.2. Ultra-violet Visible Spectroscopy

The Ultra-violet visible (UV-Vis) spectroscopy involves the detection of chemical groups that absorb radiation in the visible region (390-750 nm) of the electromagnetic spectrum.

Simply explained, the appearance of bands/peaks in the UV-Vis spectrum occurs thanks to a set of electronic transitions that arise from the incident visible light radiation over the absorbing groups of the molecule being studied (*i.e.* chromophoric units). Mainly, these electronic transitions happen for molecules that contain organic groups with π electrons (bonding) or non-bonding electrons (n) that can absorb photons at a specific position of the visible spectrum (*i.e.* energy level). This absorption of light results in the transition of these electrons (excitation) to the molecular orbitals at higher energy levels (*e.g.* antibonding orbitals like π*). The energy gap (*i.e.* band gap) between the orbital from where the electron was excited to the orbital of higher energy level, will define the energy required for the transition to occur and as a result dictate the position of the band in the UV-Vis spectrum.

It is important to note that, not only the electronic transitions contribute for the existence of peaks in the UV-Vis spectrum but also the lower-energy vibrational/rotational transitions (see Figure 47). As a result, the conjugated effect of these transition types leads to the formation of peaks where the most probable transitions contribute for the maximum absorption usually referred as λ_{max}. In most cases, the UV-Vis analysis in accomplished in liquid phase resulting in peak broadening of the electronic transitions and the hindering of the vibrational/rotational transitions (*e.g.* due to hydrogen bonding, collisions). Additionally, for a proper analysis, the sample must be diluted in a pure and “transparent” solvent that does not absorb (*cut-off*) in the UV-Vis region (*e.g.* especially water, methanol, cyclohexane). For comparison purposes, the UV-Vis spectrum of the analyte must be ideally acquired based on the same reported solvents since that the use of different solvents may influence the intensity and the position of the absorption maximum[2,16,62,91].

For a more detailed explanation regarding the fundamental concepts of UV-Vis spectroscopy, the further reading of the following book is recommended[91].

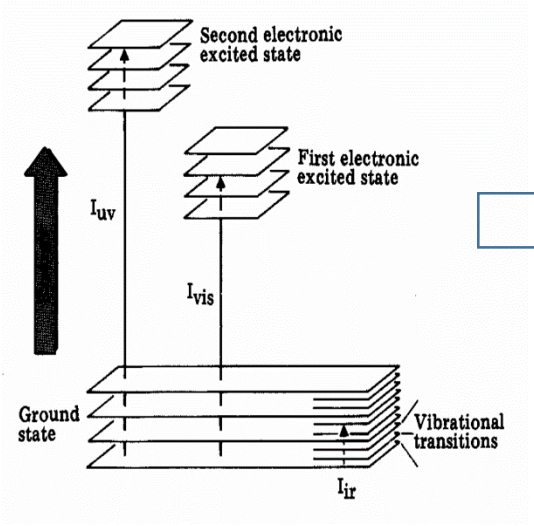

Figure 47 – Schematic representation of the different molecular energy levels where each electronic state is composed by a set of vibrational/rotational states. Note that the energy (E) is inversely proportional to the wavelength (λ). As a result, high energy transitions occur in the lower wavelengths (h = Plank's constant; c = velocity of light) (Figure adapted from Ref. 92).

Since that the UV-Vis spectroscopy is mainly a quantitative technique, there is limited ability to characterize the dendrimer structure solely based on this approach. Nevertheless, the UV-Vis analysis may help to uncover possible changes taking place on the surface or interior of the dendrimer scaffold. Moreover, the UV-Vis has also been used to determine the purity and the defect level of some dendrimers containing chromophoric units[2,16,62,93,94].

The most common electron transitions than can be observed in the dendrimer scaffold are of the type, n→π* (e.g. electron lone pairs in oxygen or nitrogen) and π→π* (e.g. carbonyl groups, double bonds, triple bonds or conjugated π systems). Since that σ→ σ* and n→ σ* transitions (e.g. simple carbon-carbon bonding) required more energy to occur, therefore they are not detected in the UV-Vis region but rather in the UV region (< 390 nm). Note that since that these transitions are sensitive to the surrounding chemical moieties, they may be used to complement other characterization techniques for further confirmation of the dendrimer surface functionalization[2,15,52].

Note also that for dendrimers containing inorganic groups, the UV-Vis absorptions that involve the d- or f- orbitals can also be detected in the spectrum (charge-transfer complex)[†]. As a result, the complexation of metal ions inside the dendrimer scaffold can be followed based on the UV-Vis analysis thanks to a change in the orbital energy levels that comes from this process. For example, the stabilization/encapsulation of metal nanoparticles in the dendrimer scaffold can also be followed

[†]For metals, the electronic transition consists of a charge-transfer complex where an electron-donor group is associated with an electron acceptor. With the absorption of photons an electron of the donor group is transferred to an orbital that is mainly associated with the acceptor.

through the UV-Vis analysis based on the appearance of characteristic surface plasmon resonance bands (SPR) in the spectrum[95,96].

As mentioned earlier, the quantitative analysis that is characteristic of the UV-Vis spectroscopy may be exploited in favor of the dendrimer characterization. Based on the Beer's Law (see Figure 48), it is possible to determine the concentration or molar absorptivity values depending on the experimental data that is available. By this way, the successful quantitative determination of chromophoric units within each dendrimer generation can be accomplished[62,97,98].

Additionally, if the basic principles of the Beer's Law are maintained (see Figure 48), it can be used to determine the purity and perfection level of the dendrimers containing UV-vis absorbing units. Interestingly, if an UV-Vis absorbing core is used, the changes in the λ_{max} may be followed in order to predict possible conformation variations in the dendrimer scaffold as a function of the environmental conditions[62,97,98].

Finally, the UV-vis analysis has also been applied to follow the conjugation of chemical moieties to the dendrimer scaffold. For example, fluorochromes can display distinct λ_{max} positions when coupled with the dendrimer scaffold and which may be used to differentiate from the non-conjugated counterpart[62,97,98].

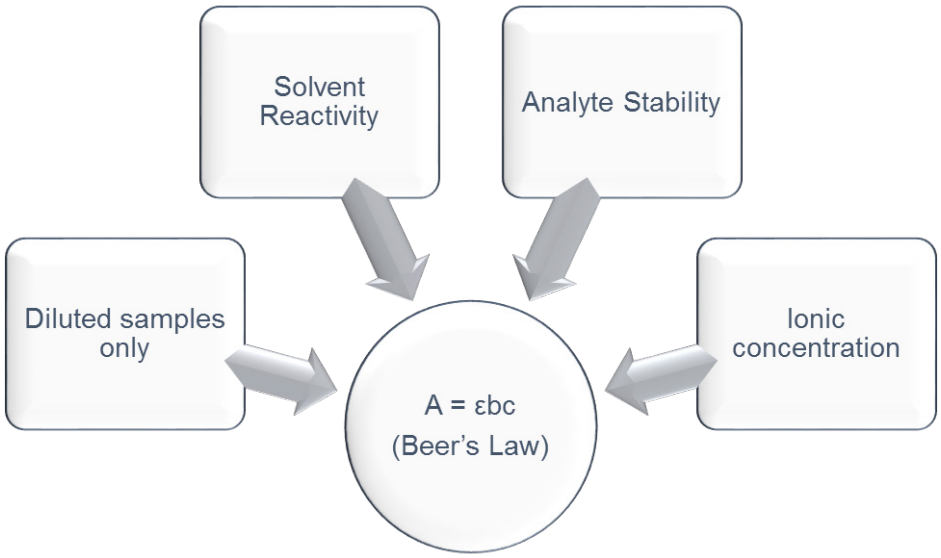

Figure 48 – The Beer's law and its real and chemical limitations (A = absorbance; ε = molar absorptivity; b = path length; c = concentration).

1.4.3. Infrared spectroscopy

The infrared (IR) spectroscopy has been largely used for the identification of functional groups that typically present characteristic bands in the infrared region. The basic concept of the infrared spectroscopy relies on the use of light with a longer wavelength than the visible light (*i.e.* infrared

radiation), that passes through the sample and leads to specific modes of vibration/rotation of most chemical bonds. A wide range of functional groups are well reported in the literature in relation to their modes of vibration and the associated energies of the corresponding vibrational transitions (*e.g.* amine, carbonyl, carboxyl groups). The Fourier transform mid-infrared (FTIR) spectroscopy ($\bar{\nu}$ = 4000-400 cm^{-1}) has been mainly employed to study the vibrational and rotational-vibrational structure of the dendrimer terminal groups. By this way, the chemical transformations occurring in the dendrimer surface can be followed either during their synthesis or to assess the post-synthetic functionalization (*e.g.* drugs, targeting groups)[2,16,62].

The FTIR spectrum can be obtained either in solution or solid phase; however, the latter is the most commonly used approach for the dendrimer characterization. Mainly, in solid phase, the spectrum can be obtained by pressing the sample with KBr at high pressures (KBr pellets) or through the direct sample measurement using an Attenuated Total Reflectance (ATR) cell (see Figure 49). The FTIR-ATR characterization is especially useful for the analysis of certain functional groups such as isothiocyanates (-N=C=S), carbonyl (-C=O) or nitriles (-C≡N)[2,16,62].

Note that many other IR related techniques have been used for the analysis of dendrimer properties which will not be discussed here (*e.g.* Raman, FTIR-ERS). For example, FTIR-ERS (see Figure 49) can also be employed to explore possible conformational or chemical changes on the dendrimer surface[99]. Moreover, low-frequency Raman spectroscopy has been applied to investigate the end group steric crowding of the high generation dendrimers[100]. Also, the near infrared spectroscopy (NIR) was successfully used for the analysis of π- π interactions[2].

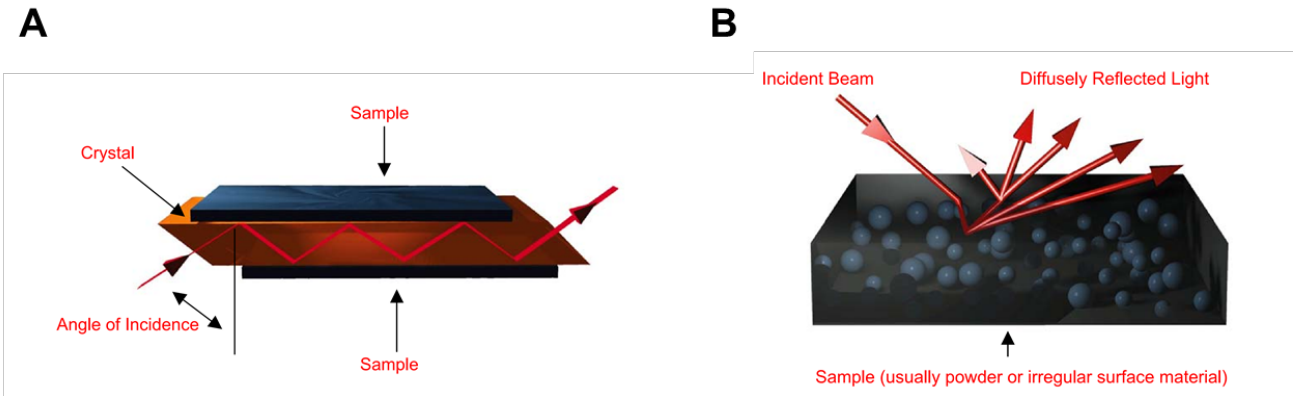

Figure 49 – Schematic representation of the differences between the ATR (A) and ERS (B) spectroscopies (Figure adapted from Ref. 101).

The FTIR has also been used to study dipole-dipole interactions and conformational changes between dendrimer end groups and other chemical moieties (*e.g.* drugs, nanoparticles) based on the energy changes of the vibrational/rotation level (wavenumber ($\bar{\nu}$) shift). Additionally, based on the

wavenumber shift of the interior functional groups, FTIR has been applied to assess the possible encapsulation/endo-complexation of drugs, fluorochromes or metals in the dendrimer scaffold[102–109].

1.4.4. Fluorescence spectroscopy/microscopy and fluorochromes

The term fluorescence refers to the phenomenon of energy reemission by a molecule that was initially excited by the absorption of incident radiation. The time difference between the absorption and emission of radiation is usually referred as fluorescence lifetime and defines the time that a molecule remains in the excited state.

As described in the previous sections, the absorption of UV radiation by a molecule results on the electron transition from a lower energy orbital to a higher energy one (see Figure 50). In order for that transition to occur, the energy of the incident photons must match the corresponding energy gap between the lower energy and the higher energy orbitals (energy conservation principle)[91,110].

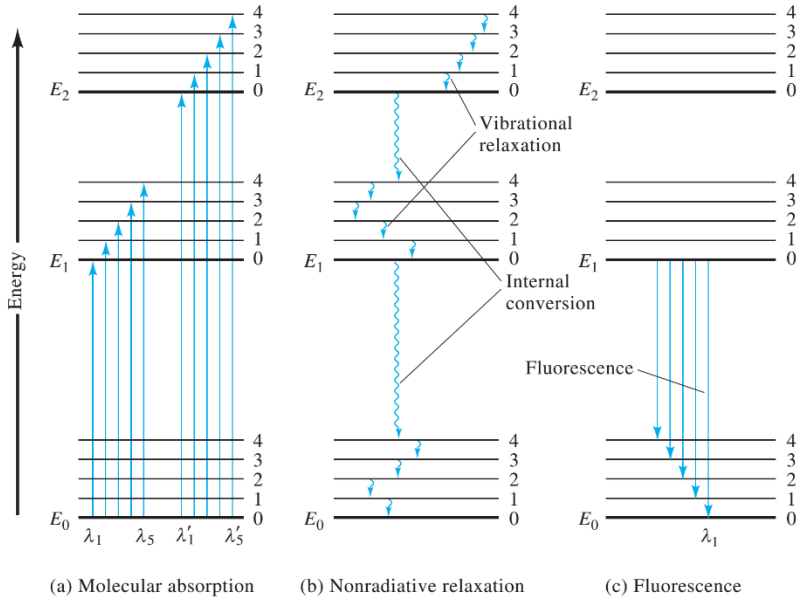

Figure 50 – Schematic representation of the different energy levels and the possible transitions that may occur as a function of incident radiation (Figure adapted from Ref. 91).

As shown in Figure 50, after achieving the excited state, distinct electronic processes usually happen in order for a molecule to return to the lower and stable energy state. As a result, competing with the fluorescent emission, fast internal conversions (IC, ~10^{-12} s) along with a set of vibrational relaxations (~10^{-10}-10^{-11} s) take place in the molecule (*i.e.* known as nonradiative relaxations). The

nonradiative mechanisms are characterized by electronic relaxation processes that involve the conversion of excited species to lower energy/vibrational states*.

On the other hand and less frequently, the fluorescent emission can also occur depending on the molecule and the surrounding conditions. This process involves the slower (~10^{-10}-10^{-5} s) transition of electrons from the lowest excited energy state at E_1 to the several vibrational levels at the ground energy state (E_0). By this way, the fluorescent emission involves the transmission of photons with specific energy that are at lower wavelengths than the ones absorbed. This difference between the absorption and emission maxima is known as Stokes-Shift[91,110].

For most of the fluorochromes very small quantities of the dye are required in order to attain a fluorescent signal (in the order of the ppm). Note that a proper selection of the ideal fluorochrome is important when a reliable fluorescence analysis is intended. As a result, the physicochemical properties (*e.g.* nature, size, cytotoxicity) of the selected fluorescent dye along with the environmental conditions where the fluorochrome will be employed should be taken into consideration for any type of analysis.

Ideally, for cell studies, the selection of the proper fluorescent dye relies on the sufficient photostability, the excitability upon conventional light sources, the minimal fluorescent background from the biological matrix and the capability to produce sufficient brightness to be detected with the most common instrumentation. Also parameters such as solubility, size/steric effects, temperature†, viscosity or pH dependence must be taken into consideration.

Another interesting factor that should be addressed is the structural exposure of the fluorochromes to the components in the environment. For example, while most of the organic dyes may lose their fluorescent ability or photobleach in the presence of molecular oxygen (*i.e.* due to changes in the π system), "rigid" dyes (*e.g.* inorganic nanoparticles) tend to be more photostable under such conditions.

It is important to outline that for most of the fluorescent dyes, the fluorescence intensity strongly depends on the concentration of the dye. However, after a specific threshold and at very high concentrations this relationship is broken. With the continuous increase in the concentration the fluorescence intensity starts to decline due to the well-known primary and secondary absorption processes (*i.e*. inner filter effects) that are caused by the excess of surrounding molecules (see Figure 51).

For molecular conjugation purposes, the selection of the proper fluorochrome should rely on additional considerations. The chemical availability of the coupling site and the possible concentration/localization effects should be taken into analysis. For example, in the case of the

*In the liquid medium, the transfer of the excess energy is accomplished from the excited molecule to the solvent molecules.

†High temperatures lead to a hindered fluorescent activity due to the increased number of collisions between the molecules of the solvent and the fluorochrome.

fluorochrome-dendrimer surface functionalization, the selection of the ideal fluorescent marker depends on the reactivity/specificity of the dye to the terminal groups of the dendrimer. Moreover, due to the nature of the dendrimer scaffold possible steric and quenching* effects should also be taken into account.

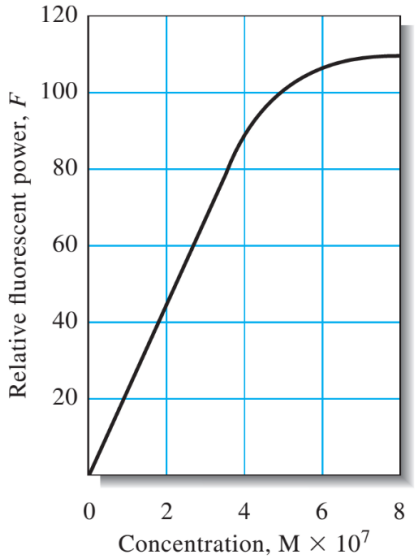

Figure 51 – The fluorescent signal of organic dye with the continuous increase in the concentration. Due to this behavior, the conjugation of fluorescent probes with dendrimers must not be extensive (Figure adapted from Ref. 91).

The Table 2 outlines some of the fluorescent markers and compares the aforementioned key properties that should be taken into account when selecting a fluorescent probe for dendrimer functionalization.

Table 2 – Different types of fluorescent dyes and the relationship of some key parameters (each parameter is valued from 1 (low) to 4 (high) – Data adapted from Ref. 110).

Class	Example	Brightness	Photostability	Biocompatibility	Environmental sensitivity	Excitation (λ_{max}, nm)	Emission (λ_{max}, nm)
AlexaFluor	AlexaFluor 488	4	4	4	2	499	519
Cyanines	Cy5	3	4	3	2	650	670
Fluorescein	FITC	3	1	3	4	495	519
Rhodamine	Rhodamine 6G	3	4	2	3	525	548
Quantum Dots	CdSe	4	4	1	1	Variable	Variable
GFP-like proteins	EGFP	2	2	4	2	488	507
Phycobiliproteins	R-phycoerythrin	4	2	2	2	480	578

*Quenching is the term used to describe a decrease or complete depletion of the fluorescence emitted by a fluorochrome.

Several parameters can be used to differentiate the fluorescent applicability and efficiency of the molecules. Mainly, the quantum yield (QY) may be applied for these comparative purposes. Simply, this parameter is defined by the ratio between the number of photons emitted and the ones that were absorbed. While highly fluorescent molecules exhibit high QY (near 1), weakly fluorescent molecules tend to show very low QY (almost 0). Another parameter that may be used to classify the fluorescent applicability of different molecules is the molar extinction coefficient (ε, $M^{-1}cm^{-1}$). Ideally, fluorochromes should exhibit high extinction coefficients, meaning that they have a higher ability to absorb photons at a particular wavelength.

Many different organic or inorganic fluorescent dyes are available. These are classified as biological (*e.g.* fluorescent proteins, etc.) or synthetic (*e.g.* fluorescein, fluorescent inorganic nanoparticles, etc.) depending on their origin and nature.

Since that in the current work only synthetic organic dyes were conjugated to the PAMAM dendrimer scaffold, only the basic concepts regarding this class of fluorochromes will be discussed. If additional information regarding other fluorescent dyes is desired, the further reading of the following references is recommended[91,110].

A large variety of organic dyes with distinct wavelength emissions can be commercially obtained covering the whole region of the UV-vis spectrum. Although a small number of organic aliphatic or conjugated double-bound structures exhibit fluorescence, the most common fluorescent organic molecules are the compounds that contain polycyclic aromatic systems. As a result, the most efficient and usual organic fluorochromes present a rigid and planar structure containing a multitude of conjugated π systems. Furthermore, the most commonly used dyes exhibit a typical molecular weight of ~250-1500 $g.mol^{-1}$.

While simple aromatic structures do not display high fluorescent activity, highly fused aromatic ring structures tend to exhibit strong molecular fluorescence. This phenomenon happens thanks to the characteristic electronic systems on the fused aromatic structures that cause a shift of the absorption/emission maximum into the visible region of the electromagnetic spectrum. Additionally, more rigid conjugated π systems tend to exhibit improved molecular fluorescence. The increased molecular rigidity decreases the rate of nonradiative relaxations, giving more time for the fluorescent relaxation to occur.

The most efficient organic fluorescent dyes present high ε and QYs along with Stokes-shifts that range from 20 to 40 nm. Some examples of organic dyes are presented in the Figure 52, including the one that was used in the current thesis for PAMAM dendrimer functionalization, the FITC.

As shown in the Figure 52, each organic dye is characterized by advantages and limitations. Thanks to the improved knowledge related with the fluorescent behavior of molecules, many fluorescent dyes with unique properties are currently available in the market. Some of them include special functional groups for an improved stability and a facile conjugation with dendrimers or biomolecules. Nonetheless, some of these dyes are still very expensive to obtain (> 200 € per mg).

Additionally in some cases, even with the best fluorochromes, the controlled and equivalent surface functionalization within each dendrimer is extremely difficult to achieve.

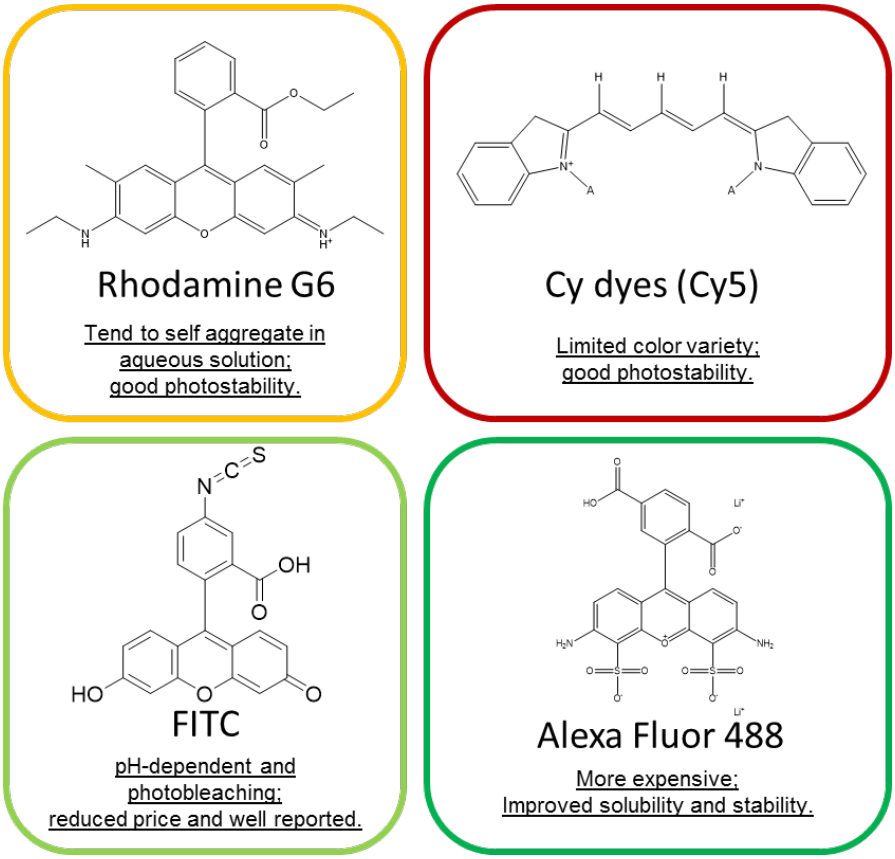

Figure 52 – Some of the most commonly used fluorochromes and the associated limitations/advantages.

Different types of instrumentation may be used for the analysis of dendrimer conjugates containing fluorescent moieties. Some examples explained below include fluorescence spectroscopy or microscopy.

In fluorescence spectroscopy, an emission spectrum is acquired mainly through the use of a spectrofluorometer. Similarly to the absorption spectrum in the UV-Vis analysis, the emission spectrum is built based on the different fluorescent relaxation transitions that are represented in the Figure 50. Likewise, the emission maximum corresponds to the transitions that are more probable to occur. Note that in the emission analysis, each fluorescent relaxation contributes for a single line in the spectrum, however due to the global effect of each individual relaxation processes along with the fluorochrome-solvent collisions (higher in polar solvents), a broader peak is obtained rather than the mentioned single lines[91,110].

Although the fluorescence spectroscopy is not a major qualitative technique, it can be used along with other techniques to predict the behavior of fluorescent dyes and their conjugates in specific conditions (*e.g.* effect of pH, buffers or metal ions or stability in the biological medium). For example,

Staneva *et al.* have reported the preparation of fluorescently labeled PAMAM dendrimers (see Figure 53A) that have the capability to act as sensors for metal cations (*e.g.* Ag^{2+}, Cu^{2+} or Fe^{3+}). Based on the spectroscopic analysis, the authors verified that in the presence of some metal cations, the fluorescent intensity increased in several orders of magnitude. Moreover, under distinct pH and solvent conditions the authors have shown that these fluorescent PAMAM dendrimers exhibited unique changes in the emission spectrum elucidating the possible use of these structures as sensors for the detection of metals or ions in solution[62,111].

The fluorescent spectroscopic analysis can provide important additional information over the UV-vis characterization, thanks to the impressive sensitivity of the most recent spectrofluorometers. The basic explanation behind such sensitivity is that while the absorbance is independent of the source intensity, in fluorescence, the radiant power that is emitted by the sample is strongly dependent of the source power[91,110].

Additionally, the fluorescence spectroscopy may be used along with other characterization techniques to assess the successful conjugation of fluorochromes into the dendrimer scaffold. However, it can only be done under optimal conditions and if the complete purification from the unconjugated dye is assured. Furthermore, fluorescence spectroscopy has also been applied to aid in the quantification of defects in dendrimers containing covalently bound fluorescent groups[91,110].

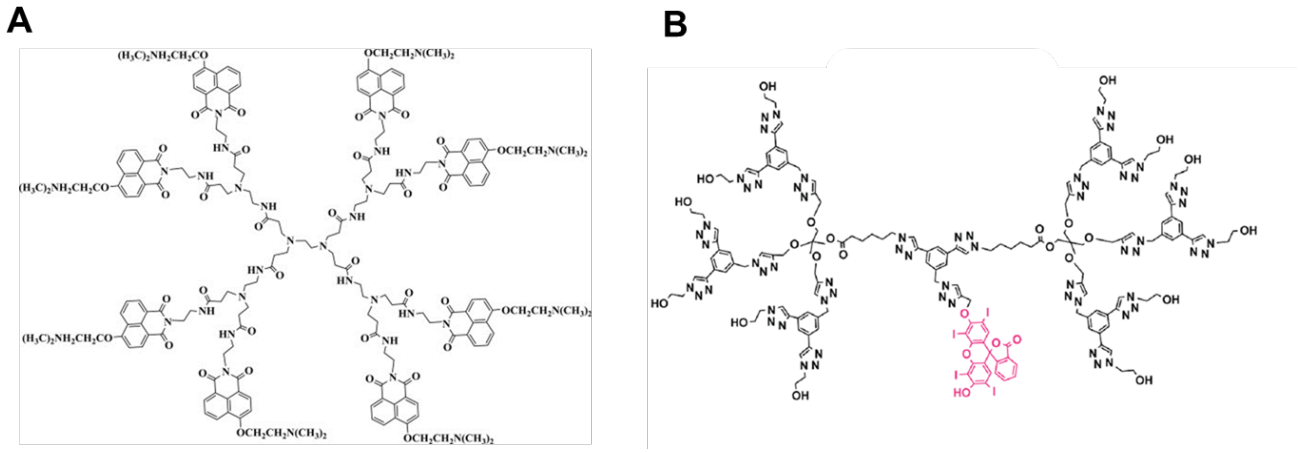

Figure 53 – Example of dendrimers containing fluorescent units: (A) G1 PAMAM dendrimer containing the fluorescent 4-N,N-dimethylaminoethyloxy-1,8-naphthalimide at the periphery, as reported by Staneva *et al.*; (B) the dendrimer structure containing the 2',4',5',7'-tetraiodofluorescein (TIF) coupled to the core as reported by Sharma *et al.* (Figure adapted from Refs. 111 and 114).

The fluorescence spectroscopy can also help in the characterization and determination of the fluorescent power of dendrimers presenting fluorescent units in the core, branching cells or at the periphery[112,113]. Recently, Sharma *et al.* have reported the successful preparation of multifunctional traceable dendrimers for drug delivery applications (see Figure 53B)[114]. The authors have reported the preparation of dendrimers containing the 2',4',5',7'-tetraiodofluorescein (TIF) coupled to the core.

Based on the spectroscopic analysis, the authors observed that these fluorescent dendrimers could be effectively used for cell studies since that no deep changes in the fluorescent activity of the TIF fluorochrome was observed after coupling. Moreover, the authors also verified that, after conjugation, a red shift in the absorption maximum of the conjugated TIF (~ 10-20 nm) could be detected and used to differentiate from the unconjugated fluorescent dye[114]. Similar observations have been done for other dendrimer-fluorochrome conjugates, including the FITC[115,116].

Furthermore, the emission spectrum has also been applied to exploit the quenching power or to investigate the surface crowding during generational growth of some dendrimer families[62]. Also, other fluorescence techniques have been recently used to smartly identify possible morphological changes in dendritic structures upon a range of temperatures[117].

The fluorescence microscope can be primarily applied to preview the behavior of the dendrimer-fluorochrome conjugates in an intact biological medium before using more complex techniques. Basically, the fluorescence microscopy uses an optical microscope that takes advantage of analytes containing fluorescent units. In this type of microscopy the analyte is excited by an incident source of radiation (*e.g.* mercury arc lamp) where the emitted fluorescence is then "optimized"* in order for the fluorescence light to reach the observer or electronic detector[110].

A preliminary analysis of the cellular trafficking of dendrimer conjugates containing fluorescent units may be followed based on the microscopy observations (especially with higher resolution techniques like confocal microscopy). As a result, the coupling of fluorescent units to a nonfluorescent dendrimer scaffolds can serve as a useful tool to understand the cellular fate of dendrimers specifically designed for drug or gene delivery[118–121]. For example, based on the microscope visualization along with other characterization techniques it was found that PAMAM dendrimers tend to exhibit intrinsic fluorescent activity under specific aging conditions (*e.g.* action of molecular oxygen present in the air or heat), due to the existence of amide resonance structures[109,122,123].

1.4.5. Surface Charge and Zeta potential

When in ionic solutions, the dendrimers possessing a net-charge will be surrounded by a strongly bound layer of counter ions (*i.e.* Stern layer). As the distance from the dendrimer surface increases, a second layer of loosely bound counter ions is also present. This set of two ionic layers is usually referred as electrical double layer.

As the dendrimers move in solution (*e.g.* due to Brownian motion), a potential is observed between the second layer (slipping plane) and the ions dispersed in the medium. This potential is known as zeta-potential (ξ, expressed in mV) and it is characterized to decay exponentially as the

*Note that the fluorescence is emitted in all directions, however only a small fraction is "selected" through a light cone. A set of high quality optical filters is then used to give rise to an "optimized" final image.

distance from this boundary increases (see Figure 54). By this way, the determination of the zeta-potential is a plausible method to characterize the surface charge of the dendrimer scaffold.

Moreover, the determination of the zeta potential can also provide useful information regarding the stability of the dendrimers in solution. Usually, when the ξ value is not sufficient enough to produce repulsion forces capable of surpassing the kinetic energy that arise from the particle collisions, agglomeration may occur through Van der Waals interactions, indicating poor stability in the analyzed conditions. As indicative values, usually dendrimers and other particles presenting ξ values superior to + 30 mV and inferior to - 30 mV, show improved stability than the structures with ξ within this range[124,125].

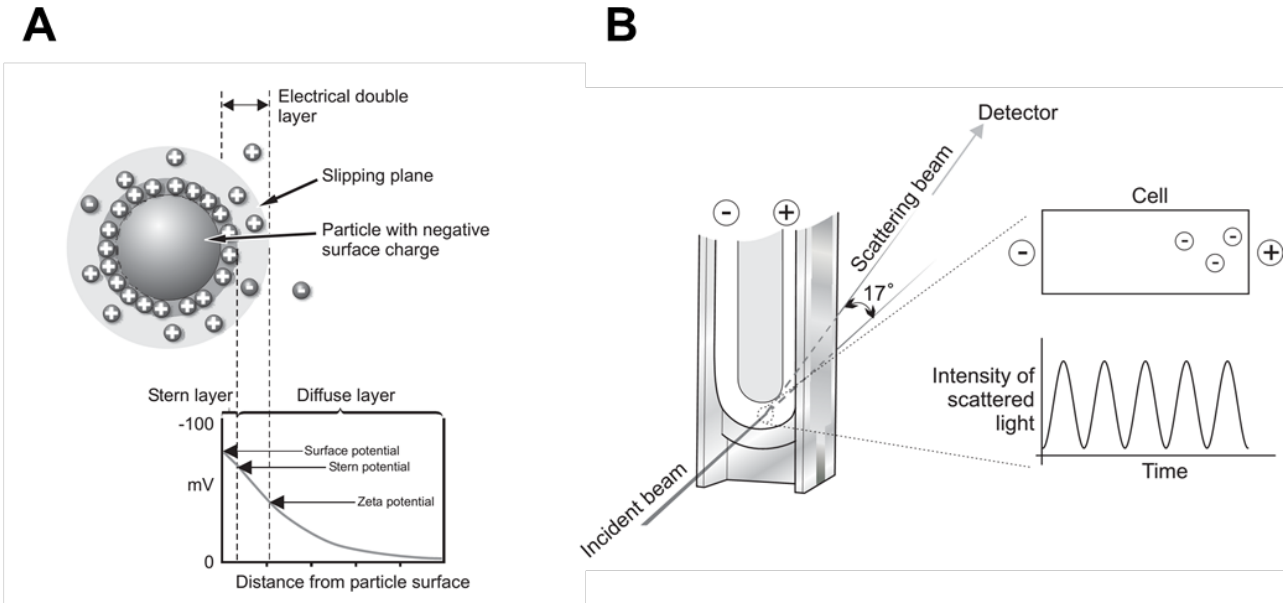

Figure 54 – Schematic representation of (A) the zeta potential boundary and (B) its determination through an incident laser and based on the electrophoretic mobility of the particles in solution (Figure adapted from Ref. 126).

In the zeta potential measurements, the final value, in mV, is not a product of the direct surface charge measurement but rather a determination of the particle movement. After placing the sample in a capillary cell and under optimal conditions, an electrical field is applied across the whole sample. This potential will force the particles in solution to move to the electrodes of opposite charge. As a result, this movement of the dispersed particles, called electrophoretic mobility, is measured based on the scattering of an incident laser (see Figure 54) and converted into ξ through a mathematical formula (Henry equation)[125,126].

It is important to note that the ξ does not only depend of the dendrimer surface charge but also on the properties of the dispersing solution (*e.g.* pH, ionic strength, viscosity, impurities, sample concentration). For example, while the quantity of ions in solution has an impact over the density

charge around the dendrimer surface, the pH has a strong influence on the shape and net-charge of some dendrimer families. Additionally, the ξ measurement of the dendrimer conjugates (*e.g.* functionalized with drugs or fluorochromes) is a way to predict the behavior and stability of these conjugates in solution (*e.g.* biological medium)[125,127].

As an example, at physiological pH conditions (pH ~ 7.4), the PAMAM dendrimers may exhibit distinct ξ values depending on the surface functionality. The PAMAM dendrimers with primary amine end groups exhibit a positive ξ since that most of end groups are protonated at pH 7.4. On the other hand, the PAMAM dendrimers with carboxyl terminal units are characterized by a negative ξ due to the ionization level of the terminal units at physiological pH. Moreover, in both cases, the ξ value is greater for higher generations, since that the number of terminal groups also increases. Additionally, the PAMAM dendrimers containing hydroxyl terminal units exhibit almost neutral ξ values, under the same conditions, due to the partial protonation state of the end groups[36,128].

It is worth to mentioning that the interior amides of the PAMAM dendrimer scaffold are also strongly dependent on the pH of the dispersing medium. For example, as the pH of the medium decreases the interior tertiary amines start to protonate leading to molecular expansion and shifting the ξ to more positive values[129].

1.4.6. Purification techniques

In order to obtain a complete and unequivocal characterization of the synthesized dendrimers or related conjugates, it is essential to assure that the final products are free of by-products or unconjugated chemical moieties. Several separation and purification techniques have been successfully reported as useful approaches for the removal of by-products from the final dendrimer structures. Some examples include: chromatographic techniques, electrophoretic separation, dialysis or ultrafiltration[2,12,16,62,130].

In the current thesis, two distinct purification techniques were explored with the intention of removing as much as possible the secondary products (*i.e.* unconjugated dye and unreacted coupling agents) from the final dendrimer-FITC conjugates. As a result, only the techniques that were applied in the current work will be effectively discussed below. If a better understanding of other purification techniques is desired, we recommend the further reading of the following works[2,12,16,62,87,88,131].

Despite the great efforts accomplished until today for the purification of dendrimer products, we defend that this subject is still lacking of a more methodological and standardized approach. As we will see later on, in some cases many of the reported purification methods are not so efficient for the complete removal of by-products from the final dendrimer structures or conjugates. Additionally, many of the commercially available dendrimers are not completely free of structural defects or by-products (see Figure 55). As reported by several research groups, commercially available PAMAM dendrimers

may exhibit missing arms, dimers or trailing generations which can increase even further the difficulty of an efficient conjugation or complete purification of final dendrimer products[88,130,132].

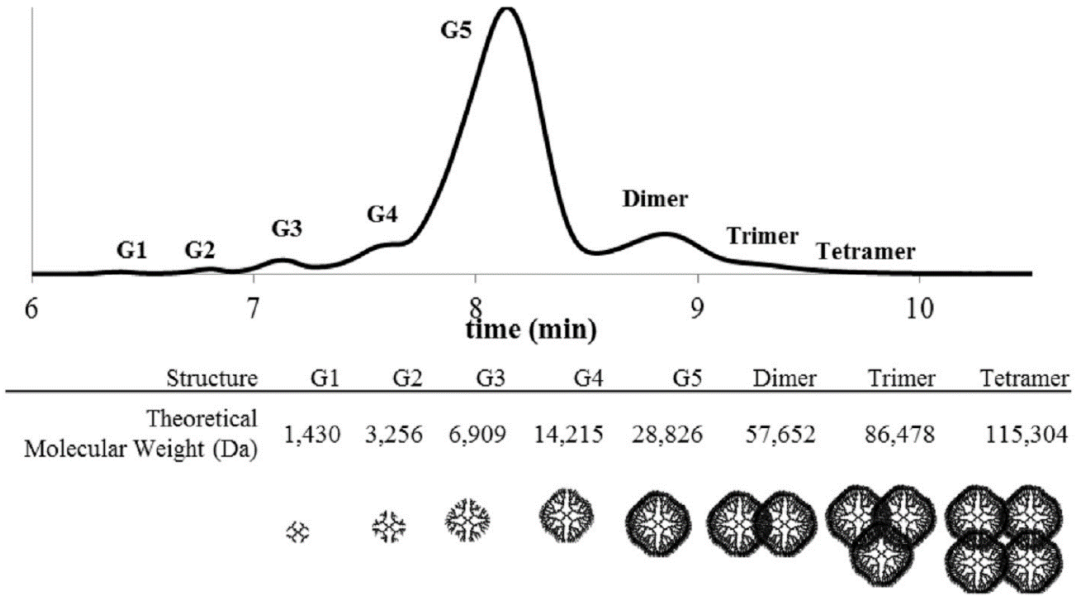

Figure 55 – Chromatographic analysis of commercial G5 PAMAM dendrimers (Figure adapted from Ref. 132).

A) Dialysis

The separation of small molecules from biological macromolecules through dialysis has been widely used for several years in the biochemistry field. As mentioned before, since that high generation dendrimers usually exhibit a very high molecular weight, the membrane separation through dialysis has also been largely applied for the preliminary purification of dendrimers from low molecular weight impurities[98,133–136].

The dialysis separation occurs in size and time-dependent manner. Briefly, the solution containing the sample is placed inside a semi-permeable membrane that will be in contact with a "buffer" (i.e. dialysate) that is in several order of magnitude greater in volume than the sample volume.

The degree of the membrane permeability should be properly selected depending on the material to be purified. Currently, many different kinds of membranes with distinct pore-sizes (cut-off between 100-100 000 D) and chemistries (*e.g.* cellulose ester or regenerated cellulose) are commercially available. As a result, depending on the membrane pore-size, molecules with high MW will be retained, while molecules with an MW below the membrane cut-off will freely pass in both directions. The concentration of smaller molecules between the sample and the dialysate will define their diffusion through the membrane pore in a time-dependent manner (see Figure 56). Consequently, due to the existence of an osmotic pressure gradient, the small molecules will mainly

move from regions of high concentration to low concentration gradients (Flick's Law). Usually, through this approach up to 90%* of the sample is recovered and successfully separated from smaller molecules.

For an optimal separation, a continuous change of the dialysate is essential to assure the continuous diffusion of the impurities throughout the membrane and prevent the by-product concentration equilibrium in both sides of the membrane.

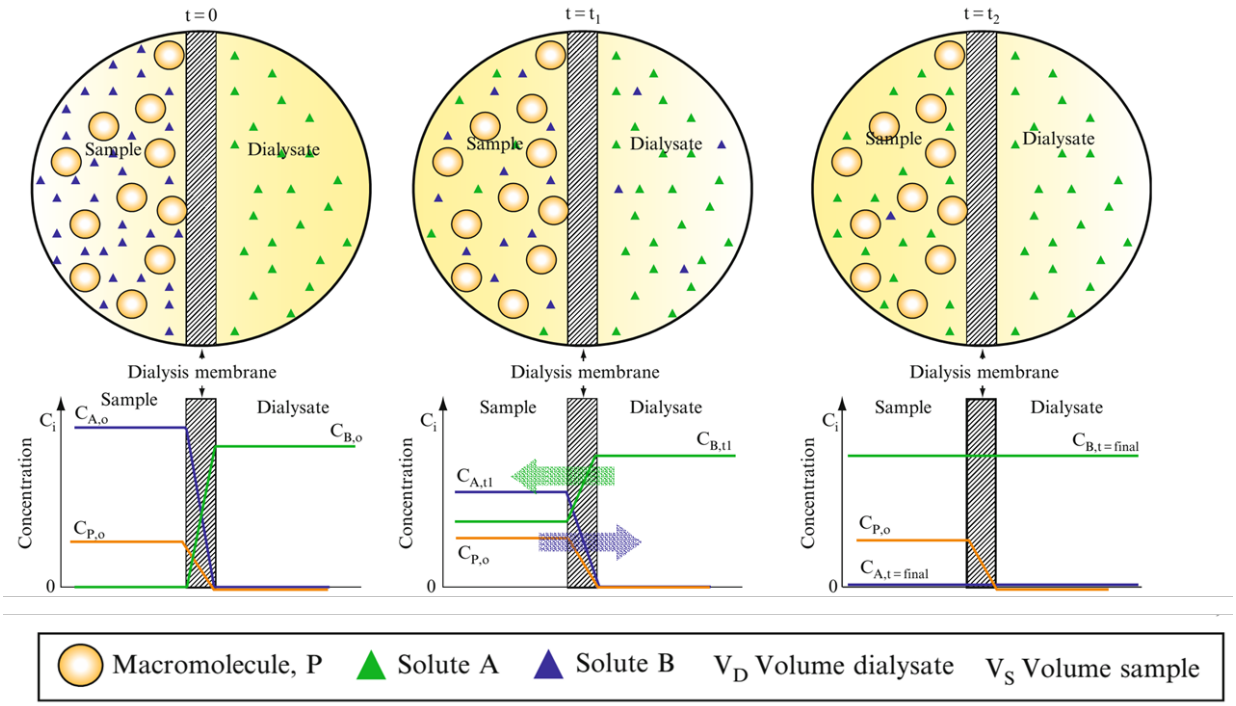

Figure 56 – Time-lapse of molecular separation by dialysis: at t=0, the sample is placed in a container where V_D is much higher than V_S; after some time (t_1), the molecules with a MW below the membrane cut-off (blue) can freely pass through the membrane from regions of higher concentration gradient (inside the membrane, left side) to lower ones (dialysate, right side). Note that small molecules from the dialysate will also move in the opposite direction into the membrane; at the final phase of the dialysis (t_2) since that V_D is much higher than V_S the impurities are present at almost undetectable levels (Figure adapted from Ref. 137).

Several factors may influence the separation efficiency and the acquisition of a stable product. As a result some of the parameters that should be taken into consideration during dialysis are: (a) ideal diffusion time for separation, which is highly dependent of the membrane area, temperature, viscosity, sample concentration or ionic strength; (b) membrane chemistry and its resistance to the dialysate; (c) set-up of the dialysis system (*e.g.* higher dialysate volumes result in improved separation; moreover, the dialysate flow around the membrane may also help in the separation)[137].

Although dialysis does not assure the complete removal of by-products from dendrimer conjugates, it is a facile and simple technique that may be followed as a preliminary approach for the

*There is always an associated sample loss, *e.g.* sample adsorption in the membrane.

purification. Additionally, this technique does not require extreme chemical or physical conditions which may be ideal for the initial purification of more sensitive dendrimer conjugates containing drugs or fluorescent dyes. Contrary to the linear polymers, the dialysis has been largely applied for the purification of dendrimers since that no reptation is observed, especially in the case of the higher generation globular dendrimer structures[2,137].

Since that in most of the cases, a complete purification cannot be achieved by dialysis, a conjugated set of purification methods (*e.g.* chromatography) are applied in order to improve the purity of the final dendrimer conjugates. It is also worth to mention that the dialysis separation is usually verified with the aid of other analytical techniques like thin layer chromatography (TLC), mass spectrometry (MS), NMR, fluorescence or UV-Vis spectroscopy.

B) Chromatography and the Size-exclusion chromatography (SEC)

The chromatography refers to a collective set of separation methods that rely on the physical individualization of each chemically distinct component that may be present in a mixture. This separation is accomplished through a set of equilibrium processes between the mobile and the stationary phase. In liquid chromatography, the sample is dispersed into a liquid medium (mobile phase) that will pass through a stationary phase (this process is termed elution). The further elution of the mobile phase with the aid of gravity or pressure will promote the movement of the sample throughout the stationary phase.

The degree of differential partitioning between the mobile and stationary phases will define the retention time of the components existing in a mixture and cause their separation (see Figure 57). Mainly, sample molecules that interact more strongly with the stationary phase will be retained longer that the ones that interact less. As a result, if a proper detector is placed at the end of the stationary phase, a graphical representation may be obtained (chromatogram) and provide useful information regarding the analyte concentration as a function of time (retention time).

Different types of chromatographic techniques may be use for separation (see Figure 58), where the main distinction between them relies on the way that the samples are eluted and on physicochemical nature of the mobile and stationary phases. For example, the mobile phase may be liquid or an inert gas depending if liquid or gas chromatography are used, respectively. In contrast, the stationary phase can be packed in either a column or planar surface in the case where column or layer chromatography is applied, respectively. The physicochemical nature (*e.g*. polarity, composition, column diameter or pore-size or temperature) of both phases may be tuned in order to provide improved separation of the individual sample components.

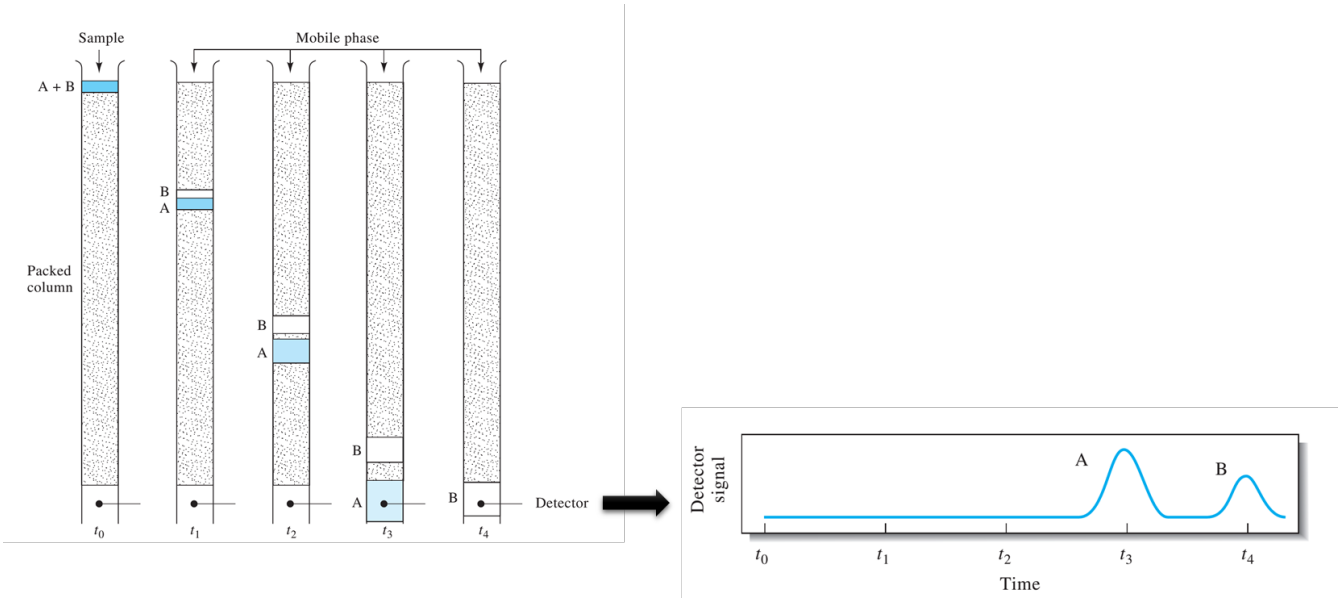

Figure 57 – An example of a chromatographic separation where the stationary phase is packed inside a column. The analytes A and B that were initially together (t = 0), are progressively separated during their elution. Since that analyte B had a greater affinity with the stationary phase, it stayed longer inside the column than A. If a detector is placed at the end of the column a chromatogram can be obtained (Figure adapted from Ref. 91).

In chromatography, the separation can be done with two different objectives: (a) preparative or (b) analytical. In the preparative chromatography, the goal is to separate the different components of a mixture for further application or characterization. On the other hand, in the analytical chromatography, smaller amounts of sample are used with the main objective of identifying and quantifying the individual components of the mixture.

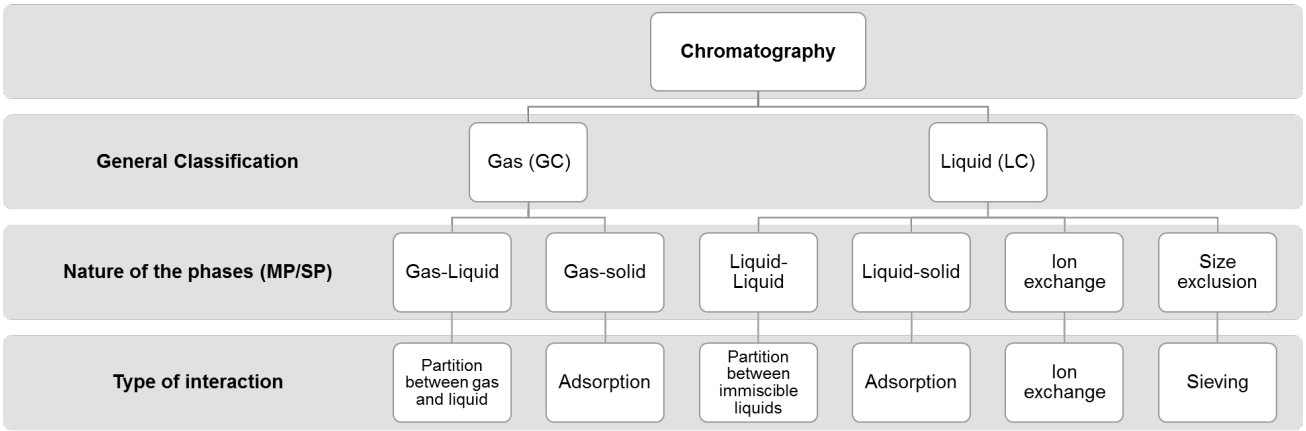

Figure 58 – Schematic representation of the different chromatographic techniques (Note: GC = Gas Chromatography; LC = Liquid Chromatography; MP = Mobile Phase; SP = Stationary Phase) (Figure adapted from Ref. 91).

Any of the chromatographic techniques may be coupled with a multitude of other analytical techniques (*e.g.* spectroscopic or spectrometric) allowing the immediate identification and quantification of the mixture components right after their separation.

For a better understanding of the different chromatography techniques, we recommend the further reading of the following references[91,138–140].

Many different types of chromatographic techniques have been successfully applied in the dendrimer chemistry. Some examples include the quantitative and qualitative analysis of the functionalization or solubility degree of PAMAM dendrimers through LC coupled with MS or UV-Vis[141,142]. Other novel applications comprise the quantitative study of the PAMAM dendrimers present in the urine[143] or even the use of some dendrimer families as stationary phase for the ion-exchange separation of biomolecules[144].

Usually, the efficient separation of higher generation dendrimer samples is mainly accomplished through high-performance liquid chromatography (HPLC) since that structures with high molecular weight are very difficult to volatilize and, as a result cannot, be separated through GC[12]. It is worth mentioning that since the dendrimer surface mainly defines its interaction with the stationary phase, the polarity of the end groups should be taken into consideration in order to achieve a successful separation from the secondary products. For example, if the polarities of the dendrimer end-groups and stationary phase are too similar a strong retention may occur in which can hamper the successful elution of the dendrimer[2,12].

Several works have reported the use of a preparative approach for the purification of dendrimers or dendrimer conjugates. For example, preparative LC has been widely applied for the purification of dendrimers since that it allows the loading and separation of large samples (> 1 g). Additionally, thin-layer chromatography (TLC) is routinely used during dendrimer conjugation or synthesis, since it allows the facile and preliminary identification of impurities.

Another facile and widely used approach for the purification of dendrimer is by size-exclusion chromatography (SEC). In this separation method, the packing of the column is composed by a well-defined and uniform porous polymeric gel (*e.g.* dextran - Sephadex™). The SEC is characterized as a sub-type of liquid chromatography that allows the separation of dendrimers from by-products mainly based on the differences of their molecular sizes in solution (*i.e.* hydrodynamic volume). Contrary to the traditional chromatographic techniques, in SEC the dominant factor for a successful separation is the molecular size and not the affinity to the stationary phase.

The SEC separation may be accomplished in different ways depending on the set-up used to perform the purification. Mainly two types of SEC set-ups can be used, containing: (a) high-pressure columns or; (b) high-throughput columns. In recent years, many works have focused in the purification of dendrimers based on the use of high-throughput SEC columns since that the separation is faster and simpler. However, it is important to note that a more efficient separation is usually achieved based on the use of high-pressure SEC columns.

Currently, many different types of SEC columns are commercially available with distinct packing chemistries and pore sizes. The selection of the proper column depends on the size of the molecules to be separated and on the elution conditions[139].

The separation through SEC occurs based on the use of a mobile phase containing the sample that will pass through the porous column. As a function of the column pore size, large molecules will pass through the interstitial spaces of the pores, while smaller molecules will penetrate into the pores and be temporarily retained inside the column. By this way, since that the dendrimers exhibit a high molecular size, they do not penetrate into the pores of the column and as a result they are generally eluted first than the small molecular size contaminants (see Figure 59). As a result, this strategy may be applied for the separation of dendrimer conjugates from unconjugated fluorescent dyes or drugs that are usually much smaller[145,146].

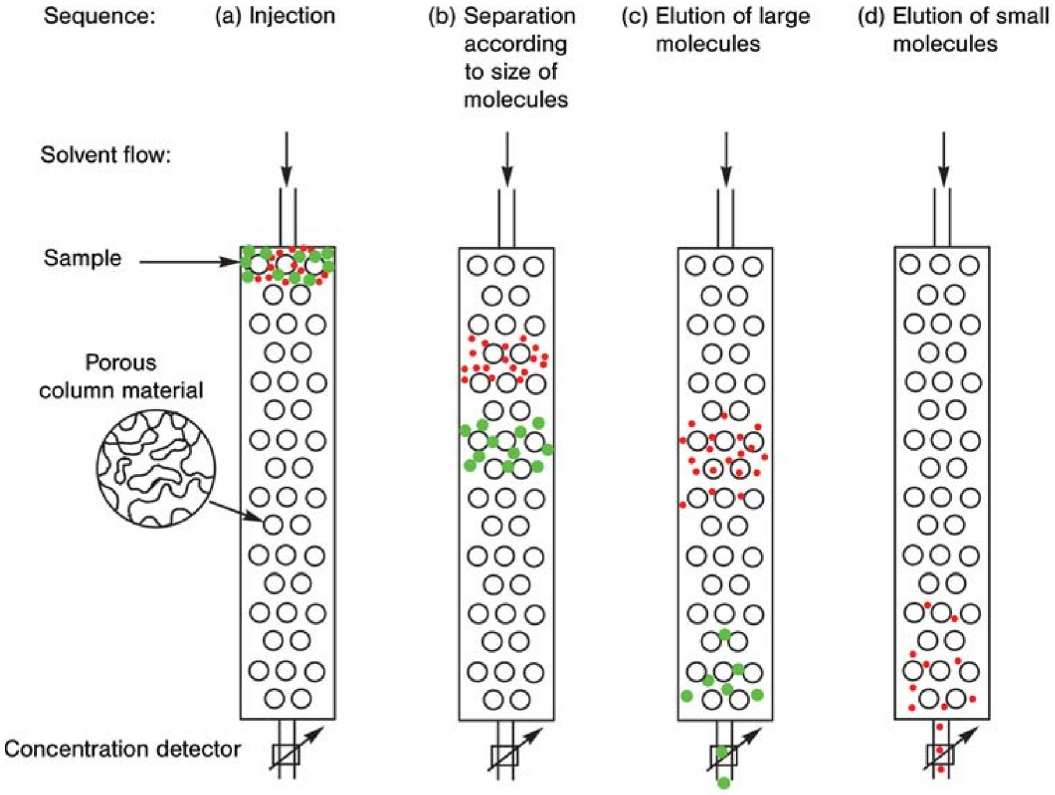

Figure 59 – Schematic representation of dendrimer purification through SEC (Figure adapted from Ref. 12).

Ideally, if a detector (*e.g.* fluorescence or UV/vis) is placed at the end of the column, it can provide useful information regarding the elution time and by this way allow the collection of the ideal fractions containing the purified dendrimer product. Provided with the proper detector, the SEC may also be used for the molecular-weight (MW) characterization of different dendrimer generations. This technique may also be useful for the removal of residual monomers or highly defective dendritic

structures that are usually present in the divergently synthesized dendrimers. Note however, that dendrimers with low degree of defects cannot be removed through SEC since that their hydrodynamic volume is relatively similar to the defect-free dendrimers[12,139].

1.5. Physicochemical properties of dendrimers

In the current section, some of the unique physicochemical properties of dendrimers and especially the ones that can be applied for cargo delivery to cells (*e.g.* drugs) will be explored. Moreover, since that the studies of the current thesis relied on the use of PAMAM dendrimers, we will give a more detailed perspective regarding this dendrimer family. Additionally, the PAMAM dendrimers are currently the most widely explored dendritic structures in the literature. The main reason behind this is that they were the first dendrimers to become commercially available at high generations (until 11th), and their synthesis is relatively simple and inexpensive. Although with some limitations, the PAMAM dendrimers exhibit exceptional physicochemical properties that are specific to this dendrimer family, and that can be exploited for several applications, including in the biomedical field[2,12,13,147].

Before describing the specific physicochemical properties of dendrimers it is important to understand in the first place this new era of nanoscale pharmaceuticals and clarify the position of the dendrimers in this new “nanoperiodic” paradigm.

A) Dendrimers in nanomedicine and the new “nanoperiodic” paradigm

The primordial pharmaceutical era relied on the exploitation of the physical and chemical properties of basic elements or sub-nanoscale molecules. Mainly, the successful design of biologically active drugs depended on the manipulation of parameters specifically associated with this class of elements or molecules. Such parameters were widely described as “critical atomic/molecular design parameters” (CADPS/CMDPs) and were mainly used to define the ideal molecular compositions and architectures for an improved interaction with the biological systems.

With the recent developments in the preparation and characterization of nano-sized materials, highly complex nanostructures with unique physicochemical properties started to emerge in which have led to the identification of new critical hierarchical design parameters (CHDPs). This new set of parameters started to be described as “critical nanoscale design parameters” (CNDPs) and relied not only on the composition and architecture but also on other physicochemical properties as flexibility, surface chemistry, shape or size (see Figure 60). The introduction of these new CNDPs provided important insights for the manipulation of such parameters with the intention of preparing bioactive nanostructures[58,148].

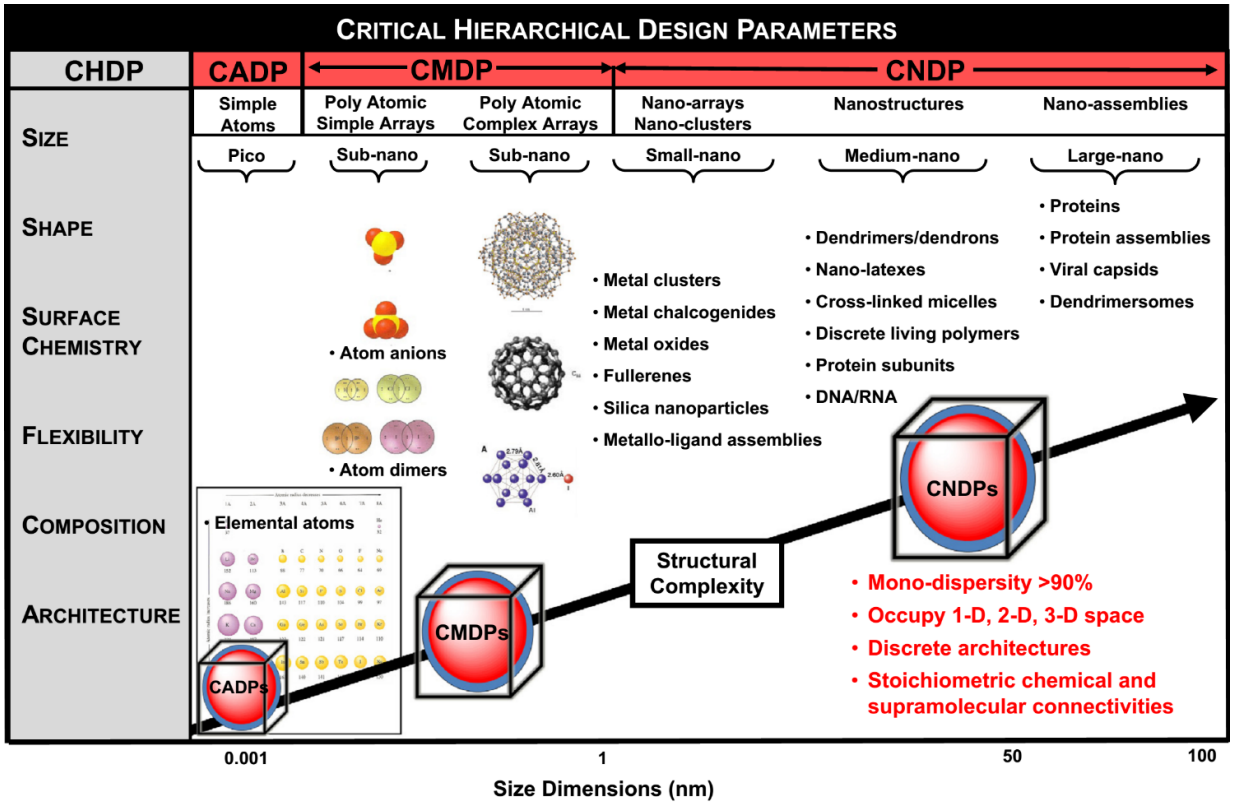

Figure 60 – The critical design parameters associated with the preparation of new bioactive compounds at each specific scale. The controlled synthesis of nanostructures (like dendrimers) have required the manipulation of parameters such as size, shape, surface chemistry or molecular flexibility (Figure adapted from Ref. 58).

The appearance of unique physicochemical properties associated with these novel nanoscale materials resulted in the need to define a new nanoperiodic system in analogy to the well-known Mendeleev's periodic table. The traditional periodic system has been largely used for the determination of powerful periodic patterns and predictive principles that were needed for design of the traditional pharmaceuticals. As a result, the introduction of a new nanoperiodic table could provide useful information for the structure-controlled synthesis of nanomaterials.

Basically, the introduction of dendritic structures like the dendrimers, have contributed for a whole new level of structural control that could not be attained in the traditional molecular structures. Until then, such degree of structural control could only be observed in the biological systems where highly efficient mechanisms are capable of producing extremely complex nanoscale structures from picoscale building-blocks. Currently, a mimicry of such structural control can be achieved for a multitude of synthetic materials at the nanoscale (*e.g.* fullerenes, dendrimers, metal nanoparticles and many others)[2,58].

Furthermore, the ability to manipulate the CNDPs along with the creation of a nanoperiodic system could allow a better understanding of the physicochemical properties that rule the synthetic nanostructures, including the dendrimers. With the developments made in the last decade in that way,

the “nanoperiodic concept” started to involve, by allowing the preparation of highly complex nanostructures with well-defined size, shape, surface chemistry, composition or flexibility. The development of this concept will be fundamental for the application of dendrimers and other nanostructures in the biomedical field since that it will allow the prediction of the ideal functions and properties (*i.e.* toxicity or pharmacokinetics) that are required for this type of applications.

With the introduction of different dendrimer preparation methods, we can see that the synthesis of such complex structures follows the universal CHDPs. Based on a hierarchical assembly of the individual building blocks (*i.e.* branch cell monomers) the preparation of highly complex multifunctional structures can be achieved[58].

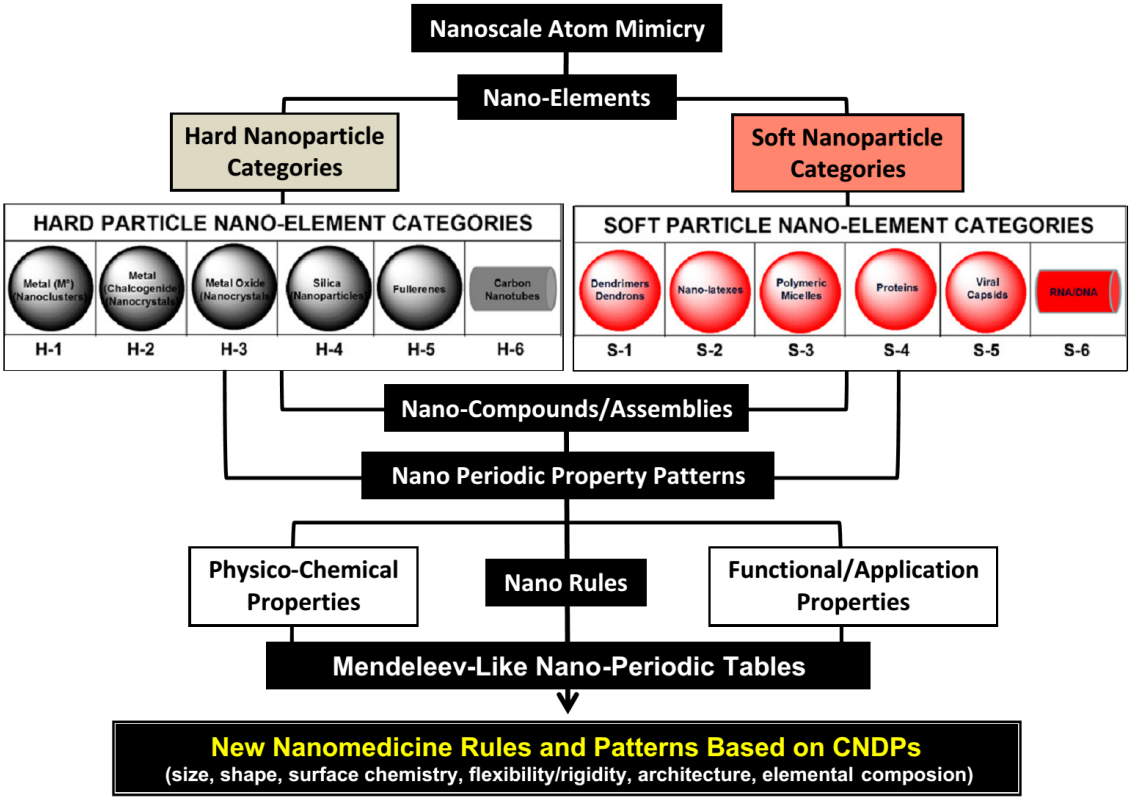

Figure 61 – The nanoperiodic concept built from the application of hard/soft building blocks. More complex structures are formed based on the stoichiometric hierarchical assembly of the individual building blocks. Note that the nature of the building blocks that is ruled by distinct CNDPs, will define the ultimate physicochemical properties of the final structure (Figure adapted from Ref. 58).

Based on the hierarchical assembly, the use of hard or soft building blocks that mimic elemental atomic units are applied to build a multitude of nanostructures. Referred as “superatoms” these individual hard/soft building blocks give rise to more complex structures that can be organized into distinct nanoelemental categories. As shown in the Figure 61, the dendrimers are built based on the stoichiometric assembly of soft building blocks resulting in nanostructures with unique physicochemical properties that are distinct from the other nanoelemental categories. As a result, the

building blocks applied during the nanomaterial preparation will define the physicochemical properties and consequently its possible applications[2,58].

B) PAMAM dendrimers: Size, Shape and Multifunctionality

The nano-size and unique shape of dendrimers can be exploited for multiple applications, especially in the biomedical field[15,48]. For example, the nanosize of the dendrimers provides a way of passive targeting, leading to a reduced non-specific toxicity of conjugated drugs[149].

Additionally, the ability to prepare multifunctional dendrimers with distinct generations provides a larger set of dendrimer scaffolds that contain well-defined sizes, shapes and terminal groups. For example, it was recently reported that dendrimers presenting slight changes in their size exhibit selective organ affinity and distinct renal/liver clearance properties[58,150].

Furthermore, several works have shown that thanks to the dendrimer nanosize and shape, a unique pattern in terms of cellular uptake, transport and bioaccumulation can be observed *in vitro* and *in vivo*[16,58,149].

Due to the high-molecular weight and shape of some dendrimer families, they may be used to mimic biomolecules like proteins. Besides of these two similar properties, both, dendrimers and proteins also contain exposed terminal groups that provide additional functionality. For example, the G5 PAMAM dendrimer exhibits a similar size and shape to hemoglobin. Moreover, PAMAM dendrimers at other generations also exhibit similar shapes and sizes to other biomolecules as the cytochrome C or insulin (see Figure 62)[4,16,147].

Given the shape similarities between the PAMAM dendrimers and proteins, several approaches have been explored in order to produce dendrimer scaffolds that mimic several biological processes as the angiogenesis or the tooth regeneration of hydroxyapatite[147]. For example, recent works have shown that PAMAM dendrimers containing carboxylic acid terminals along with alendronate (ALN) shown improved capability for the in situ remineralization of the human tooth enamel thanks to the improved capability to absorb the hydroxyapatite crystals[151].

Although the dendrimers possess great morphological similarities with globular proteins, they also show some important differences. The proteins are quaternary structures formed through the folding of simpler linear proteins. Due to the nature of this folding (mainly of non-covalent nature), the proteins are usually sensitive to even slight changes in the medium (*e.g.* pH or temperature), which can lead to deep morphological changes (denaturation). On the other hand, the dendrimers are more robust structures being mainly formed through covalent bonding and with a mathematically defined size and number of terminal groups[147].

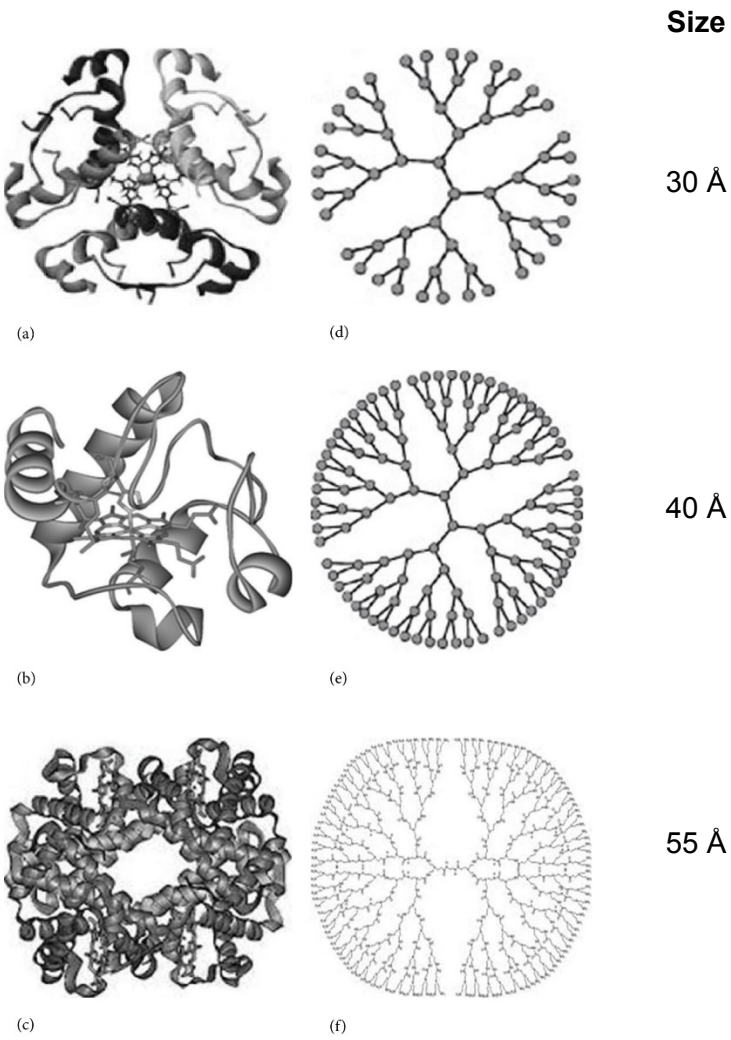

Figure 62 – Size and shape relationship between the G3 (d), 4 (e) and 5 (f) ammonia core PAMAM dendrimer and the following biomolecules (a) insulin, (b) cytochrome c and (c) hemoglobin. As shown, the degree of packing increases with the dendrimer generation (Figure adapted from Ref. 147).

Some dendrimer families can be tuned during their synthesis with variable cores or surface functionalities. As described in the section 1.3, the PAMAM dendrimers are an example of this situation where they can be prepared with distinct cores (*e.g.* ethylenediamine (EDA); cystamine core and many others) or terminal groups. Commonly, the full-generation PAMAM dendrimers are synthesized with primary amines (-NH_2) or hydroxyl (-OH) terminal groups. On the other hand, the synthesis of the PAMAM dendrimers can be halted at half-generations resulting in scaffolds with carboxylic acid terminal units. However, many other surface functionalities can be introduced during the PAMAM synthesis and in which are commercially available. Some examples include: N-2-hydroxydodecyl, trimethoxysilyl, tris(hydroxymethyl)amidomethane or 3-carbomethoxypyrrolidinone terminal groups (see Figure 63).

The impressive multivalence of the commercially available PAMAM dendrimers provides unique physicochemical properties in terms of solubility and reactivity. For example, by preparing PAMAM dendrimers with distinct terminal groups it is possible to obtain structures with the desired surface

charge. The ability to play with the surface charge provides another way to selectrivelly control the cellular fate of the dendrimer scaffold.

Moreover, the specific reactivity of the different terminal groups allow the conjugation with an almost unlimited number of other guest moieties including drugs, fluorescent dyes, nanoparticles, polymers or biomolecules (*e.g.* antibodies, DNA or RNA).

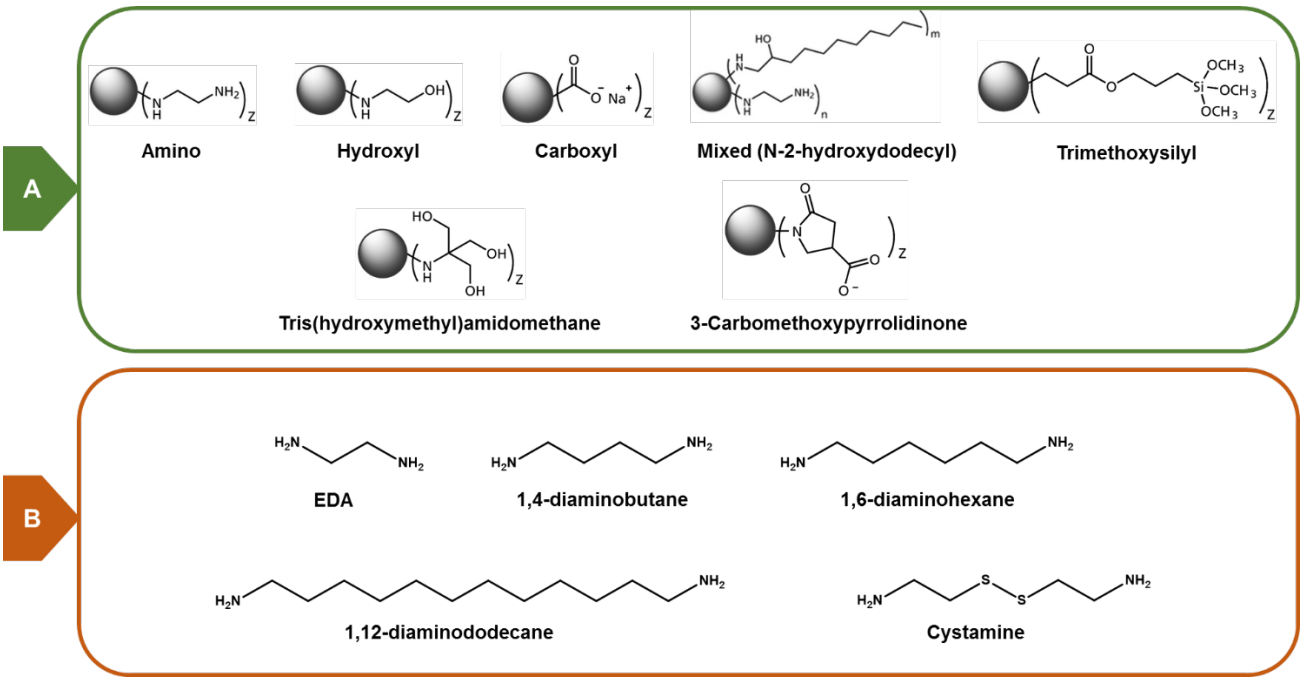

Figure 63 – The surface functionalities (A) and the cores (B) that may be introduced during the preparation of PAMAM dendrimers and that are commercially available. Note that the cystamine is a biologically cleavable core which may have useful applications in the biomedical field.

Another incredible set of possible applications may arise from the conjugation of PAMAM dendrimers with other chemical identities (*e.g.* gene/drug delivery, MRI contrast agents, many others). For example, the ability to change the surface nature (*i.e.* charge or polarity) by the covalent or non-covalent coupling with other molecules, provides a unique way to control the cytotoxic and hemolytic effect of some terminal groups.

The conjugation between the primary amine groups of the PAMAM dendrimers with polyethylene glycol (PEG) or carbohydrate units is one of the ways to reduce the cytotoxic effect of this dendrimer scaffold. The conjugation of PEG with PAMAM dendrimers has become one of the most widely approaches for surface functionalization since that it provides improved water solubility, biocompatibility and the capability to tune the dendrimer biodistribution[16,133,149,152,153]. For example, Cai *et al*. explored the antimicrobial activity of G5 PAMAM dendrimers where about 43% of the amines were “protected” with PEG. The authors found that while the antimicrobial activity against gram-negative bacteria was high (EC_{50} = 0.9 – 1.5 μg/mL), the toxicity to the eukaryotic cells was still low at the same concentration levels[154].

The terminal groups and shape of the PAMAM dendrimer scaffold can also be exploited for the passive or targeted delivery of drugs. As mentioned in the section 1.2, the shape can be tuned based not only on the generation but also by the preparation of PAMAM dendrimers with cores containing distinct natures (see Figure 63).

In the case of active targeted delivery, the optimal terminal groups are selected for an efficient conjugation with drugs and targeting moieties (*e.g.* folic acid; octreotide; RGD containing peptides; riboflavin; transferrin; or endogenous growth factors). As we shall see later on, depending on the generation and nature of the end groups distinct uptake pathways may contribute for the cell internalization of the PAMAM dendrimers[155,156].

In the passive targeted delivery, the shape and nanosize of PAMAM dendrimers can be explored for a selective diffusion of dendrimer-drugs and enhanced retention in the tumor sites (enhanced permeation and retention effect, EPR*). Additionally, by playing with the dendrimer surface charge and functionality it is possible to design PAMAM dendrimers capable of avoiding the reticulum endothelial system (RES) resulting in a reduced macrophage uptake and improved delivery to the desired tissues, other than the immune system[16,147–149,153,157].

Thanks to the ability of the PAMAM-NH_2 dendrimers to condensate the DNA† and act as buffering agents, they may be used as platforms for gene delivery. While the buffering capacity of the PAMAM dendrimers may facilitate the endosomal escape of the dendriplex (*i.e.* proton sponge effect), the condensation ability promotes the cell internalization of the genetic material and its protection from degrading conditions (*e.g.* pH or enzymes)[158]. Recently, Lee *et al.* have reported an enhanced gene transfection based on the use of PAMAM dendrimers containing a nuclear localization signal peptides[159].

Moreover, the conjugation of terminally distinct PAMAM dendrimers with fluorescent moieties (*e.g.* FITC, Py-5, dansyl chloride) or with radiodense magnetic nanoparticles can be exploited to understand the dendrimer cellular fate or be used as MRI contrasts agents respectively[107,115,128,145,160,161].

Table 3 exemplifies some of the bioactive agents/drugs already conjugated/loaded with the PAMAM dendrimers.

Although the library of molecules that can be conjugated with PAMAM dendrimers is great, there are some limitations associated with the post-functionalization. As reported by Holl *et al.* the uniform post-functionalization of all dendrimers in a sample is very difficult to achieve (especially through the traditional approaches, see section 1.6). For example, the authors verified the calculation of a mean value was very far from the true functionalization degree. By functionalizing the G5 PAMAM

*Profound differences between the normal and the tumor tissue allow the use of PAMAM dendrimers as passive targeting agents. The anomalous vasculature in the tumor site leads to an improved permeability of the endothelial lining due to the existence of gaps in the order of 600-800 nm. Moreover, the poor lymphatic drainage also leads to a prolonged accumulation of the dendrimers in the tumor sites.
†The nature of the PAMAM-DNA interaction is mainly electrostatic.

dendrimers with several ligands, the authors observed that the obtained mean of 12.9 ligands per dendrimer was not the best estimation of the sample, since that 27 different species were found in the final product. Interestingly, the authors found that while some dendrimers were not conjugated with any ligand, others contained about 26 ligands. Consequently, they also found that the post-conjugation of additional ligands increased even more the heterogeneity of the dendrimer sample[13,162].

Besides of the surface multivalency, the interior of PAMAM dendrimers is characterized by the existence of void spaces that can be further explored for the encapsulation of a multitude of chemical moieties. Through this approach, it is possible to improve the solubility of hydrophobic drugs in physiological conditions. Also the non-covalent encapsulation of bioactive compounds, may provide a way for improved cell delivery by facilitating the cell internalization and protection the cargo from possible sources of degradation (*e.g.* enzymes). Furthermore, since that the shape of the PAMAM structure is dependent of the surrounding conditions (*e.g.* pH or temperature) the release of hydrophobic drugs can be controlled based on such parameters. Similarly, the introduction of PEG chains at the surface can also be applied for the controlled release of the dendrimer encapsulated drugs[52,149,163].

Likewise, the physical entrapment of high atomic density metal nanoparticles into the dendrimer scaffold have been explored as possible MRI contrast agents[136,164].

Table 3 – Summary table describing some of the bioactive agents/drugs already conjugated with the PAMAM dendrimers. An extensive list with more examples can be found in the references 52 and 149.

Application	Bioactive agent/Drug	Role of the dendrimer
Gene delivery	DNA/siRNA	Complexation
Antibody conjugates	Antibody	Binding
Transdermal delivery	Indomethacin	Permeation enhancer
Ocular delivery	Pilocarpine & Tropicamide	Vehicle
Oral delivery	Niclosamide	Solubility enhancer
Colon delivery	5-Aminosalicylic acid	Carrier
Topical Gels	Nifedipine	Solubility and permeation enhancer

The conjugation/encapsulation of selective chemical moieties into the PAMAM dendrimer scaffold can also be useful for the preparation of electrochemical biosensors. Recently, a huge number of research groups have dedicated their work for the development of highly efficient electrodes containing PAMAM dendrimers for an improved detection of specific biomolecules (*e.g.* DNA or proteins)[165–171]. The development of such biosensors may provide another way for the early detection of diseases[147]. Recently, Kasovi *et al.* reported the preparation of an electrochemical

immunoassay system based on the covalent immobilization of PAMAM dendrimers containing gold nanoparticles. The authors have shown, that this system was ultrasensitive for the detection of the cancer biomarker α-fetoprotein. Additionally, the authors defended that the great conductivity of the PAMAM-Au nanocomposites along with their large surface area, provided the crucial elements for an improved electrochemical performance[172].

Finally, as referred in the previous paragraphs the dendrimers exhibit unique physicochemical properties as a function of their size/generation. The term collectively used to define this unusual property in the dendrimer structures is called “dendritic effect”. Usually, the dendritic effects are considered positive or negative depending if a specific property is enhanced or reduced along each generation. Some clear examples of such effects are the differences in the dendrimer shape, solubility or encapsulation ability along each generation (see Figure 64).

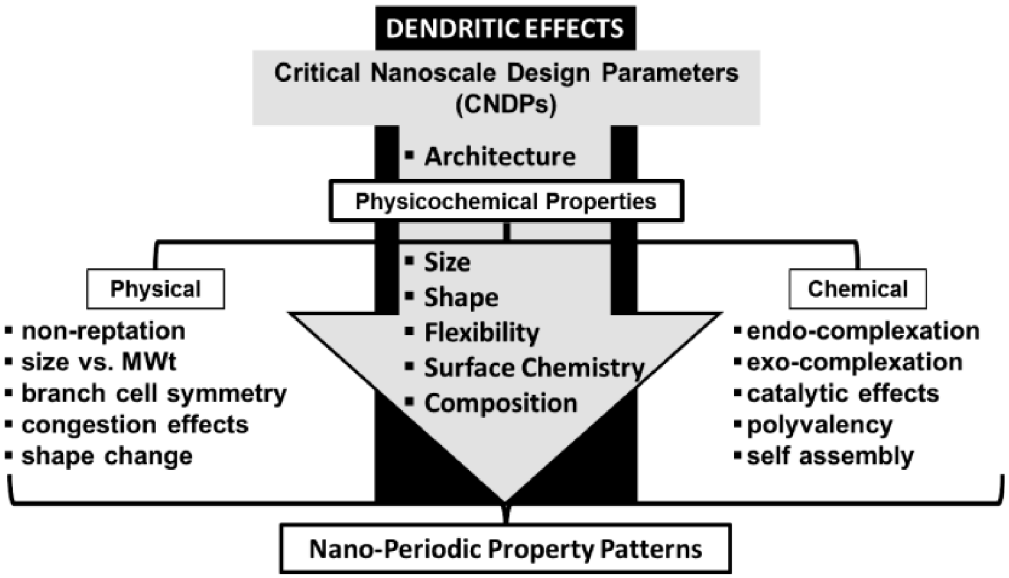

Figure 64 – Relationship between the special physicochemical properties of dendrimers and their design considerations (Figure adapted from Ref. 2).

The Figure 64 establishes a relationship between the CNDPs and the effects observed in the previous paragraphs. For example, the branch cell monomers that produce highly symmetric dendritic structures usually facilitate the endo-complexation of drugs. Moreover, the flexibility of the end groups affects the degree of functionalization with targeting molecules or drugs. Overall, the PAMAM dendrimers exhibit a generation dependent loading capability, cytotoxicity, cell internalization or biodistribution[2,163].

The PAMAM dendrimers and many others dendrimer families have been used beyond the biomedical field. Many of the dendritic effects have been exploited for other applications as environmental sensors, biofuel cells or catalysis[173–175]. For more information regarding further

applicability of PAMAM dendrimers in other areas we recommend the reading of the following references[2,12,59].

1.6. Methods of conjugation of chemical identities to the PAMAM dendrimer scaffold

As already depicted in the previous section, the stable coupling of drugs, fluorescent dyes or any other chemical moieties into the dendrimer scaffold can be accomplished mainly in two ways: (a) non-covalent encapsulation or; (b) covalent/non-covalent surface functionalization. The non-covalent interactions are mainly of the type hydrophobic, dipole-dipole, electrostatic or van der Waals forces. The Figure 65 summarizes this set of possible interactions that can be exploited for the conjugation of chemical moieties into the PAMAM dendrimer scaffold[25,163,176,177].

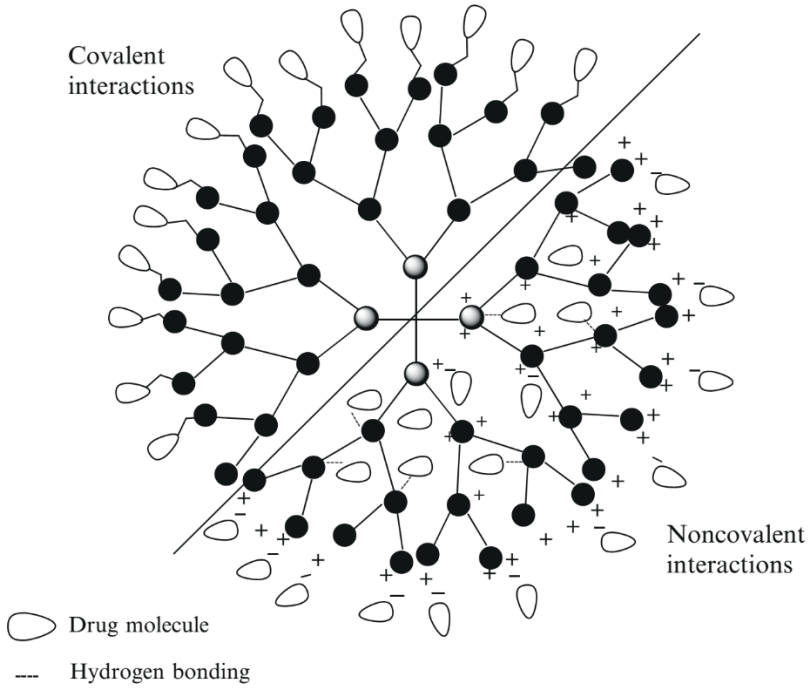

Figure 65 – Interactions that may be exploited for the loading of drugs, fluorescent dyes or any molecule of interest in the PAMAM dendrimer scaffold (Figure adapted from Ref. 25).

The introduction of a specific functionality to the dendrimer scaffold can be accomplished during (pre-functionalization) or after (post-functionalization) the dendrimer synthesis. In the pre-functionalization, only the chemical functionalities that exhibit acceptable stability and solubility can be employed during the synthetic process. On the other hand, on the post-functionalization approach, sensitive species that cannot be coupled during the synthetic conditions, may be introduced in a “convergent-type” strategy through a library of many different coupling chemistries. In either approach, depending on the way that the functionalities are organized at the dendrimer surface they

can be classified as random, block or alternate. Note that, depending on the conjugation conditions, not only small molecules can be incorporated but also larger structures may be coupled (*e.g.* another dendron containing distinct functionalities)[63,176,177].

In the recent years, many different types of chemistries and novel functionalization techniques were described in the literature. Considering that the approaches used in the current thesis relied on post-functionalization chemistries (mainly "stochastic" and based on molar ratios), only this type of functionalization methods will be discussed below. For further information regarding other functionalization methods, we recommend the further reading of the following review article[63].

The "stochastic" conjugation/encapsulation of several functionalities to the dendrimer scaffold provides a cost-effective and "easy" way to prepare multipurpose architectures that can be used for several applications. However, in most of the cases the unequivocal synthesis and characterization of such structures prepared by stochastic methods may be difficult to achieve. Some of these limitations come from the difficulty to obtain an uniform distribution of the diverse functionalities along each dendrimer scaffold or due to the problematic purification of the final sample containing many by-products. Usually, such heterogeneity arises due to the molar excess of ligands in comparison to the dendrimer scaffold. As shown in Figure 66, this stochastic functionalization proceeds with a very limited control[63]. Moreover, when using this post-functionalization approach and given the degree of heterogeneity, the conclusions related to its biological applicability must be carefully made. For example, Baker *et al.* have shown that a uniformity in terms of functionality is essential to attain reproducible biological results[178].

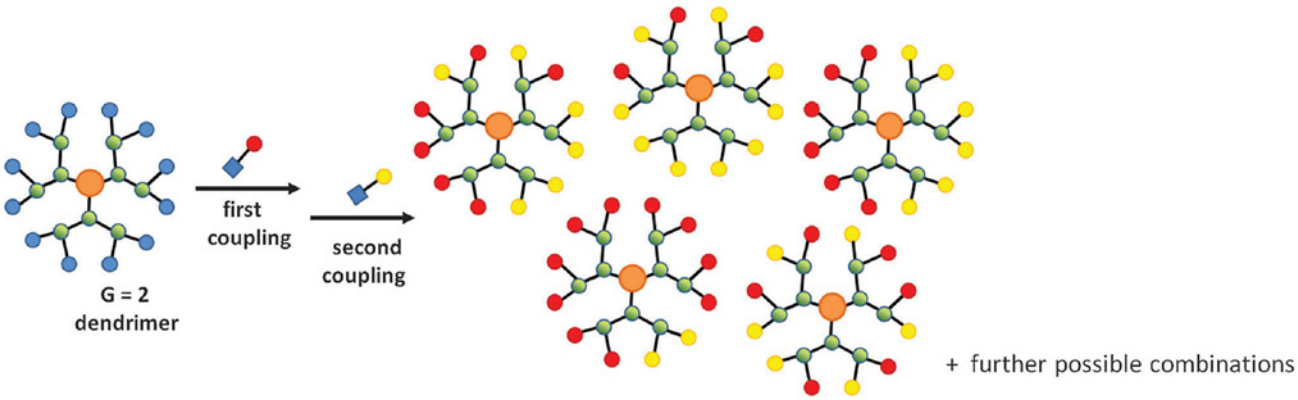

Figure 66 – Schematic representation of the stochastic functionalization of dendrimers. The greater the number of couplings, the higher will be the sample heterogeneity (Figure adapted from Ref. 63).

In contrast to the traditional post-functionalization methods, some novel methods provide a better control over the functionalization pattern within the dendrimer sample. Some examples include pre-functionalization approaches through the convergent assembly of dendrons containing distinct but well-defined functionalities or through the use of orthogonal chemistry pairs that promote a more selective post-functionalization (see Figure 67). Additionally, other post-functionalization approaches

include the controlled protection/deprotection steps allowing a selective modification of the terminal groups[63].

Although the novel approaches offer a better control in terms of functionalization, they usually require more complex and laborious techniques when compared with the traditional stochastic functionalization methods.

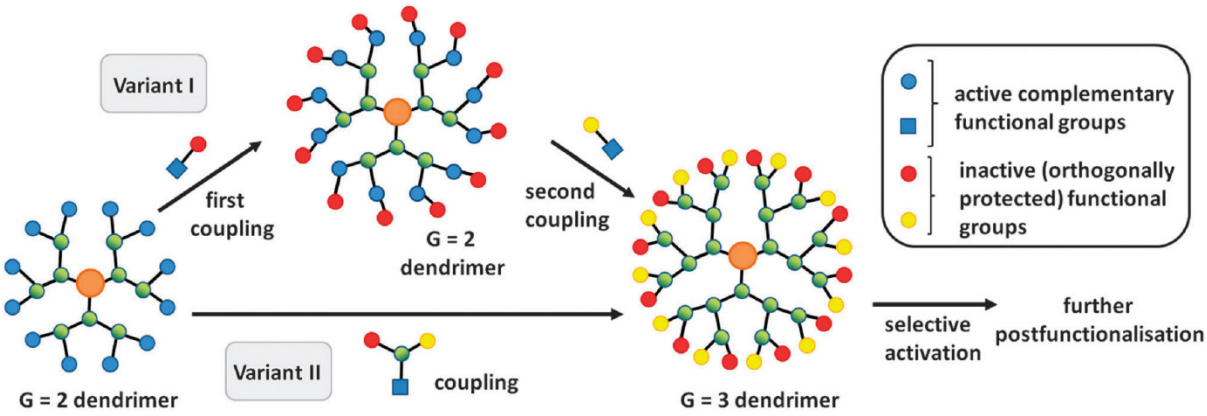

Figure 67 – Several strategies for a controlled functionalization of the dendrimer scaffold (Figure adapted from Ref. 63).

Independently of the functionalization approach, the covalent or non-covalent conjugation can be applied depending on the intended application and the nature of the dendrimer scaffold.

The non-covalent interaction of chemical functionalities is usually accomplished taking into advantage the nature of the dendrimer and the ligand, along with the possible interactions that they may establish. This strategy is mainly used to improve the solubility of hydrophobic drugs or to promote the molecular condensation for the protection of the cargo (*e.g.* DNA).

In the case of PAMAM dendrimers, the hydrophobic tertiary amines in the interior promotes the non-covalent inclusion of drugs, while that the hydrophilic surface improves the drug solubilization[25].

Moreover, since that PAMAM-NH_2 dendrimers contain a positive net-charge under physiological conditions, the condensation of DNA can be accomplished. Mainly this condensation occurs based on the electrostatic interaction between the negatively charged phosphate groups of the DNA and the positively charge primary amines of the dendrimer. This type of functionalization can be exploited to build non-viral vectors for gene delivery[179].

Due to the nature of the non-covalent functionalization, the sucessful conjugation of molecules with the PAMAM dendrimer scaffold is strongly dependent on several factors, including the dendrimer generation size and concentration, nature of the branching units and terminal groups, pH, ionic strength or temperature[25]. In contrast with the traditional covalent methods, the controlled functionalization through the non-covalent conjugation may be even more difficult to achieve[177].

The covalent coupling of chemical identities onto the dendrimer surface or branching points has been widely reported in the literature. Besides of drugs and fluorescent dyes, other molecules have

also been coupled through covalent conjugation including specific cell targetting ligands or radioligands. It is worth mentioning that the successful covalent conjugation depends essentially of two factors:

(i) the steric crowding of the dendrimer surface groups; *e.g.* PAMAM dendrimers of higher generations (> G5) are more difficult to functionalize due to the limited accessibility of the terminal groups; moreover the size of the ligand to be coupled can also limit the degree of conjugation;

(ii) type of the dendrimer surface functionality and ligand functionality should allow an easier coupling without the need of many reaction steps.

The covalent conjugation methods have been widely applied in order to achieve an improved functionalization of ligand payload with the desired stability. For example, the covalent attachment of drugs with predefined cleavable linkers (*e.g.* amides, esters, etc.) has been exploited for the controlled release of drugs under disease-specific environmental conditions (*e.g.* enzymes, pH, light, etc.).

The covalent coupling of molecules to the dendrimer scaffold can be accomplished: (a) directly; (b) through the use of spacers/cross-linkers that promote or improve the conjugation between the dendrimer terminal units and the molecules of interest. Moreover, some commercially available dendrimers are designed with internal groups that allow the covalent conjugation in the interior of the dendrimer[176,177].

Note that depending on the intended application, the necessary functionalization degree of the dendrimer scaffold may vary.

For example, for the targeted delivery of PAMAM dendrimers functionalized with folic acid (FA), the interaction kinetics with the folic acid receptors (FAR) is related with the functionalization degree of the dendrimer scaffold. Nevertheless, recently Holl *et al.* reported the successful preparation of homogenous monovalent FA-G5PAMAM conjugates where the authors found that a unique interaction between the dendrimer conjugate and the FAR could be observed. These findings disapproved previous observations that claimed the need of high functionalization degrees of FA with PAMAM for an improved interaction[146].

Another example is related with the fluorescent labeling of the dendrimer scaffold. The extensive conjugation of the PAMAM dendrimers with an unnecessary number of fluorescent moieties may result on undesired modifications of the dendrimer surface nature or lead to fluorescence quenching due to the great proximity of functionalized terminal groups[176,177].

The functional units of the PAMAM dendrimers and the molecules to be coupled will define the different strategies that may be followed for the covalent conjugation. Some traditional examples include the formation of distinct types of bonds such as amide, ester, thiourea or ether. Some of the different conjugation chemistries involve: (i) reductive amidation; (ii) cross-linkers (*e.g.* Sulfo-NHS family; EDC; DCC) or (iii) epoxy activation[176,177].

The use of biodegradable spacers is also another way to improve the conjugation of a drug with the dendrimer and ensure its effective release in the biological environment under specific conditions (*e.g.* action of enzymes). Moreover, in some cases the application of a spacer between the fluorescent dye and the dendrimer is recommended in order to reduce the possible energy transfer between both structures and minimize quenching effects[180,181].

The Figure 68 provides some insights regarding the versatility level of the PAMAM dendrimers terminal groups and the corresponding functionalization possibilities.

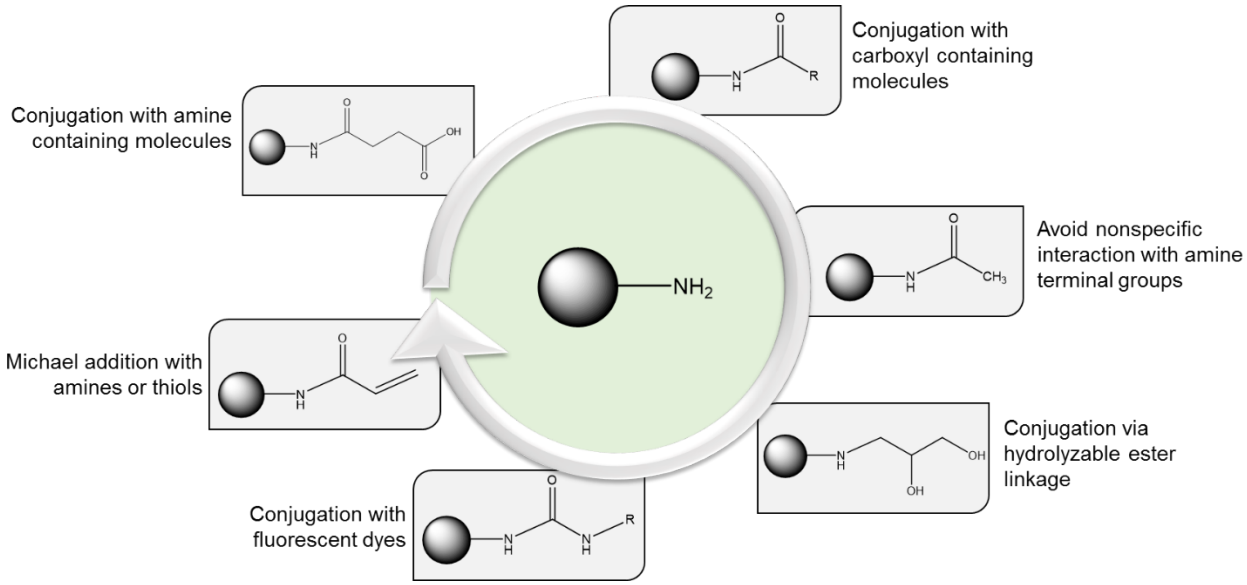

Figure 68 – Possible surface modifications of the PAMAM-NH_2 dendrimers terminal groups (Figure adapted from Ref. 182).

As we shall see later on, different strategies were used in the current thesis in order to proceed with the functionalization between the PAMAM dendrimers, containing distinct terminal groups (-NH_2; -COOH; -OH), and the fluorescent dye, FITC.

1.7. The cell membrane interactions and internalization pathways of PAMAM dendrimers

Firstly, in order to understand the interaction of the PAMAM dendrimers with the eukaryotic cells it is essential to have in mind the basic functional units that characterize this type of cells. As a result, in the next paragraphs we will give some insights regarding the membrane nature of the eukaryotic cells and the several mechanisms that may contribute for the cell internalization of the PAMAM dendrimers.

The cell membranes are the basic structural and functional units of the cell that are essential for life. For example, the plasma membrane is responsible for defining the boundary between the internal (cytosol) and the external cell environments. Even inside the eukaryotic cells, several

organelles contain similar cell membranes that are important to separate and maintain the characteristic differences of each organelle from the cytosol. As shown in the Figure 69, all cell membranes are composed by a dynamic and fluid phospholipidic bilayer that along with other biomolecules (*e.g.* proteins) are fundamental to accomplish a multitude of specific functions. For example, some of the plasma membrane proteins are responsible for the transmission of vital signals from the extracellular medium into specific intracellular targets. On the other hand, a distinct set of functional proteins have the capability to specifically define ion gradients along the membranes and promote the movement of vital solutes between the two sides. All the components of the eukaryotic cell membranes all mainly held by a set of non-covalent interactions (*e.g.* hydrophobic, dipole-dipole).

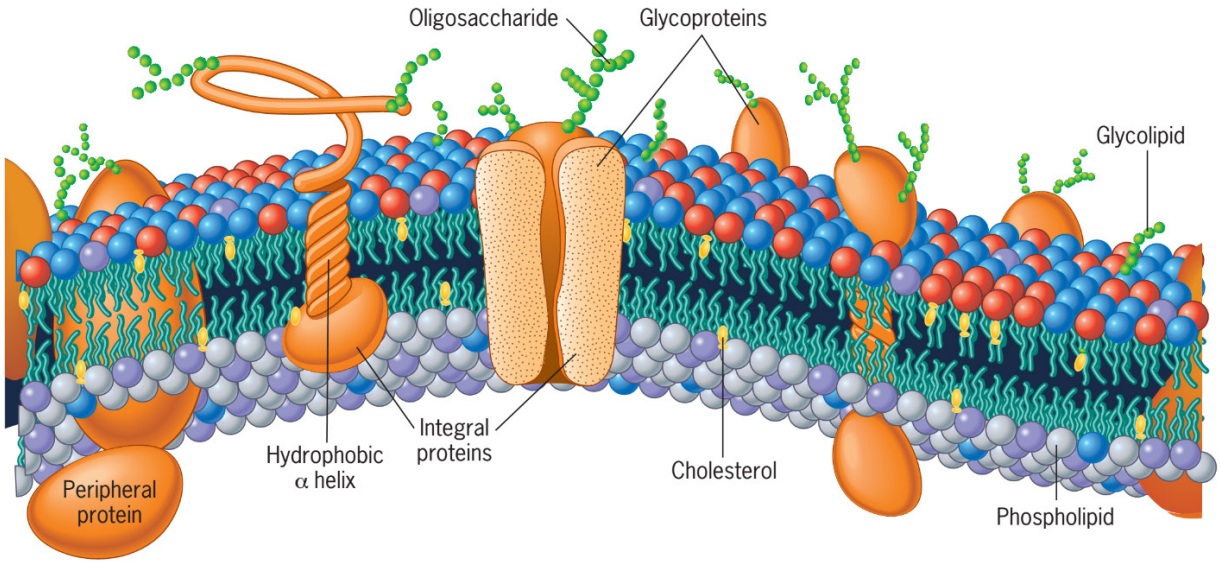

Figure 69 – Generic representation of the cell membrane (*e.g.* plasma membrane) composition: as shown, the external layer (upper), is composed by a fraction of proteins and phospholipids that contain covalently bound sugar chains (*i.e.* glycoproteins and glycolipids). Moreover, the phospholipidic bilayer also contains different types of lipids where the outer layer may exhibit microdomains ("rafts") with clusters of specific lipid species (red) (Figure adapted from Ref. 183).

Specifically, the plasma membrane is ~5-10 nm wide and is mainly responsible for acting as a selective barrier between the extracellular and the intracellular mediums. Note that the lipids that form the plasma membrane are amphipathic, exhibiting a hydrophilic "head" and a hydrophobic "tail" (see Figure 70). As a result, due to the nature of the membrane interactions and its hydrophobic "interior", the plasma membrane has the capability to selectively block the passage of high molecular size water-soluble molecules. On the other hand, the proteins that cross the lipid bilayer mediate all the other cell membrane vital functions. Some of these functions include the transport of hydrophilic molecules across the membrane or the communication between neighboring cells. Due to the

functional diversity of these proteins, almost 30% of the eukaryotic genome encodes membrane proteins with a distinct set of roles[183–185].

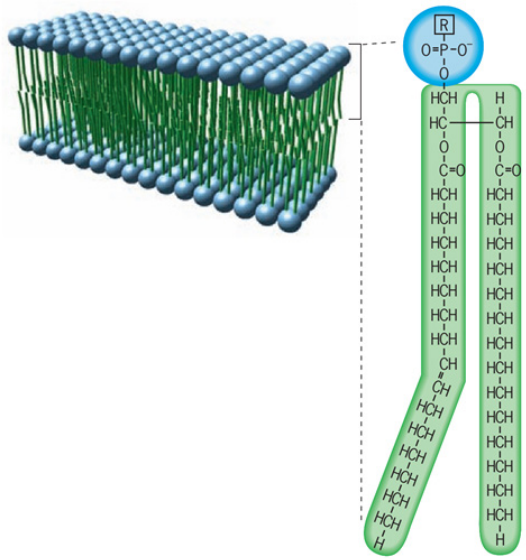

Figure 70 – The nature the cell membranes lipid bilayer. Due to the amphiphilic nature of these lipids, they establish a set of non-covalent interactions where the hydrophilic groups stay exposed to the interior/exterior of the cell and the hydrophobic tails face each other. Since that, most of the membrane lipids contain a phosphate group (blue) and are built from a glycerol backbone (R) they are referred as phospholipids or more precisely as phosphoglycerides. Other major classes of lipids that also compose the cell membrane are mainly the sphingolipids and cholesterol. Although in low quantities, the cholesterol, for example, is important to keep the fluidity of the membrane at an optimal level (Figure adapted from Ref. 183).

Due to thermodynamic factors and under normal conditions, the hydrophobic part of the lipid bilayer is never exposed to the extracellular medium that is usually in aqueous solution. For this reason, the cell membranes are known for its continuum and edge-free structures.

Interestingly, different types of eukaryotic cells exhibit unique profiles in terms of their plasma membrane lipid composition (*i.e.* distinct tail chains or backbones). As a function of this lipid diversity, it is expected that they contribute for a distinct set of functional capabilities like the definition of the physical state of the membrane (*e.g.* fluidity, flexibility, stability) or the ability to provide specific precursors that regulate the cell function.

The unique flexibility and fluidity of the cell membranes are two of the most important physicochemical properties of these cell structures.

The fluidity given by its lipid composition at physiological conditions, is a perfect way to provide a balance between a rigid/ordered structure and a lower viscosity that is essential for the movement of cell cargo along the membrane. For example, the special fluidity of the membrane allows the movement and assembly of proteins at specific points of its structure in order to accomplish specific time-space actions (*e.g.* cell division). As a result, depending on the surrounding conditions (*e.g.*

temperature) the cells have the capability to change their membrane lipid composition in order to provide an optimal fluidity level while maintaining its structural organization.

On the other hand, the natural flexibility of the cell membranes, allow them to change their overall shape during fundamental cell processes (*e.g.* locomotion, cell division or endocytosis/exocytosis) without compromising their structural function[183–185].

Due to the asymmetric distribution of different types of lipids along the plasma membrane, the composition of the inner and outer layers is usually distinct. Mainly, while the phosphoglycerides/sphingolipids that comprise the outer layer are the phosphatidylcholine (PC) and sphingomyelin, respectively, in the inner layer the phosphatidylethanolamine (PE) and phosphatidylserine (PS) are the dominant phosphoglycerides. Moreover, it is defended that such heterogeneous distribution of the lipids provide greater structural stability to the membrane and regulates the localization of proteins that are involved in several cellular processes including the endocytosis. Given the physiological pH conditions and the nature of the PS headgroups, the cytosolic "leaflet" for the plasma membrane is characterized by a negative charge[183,186].

For a better understanding, the Figure 71 summarizes the most common components of the plasma membrane and the main functionalities associated with them.

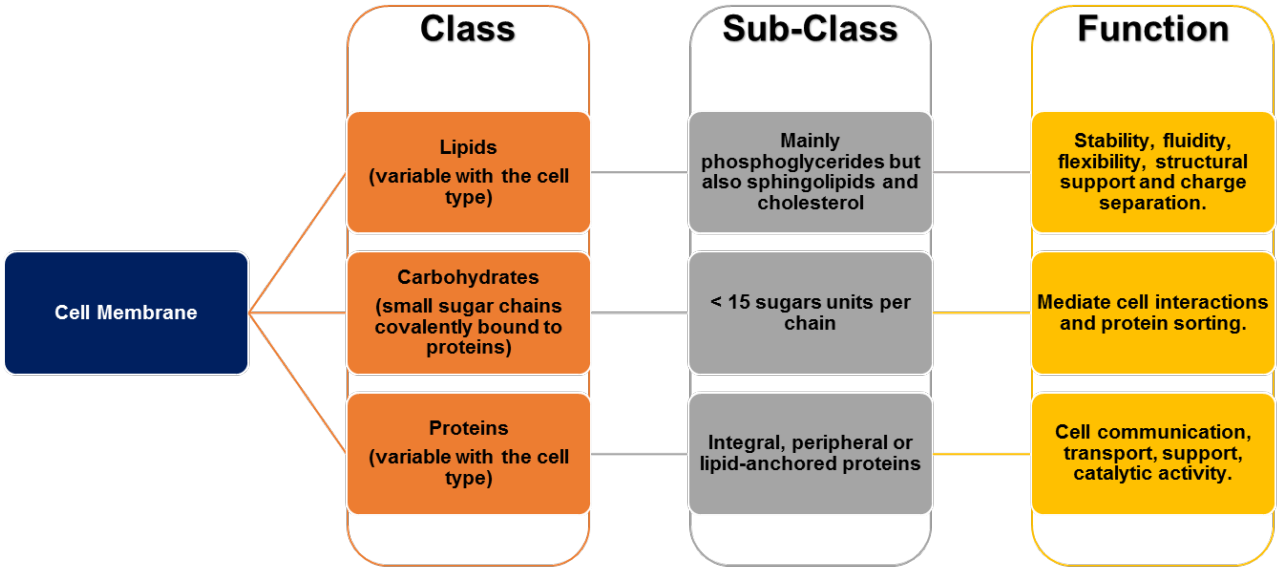

Figure 71 – The plasma membrane components and their main functions.

The aforementioned unique characteristics of the cell membranes will provide essential means for the flux of cargo into (influx) and out (efflux) of the cell. Given that all the cell contents are enclosed within the plasma membrane, the exchange of content and information must be done through this structure.

The transport of cargo through the membrane can occur in two ways depending on the energy requirement. Usually, molecules that have the capability to pass through the membrane without the need of energy are said to cross this barrier based on a passive diffusion. In a general way, the movement based on passive diffusion occurs from higher concentration regions to lower concentration ones.

On the other hand, some molecules are not able to directly move through the plasma membrane and require an energy-coupled transport process where they move actively.

Usually, the only molecules that have the capability to pass directly through the plasma membrane without energy requirement are small hydrophobic solutes that can move freely through the hydrophobic interior of this cell structure. Also, other small molecules like O_2, CO_2, or NO, have the capability to pass rapidly through the membrane since that they can slip between adjacent phosphoglycerides. On the other hand, big polar molecules show poor membrane permeability and require more specialized mechanisms to penetrate the plasma membrane. This semipermeable nature of the plasma membrane allows a better regulation of the influx/efflux of molecules.

Life essential chemical identities as water, ions (*e.g.* Na^+, K^+, Cl^-) or glucose can also transverse the membrane without the need of energy. Mainly, the chemical influx/efflux of these identities occurs through: (i) specific channels (*e.g.* aquaporins); (ii) unique ion gated channels or; (iii) facilitative transporters, respectively. In all of these cases, these channels or transporters are integral proteins organized along the plasma membrane.

On the other hand, the trafficking of molecules with a lower plasma membrane permeability can occur based on a great diversity of energy dependent mechanisms. In these situations, the transport of molecules happens against the concentration gradient and requires the input of energy promoted by the hydrolysis of ATP (*e.g.* Na^+/K^+ ATPase) or through the flux of electrons. Nonetheless, these processes are usually associated with the translocation of small molecules through the plasma membrane.

As a result, the trafficking of bigger cargo (*e.g.* proteins, cholesterol/LDL) between the interior/exterior of the cell happens by a complementary set of energy dependent processes called endocytosis/exocytosis[183–186].

Thanks to the fluid and flexible nature of the plasma membrane, in endocytosis, the material is internalized by the cell through the membrane invagination, in which the cargo is surrounded by the plasma membrane that then buds off into the cytosol to form a vesicle. Inversely, the exocytosis is the process in which the cell expels content through the intracellular formation of vesicles that will then fuse with the plasma membrane to deliver the cargo to the extracellular medium[183,185,186]. Since endocytosis and exocytosis are extremely dynamic and regulated processes, it has been predicted that the mammalian cells may be capable of internalizing or expelling up to five times their volume and membrane area[187]. These two processes are depicted in the Figure 72.

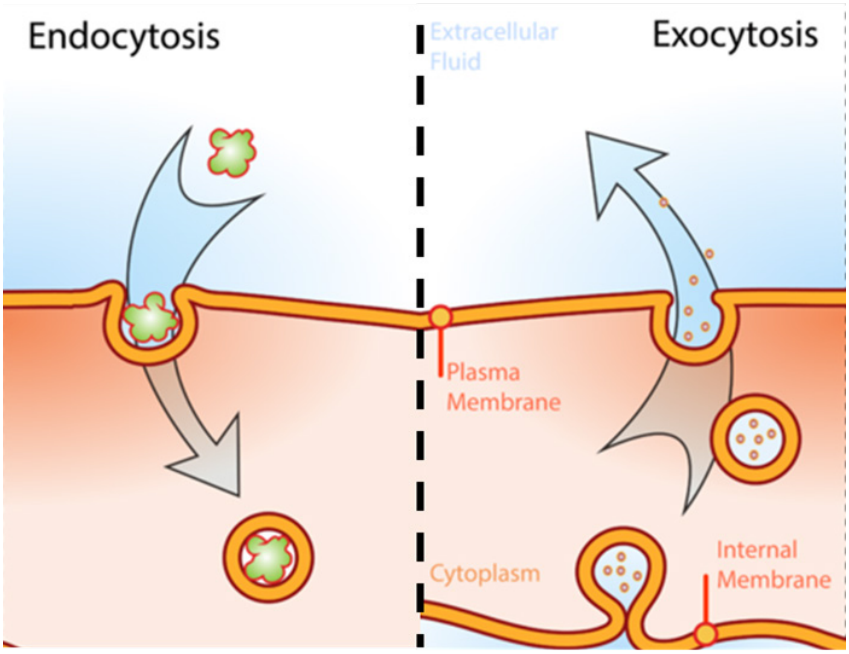

Figure 72 – Schematic representation of the two complementary ways for the cells to internalize (left) or expel (right) large molecules (Figure adapted from Ref. 188).

With the recent advancements in the molecular biology, it is now known that distinct endocytic processes may contribute for the cargo internalization in the mammalian cells. Mainly, depending on: (i) the cargo to be internalized; (ii) the associated signals; (ii) the protein/lipid machinery involved and (iv) the fate of the materials; the cell internalization of cargo through endocytosis can be divided into two main groups: (a) phagocytosis (*cell eating)* and; (b) pinocytosis (*cell drinking*).

While that phagocytosis is mainly accomplished by highly specialized cells (*e.g*. dendritic cells, neutrophils or macrophages), the pinocytosis happens in almost all eukaryotic cell types. Several variants of the pinocytosis may be observed. The most investigated are: (i) clathrin-mediated endocytosis (CME); (ii) caveolae-mediated endocytosis (CavME); (iii) macropinocytosis and; (iv) several clathrin/caveolae-independent endocytosis[186,189–193].

Nevertheless, some of the sub-pinocytic mechanisms are still highly debated due to the inherent difficulties to clearly understand the mechanisms that regulate these endocytic processes[186,189–193]. For example, very recently, Nichols *et al.* have reported that the predominant endocytic pathway in mammal cells relies on the formation of clathrin-coated vesicles, where at least 95% of the total protein influx occurs by this way. As a result, the authors concluded that the other clathrin-independent endocytic pathways do not have a significant contribution for the influx of cargo[194].

The major difficulties for the clear identification and analysis of the endocytic pathways comes from:

(a) the lack of standardized markers and inhibitors that may help to elucidate the different mechanisms;

(b) limited spatial resolution of the current imaging techniques;

(c) some methods involve the perturbation of the cell homeostasis, in which can influence the endocytic pathway *per se*, or;

(d) the possible cross-talking between the distinct pinocytic pathways[195].

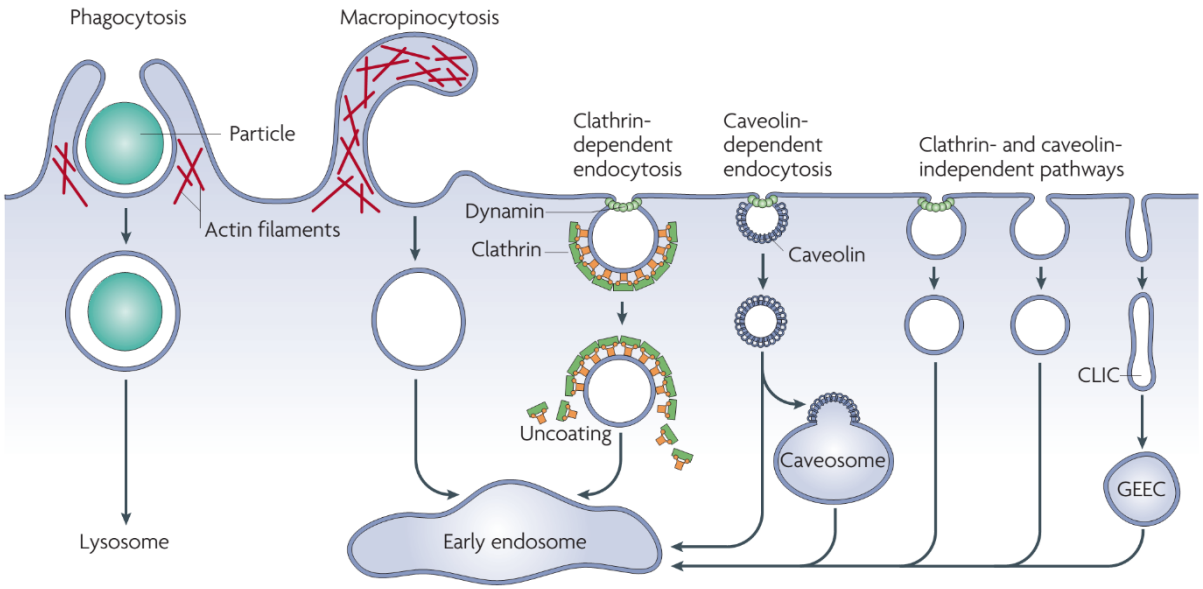

Figure 73 – The distinct endocytic pathways that contribute for the internalization of cargo into the mammalian cells. Mainly, the endocytosis route is highly dependent of the cargo size. While big particles are internalized through phagocytosis or macropinocytosis, smaller particles (< 100 nm) are usually endocytosed by the other pathways. In a classical point of view, most of the cargoes are delivered to early endosomes through vesicles or through tubular intermediates (CLIC) that will then experience further maturation. Some cargoes may first pass by intermediary compartments like the caveosomes or the glycosyl phosphatidylinositol-anchored protein early endosomal compartments (GEEC) (Figure adapted from Ref. 193).

Most of the pinocytic pathways shown in the Figure 73 involve four common mechanisms: (i) specific interaction of the cargo at the cell surface (see Figure 74); (ii) structural change of the plasma membrane and pitching off; (iii) complete enclosure of the cargo into a vesicular/tubular structure and; (iv) targeted movement of the cargo into predefined subcellular organelles.

Furthermore, during the secretory* or endocytic pathways the vesicles possessing the cargo are accompanied by sorting signals that will be fundamental for the recognition and sorting of the vesicular contents to the correct cell compartments. The sorting and regulatory mechanisms existent in the cell rely on a range of channels, adaptors, retrieval and coating proteins, including the, transient receptor potential-mucolipin (TRPML1)[196], Rab GTPases and the soluble N-ethylmaleimide-sensitive factor accessory protein receptors (SNARE) that define the precise delivery of the internalized content to the intracellular compartments[191].

*Note, the secretory pathway specifically refers to a conjugated set of invents that happen inside the cell and that are responsible for the delivery of newly synthesized membrane proteins to their correct location.

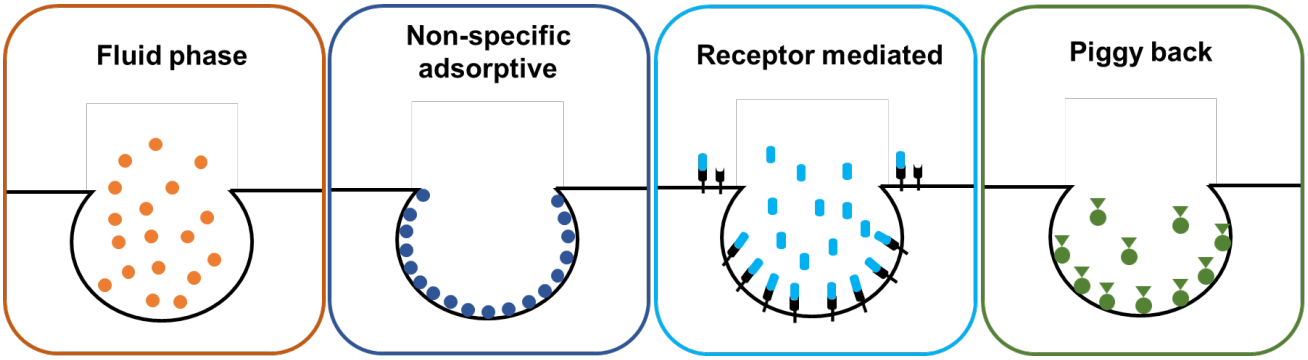

Figure 74 – Nature of the interaction between the materials to be internalized and the components of the plasma membrane. The type of the interaction with the plasma membrane depends on several factors like size, shape, chemistry and net-charge of the molecule. Note: "Piggy back" endocytosis relates to the uptake of a molecule complexed with a carrier (*e.g.* protein) that promotes its internalization.

Keeping with the scope of the current work, we will only give some insights regarding the most commonly discussed endocytic pathways (*i.e.* CME, CavME, macropinocytosis and phagocytosis) that may contribute for the cell internalization of nanomaterials, including the PAMAM dendrimers. For further reading regarding this topic, we recommend the following excellent reviews that discuss in detail the alternative endocytic pathways[187,192,195,197–199].

First of all it is worth mentioning that although all pinocytic pathways are common to almost all eukaryotic cell types some mechanisms are more frequent in one cell type than another. For example, CavME factors (~ 70%) are frequently present in vascular endothelial cells, while the CME factors are more commonly found in epithelial cells[197,199].

The clathrin-mediated endocytosis (CME) is the most widely studied and characterized internalization pathway of the pinocytic routes. It has also been described as the main internalization route in the eukaryotic cells for the uptake of nutrients or signaling molecules. Usually, macromolecules or particles presenting a size in the range of 120-200 nm are mainly internalized through CME. The way that the cargo is internalized through this pathway is either adsorptive or receptor-mediated. In the adsorptive CME, cationic cargo interacts non-covalently with the negatively charged plasma membrane. In contrast, in the receptor-mediated internalization, the cargo is taken by the cell through highly selective and specific membrane receptors (*e.g.* LDL, growth factors, insulin are all internalized based on receptor-mediated internalization).

After the interaction of the cargo with the plasma membrane several mechanisms are triggered that will promote the migration of the clathrin coat protein complex. As a result, in the early stages of the CME an intricate protein machinery will be directed to the inner layer of the plasma membrane to promote the initial formation of the clathrin-coated pit. The formation of the pit is promoted through

the action of clathrin as the main structural unit but also with the help of other elements like the adaptor proteins (APs), modeling proteins and sorting adaptors.

The clathrin is a triskelion protein with three heavy chains (~ 190 kDa) where each is associated with a single light chain (~ 25 kDa). While the heavy chains give the required structural support, the light chains (along with APs) are fundamental to regulate the assembly and disassembly of the clathrin pit. In later stages, the action of the APs will promote deformation of the internalization sites through the assembly of a curved polygonal web that will lead to the initial plasma membrane curvature (nucleation). The invagination of the membrane is then continuously promoted by the action of modeling proteins (*e.g.* FCHO, EPS15) that will then direct the migration of sorting adaptors. Usually, these sorting adaptors will work as specific recognition sites for many different kinds of cargoes and sorting signals that will define the fate of the cargo.

In the final stage, the action of the GTPase dynamin will force the formation of a "neck" and the separation of the clathrin-coated structure from the plasma membrane. This complete separation results in the formation of the clathrin-coated vesicle (CCV). Once in the cytosol, the protein complex around the CCV will disassemble through the action of specific proteins (*e.g.* auxilin), where the resulting naked vesicle will experience further maturation (*e.g.* endosomes or lysosomes) until the cargo reaches the target[186,187,195,197,199–201].

The whole process of the CME vesicle formation is simplified in Figure 75.

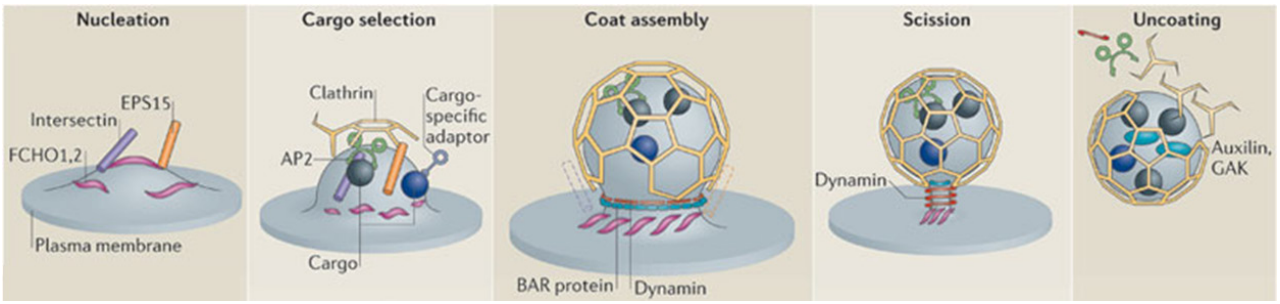

Figure 75 – Simplified representation regarding the formation of the clathrin-coated vesicle during CME (Figure adapted from Ref. 201).

Most of the materials containing targeting agents (including dendrimers) are internalized through receptor-dependent CME. Moreover, for the non-targeted delivery, the internalization through CME is highly dependent of the material size, net-charge and surface chemistry. For example, Pei *et al*. explored the cell internalization of PEGylated PAMAM dendrimer-doxorubicin conjugates (size < 50 nm) in SKOV-3 cells (ovarian cancer). The authors concluded that the main internalization pathway of these dendrimer conjugates in the SKOV-3 cells was through CME[202].

On the other hand, recently, Qi *et al.* studied internalization pathway of PEGylated PAMAM dendrimer polyplexes (*i.e.* with DNA, size > 200 nm) in HepG2 cells (liver cells). The authors observed that the main internalization pathway was through CavME[203]. It is important to note that the type of

endocytic internalization pathway is not only dependent on the size or targeting moieties, but also on the cell type being studied. As a result, it is important to mention that both research groups explored the internalization pathways between different cell types, and this factor must be considered when taking any conclusion[187,197].

The CavME is the most explored clathrin-independent endocytic internalization and it is reported to play an important role in the cell uptake of signaling molecules but also in the regulation of the lipid distribution along the plasma membrane. This pathway is more commonly observed in the endothelial cells but can also occur in smooth muscle cells, adipocytes or fibroblasts. In contrast, this endocytic pathway is mainly absent in neurons and leukocytes. It has also been reported that the CavME may be related with several diseases as cancer, diabetes or even bacterial/viral diseases (*e.g.* cholera toxin or Simian virus 40).

Although some of the processes associated with the CavME are now clearer, there is still a hot debate regarding the function and intervention of some proteins and the cellular fate of the cargo. Despite that, it is known that the CavME is characterized by the formation of caveolae that contribute for the cell update of cargo. These caveolae (means little caves in Latin) are flask-shaped membrane structures with sizes ranging between 50 and 80 nm.

It is known that the caveolae are mainly composed with distinct caveolin proteins (caveolins 1, 2 and 3) and signaling molecules, in which vary with the cell type. The caveolins (~ 21kDa) are anchored proteins distributed along the plasma membrane through a hydrophobic amino acid sequence in the cytosol side. Along with the caveolins, the cavins are known to play an important role in the caveolae formation and cargo destiny, however the exact mechanisms of these processes are still unidentified. Moreover, besides of this intricate network of proteins it is known that the action of the GTPase dynamin promotes the invagination process especially in hydrophobic plasma membrane domains (*i.e.* higher content in cholesterol and glycosphingolipids, known as “lipid rafts”).

Although still highly discussed, it is assumed that during CavME special caveolar endosomes (known as caveosomes, with neutral pH) may be formed. As a result, due to the nature of these caveosomes, it is defended that the internalization of drugs through this approach may be a way to avoid the harsh acidic conditions of the lysosomes. Nevertheless, some works defend that the lysosomal degradation in the CavME cannot be completely discarded due to possible cross-talk between the different endocytic pathways.

Additionally, since that most of the caveolae contents are directed to the Golgi apparatus and endoplasmic reticulum it may provide a way for the delivery of bioactive agents to these cell compartments. Unfortunately, the mechanisms that may allow the targeted CavME delivery are still subject of studies.

It is currently known that the small size of the cargo (nano range: 20-50 nm) along with the action of specific targeting ligands (*e.g.* folic acid, FA) may promote the cell internalization through the CavME pathway[187,193–195,199]. Recently, it has been described that the conjugation of FA with drug

carriers (*e.g.* dendrimers) may promote its binding with folic acid receptors that are present in caveolae[204].

The Figure 76 represents, in a simple way the CavME and its relationship with other endocytic internalization pathways.

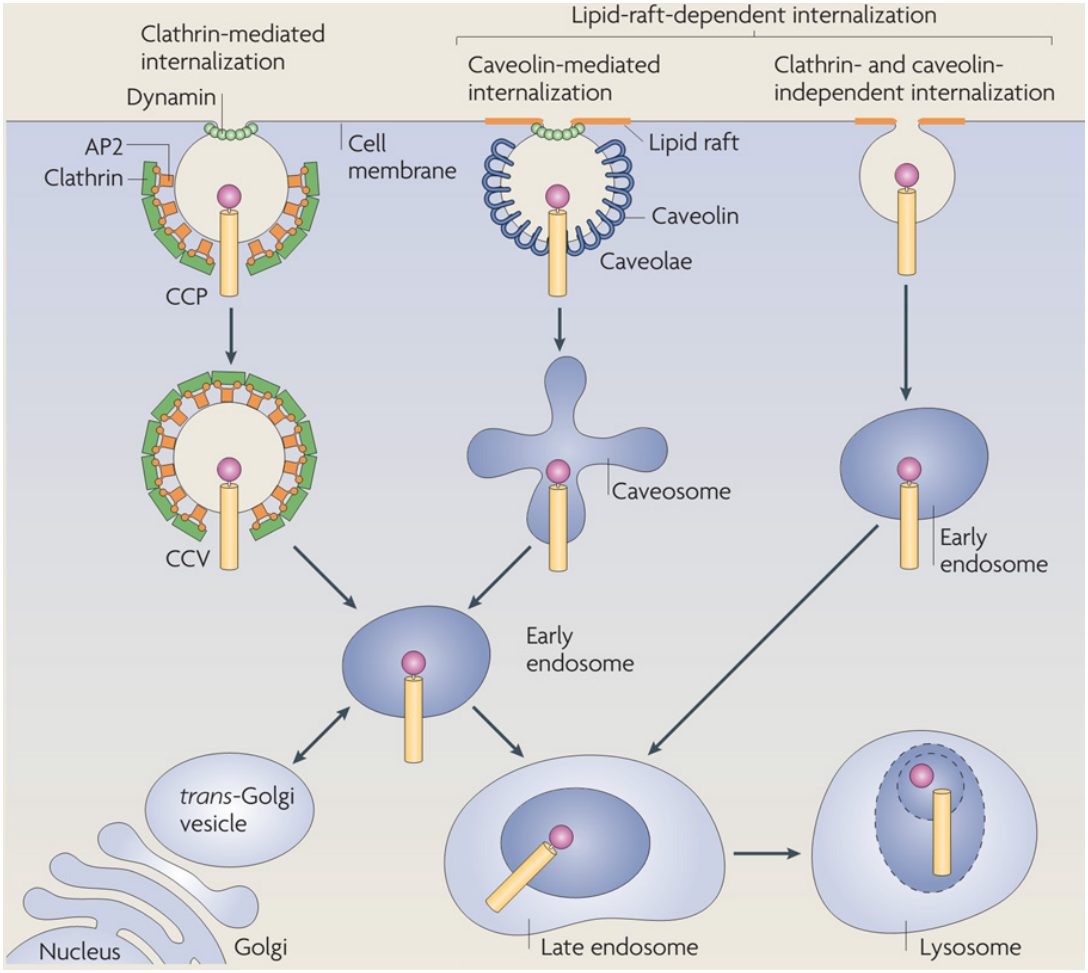

Figure 76 – Simplified representation of the CavME (middle) and its relationship with other internalization pathways. Note that some endocytic pathways may occur in certain microdomains of the plasma membrane but do not require the presence of dynamin (right side). Moreover, all the cases represented in the scheme are related with receptor-dependent internalization – yellow cylinder (Figure adapted from Ref. 205).

The macropinocytosis is a non-specific actin-dependent cell internalization process that involves the uptake of great quantities of the extracellular fluid through the formation of large vesicles with variable shapes. Multiple vesicle sizes have been linked to this internalization process ranging from 0.5 μm up to 1 μm. Given the size of the formed vesicles, the macropinocytosis was the first endocytic pathway to be identified in the eukaryotic cells.

Contrarily to the aforementioned endocytic pathways, the internalization through macropinocytosis is not accomplished based either on the type of cargo or on the material interaction

with specific receptors. Consequently, the macropinocytosis is usually promoted through the activation of growth factor receptors (*e.g.* epidermal grow factors, EGF) or due to the presence of apoptotic cells, bacteria or viruses in the extracellular medium. It is known that the interaction of these agents with the plasma membrane induces the actin polymerization, ruffling and the formation of the macropinosome. Additionally, the actin polymerization is also conducted based on the action of other elements like the small family Rho GTPases that work along with specific phospholipids like the phosphoinositide 4,5-bisphosphate (PI(4,5)P2).

It has also been found that the macropinosomes exhibit common proteins with other endocytic pathways (*e.g.* Rab5) in which further confirms the cross-talk between the distinct endocytic routes. Depending on the cell type, the nature of the membrane ruffles can be planar, circular cup-shaped or large extrusions. The collapse of these ruffles with the plasma membrane results in the formation of the macropinosomes containing the extracellular fluids and its contents. As a result of this collapse, the macropinosomes are larger than other endocytic vesicles and they do not exhibit the intricate protein coat. It is important to note that the macropinosome closure is usually aided by the action of the GTPase dynamin, however depending on the ruffle nature, the action of the dynamin may not be necessary.

The formation of the macropinosomes happens in a random manner where not all the membrane protrusions effectively result in the formation of vesicles. Moreover, due to their nature, the macropinosomes are sensitive to the cytoplasmic pH where they usually fuse with the endosomal/lysosomal routes. Since that the ruffling is a random and continuous process that happens in almost all eukaryotic cell types, they typically contribute along with other endocytic pathways for the internalization of cargo in a non-specific manner[187,195,197,199].

For example, it has been found that PAMAM dendrimers (G2, G4 and G6) containing distinct functional end groups (neutral, cationic or lipidated) are mainly internalized by both CME and macropinocytosis in the HeLa cells[206]. Nevertheless, these studies are still inconclusive since that contradictory observations were reported for dendrimer containing distinct composition but with similar size. For example, other research groups have reported that the main cell internalization pathway of FITC-labelled gallic acid-triethylene glycol (GATG) dendrimers in the same cell type (HeLa cells) was through macropinocytosis where the other endocytic pathways did not played a significant role[207]. It is clear that the complexity and versatility of the endocytic pathways and the lack of standardized analytic approaches may strongly limit the acquisition of deeper conclusions[186,197,208].

The Figure 77 shows the plasma membrane protrusions that may lead to the formation of macropinosomes and the overall internalization process through macropinocytosis.

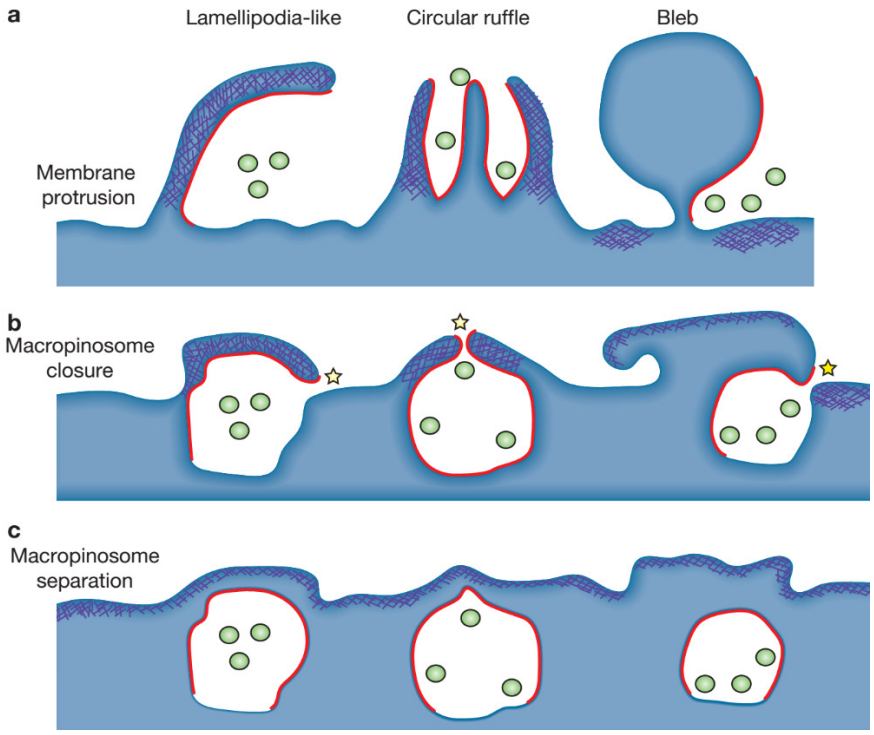

Figure 77 – Schematic representation of (a) the possible protrusions that may lead to the formation of macropinosomes; (b) the events that lead to the macropinosome formation through the collapse of the ruffles with the plasma membrane; (c) the formation of the macropinosome devoid of an intricate network of proteins (Figure adapted from Ref. 209).

It is important to mention that the actin cytoskeleton plays a central role not only in the macropinocytosis but also is many other endocytic routes. The actin is a globular protein (~ 43 kDa) in which polymerizes through non-covalent interactions giving rise to highly flexible microfilaments. These microfilaments have a central role in many cellular processes including cell migration, cell division or endocytosis. Futhermore, it is now known that the application of drugs that interfere with the actin expression may deeply hamper the internalization of cargo through endocytosis[186,197,208].

The Figure 78 shows the great importance of the actin polymerization for the different endocytic pathways. For a more detailed analysis regarding the importance of actin polymerization during endocytosis, the reading of references 208 and 210 is highly recommended.

The phagocytosis is an endocytic pathway that mainly occurs in specialized immune cells (*i.e.* macrophages, monocytes, neutrophils or dendritic cells). Nevertheless, it has also been observed to take place in other eukaryotic cell types including fibroblast (*i.e.* collagen phagocytosis), epithelial cells or cells responsible to generate inflammatory agents (*e.g.* basophils). The phagocytic pathway has been largely associated with the uptake of pathogens or dead cells, but it is also known to play an important role in the internalization of nutrients[187,195,199].

The phagocytic process may be triggered either through the interaction of plasma membrane receptors with exposed chemical moieties of a foreign body or by the receptor-mediated recognition

of specific soluble cell factors that “mark” the cargo. The process in which the cargo is marked by recognition factors is called opsonization and relies on the adsorption of small proteins (opsonins) over the surface of the material to be internalized. Some of these« opsonins include immunoglobulins of type G and M, complement factors or blood serum proteins like the fibronectin[187,195,199].

After opsonization specific plasma membrane receptors (*e.g.* Fc receptors) have the capability to recognize these “marked” bodies resulting in the activation of the phagocytic pathway. Note that the nature of the different opsonins and its interaction with the distinct membrane receptors will define the response of the cell and the fate of the cargo[187,195,199].

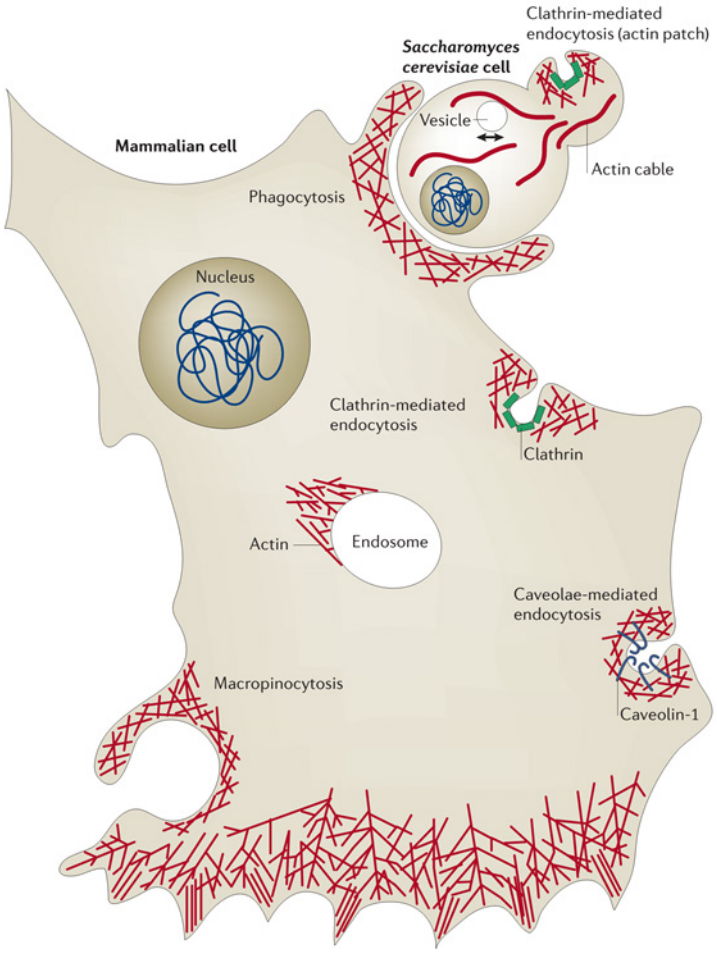

Figure 78 – The importance of the actin microfilaments (red) for the different cellular processes including the membrane reshape (*i.e.* membrane invagination and vesicle scission) during endocytosis (Figure adapted from Ref. 208).

For example, as shown in Figure 78, the phagocytosis starts with a series of signaling events that promote the actin polymerization and the formation of several plasma membrane elongations. These cell membrane distortions allow the engulfment of the material by the phagocytic cell and results in the formation of an intracellular vesicle called phagosome.

Phagosomes presenting distinct sizes (0.5 – 10 μm) and shapes (spherical or elongated) have been reported, and are known to be associated with the same morphological properties of the internalized cargo. Taking into consideration that the phagocytosis requires relatively large volumes of plasma membrane, it is known that many other cell compartments also intervene in the phagocytic process. For example, after the phagosome formation, the maturation process takes place over a series of fusion/fission processes with endosomes (phagoendosomes) and lysosomes (phagolysosomes). The materials internalized by this route are usually sorted to the degradative cellular pathway given the harsh hydrolytic conditions of the phagolysosomes[187,195,199].

The phagocytosis is associated with the internalization of relatively large particles (> 500 nm) since that they are preferentially marked through opsonization. Nevertheless, it has been observed that much smaller particles (~ 100 nm) may also be internalized through this endocytic pathway[211,212]. The phagocytosis may strongly limit the desired targeted delivery of dendrimer-drug conjugates. It is known that depending on the surface stability (*e.g.* agglomeration) and net-charge (*i.e.* cationic particles favor the adsorption of opsonins), the phagocytic uptake by the macrophages can easily happen. Such phenomena usually results in the low targeted delivery of drugs and, their accumulation in the mononuclear phagocytic system (MPS) organs (*e.g.* liver or spleen - resulting in systemic toxicity effects)[212–215].

Besides of the aforementioned cell internalization pathways, many other endocytic routes have also been discovered in the last decade. Many of these new discoveries occurred thanks to the great developments associated with the imaging techniques (*e.g.* electron microscopy), proteomics and targeting moieties. Some of the knowledge associated with these novel endocytic routes are still preliminary, and their influence is still unknown for the cargo uptake. Some examples of the alternative endocytic routes are shown in the Figure 79.

It is worth mentioning that all the endocytic processes require relatively high energy levels since that the formation of vesicles involves the overcoming of the plasma membrane resistance. Besides of the aforementioned proteins, other proteins complexes that exist in the cytosol are common to almost all the endocytic pathways and are responsible for facilitating the plasma membrane deformation. An example includes the superfamily of proteins that contain the BAR domains. It is known that these proteins are largely associated with several endocytic routes and are responsible for mediating the membrane deformation, curvature and enclosure during vesicle development[195].

As shown in Figure 79, the fate of the cargo may be variable as a function of the different endocytic routes. In the recent years, the preparation of dendrimers and other materials that specifically target some of these pathways have been explored. Unfortunately, the desired targeted drug delivery is still a great challenge to overcome[191,206].

It is clear that the study of the endocytic pathways provides a way to understand the mechanisms behind the cell internalization and allow the development of more efficient delivery

vehicles (*e.g.* genes, drugs, etc.) that present a maximized cellular internalization and a reduced cytotoxic effect[191,206].

The current pharmaceutical field relies mainly on the development of drugs that can diffuse through the plasma membrane and pervade the entire cell. However, such approach carries several limitations including drug sequestration in undesired cell compartments (lysosomes) or non-specific interactions with other organelles. In recent years, novel approaches have pursued the development of highly specific drugs that have the capability to escape certain cell compartments (see Figure 80) and achieve the desired cellular target[191,216–218]. It is clear now that the development of such systems is strongly dependent on the analysis of the interactions between the plasma membrane and the material in study. Moreover, with the ever increasing application of dendrimers to the biomedical field it becomes essential to understand their internalization pathways and cell compartment accumulation for the elucidation of possible toxicity effects[195].

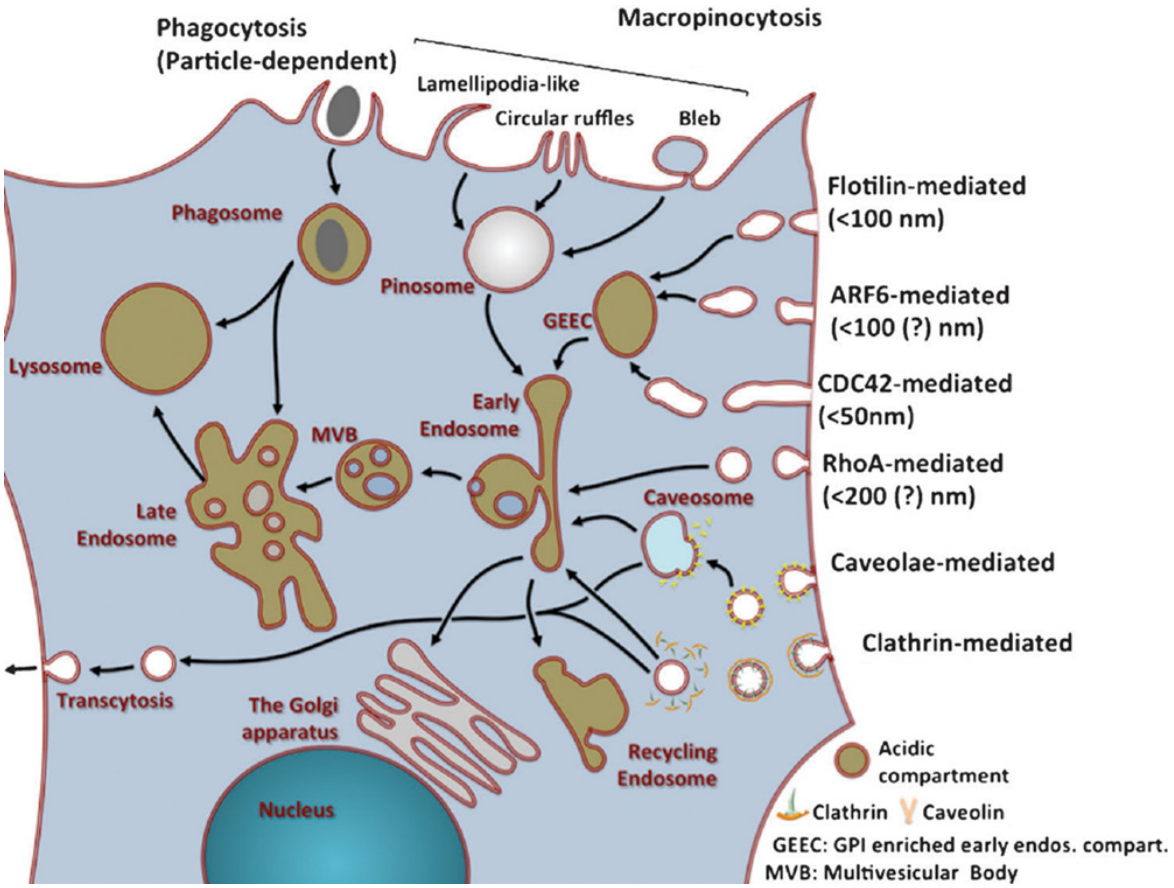

Figure 79 – The possible endocytic mechanisms of eukaryotic cells (Figure adapted from Ref. 195).

Currently, some methodologies may be used *in vitro* to explore the cellular internalization and trafficking of cargo. Usually, this analysis may involve two approaches:

(i) colocalization of the materials in study* with well-known tracking units or endocytic markers;

(ii) exclusion of endocytic pathways through the use of chemical, biological or physical inhibitors before exposing the materials to the cells.

With the recent developments, several advanced biological probes and chemical inhibitors have been developed aiding in the investigation of the cell internalization of cargo.

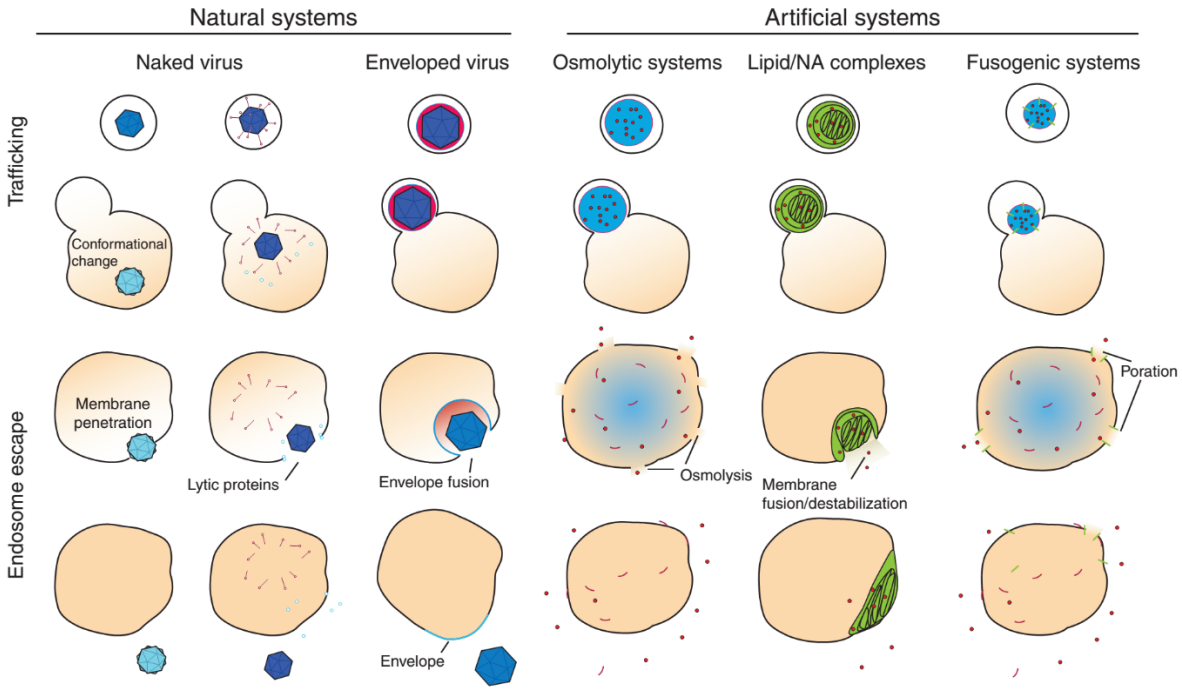

Figure 80 – Schematic representation of the effects that may be exploited for endosomal escape of cargo. For example in osmolytic systems, highly cationic particles, like some dendrimers, may lead to an increased influx of protons and ions which results in a higher osmotic pressure. The increasing osmotic pressure will cause the vesicles to swell and rupture, allowing its cargo to escape to the cytosol (Figure adapted from Ref. 217).

Also, it is worth mentioning that several imaging techniques may be used to explore the interaction between the materials and the biological interface. Some of these techniques include the direct observation by using high resolution fluorescence microscopy or by electron microscopy techniques (*e.g.* environmental SEM, TEM cryomicroscopy)[219–223].

Also, other techniques may be complementarily used to aid in the analysis of the cargo internalization by the cells. For example, flow cytometry may be employed for a quantitative analysis of the cell uptake and also to investigate the endocytic trafficking of cargo[224,225]. On the other hand,

*The materials are usually fluorescently tagged to allow the live observation of the internalization process. However, such observations may be limited to the spatial resolution of the current microscopes.

AFM can be applied to study the degree and nature of the interactions between the materials and the biological membranes[226–228]. Some of the mentioned techniques allow the live investigation of the endocytic process without compromising the cell homeostasis.

Besides of aforementioned analytic techniques, some of the complementary methodologies used to explore endocytosis of dendrimers, or other materials are briefly described in the Table 4.

The investigation of endocytosis based on the application of chemical inhibitors is still the most widely followed method since that it provides a time and labor efficient approach. Moreover, the use of well-characterized pharmacological inhibitors can be easily quantified and titrated since that it affects the overall cell population in a similar way and its cytotoxic behavior can be predicted. Despite its advantages, the use of chemical inhibitors has led to hot debates in the scientific community due to the increasing reports that claim the lack of specificity and misleading results due to endocytic cross-talking[197,212,218].

Table 4 – The several techniques that may be used to explore the endocytosis of materials, including dendrimers. Due to the limitations of each approach, they are usually employed in conjugation for a more reliable identification of the cell internalization pathway.

Method	Role	Type of study	Examples
Colocalization techniques			
"Pulse-chase"	Colocalization of the material in study using proteins with well-known internalization pathways	Live cells	Transferrin (clathrin) or cholera toxin B (caveolae)
Fusion proteins	Transfection of fluorescently marked proteins that are associated with the endocytic process	Live cells	Rab5, caveolin-1, etc.
Molecular Probes	Application of probes that mark specific endocytic compartments	Live cells	Lysotracker™ or MitoTracker™
Immunocytochem.	Conjugation of fluorescently tagged agents that recognize proteins associated with endocytosis	Fixed cells	Antibodies
Exclusion of endocytic pathways			
Chemical or physical inhibition	Expose cells with pharmacological agents or low temperatures that hamper specific endocytic pathways	Live cells (conditions vary with the cell type)	Chlorpromazine or cholesterol depletors

We recommend the further reading of the following works that describe in detail the advantages and disadvantages of current methods that are traditionally used to explore the endocytic pathways[218,229].

Additionally, some of the most commonly employed pharmacological or chemical inhibitors are described in Table 5.

Despite the great advancements of the analytical techniques that may be used to study the endocytosis pathways, the scientific community is still far from completely unveiling all the mechanisms and parameters associated with it.

Moreover, given the great diversity of materials and cell type used to explore these trafficking pathways, it has become increasingly difficult to establish common factors between the different studies. For example, even when the materials, like dendrimers, are functionalized with specific targeting agents, these material will still be internalized by other endocytic pathways at the same time. Besides that, many of the techniques shown in Tables 4 and 5 are mainly applied *in vitro* where in most of the cases the conclusions taken from such analysis overlook the *in vivo* conditions[197,212,218].

Table 5 – The most commonly used inhibitors for the distinct endocytic routes. The employed concentration of the inhibitors are not described since that they usually vary with the cell type (Data obtained from Ref. 229).

Endocytosis pathway	Inhibitors	Mechanism	Specificity
Clathrin	Hypertonic Sucrose (0.4-0.5 M)	Cytosol dispersion of the clathrin protein complex	Influences other pathways (CavMe)
	K^+ depletion	Blocks plasma membrane proteins associated with clathrin assembly	May have some effects over macropinocytosis
	Cytosolic acidification	Inhibits the vesicle enclosure	May have some effects over macropinocytosis
	Chlorpromazine	Blocks the activity of adaptor proteins	Influences other pathways like CavMe or phagocytosis
	Monodansylcadaverine	Inhibits the vesicle enclosure	May have some effects over macropinocytosis and phagocytosis
	Phenylarsine oxide	Still unknown	May have some effects over macropinocytosis and phagocytosis
Caveolae	Statins, Methyl-β-cyclodextrin, Filipin, Nystatin and Cholesterol Oxidase	Changes in the cholesterol synthesis, structure and its distribution along the plasma membrane	May affect other endocytic pathways or change the membrane integrity and permeability
Macropinocytosis and phagocytosis	Amiloride	Inhibits the sodium-proton exchange in which affects the actin polymerization	May have an influence on other endocytic pathways.
	Wortmannin	Works as an inhibitor of phosphoinositide metabolism in which affects actin polymerization and signaling molecules	
	Cytochalasin D	Blocks actin polymerization	

Apart of the current limitations, it is now accepted that many distinct physicochemical parameters of the materials (*i.e.* size, shape, compressibility, surface chemistry, charge and topology) can be exploited to optimize the internalization through a specific endocytic pathway (see Figure 81).

For example, several works have shown that the aspect-ratio of the materials can strongly influence the internalization behavior by different cell types. While some cells (*e.g.* macrophages)

preferentially uptake rod-like particles, other cell types (*e.g.* HeLa cells) exhibit an improved uptake of spherical particles. Although the mechanism that rules this process is still unknown, it is supported that this behavior is strongly dependent of the cell type and the contact angle formed between the material-biological interface (see Figure 82)[212,217].

Another example is the well-known formation of a protein-corona around the material surface. When in the biological fluids (*e.g.* blood) and depending on the material surface nature, a coating through the adsorption of specific proteins (*e.g.* serum albumin or fibrinogen) may be observed. Usually, this event results in altered cellular interactions leading to the reduction of the material functionality. In contrast, in some cases this protein adsorption may be desired for targeted cell delivery (*e.g.* opsonization for the delivery to the cells associated with the RES)[213].

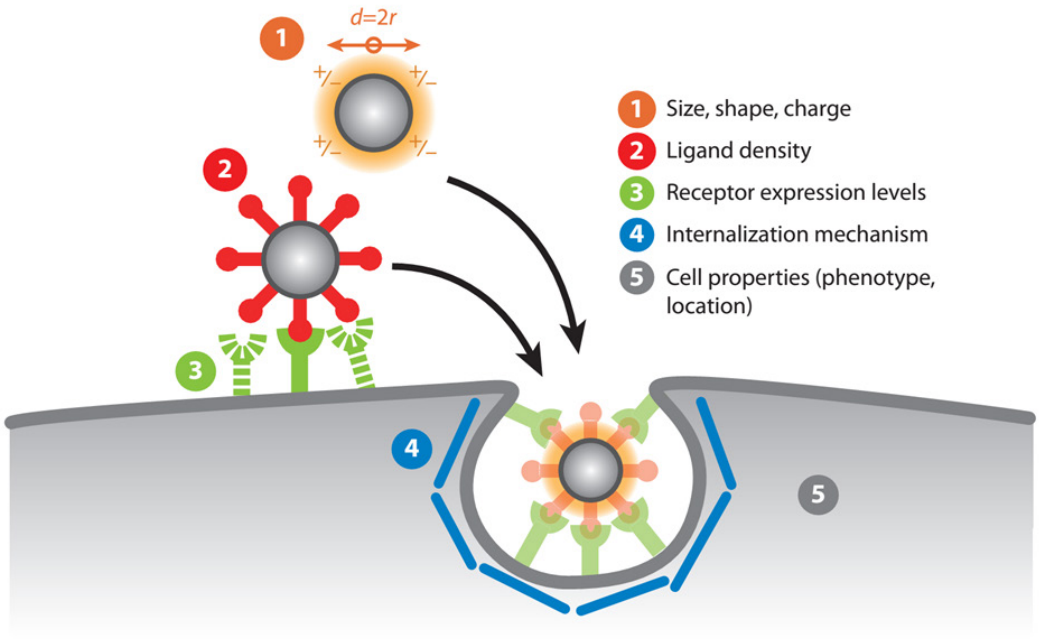

Figure 81 – The parameters that may affect the endocytosis of dendrimers and other materials. (Figure adapted from Ref. 214).

Additionally, some internalization pathways are favored based on a specific particle diameter interval. It has been shown that some materials exhibit an optimal internalization at a specific size range, where the uptake effectiveness decreases when the particle sizes fall beyond this range (see Figure 82). Moreover, it has been shown that such effect is strongly dependent on the cell type and material composition. Besides that, many *in vivo* events are strongly dependent on the particle size including circulation time or clearance.

The surface functionalization also plays a fundamental role on the cell internalization of cargo. The existence of specific functional groups or an overall net-charge may result in distinct cell uptake

events when compared with the materials that do not present such modifications. For example, the functionalization of nanoparticles with polymer chains (like PEG) may be exploited to avoid the uptake by cells from the RES by decreasing protein adsorption and particle agglomeration. As a result, by playing with surface charge (*e.g.* cationic, anionic or neutral) it may result in personalized internalization patterns and variable cytotoxic effects, being always dependent of the cell type[212].

Several excellent works have debated in detail the effect of the material's physicochemical properties over its cell internalization and as a result we recommend the further reading of the following reviews for a better understanding of this topic[199,206,213–215,217,218,230].

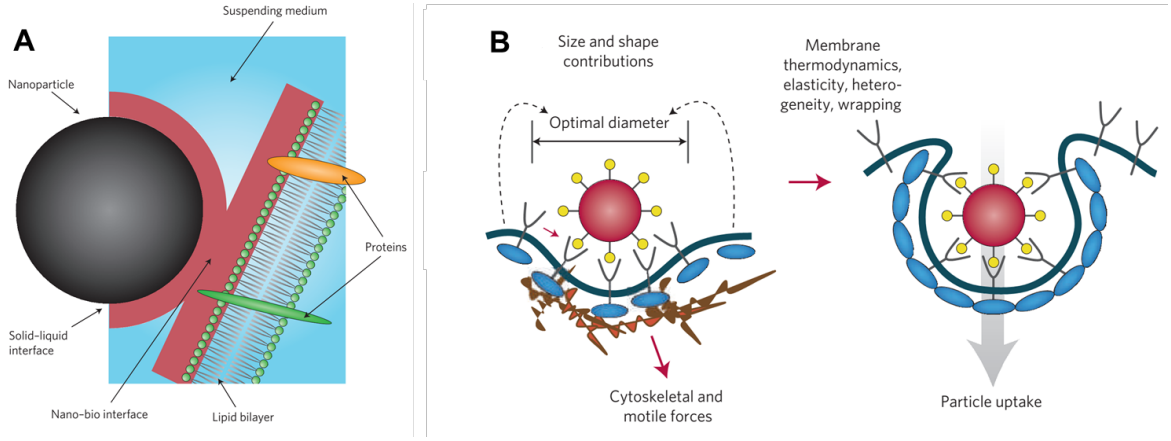

Figure 82 – The interactions at the material-biological interface. (A) The angle of the interaction may influence the cell uptake; (B) the optimal diameter that provides the ideal cooperative thermodynamic energy to overcome the resistance provided by the cell membrane (Figure adapted from Ref. 213).

To conclude this section, we will discuss in the next paragraphs the influence of the PAMAM dendrimers physicochemical properties (*e.g.* in terms of size, shape, surface chemistry and charge) over the endocytosis of some eukaryotic cell types. Finally, we will then give some insights regarding the strategies that rely on the use of PAMAM dendrimers to achieve an improved internalization of cargo through endocytosis.

As already mentioned in the previous sections, the higher generation PAMAM dendrimers exhibit a shape that resembles some proteins. As a result, given this mimicking ability of the PAMAM dendrimers, they may be exploited for the delivery of cargo by interacting with the cell machinery in a similar way that some biomolecules do.

It is currently known that the cytotoxicity of the PAMAM dendrimers is strongly dependent of the generation and nature of the terminal groups. This generation-dependent cytotoxicity happens mainly for two reasons. First, at the same molar concentration, higher generation PAMAM dendrimers exhibit a greater number of end groups that results in a superior charge-density. Second, an increased contact area between the dendrimers and the cell membrane is observed at higher generations.

Also, as already referred in the previous sections, the amine-terminated PAMAM dendrimers show an improved cytotoxic effect when compared with other end groups (*i.e.* acetylated, carboxylated or hydroxylated terminal units).It has been postulated that this increased cytotoxic effect happens due to the positive net-charge of the amine-terminated PAMAM scaffold at physiological pH. Although the associated mechanism is not completely understood yet, it has been shown that such effect comes from the increased electrostatic interactions between the PAMAM primary amine terminal groups and the cell membrane. On the other hand, a lower cytotoxic effect is observed for the neutral or cationic PAMAM dendrimers due to the lower degree of interactions that are established between the dendrimer and the plasma membrane[182,231a,b].

It has been recently reported that the interaction of the PAMAM dendrimers with the plasma membrane is not only dependent of the surface groups but also on the nature of the core. For example, the properties of the core may define the thermodynamic stability of the PAMAM dendrimer in the plasma membrane interior[231c,d].

Additionally, simulations have shown that the interaction between the PAMAM dendrimers and the cell membrane is also dependent on the constitution of the lipid bilayer. For example, while the interaction of cationic PAMAM dendrimers with anionic lipids may result in the formation of liposomes, in the case of zwitterionic lipids, micelles are observed[231c,e,f]. Besides of these parameters, the aggregation state and generation of the PAMAM structure also defines the way that dendrimer interacts with the biological interface. The effect of these parameters is discussed in the next paragraphs[231c].

Holl *et al.* have investigated the possible interaction of higher generation PAMAM dendrimers with the cell membrane based on the use of lipid bilayer models along with live cell membrane studies (KB and Rat2 cells). According to their investigations on the lipid bilayer model, it was found that high generation PAMAM-NH_2 dendrimers (>G5) may lead to the formation or expansion of nanoholes in the lipid bilayer. On the live cell studies, the authors also observed that the interaction between the plasma membrane and higher generation polycationic PAMAM dendrimers resulted in augmented membrane permeability while that polyanionic polymers did not induce any profound changes on the plasma membrane[182,232].

Many other works also explored the effect of PAMAM dendrimers containing distinct terminal groups on several cells lines (*e.g.* HeLa, Caco-2, B16F10, HepG2, hMSCs, V79) and based on the use of specific incubation times (*i.e.* minutes to days), molar concentrations and assay methods. Independently of the conditions, a general trend could be observed among all studies. In all cases the -NH_2 terminated PAMAM dendrimers exhibited an increased cytotoxic effect when compared with other anionic or neutral structures. Another common behavior observed in several works is that these cytotoxic effects were dependent of the generation (charge density), nature of terminal groups and the cores, molar concentration and cell type[16,206,231,233–236].

For example, Ghandehari *et al.* reported that the end group acetylation of the PAMAM-NH_2 dendrimers reduces the cytotoxicity of the dendrimer scaffold in 10 fold while maintaining its membrane permeability on Caco-2 cell monolayers. The authors explained that this behavior could be observed thanks to the reversible modulation of the cell tight junctions upon the cell exposure to the acetylated PAMAM dendrimers[133].

Moreover, it was also found that PAMAM dendrimers exhibiting distinct generations interact differently with the lipid bilayer membrane models. For example, while low generation cationic PAMAM dendrimers interact electrostatically with the plasma membrane without compromising its integrity, higher generation cationic PAMAM dendrimers present a higher degree of electrostatic interactions in which induces the formation of nanoholes and leads to cell death[16,237].

Other studies have also shown that the PAMAM dendrimers with distinct functional groups exhibit different permeability levels across Caco-2 cell monolayers[16]. For example, regarding the permeability across the Caco-2 cell monolayers, Ghandehari *et al.* found the anionic PAMAM dendrimers (-COOH) exhibited greater permeability than the cationic (-NH_2) and neutral (-OH) PAMAM scaffolds. As a result, the authors defended that the low cytotoxicity of the PAMAM-COOH dendrimers along with its capability to reversibly modulate the tight junctions may be explored as oral drug delivery carriers[234]. It is currently known that this increased permeability of the PAMAM dendrimers across the endothelial cell layers occurs mainly through transcellular or paracellular routes[149].

Nevertheless, the tight junction modulation effect of some PAMAM dendrimer terminal groups is still controversial where the associated mechanisms are not yet completely elucidated. Very recently, Swaan *et al.* reported that while half-generation PAMAM dendrimers (-COOH) exhibited little modulating ability, the PAMAM-NH_2 dendrimers were able to effectively change the behavior of the tight junctions through its effect on the calcium signaling processes and nonspecific membrane interactions. The authors defended that such contradictory results come from the fact that many works have overlooked the possibility of the half-generation PAMAM dendrimers to pass through endocytic pathways rather than the previously reported paracellular routes[238].

It is worth mentioning that due to the inherent limitations of PAMAM dendrimers in clinical applications (*e.g.* relative toxicity and poor degradability) other approaches have emerged involving the use of less cytotoxic and biodegradable dendrimers, like the biodegradable polyester dendrimers* (*e.g.* based on the 2,2-bis(hydroxymethyl) propionic acid)[182].

For example, very recently, Byrne *et al.* presented a systematic study regarding the cytotoxic effect of the G4, 5 and 6 amine-terminated PAMAM dendrimers. The authors found that the mechanisms underlying the cytotoxic effect of these PAMAM dendrimers are based on two stages. In

*The reduced cytotoxicity of the hydroxyl-terminated polyester dendrimers is associated with the minimized nonspecific cell interactions.

the early-stages, the PAMAM dendrimers enter by endocytosis or through the generated plasma membrane nanoholes resulting in endosomal entrapment. During this phase, the authors observed a reversible oxidative stress in which was the result of the reactive oxygen species generated by the -NH_2 dendrimer surface groups. It was verified that this initial oxidative stress could be effectively hampered by intracellular mechanisms. In the second-stage, it was found that the PAMAM dendrimers could effectively escape the endosomal compartments (through osmolytic process) and interact directly with other cell organelles. In HaCaT cells, the authors verified that after 16 hours, the dendrimers could be located in the mitochondria in which resulted in an increased non-reversible oxidative stress and in the activation of distinct cell-death pathways[239].

Nevertheless, thanks to the novel functionalization approaches, new advancements have been made for the design of PAMAM dendrimer drug carriers with reduced cytotoxic effects. For example, recent approaches include the functionalization/protection with biodegradable or biocompatible units that improve the cell internalization and minimize the cytotoxic effect (*e.g.* PAMAM dendrimers containing PEG[240], oxyethylene[241] or arginine/lysine terminal units[242]).

In the recent years, several works have explored the endocytosis internalization pathways of PAMAM dendrimers based on the effect of distinct terminal groups and over diverse eukaryotic cell types. Despite the growing amount of works regarding this topic, the mechanism by which the PAMAM dendrimers are internalized is still a question of great debate. Besides that, due to the nonspecific uptake (adsorption) of the PAMAM dendrimers (mainly with –NH_2 end groups), it is very difficult to define a single internalization pathway since that other fluid-phase uptake mechanisms (*e.g.* macropinocytosis) may also contribute for the concomitant internalization. For example, it was recently found that the G7 PAMAM-NH_2 dendrimers were still internalized under energy-dependent internalization blocking conditions. Even at 4 ºC, the internalization of G7 PAMAM-NH_2 dendrimers was still observed, confirming the formation of the nanoholes and an increased plasma membrane permeability[182].

According to the data shown in the Table 6, the certain identification of the PAMAM dendrimer endocytosis pathway is far from being unanimous. We defend that a more rigorous study taking into consideration several parameters (*e.g.* terminal groups, generations and cell types), should be accomplished in order to shed some light over this highly controversial topic.

It is now clear that future studies should take into attention the *in vivo* conditions and have in mind that several endocytic pathways may surely contribute for the internalization of the PAMAM dendrimers, independently of the cell type. Finally, we also defend that the development of more reliable and standardized analytical methods will provide valuable tools for the acquisition of more consistent results.

Table 6 – Summary table with the reported endocytosis internalization pathways based on PAMAM dendrimer with distinct terminal units/complexes and several eukaryotic cell types.

Type of Terminal group	Generation	Nb. End groups	Cell Type(s)	Reported Endocytosis pathways	Ref.
-NH_2	2	16	HeLa	CME and macropinocytosis	182
			Caco-2	CME	182
			B16F10	Cholesterol-dependent	243
	4	64	Caco-2	Cholesterol-dependent	182
			HeLa	CME and macropinocytosis	182
			A549	Non-CME and non-CavME	235
			B16F10	Cholesterol-dependent	243
	6	256	HeLa	CME and macropinocytosis	182
	7	512	KB, Rat2, C6	Membrane nanoholes	182
-OH	4	64	A549	Non-CME and non-CavME	235
-COOH	3.5	64	A549	CavME	235
			Caco-2	CME, CavME and other dynamin dependent	244
-NH_2/Propanolol	3	30/2	HT-29	CavME and macropinocytosis	245
-NH_2/Lauroyl	3	30/2	HT-29	CME, CavME and macropinocytosis	245
-NH_2/Lauroyl/Propanolol	3	28/2/2	HT-29	CME and CavME	245
-NH_2/PEG-lactoferrin/pDNA	3	125.6/2.4/-	Brain capillary endothelial cells	CME, CavME and macropinocytosis	246
-NH_2/PEG/DOX	4	30/20/14	SKOV-3	CME	120
-NH_2/Polyrotaxane of PEG and α-cyclodextrin/pDNA	1	-	HEK293A	CavME	247
-NH_2/FITC	4	58/6	Human myometrial cells	CME	248
-NH_2 siRNA polyplex	5	128	PC-3	Mainly macropinocytosis but also CME and CavME	249
	7	512	T98G glioblastoma	CavME	250
			J774 macrophages	CME and CavME	
-NH_2/oxyethylene units/FITC	3,4, and 5	30/33/1	HeLa	CME and CavME	241
-NH_2/Alexa Fluor 488 pDNA complex	5 and 7	-	Cos-7, HEK293A, C6, HeLa, KB and HepG2	Non-CavME	251
-NH_2/chondroitin sulfate pDNA complex	5	-	B16-F10	CME, CavME and other energy dependent pathways	252
-NH_2/FITC/PEG-PLGA pDNA complexes	2	-	HEK293A	CME and CavME	253

-NH_2 /FITC/hyaluronic acid with entrapped DOX or siRNA complex	5	-	NCI/ADR-RES	CME	254

1.8. Objectives of the work

In this thesis, the synthesis of the FITC-PAMAM dendrimer conjugates is explored for *in vitro* cell studies. For this purpose, the conjugation efficiency of the FITC fluorescent dye with the PAMAM dendrimers is investigated taking into consideration the wide number of reported works that have used this system for the endocytosis investigation of the PAMAM dendrimer scaffold.

Given the great diversity of FITC-PAMAM functionalization methods already described in the literature, this work intends to provide new data regarding the applicability of some of the reported conjugation chemistries. With this goal in mind, we expect to investigate the stochastic conjugation based on distinct PAMAM:FITC molar ratios and based on the use of discrete PAMAM dendrimer generations and terminal groups (see Figure 83).

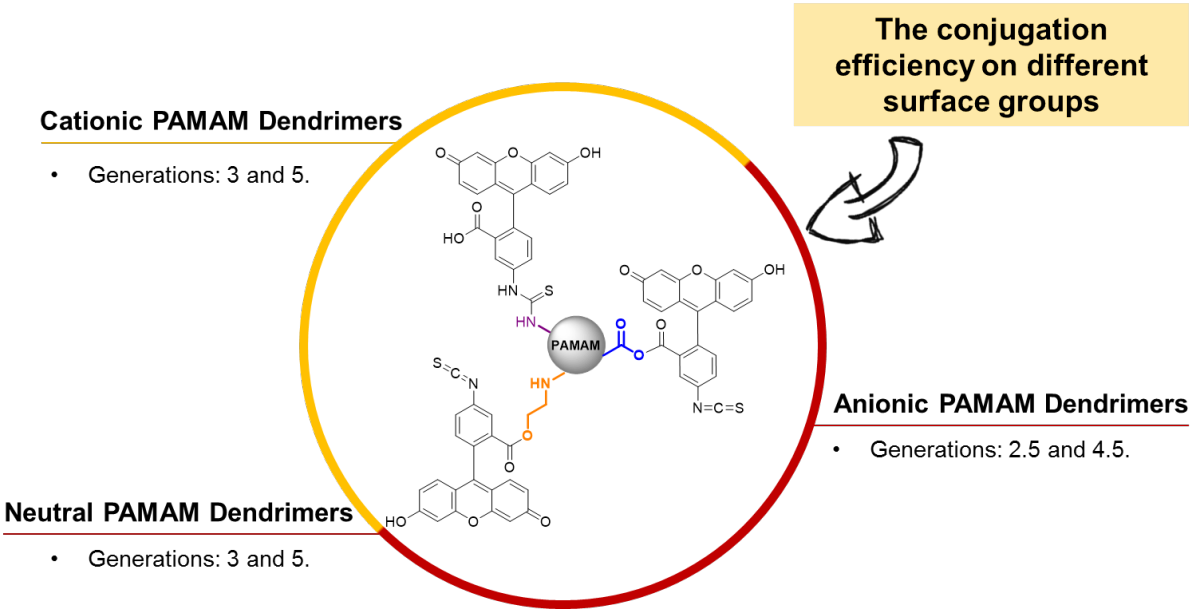

Figure 83 – Representation of the distinct FITC-PAMAM conjugates that are intended to be investigated and explored in the current thesis.

In order to investigate the conjugation efficiency of FITC with the PAMAM dendrimers, the aim of this thesis is to characterize all the products by distinct analytical techniques (*i.e.* ^{1}H NMR, UV/Vis, FTIR). Additionally, the study of other physicochemical properties of the FITC-PAMAM conjugation products is also expected including, surface charge measurements and assessment of fluorescent intensity at distinct concentrations and pH conditions.

Furthermore, we intend to verify the applicability of FITC-PAMAM conjugates for cell studies through a preliminary analysis of the *in vitro* cytotoxicity (resazurin assay) on the mouse embryonic fibroblast cell line NIH 3T3.

The Figure 84 gives a more detailed information regarding the main objectives of the current thesis.

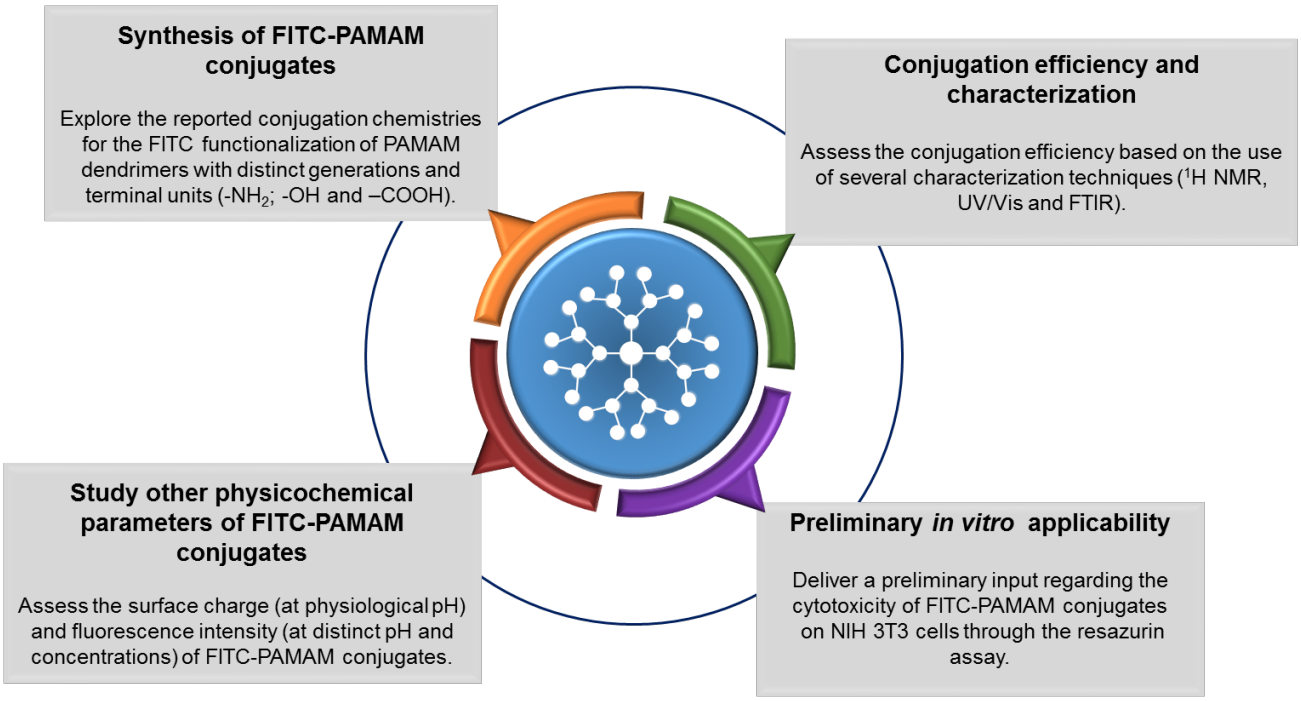

Figure 84 –The main objectives of the current thesis.

Part 2. Materials and methods

Contents

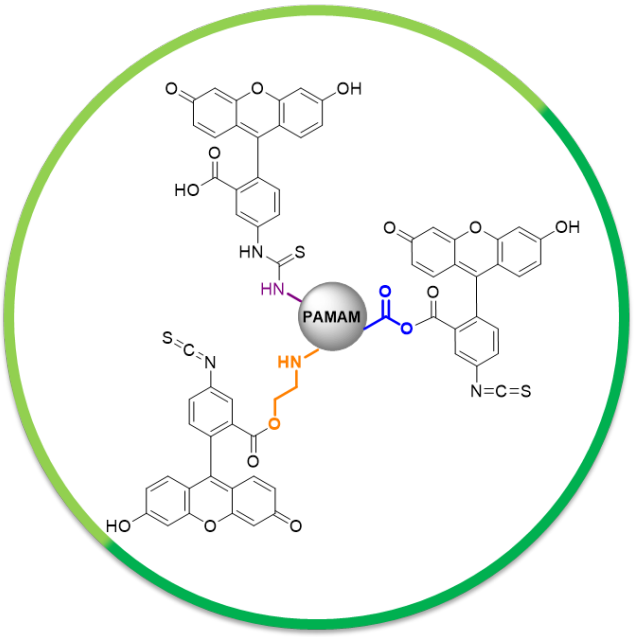

2. Materials and methods

In this section, we report the adopted procedures for the surface functionalization of PAMAM dendrimers with the FITC fluorescent probe. As such, herein we describe the reaction conditions and purification methods that we found to be the most suitable for the acquisition of the best yields and conjugation efficiencies. The characterization methods used for the analysis of the conjugation products are also described in detail.

At the end of this section, the parameters used in the studies of the cell cytotoxicity and effect of pH on the fluorescence of the FITC-PAMAM conjugates are also presented.

2.1. Synthesis of FITC-PAMAM conjugates

2.1.1. Materials

The Fluorescein isothiocyanate (FITC, Isomer I, ≥ 90%), N-(3-Dimethylaminopropyl)-N'-ethyl-carbodiimide hydrochloride (EDC, purum > 98%) and the phosphate buffered saline (PBS) were from Sigma-Aldrich. The N-dimethylamino pyridine (DMAP, 99%) was from Acros Organics. The EDA-core PAMAM dendrimers, in methanol, with 100% -NH_2, -OH and –COONa end groups, respectively, were from Dendritech ® (Midland, MI, USA). The dimethyl sulfoxide (DMSO, analytical grade) was from Fisher Scientific. The Methanol (AnalaR Normapur, Reagent Ph. Eur.) and Chloroform (AnalaR Normapur, Reagent Ph. Eur., stabilized with about 0.6% of ethanol) were from VWR. The absolute Ethanol (Pro Analysis, 99.5 %) was from Panreac. The dialysis membranes were from SpectrumLabs (Spectra/Por ® 7 Dialysis Membrane with MWCO cut-off of 1000 D (flat width: 38 mm)). The PD-10 desalting columns (Sephadex G25M) were from GE Healthcare. The ultra-pure (UP) water used in all experiments was obtained through the Millipore Milli-Q purification system with a resistivity higher than 18.2 MΩ.cm (at 25 ºC). The TLC plates (Silica Gel 60) were from Merck.

2.1.2. Preparation and purification of FITC-PAMAM-NH_2 conjugates

For the preparation of the FITC-PAMAM-NH_2 conjugates, the G3 and G5 EDA-core PAMAM dendrimers with 100% -NH_2 surface groups were used.

Although several attempts were accomplished for the preparation and purification of these conjugates based on distinct molar ratios PAMAM:FITC (1:5; 1:12; 1:14; 1:17; 1:20), reaction conditions (*i.e.* such as conjugation time, solvents, pH) and purification techniques (*i.e.* dialysis and PD-10 desalting columns), herein we only report the optimized procedures that produced a quantity of product that was enough for their characterization and biological study. The preparation and purification conditions were adapted from previous published works[128,248,255–257].

The conditions used for the preparation of the FITC-G3PAMAM-NH_2 conjugate are schematically shown in Figure 85 (1:14 PAMAM:FITC ratio). Briefly, the G3 PAMAM-NH_2 dendrimer (300 mg, 43.4 μmol) in methanol was dispersed in 25 mL of PBS solution (0.1 M, pH 9.1). Then, the conjugation was started by dropwise addition of the FITC solution (91 mg, 233.7 μmol in 18 mL of DMSO). The reaction was allowed to proceed for 18 hours with stirring under dark conditions and at room temperature. No precipitation was observed during this reaction. After that time, the orange solution was extensively dialyzed against distilled and UP water for 3 days. The dialyzed solution was then lyophilized yielding *ca.* 129 mg of an orange solid. The efficiency of the dialysis was followed through TLC using methanol:chloroform (1:1) as mobile phase. Despite the fact that the characterization indicated a successful conjugation, we were unable to purify the final product completely, even when using the PD-10 desalting columns. The spot related with the free FITC was always detected in the TLC (see Annexes – Section B). Given the complexity of the conjugate spectra, only the most important peaks from the ^{1}H NMR, FTIR and UV/Vis characterization are reported in the Table 7.

Table 7 – Summary table containing the key data associated with the characterization of the FITC-G3PAMAM-NH_2 conjugate.

Technique	Main peaks
^{1}H NMR*	δ (ppm) = 2.37-3.39 (m, overlapping, protons of the –C*H*$_2$- groups of the dendrimer), 3.71 (b, aliphatic proton from C*H*$_2$NHC=S); 6.50-7.54 (b, aromatic protons of FITC).
UV/Vis	λ_{max} of FITC-G3PAMAM-NH_2 conjugate = 502 nm.
FTIR**	ATR (*v*, cm^{-1}): 3252 (w, b, -NH_2 PAMAM); 1100 (w, b, thiourea bond from FITC-PAMAM).
Zeta potential	ξ (mV) = 12.73 ± 0.29 (in PBS, pH = 7.4).

* The ^{1}H NMR data is expressed as follows: chemical shift, peak nature and multiplicity (m, multiplet; b, broad);

** The FTIR data is expressed as follows: wavenumber (cm^{-1}) and peak nature (w, weak; b, broad);

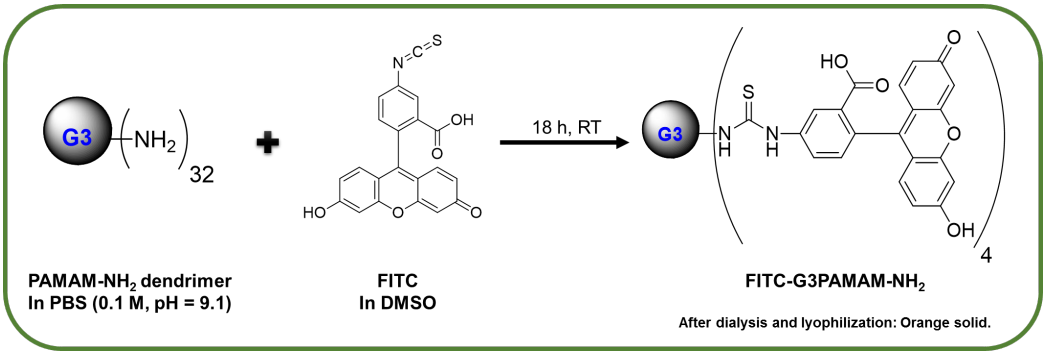

Figure 85 – Conjugation conditions for the preparation of the FITC-G3PAMAM-NH_2 conjugate (1:14 PAMAM:FITC molar ratio).

The conditions used for the preparation of the FITC-G5PAMAM-NH_2 conjugate are schematically shown in the Figure 86 (1:17 PAMAM:FITC molar ratio).

The G5PAMAM-NH_2 dendrimer (252 mg, 8.74 μmol) in methanol was dispersed in 25 mL of PBS (0.1 M, pH 9.1). Then, the conjugation was started by the dropwise addition of the FITC solution (55 mg, 152 μmol in 12 mL of DMSO). The reaction was allowed to proceed for 18 hours with stirring under dark conditions and at room temperature. After that time, the orange solution was extensively dialyzed against UP water for 3 days. The dialyzed solution was then lyophilized yielding *ca.* 300 mg of an orange solid. The efficiency of the dialysis was followed through TLC using methanol:chloroform (1:1) as mobile phase. As referred before for G3PAMAM-NH_2, despite the fact that the characterization indicated a successful conjugation, we were unable to completely purify the final product from the unconjugated FITC fluorescent dye even when using the PD-10 desalting columns (Sephadex G25M). The spot related with the free FITC was always detected in the TLC (see Annexes – Section B). Given the complexity of the conjugate spectra only the most important peaks from the ^{1}H NMR, FTIR and UV/Vis characterization are reported in the Table 8.

Table 8 - Summary table containing the key data associated with the characterization of the FITC-G5PAMAM-NH_2 conjugate.

Technique	Main peaks
^{1}H NMR*	δ (400 MHz, D_2O, ppm) = 2.38-3.39 (m, overlapping, protons of the –CH_2- groups of the dendrimer), 3.71 (b, aliphatic proton from CH_2NHC=S); 6.52-7.54 (b, aromatic protons of FITC).
UV/Vis	λ_{max} of FITC G5PAMAM-NH_2 conjugate = 503 nm.
FTIR**	ATR (*v*, cm^{-1}): 3252 (w, b, -NH_2 PAMAM); 1100 (w, b, thiourea bond from FITC-PAMAM).
Zeta potential	ξ (mV) = 18.83 ± 1.45 (in PBS, pH = 7.4).

* The ^{1}H NMR data is expressed as follows: chemical shift, peak nature and multiplicity (m, multiplet; b, broad);

** The FTIR data is expressed as follows: wavenumber and peak nature (w, weak; b, broad);

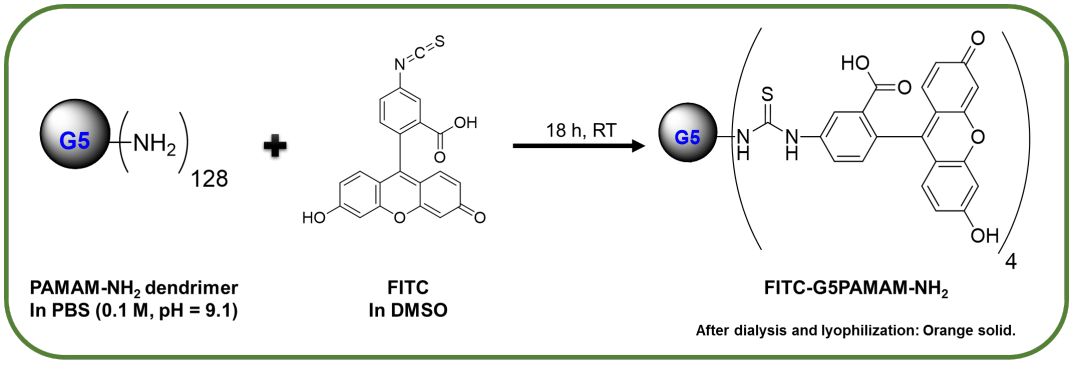

Figure 86 - Conjugation conditions for the preparation of the FITC-G5PAMAM-NH_2 conjugate (1:17 PAMAM:FITC molar ratio).

2.1.3. Preparation and purification of FITC-PAMAM-OH conjugates

G3 and G5 EDA-core PAMAM dendrimers with 100% -OH surface groups were used for the conjugation with the FITC fluorescent dye. Similarly to the $–NH_2$ conjugates, several reaction parameters were tuned in order to obtain the FITC-PAMAM-OH reaction products in enough quantities for their characterization and biological analysis. Given that some of the employed purification methods resulted in the loss of great quantities of product only the methods that provided a balance between the efficiency and yield were applied. All the preparation and purification steps reported below are adapted procedures from previous reported works[128,235,257].

As a result, the reaction conditions followed for the preparation of the FITC-G3PAMAM-OH conjugate are schematically shown in Figure 87 (1:8 PAMAM:FITC molar ratio). To the FITC solution (60 mg in 12 mL of DMSO, 154 µmol), the EDC (90 mg, 469 µmol) and catalytic amounts of DMAP (*i.e.* 10 % mol in relation to the limiting reagent) were added. This mixture was stirred for about 20 minutes. After that time, the G3PAMAM-OH (130 mg, 19 µmol) was added to the previous mixture and the materials were left to react for 48 hours, with stirring, under dark conditions and at room temperature. After conjugation, the dark orange solution was extensively dialyzed against UP water for 3 days. This orange solution was then lyophilized yielding *ca.* 147 mg of an orange solid. The purification through dialysis was followed by TLC using methanol:chloroform (1:1) as mobile phase. Although the characterization data indicated a successful conjugation, we were unable to completely purify the final product from the unconjugated FITC fluorescent dye under the conditions available in the current work. Given the complexity of the product spectra only the most important peaks from the ^{1}H NMR, FTIR and UV/Vis characterization are reported in the Table 9.

Table 9 - Summary table containing the key data associated with the characterization of the FITC-G3PAMAM-OH conjugate.

Technique	Main peaks
^{1}H NMR*	δ (400 MHz, D_2O, ppm) = 2.43-3.64 (m, overlapping, protons of the –C*H*$_2$- groups of the dendrimer); 4.08 (b, aliphatic protons from RCOO-C*H*$_2$-); 6.58-7.10 (b, aromatic protons of FITC); 7.97 – 7.99 (b, d, N*H* of dendrimer interior).
UV/Vis	λ_{max} of FITC-G3PAMAM-OH conjugate = 500 nm.
FTIR**	ATR (*v*, cm^{-1}): 3264-2825 (w, b, -OH surface groups and interior –NH of PAMAM); 1324-1200 (w, b, ester bond from FITC-PAMAM).
Zeta potential	ξ (mV) = -6.10 ± 0.48 (in PBS, pH = 7.4).

* The ^{1}H NMR data is expressed as follows: chemical shift, peak nature and multiplicity (m, multiplet; b, broad);

** The FTIR data is expressed as follows: wavenumber and peak nature (w, weak; b, broad);

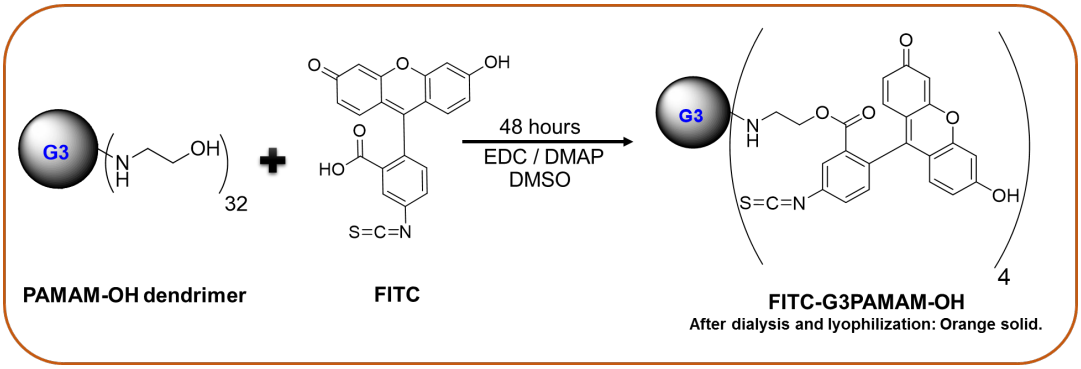

Figure 87 - Conjugation conditions for the preparation of the FITC-G3PAMAM-OH conjugate (1:8 PAMAM:FITC molar ratio).

The reaction conditions applied for the synthesis of FITC-G5PAMAM-OH conjugate are schematically shown in Figure 88 (1:11 PAMAM:FITC molar ratio). Briefly, to the FITC solution (51 mg in 15 mL of DMSO, 130 µmol), the EDC (65 mg, 340 µmol) and catalytic amounts of DMAP (*i.e.* 10 % mol in relation to the limiting reagent) were added. This mixture was stirred for about 20 minutes. After that time, the G5PAMAM-OH (333 mg, 11.5 µmol) was added to the previous mixture and the materials were left to react for 48 hours, with stirring, under dark conditions and at room temperature. After the conjugation, the dark orange solution was extensively dialyzed against distilled water for 3 days. The dialyzed sample was then lyophilized yielding *ca.* 300 mg of an orange solid. The purification through dialysis was followed by TLC using methanol:chloroform (1:1) as mobile phase. As before, although the characterization data indicated a successful conjugation, we were unable to completely purify the final product from the unconjugated FITC fluorescent dye under the conditions available in the current work. Given the complexity of the product spectra only the most important peaks from the ^{1}H NMR, FTIR and UV/Vis characterization are reported in the Table 10.

Table 10 - Summary table containing the key data associated with the characterization of the FITC-G5PAMAM-OH conjugate.

Technique	Main peaks
^{1}H NMR*	δ (400 MHz, D_2O, ppm) = 2.43-3.64 (m, overlapping, protons of the –CH_2- groups of the dendrimer), 4.09 (b, aliphatic protons from RCOO-CH_2-); 6.59-7.21 (b, aromatic protons of FITC); 7.97 – 7.99 (b, d, NH of dendrimer interior).
UV/Vis	λ_{max} of FITC-G5PAMAM-OH conjugate = 505 nm.
FTIR**	ATR (ν, cm^{-1}): 3253-2825 (w, b, -OH surface groups and interior –NH of PAMAM); 1328-1200 (w, b, ester bond from FITC-PAMAM).
Zeta potential	ξ (mV) = -5.05 ± 0.44 (in PBS, pH = 7.4)

* The ^{1}H NMR data is expressed as follows: chemical shift, peak nature and multiplicity (m, multiplet; b, broad);

** The FTIR data is expressed as follows: wavenumber and peak nature (w, weak; b, broad);

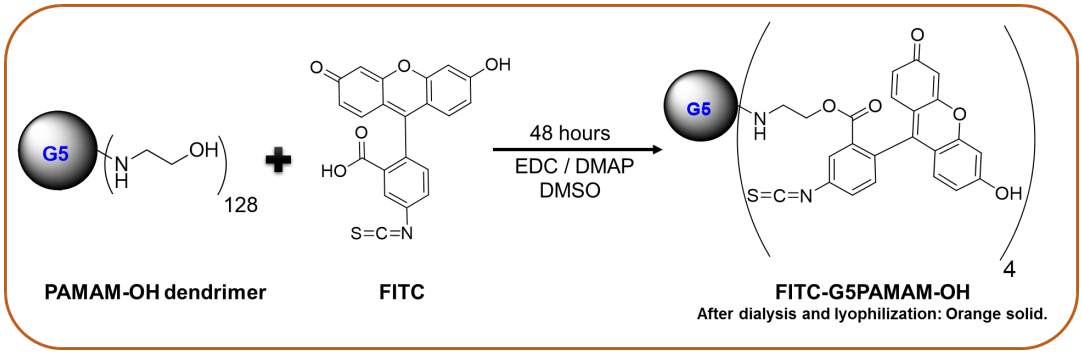

Figure 88 - Conjugation conditions for the preparation of the FITC-G5PAMAM-OH conjugate (1:11 PAMAM:FITC molar ratio).

2.1.4. Preparation and purification of FITC-PAMAM-COOH conjugates

Similarly to the previous cases, several conjugation parameters were tuned in order to prepare the FITC-PAMAM-COOH conjugates. To this end, the G2.5, and 4.5 EDA-core PAMAM dendrimers with 100% -COONa surface groups were used in order to prepare the conjugates since that they contain an equivalent number of terminal groups of the previously selected PAMAM-NH_2 and PAMAM-OH dendrimers.

Despite our efforts and several attempts, the unequivocal preparation and characterization of the final FITC-PAMAM-COOH conjugates could not be achieved using the conditions reported in this thesis. All the reaction parameters described below were adapted procedures from reported methods[128,235].

The conditions followed for the preparation of the FITC-G2.5PAMAM-COOH conjugate are schematically shown in Figure 89 (1:9 PAMAM:FITC molar ratio).

Briefly, the FITC (84 mg, 216 µmol) was dissolved in 20 mL of absolute ethanol and the EDC (105 mg, 631 µmol), catalytic amounts of DMAP (*i.e.* 10 % mol in relation to the limiting reagent) and 1 M NaOH were added. After that, these materials were left to react for about 40 minutes with stirring at room temperature and protected from the light. After, the FITC solution was added in a dropwise fashion to the G2.5PAMAM-COOH dendrimer in methanol (140 mg, 22 µmol). The reaction was allowed to proceed for 48 hours with stirring, under dark conditions and at room temperature. The resulting orange solution was extensively dialyzed against UP water for 3 days. The dialyzed solution was then lyophilized yielding *ca.* 178 mg of a yellow/pale orange solid. The dialysis purification was followed by TLC using methanol:chloroform (1:1) as mobile phase. Like the previous cases, the complete removal of the unconjugated FITC dye was unsuccessful. Furthermore, the characterization data did not provide enough evidences of an effective conjugation. Regardless of these results, the most important peaks from the ^{1}H NMR, FTIR and UV/Vis characterization are reported in the Table 11.

Table 11 - Summary table containing the key data associated with the characterization of the FITC-G2.5PAMAM-COOH conjugate.

Technique	Main peaks
^{1}H NMR*	δ (400 MHz, D_2O, ppm) = 2.63-3.66 (m, overlapping, protons of the –C*H*$_2$- groups of the dendrimer), 4.28-4.26 (?); 6.60-7.34 (aromatic protons of FITC).
UV/Vis	λ_{max} of FITC-G2.5PAMAM-COOH conjugate = 490 nm.
FTIR**	ATR (*v*, cm^{-1}): 3253-2825 (w, b, interior –NH of PAMAM); 1378-1000 (w, b, from FITC).
Zeta potential	ξ (mV) = -9.07 ± 0.64 (in PBS, pH = 7.4)

* The ^{1}H NMR data is expressed as follows: chemical shift, peak nature and multiplicity (m, multiplet; b, broad);

** The FTIR data is expressed as follows: wavenumber (cm^{-1}) and peak nature (w, weak; b, broad);

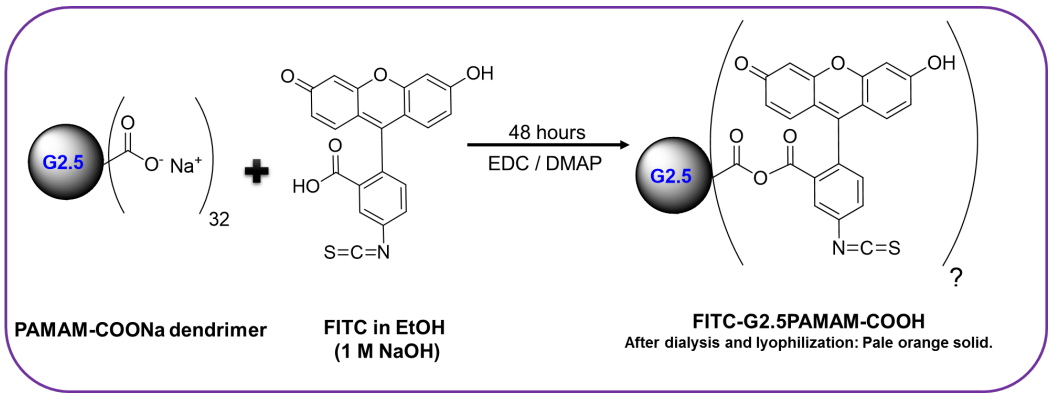

Figure 89 – The explored conjugation conditions in an attempt to prepare the FITC-G2.5PAMAM-COOH conjugate (1:9 PAMAM:FITC molar ratio).

The conjugation conditions adopted for the preparation of the FITC-4.5PAMAM-COOH conjugate are schematically shown in the Figure 90 (1:15 PAMAM:FITC molar ratio).

Summarily, the G4.5-COONa PAMAM dendrimer (200 mg, 8 μmol) was dispersed in 37 mL of UP water. The FITC (46 mg, 119 μmol) solution was then prepared in 18 mL of ethanol with 1 M NaOH. After that, the FITC solution was added in a dropwise fashion to the dendrimer solution along with the EDC (55 mg, 287 μmol) and catalytic amounts of DMAP. The reaction was allowed to proceed for 48 hours with stirring, under dark conditions and at room temperature. After that time the orange solution was extensively dialysed against distilled and UP water for 3 days. The dialysed solution was then lyophilized yielding *ca.* 147 mg of a yellow/pale orange solid.

Like the previous cases, the complete removal of the unconjugated FITC dye was unsuccessful. Also, in this case, the characterization data did not provide enough evidences of an effective conjugation. Regardless of this limitation, the most important peaks from the ^{1}H NMR, FTIR and UV/Vis characterization are reported in the Table 12.

Table 12 - Summary table containing the key data associated with the characterization of the FITC-G4.5PAMAM-COOH conjugate.

Technique	Main peaks
^{1}H NMR*	δ (400 MHz, D_2O, ppm) = 2.63-3.66 (m, overlapping, protons of the –CH_2- groups of the dendrimer), 4.33 (?); 6.60-7.34 (aromatic protons of FITC).
UV/Vis	λ_{max} of FITC-G4.5PAMAM-COOH conjugate = 502 nm.
FTIR**	ATR (*v*, cm^{-1}): 3253-2825 (w, b, interior –NH of PAMAM); 1200-1000 (w, b, from FITC).
Zeta potential	ξ (mV) = -14.50 ± 0.42 (in PBS, pH = 7.4)

* The ^{1}H NMR data is expressed as follows: chemical shift, peak nature and multiplicity (m, multiplet; b, broad);

** The FTIR data is expressed as follows: wavenumber (cm^{-1}) and peak nature (w, weak; b, broad);

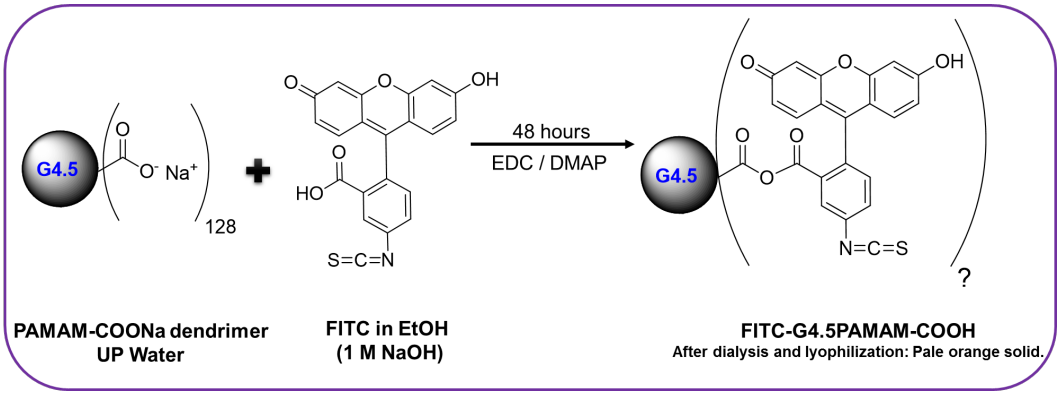

Figure 90 - The explored conjugation conditions in an attempt to prepare the FITC-G4.5PAMAM-COOH conjugate (1:15 PAMAM:FITC molar ratio).

2.2. Characterization of FITC-PAMAM conjugates

In order to assess the successfulness of the conjugation reactions, all the FITC-PAMAM conjugates and the unconjugated dendrimers/FITC fluorescent dye were fully characterized by ^{1}H NMR, UV/Vis, FTIR and zeta potential measurement as described below.

2.2.1. ^{1}H NMR

For the ^{1}H NMR characterization of all the compounds, a Bruker Avance II+ 400 MHz equipment at 25 ºC (probe temperature) was used. The chemical shifts (δ) are presented in ppm and calibrated based on the residual solvent peaks. The ^{1}H NMR spectrum of FITC was recorded by dissolving the compound in deuterated methanol (MeOD, Merck, 99.96 %). All the other compounds were dispersed in deuterated water (D_2O, Merck, 99.99 %).

Table 13 shows the minimum amounts of sample needed for an adequate ^{1}H NMR characterization of the FITC-PAMAM conjugates. Due to the differences in molecular size between

the small FITC units and the PAMAM dendrimer scaffolds, longer acquisition times (*i.e.* 128 scans, 30 minutes) were needed to obtain well-resolved NMR spectra. All the NMR data were treated using the Mnova NMR ® software, v9.1. The ^{1}H NMR spectra of the non-conjugated dendrimers were obtained with inferior acquisition times when compared with the FITC-PAMAM conjugates. As a result, some peaks associated with the dendrimer were only visible upon longer acquisition times (*e.g.* protons of interior amides, -N*H*). Additionally, the ^{1}H NMR of FITC-PAMAM conjugates was obtained using three distinct deuterated solvents (*i.e.* DMSO-d6, MeOD and D_2O). Given the greater solubility and lower interference in the spectrum, the D_2O was chosen for the acquisition of ^{1}H NMR spectra of all conjugates.

^{13}C NMR was also obtained for some of the compounds in order to investigate any change on the PAMAM dendrimer carbons in the vicinity of the newly formed bonds. However, based on the conventional acquisition times we were unable to obtain a well resolved spectra that could provide the intended information.

Table 13 – Minimum amounts of sample needed for an adequate ^{1}H NMR characterization.

Compound	Mass (in mg)	Volume of D_2O (in µL)
FITC-G3-NH_2	5.076	550
FITC-G5-NH_2	5.166	550
FITC-G3-OH	6.716	550
FITC-G5-OH	8.200	550
FITC-G2.5-COOH	8.708	550
FITC-G4.5-COOH	5.118	550

2.2.2. UV/Vis

All the UV and UV/Vis spectra were obtained using a Perkin Elmer Lambda 25 spectrophotometer. All the measurements were accomplished using a stopped quartz cell and with a scan interval between 190 and 900 nm. The conjugated and non-conjugated materials were dissolved in UP Water. The FITC-PAMAM conjugates were analyzed at the concentration of 0.02 mg/mL. The UV/Vis spectrum of unconjugated FITC was obtained by dissolving the compound in UP water at concentration of 0.01 mg/mL. The resulting spectrum was adjusted to the absorbance scale of the corresponding conjugates. As a reference, the UV/Vis spectrum of unconjugated FITC in MeOH was also acquired at concentration of 0.2 mg/mL (shown in the annexes, section A, no adjustments were done).

2.2.3. FTIR

All the FTIR spectra were obtained through an ATR coupled Perkin Elmer Spectrum Two spectrometer. The IR spectra were collected by pressing small amounts of sample on a Diamond/ZnSe crystal. All the spectra were acquired at the resolution of 4 cm^{-1}, with a minimum number of 20 scans and along the spectral range of 4000 to 400 cm^{-1}.

2.2.4. Zeta potential

The zeta potential measurements were performed using a Zetasizer Nano ZS equipment from Malvern Instruments Ltd., UK. The measurements were made at 25 °C in a folded capillary cell from Malvern. In the first measurements, the equipment was left to calibrate for 180 seconds.

In order to determine the surface charge of the conjugation products in similar conditions of the physiological medium, the samples were dispersed in 0.01 M PBS (pH = 7.4) at the optimal concentrations for this type of analysis (2 mg/mL). Each sample was measured in triplicate and the average and standard deviations were later calculated. The reported zeta potential values for the higher generation PAMAM dendrimers with the distinct terminal groups can be found in the annexes, section A7.

2.2.5. Effect of pH on fluorescence intensity of FITC-PAMAM conjugates

In order to elucidate the fluorescent behavior of FITC-PAMAM conjugates during the acidic endosomal/lysosomal maturation events, the fluorescence intensity of G4.5 and G5 FITC-PAMAM conjugates was measured at different concentrations and pH values.

The fluorescence intensity was measured through a spectrofluorometer (Perkin Elmer LS 55) by dispersing the FITC-PAMAM conjugates in 0.01 M PBS at different pH values (4, 5.4, 6.4 and 7.4) and concentrations (0-4 μg/mL). The fluorescence intensity of the unconjugated FITC dye was also measured in the same conditions to be used as reference. All the measurements were accomplished by recording the fluorescence intensity at λ = 515 nm.

2.3. Preliminary cytotoxicity studies of the FITC-PAMAM conjugates

The usefulness of the prepared FITC-PAMAM conjugates for cell studies was explored through the preliminary analysis of their cytotoxic behavior. All the conditions applied for this study are described in the next sections.

2.3.1. Cell culture conditions for cytotoxicity analysis

All cell culture studies were accomplished using a mouse embryonic fibroblast cell line NIH 3T3 acquired from DSMZ. For that purpose, NIH 3T3 cells were grown in 10 cm^2 cell culture dishes (Fisher Scientific) using Dulbecco's Modified Eagle Medium (DMEM, Sigma) supplemented with 1 % of antibiotic/antimycotic and 10 % of Fetal Bovine Serum (FBS, Gibco) – referred as complete medium from now on. The cells were cultured in an incubator (at 37 ºC with 5% CO_2 atmosphere) until the desired number of cells were achieved and before reaching confluence. For this reason, the NIH 3T3 cells were sub-cultured every 48 hours and harvested from sub-confluent cultures using trypsin-EDTA (0.1 mL/cm^2). After the removal of nonadherent cells and medium exchange at each 24 hours, the cells were harvested at day 3 for subsequent studies.

2.3.2. Effect on cell viability of FITC-PAMAM conjugates

The generation 4.5 (-COOH termini) and 5 (-NH_2 and –OH termini) FITC-PAMAM conjugation products were selected for the preliminary cytotixicity studies, since that the higher generation PAMAM dendrimers are the most commonly explored for biological applications.

The cytotoxicity of these conjugates with distinct terminal groups was evaluated through the resazurin reduction assay. This assay relies on the evaluation of metabolically active cells that convert the non-fluorescent dye, resazurin, into a fluorescent product, resorufin, which can then be measured using a fluorimeter. By this way, the cell viability was determined in percentage and in relation to the unexposed cells, by establishing a direct correlation between the cell metabolic activity and the number of viable cells.

In this study, the cell viability was evaluated as a function of the FITC functionalized PAMAM dendrimers containing distinct terminal groups (-NH_2; -OH and –COOH). For this purpose, the NIH 3T3 cells different were exposed to distinct concentrations (2.5-25 µg/mL) of the conjugates for 3 hours. In order to minimize possible interactions between the FBS and PAMAM dendrimer conjugates, the medium was depleted of serum during the incubation time.

Briefly, the NIH 3T3 cells were seeded in 48 well plates (Fisher Scientific) at the density of $2x10^4$ $cell.cm^{-2}$ with DMEM complete medium and left to incubate at 37 ºC with 5 % CO_2 atmosphere. After 24 hours, the complete medium was replaced by a fresh one without FBS. Then 50 µL of each stock solution of FITC-PAMAM conjugates in PBS (pH=7.4) were added in order to obtain the intended exposure concentration. As reference, a statistically representative number of cells were also individually treated with: a) complete medium only (positive control); b) complete medium + PBS (negative control, 10% PBS v/v); c) unconjugated FITC at the concentrations of the corresponding conjugated dye and; d) the unconjugated PAMAM dendrimers at the same concentration of the conjugated ones.

After 3 hours, the cell culture medium was removed and complete, fresh, DMEM medium containing 10% v/v of a 0.1 mg/mL resazurin solution (Sigma-Aldrich) was added to each well. The cells were then left to incubate for 2 hours at 37 ºC and 5 % CO_2. Past that time, 100 µL of the medium, from each well, were transferred to a 96 opaque well-plate and the fluorescence was measured using a microplate reader (Victor^3 1420, PerkinElmer) at λ_{ex} = 530 nm, λ_{em} = 590 nm. All the samples were analyzed based on six replicates.

Part 3. Results and discussion

Contents

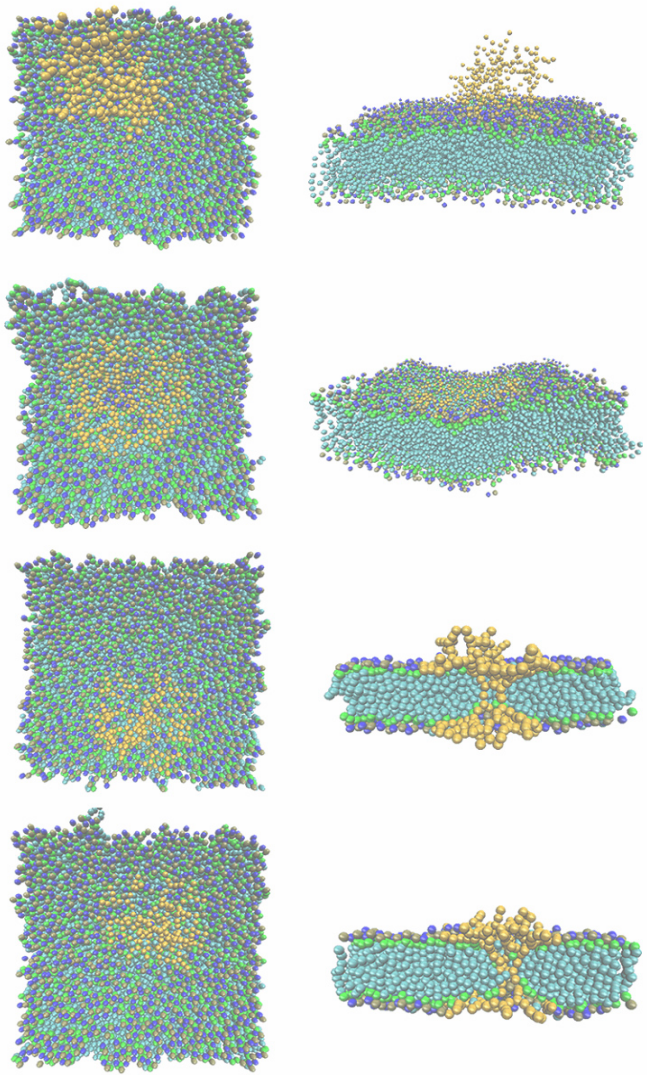

Molecular dynamics simulation of a G4 PAMAM-NH_2 dendrimer interacting with lipid bilayer. Figure taken from: Tian, W.; Ma, Y. Insights into the Endosomal Escape Mechanism via Investigation of Dendrimer-Membrane Interactions. *Soft Matter* **2012**, *8*, 6378–6384.

3. Results and discussion

3.1. Synthesis and characterization of FITC-PAMAM-NH_2 conjugates

Firstly, it is worth mentioning that the preparation of the FITC-PAMAM-NH_2 conjugates was not as straightforward as it might look, and it required several attempts for the acquisition of the proper functionalization levels and yields. Moreover, the conjugation method applied in the current thesis followed the similar conditions of many other reported works, however many of them did not provide the sufficient characterization data required for an unequivocal confirmation of the conjugation efficiency and purity[128,235,245,248,258]. By opposing these trend, herein we try to provide a more careful overview in terms of the characterization of these conjugates.

In this work, the preparation of the FITC-PAMAM-NH_2 conjugates was accomplished by covalently linking the FITC dye to the primary amine groups of the PAMAM scaffold through a thiourea bond. The literature is great regarding the reaction between primary amines and isothiocyanate groups[259,260]. Thanks to the stability of the isothiocyanate groups in most of the solvents and their readily reactivity with primary amines, the FITC has been widely used for the conjugation with several amine-containing moieties, including proteins or dendrimers[176,177].

The inherent reactivity of FITC fluorescent dye comes from the ability of the isothiocyanate groups to react under the optimal conditions with nucleophiles like the amines. Note that, usually this reaction is highly selective to primary amine groups and produces the only stable final products. As shown in Figure 91, this reaction starts with the nucleophile attack (-NH_2) on the central electrophilic carbon of the FITC isothiocyanate group. This event leads to an electron shift that results on the formation of a thiourea bond between the FITC dye and the PAMAM dendrimer[176]. Although dependent on the molar ratios and intended conjugation levels, the reaction usually proceeds completely after 18 hours[261].

It is important to note that the FITC has a better solubility in solvents like DMSO, ethanol or acetone and a low solubility in water. For this reason, when the reactions proceed in aqueous solutions, the pH of the medium must be higher than 6 in order to improve the solubility of the FITC dye*. Moreover, in this work, the FITC solutions were always freshly prepared and kept in the dark due to its light-sensitivity and relatively low stability in aqueous environments†.

Moreover, the reaction between the FITC and the PAMAM-NH_2 dendrimers requires the existence of alkaline conditions since that, at this pH, the primary amines are not completely protonated and as result are in the reactive form for the conjugation with the isothiocyanate group of the FITC[176,261–263].

*At alkaline pH, the cyclization of the FITC carboxyl groups is prevented resulting in higher solubility in water.
†A less fluorescent derivative is formed (aminofluorescein) when the FITC is exposed for long periods of time in aqueous solutions.

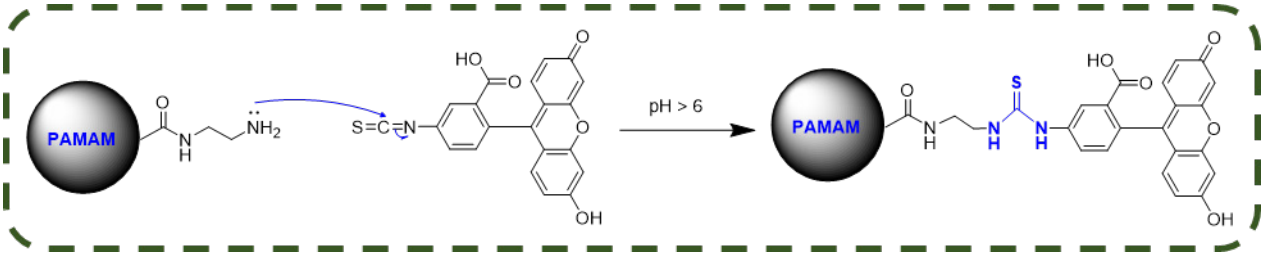

Figure 91 – Representation of the reaction between the primary amines from PAMAM dendrimers and the electrophilic carbon from the FITC isothiocyanate group.

It is important to mention that the formed thiourea bond as a limited stability due to possible hydrolytic events, however it is reported that the PAMAM-FITC conjugates are stable for at least 7 days at room temperature[248,264–266]. For the best of our knowledge although no methodological study has been done, it is expected that at low temperatures (*i.e.* 4 ºC), the hydrolysis is delayed, resulting on an increased lifetime of the conjugate.

As described before, two different purification methods were employed in order remove the unconjugated FITC dye. The extensive dialysis along with the purification through gel permeation chromatography (GPC, PD-10 columns) resulted to be ineffective for the complete purification of the final product (see annexes – section B). Such results contradict previously reported successful purifications solely based on these methods[128,248]. Always having in mind the importance of a pure product for the cell studies, different purification parameters (*i.e.* dialysis times and different elution conditions) were explored in the current thesis, however they were always ineffective to yield the desired purity level.

Furthermore, it has been reported that the stochastic conjugation method used in the current work produces heterogeneous populations that are very difficult to purify by dialysis or standard column chromatography techniques (see section 1.6). More recently, it has been shown that preparative HPLC has proven to be useful for the purification of these conjugates yielding products of higher homogeneity[160,234,264]. Unfortunately, due to technical limitations we were unable to proceed with the purification of the FITC-PAMAM-NH_2 conjugates by this approach.

It is also important to mention that, herein, higher molar ratios of FITC fluorescent dye were used in order to achieve a successful conjugation. Although not shown here, our observations suggested that lower molecular ratios (< 1:10 PAMAM-NH_2:FITC) usually resulted in very low conjugation efficiencies (< 1 dye per dendrimer). As a result, our increased FITC molar ratios may have escalated the difficulty to purify the conjugates simply based on dialysis or the gravimetric separation by GPC.

Despite the high molar ratios, it is important to have in mind that our purpose was always to proceed with a limited FITC surface functionalization of the PAMAM-NH_2 scaffold, mainly for two reasons. Firstly, the extensive conjugation of the FITC would result in a distinct dendrimer surface

nature and in which could affect its interaction with the biological interface. Secondly, it is known that 2 to 5 FITC molecules provides the optimal level for posterior visualization. Usually a higher degree of conjugated dye results in self-quenching effects due to the greater spatial proximity of the fluorescent molecules and their relatively small Stokes shifts[160,262].

Furthermore, with the procedures applied in the current work, the yields were always limited due to the high number of manipulations associated with the purification steps. For that reason, in the final preparation attempts only extensive dialysis was used with the goal of purifying as much as possible the final conjugates but at the same time with a reduced impact over the yield. Due to the possible existence of unconjugated FITC and its unclear effect on the final mass, the yields were not calculated in percentage (see section 2.1.2).

The conjugation efficiency between the G3 and G5 PAMAM-NH_2 dendrimers and the FITC was assessed through the ^{1}H NMR characterization. The ^{1}H NMR spectra of both FITC-PAMAM-NH_2 conjugates are shown in the Figures 92 and 93.

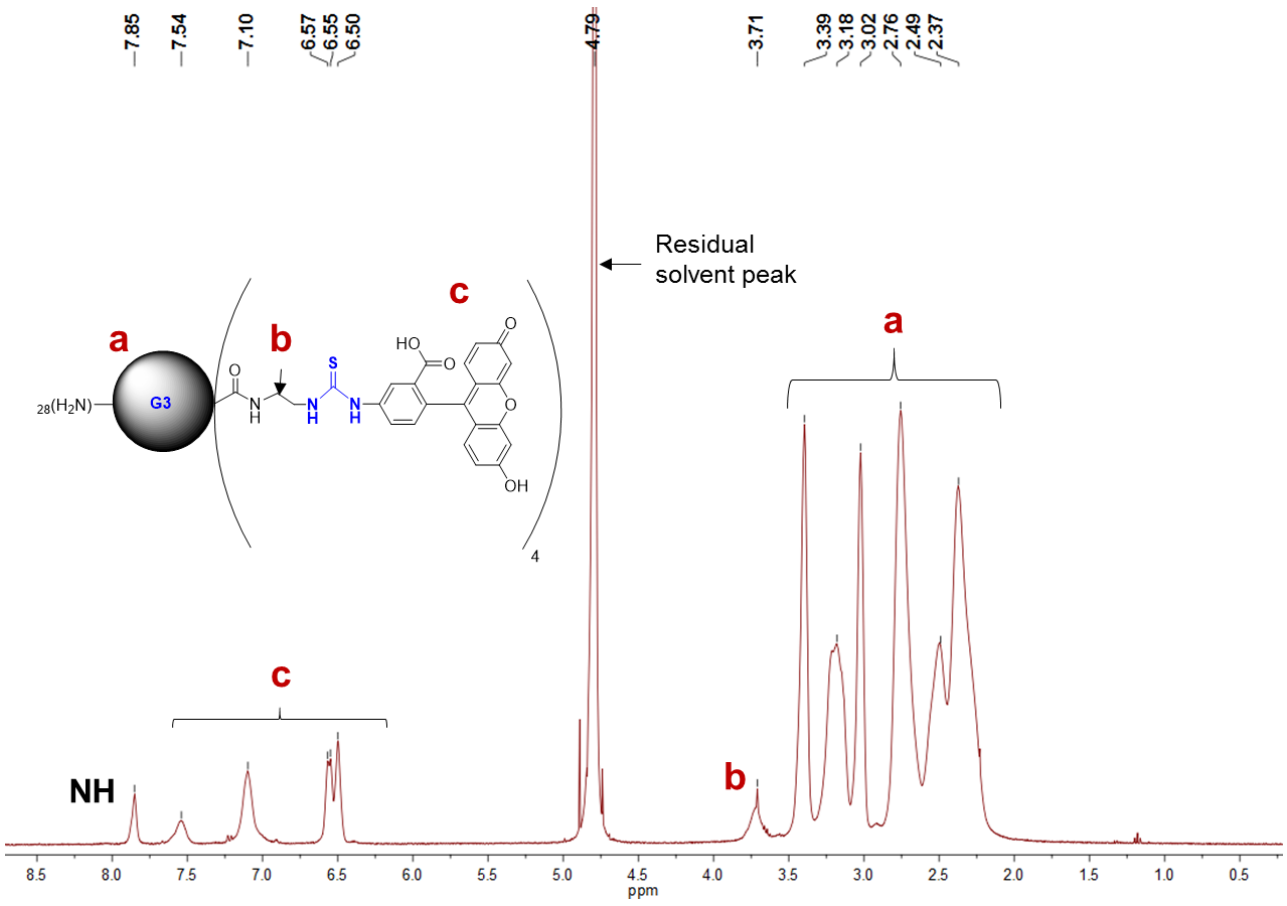

Figure 92 – The ^{1}H NMR spectrum of the FITC-G3PAMAM-NH_2 conjugate in D_2O (at 400 MHz).

As shown in the Figures 92 and 93 and despite the purity level of the synthesized conjugates, the appearance in both spectra of the peaks between 6.50-7.13 ppm (aromatic protons of FITC) along

with the one at 3.17 ppm provided evidences of a successful conjugation between the PAMAM-NH_2 dendrimers and the FITC. It has been previously described that the appearance of the broad peak around 3.71 ppm arises from the successful formation of the thiourea bond. This peak is observed due to the change on the chemical shift (deprotection) of the neighbor methylene protons near the newly formed FITC-PAMAM bond (marked with "b" in the spectra)[128,248]. The peaks marked with the "a" come from the methylene groups of the PAMAM scaffold. For comparative purposes, the stacked NMR spectra of the conjugates along with the unconjugated dendrimer and FITC can be found in the annexes, section A.

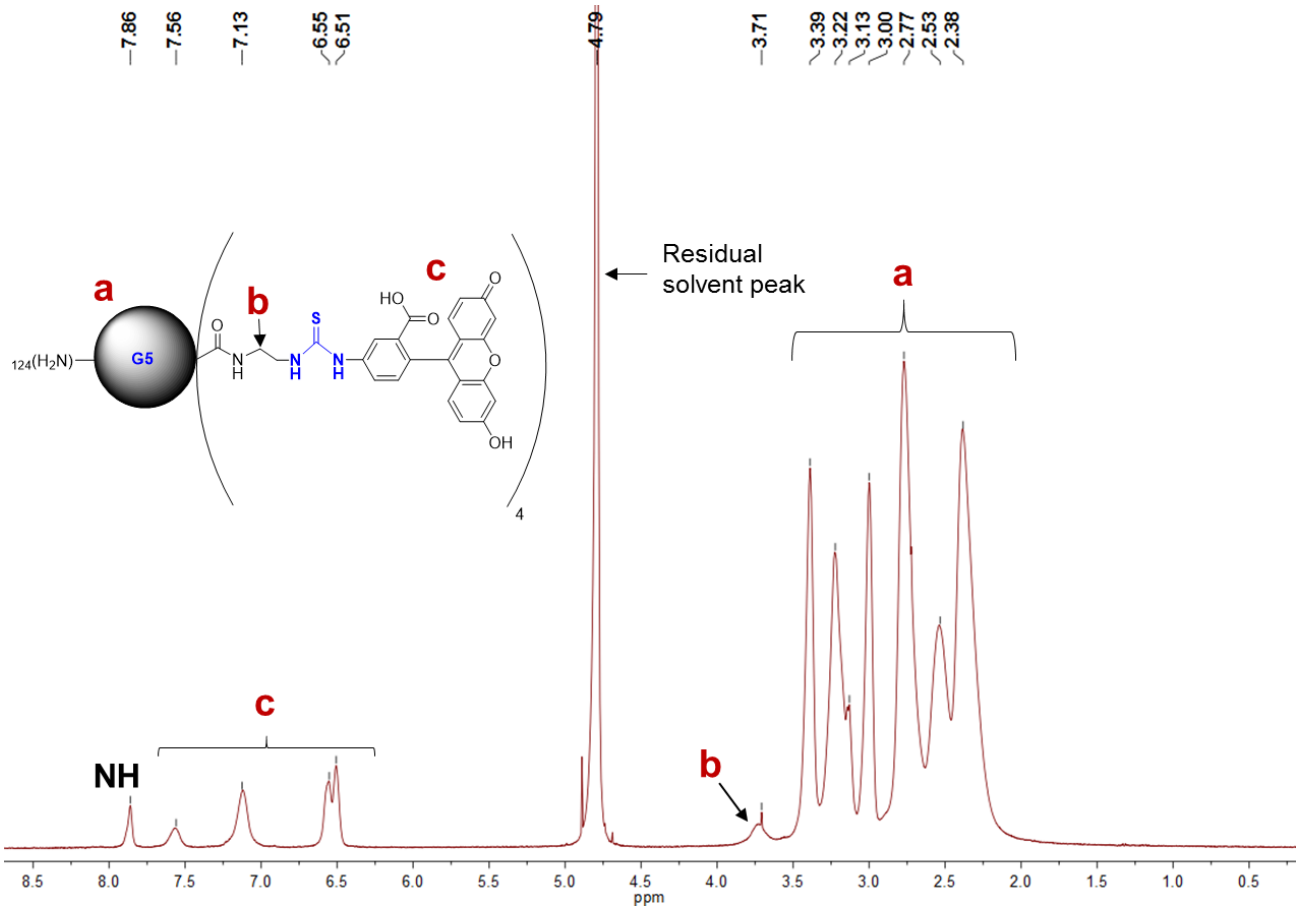

Figure 93 - The ^1H NMR spectrum of the FITC-G5PAMAM-NH_2 conjugate in D_2O (at 400 MHz).

In this case, the number of FITC molecules per dendrimer scaffold was determined based on the ^1H NMR characterization. However, it is important to note that the conjugation values presented in the Figures 92 and 93 are just an estimation and correspond to an average of whole sample population. Simply explained, the conjugation efficiency was predicted by performing the ratio between the integral values of the peaks corresponding to the dendrimer methylene protons near the thiourea bond (3.71 ppm) and the aromatic protons of the FITC dye (6.51-7.56 ppm). Based on this calculation, it was predicted that both conjugates contained an average number of 4 FITC molecules

per dendrimer. In the same way, other works have also reported similar conjugation efficiencies based on identical calculations and at analogous reaction conditions[104,128,235,248,267].

It is worth mentioning that, although the G5 PAMAM-NH_2 scaffold contains a greater number of terminal groups, the conjugation efficiency was similar to the G3 PAMAM dendrimer. Again, it is important to remember that the presented values are just an approximation of the whole population. Additionally, it is also important to have in mind that, at higher generations, the steric crowding and back-folding of the terminal groups can also limit the accessibility in post-functionalization approaches.

Although the FTIR and the UV/Vis characterization do not provide *per se* enough evidences of a successful conjugation, they were used to complement the ^{1}H NMR characterization. The UV/Vis and FTIR spectra are shown in the Figures 94 and 95, respectively. The stacked UV/Vis and FTIR spectra containing the unconjugated dendrimer and FITC can be found in the annexes (see section A).

Similarly to other reported works, herein based on the UV/Vis characterization, a shift in λ_{max} (480 nm) of the free FITC, to the 502 nm on the conjugation products, provided further evidences of a successful reaction between the both PAMAM dendrimer generations and the fluorescent dye. Although still unclear, this redshift may be attributed to a change on the aromatic system of the FITC dye, by which an energy transfer phenomenon takes place after conjugation[128,268].

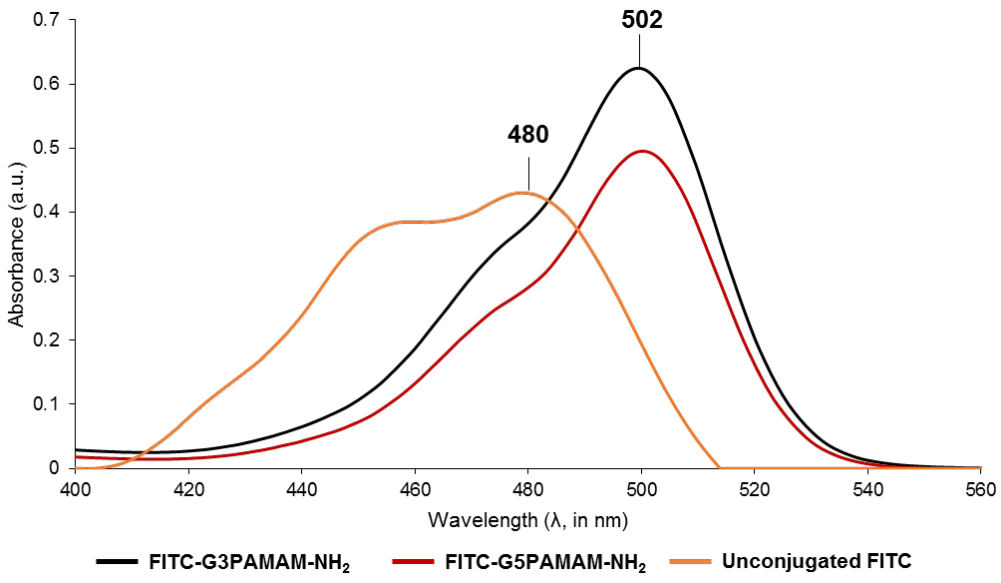

Figure 94 – UV/vis spectra of both FITC-PAMAM-NH_2 conjugates (0.02 mg/mL) and FITC (0.01 mg/mL) in UP water.

The FTIR results delivered additional evidences of a covalent conjugation between the FITC and the PAMAM scaffolds. In spite of the existence of a weak broad peak at 2100 cm^{-1} attributed to

the stretching of the unconjugated FITC isothiocyanate group, the appearance of the bands around the 1100-1300 cm^{-1} in the FTIR spectra, may be attributed to the stretching of the thiourea bond[128,266].

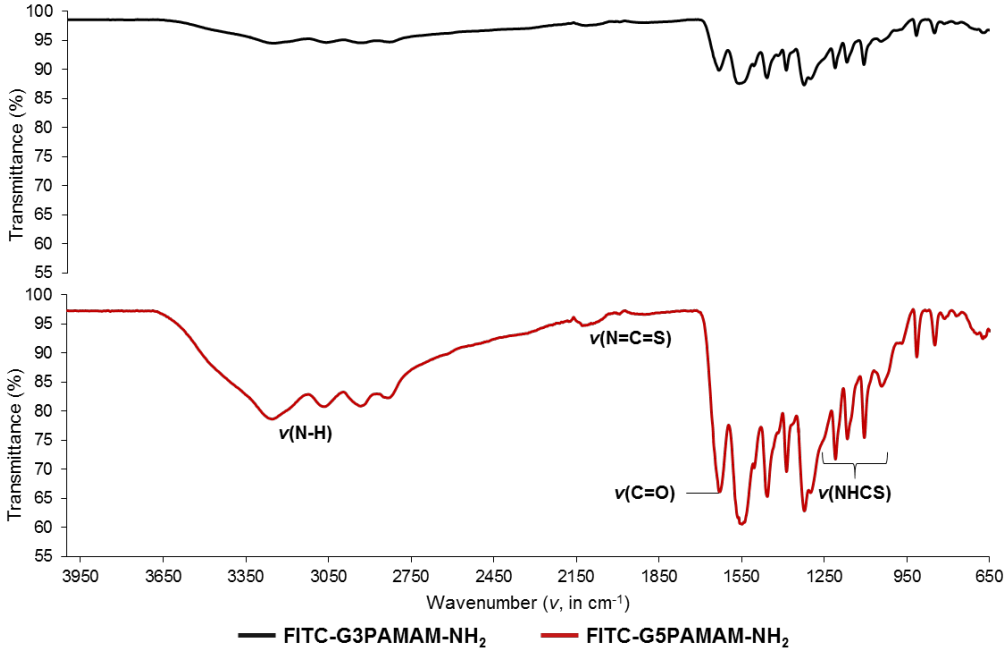

Figure 95 – FTIR spectra of both FITC-PAMAM-NH_2 conjugates.

In order to elucidate the surface charge of the FITC-PAMAM-NH_2 conjugates, their zeta potential was measured at the conditions referred in the section 2.2.4.

Similarly to previously reported observations, the reduced covalent conjugation of the FITC fluorescent dye did not induce any profound changes on the surface charge of the PAMAM-NH_2 dendrimers. Since that the conjugation extent was relatively small (average of 4 per dendrimer), only a slight portion of the dendrimer surface was consumed after conjugation[128,269,270]. However, it is important to note that this effect of surface consumption is greater for the G3 PAMAM-NH_2 dendrimers due to the lower number of terminal groups. Theoretically, in this work, while that for the G3 PAMAM-NH_2 dendrimers an average of 12 % of the surface was functionalized, in the G5 an average of 3 % of the surface groups were substituted with the FITC dye.

As shown in the Tables 7 and 8 (section 2.1.2), the zeta potential for the G3 and G5 PAMAM-FITC conjugates were 12.73 and 18.83 mV, respectively. Given the surface nature of the PAMAM-NH_2 dendrimer at the measured pH (7.4), these zeta potential values are in agreement with previous results[128,269,270]. Additionally, the increased zeta potential values of G5 conjugates arises from the greater number of charged amine end groups of these higher generation PAMAM-NH_2 dendrimers[128].

The literature is huge regarding the conjugation reactions between the FITC dye and the amine-terminated PAMAM dendrimers. The stochastic nature of these conjugation reactions produces heterogeneous samples that are difficult to purify, characterize and that may produce inconsistent results during cell studies. As previously reported, it is clear that the synthesis of monodisperse PAMAM-dye conjugates is the key for their applicability for cell colocalization studies. Additionally by clearly identifying the nature of the conjugates we can more easily relate their biological activity to certain parameters of their molecular structure[13,63,162].

As a result, with the novel methods appearing in the literature (*e.g.* one-step click chemistry reactions, see section 1.6), they are providing advancements for the applicability of more homogenous conjugates in the cell studies and in the biomedical field in general[13,63,162].

3.2. Synthesis and characterization of FITC-PAMAM-OH conjugates

Similarly to the previous conjugates, several attempts were needed in order to optimize the conjugation parameters for the preparation for the FITC-PAMAM-OH conjugates. It this case, different conjugation ratios and purification methods were used. The conjugation and purification conditions presented in the section 2.1.3 were the ones that provided a balance between the purity level and the desired yield.

Herein, the conjugation of the FITC dye with the PAMAM-OH scaffold of two different generations (G3 and G5) was accomplished by a one-step reaction through the formation of an ester bond. For this purpose, the conjugation between the -OH groups of the PAMAM dendrimer and the carboxyl groups of the FITC was made through the action of the N'-ethyl-carbodiimide hydrochloride (EDC) and N-dimethylamino pyridine (DMAP). This esterification reaction involving the EDC and DMAP is widely known as Steglich esterification[271]. The literature is great regarding this type of reactions, and many works have used this approach for the esterification between alcohols and carboxyl groups[271–275]. The proposed reaction mechanism for the Steglich esterification between the PAMAM-OH dendrimer and the FITC is shown in the Figure 96.

The Steglich esterification between the PAMAM-OH and FITC occurs at room temperature with the crucial presence of the DMAP. Usually the traditional reaction involves the use of N,N'-Dicyclohexylcarbodiimide (DCC) with DMAP, however DCC is poorly soluble on aqueous solutions and usually gives rise to by-products that a very difficult to remove at the end.

As a result, here, the conjugation was accomplished by the use of EDC, since it shows a greater solubility in aqueous solvents and the unreacted compounds can be more easily removed in this medium (*e.g.* by dialysis).

In the Steglich esterification, catalytic amounts of DMAP (~ 5 to 10 mol % of the limiting reagent) are enough to proceed with the reaction. In this situation, the DMAP as the function of an acyl transfer reagent.

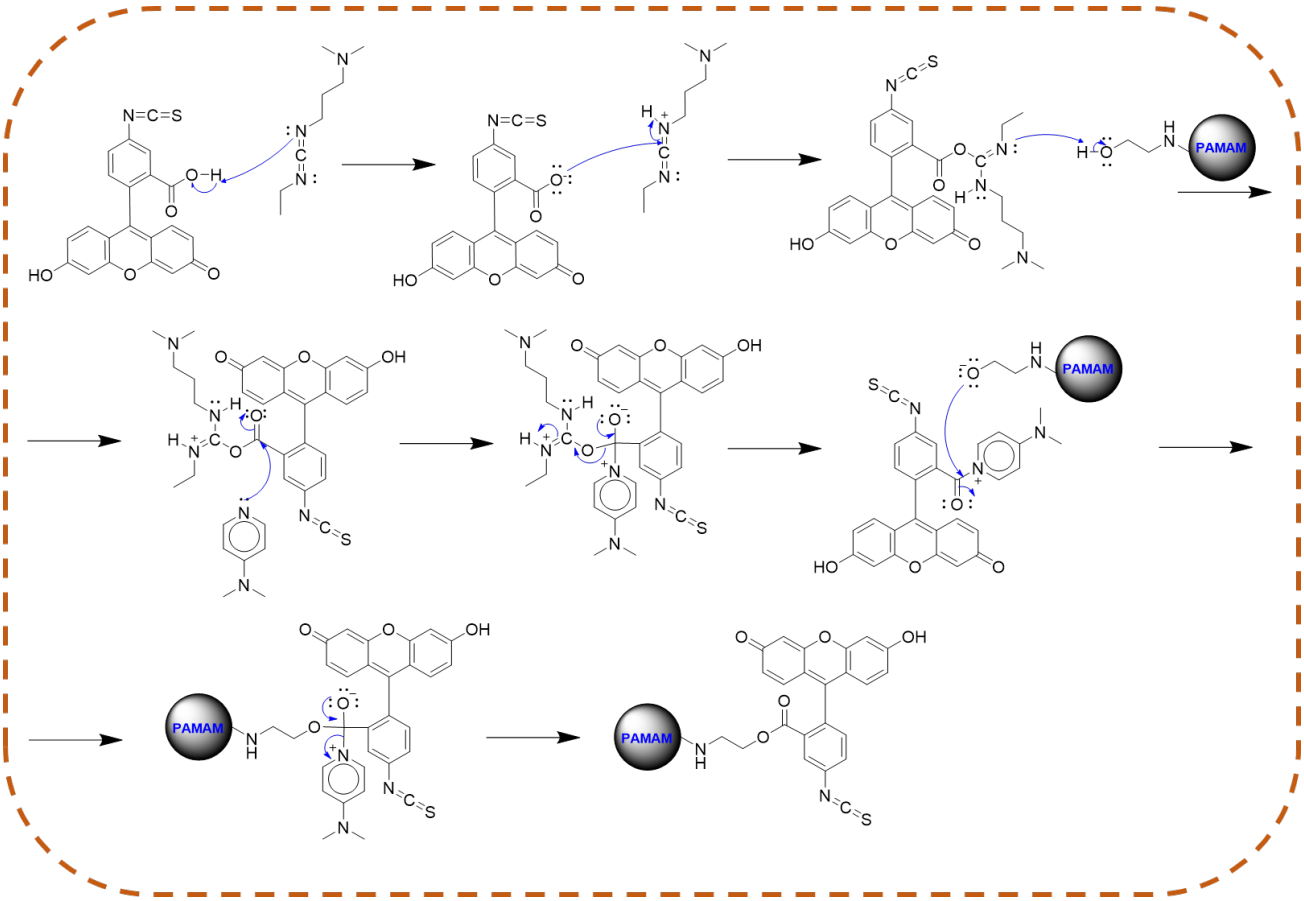

Figure 96 – The proposed Steglich esterification between the PAMAM-OH and the FITC dye through EDC chemistry and catalytic amounts of DMAP (Figure adapted from Ref. 275)

As shown in the Figure 96, the conjugation starts by the reaction between the carboxylic acid of the FITC and the nitrile of the EDC, giving rise to a more reactive intermediate, an *O*-acylisourea. This activated carboxylic acid is then able to react more easily with the alcohol terminal groups of the PAMAM dendrimer, which with the aid of DMAP catalyst gives rise to the ester bond.

It is known that the action of DMAP catalyst is crucial for the successful formation of the ester bond. The basic explanation behind this is that the DMAP is a stronger nucleophile than the alcohol, in which reacts with the *O*-acylisourea intermediate and gives rise to a reactive amide. As a result, this amide reacts rapidly with the alcohol giving rise to the ester. Moreover, since that the reaction between the *O*-acylisourea intermediate and the alcohol is relatively slow the formation of undesired by-products may occur if the DMAP is not present. Usually, these by-products arise from the rearrangement of the *O*-acylisourea intermediate into a N-acylurea that does not react with alcohols limiting by this way the final yield (see Figure 97)[274,275].

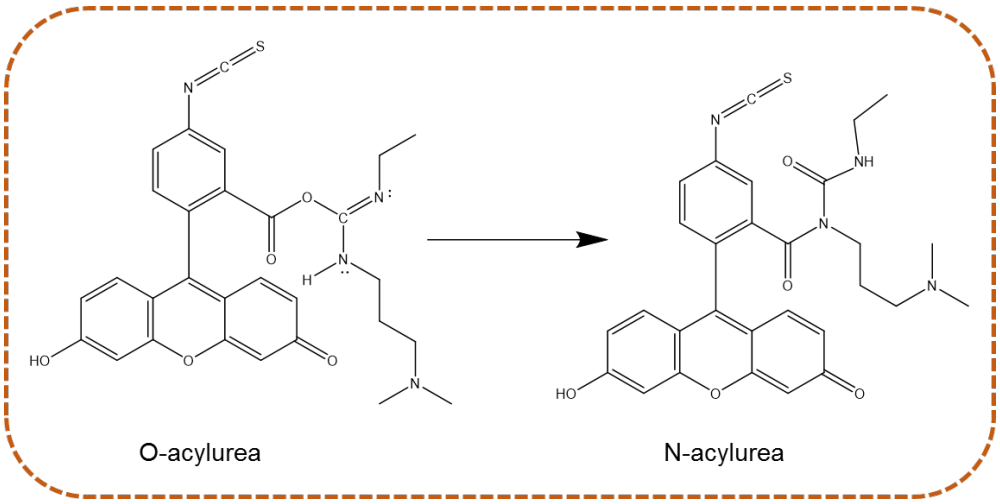

Figure 97 – The possible rearrangement of the reactive O-acylisourea form into the less reactive N-acylurea (Figure adapted from Ref. 272).

Since that in the current work the purpose was to prepare FITC-PAMAM-OH conjugates only as imaging agents, a low conjugation efficiency was intend in order to avoid any profound changes in the PAMAM-OH surface. Here, different molar ratios of FITC:PAMAM were applied for the two distinct PAMAM-OH dendrimer generations with the goal of achieving the intended low FITC-PAMAM surface functionalization. Clearly, in the case of the G3 PAMAM-OH, this ratio was lower, since that the number of terminal groups is inferior when compared with its higher generation counterpart (G5).

Both conjugates were characterized by ^{1}H NMR, UV/Vis, FTIR and zeta potential. The unconjugated PAMAM-OH dendrimers and FITC were also characterized by the same techniques to be used as a reference (see annexes, section A).

Similarly to the FITC-PAMAM-NH_2 conjugates, here, different purification techniques were also applied, however they were inefficient for the complete purification of the final products. Despite this fact, the characterization data indicates a successful conjugation of the FITC dye with the PAMAM-OH dendrimers.

Three distinct purification techniques were used including, dialysis, precipitation and gravimetric GPC (*i.e.* PD-10 desalting columns).

In the case of the dialysis, even with highly regular changes of the dialysis buffer, we were unable to purify the product completely.

On other hand, by reconstituting the conjugates in methanol and precipitating them in acetone, traces of free FITC could still be detected. Moreover, this approach always resulted in the loss of great quantities of the final product after filtration.

Finally, in the case of GPC, a sequential purification of the fractions was accomplished (see Figure 98). However, the spot of unconjugated FITC was always present in the TLC analysis (see annexes, section B). Also, this purification method resulted in the loss of great quantities of product.

Similarly to the FITC-PAMAM-NH_2 conjugates, the high molar ratios of the FITC dye used for the conjugation with the PAMAM-OH dendrimers may have increased the difficulty to purify the products solely based on the traditional purification techniques.

It is important to take into consideration that the purity analysis of these conjugates was always accomplished through TLC. As a result, based on this method, it may be difficult to determine the origin of the spot associated with the unconjugated FITC dye (see annexes, section B). For example, the probable existence of encapsulated dye cannot be disregarded and which may have been released during the TLC analysis. Accordingly, several works have reported the ability of PAMAM dendrimers to encapsulate dyes with a similar nature of FITC[276a-c]. Moreover, given the TLC separation conditions and the strong interaction of the dendrimer conjugate with the silica, the possible hydrolysis of the FITC-PAMAM bond should also be taken into consideration. Anyway, similar difficulties in terms of purification were also encountered in other published works upon comparable conditions of current thesis[276d].

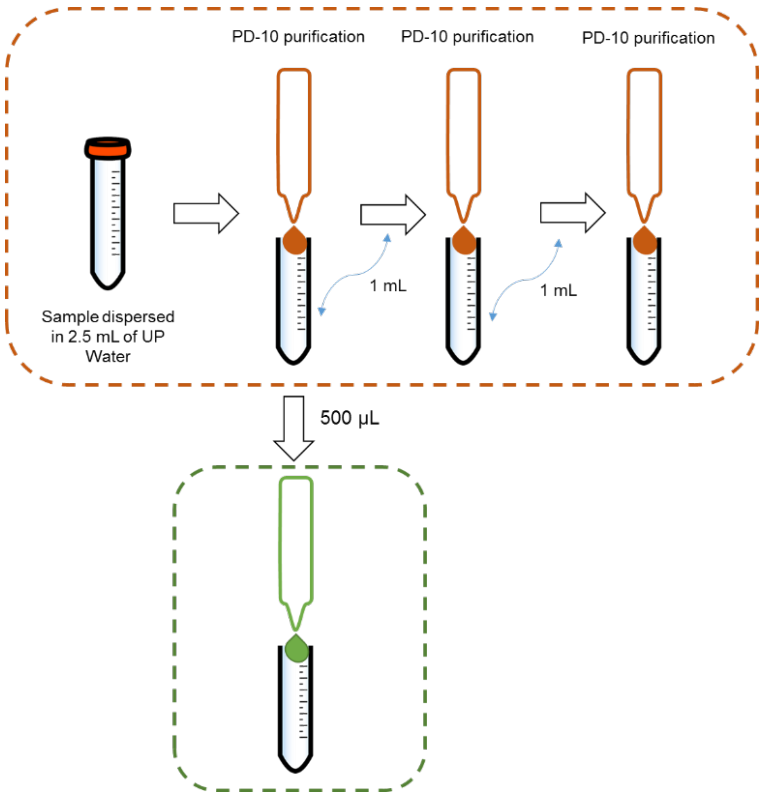

Figure 98 – The sequential purification of the FITC-PAMAM-OH conjugates by gel filtration chromatography. During the elution, several fractions were collected and verified by TLC. In any of the cases, the spot related with the free fluorescent dye was always observed. A similar approach was used for the FITC-PAMAM-NH_2 conjugates.

Provided the limited purification based on the aforementioned techniques, we decided to select a single purification technique capable of removing as much as possible the unreacted materials

without compromising too much the final yield. As a result, in the last preparation attempts, we only accomplished the partial purification of the FITC-PAMAM-OH by extensive dialysis.

Due to the possible presence of unconjugated FITC dye and its unclear impact over the final product, the yields are only presented in mass and not in percentage (see section 2.1.3).

The ^{1}H NMR spectra of the G3 and G5 FITC-PAMAM-OH conjugates are shown in the Figures 99 and 100, respectively.

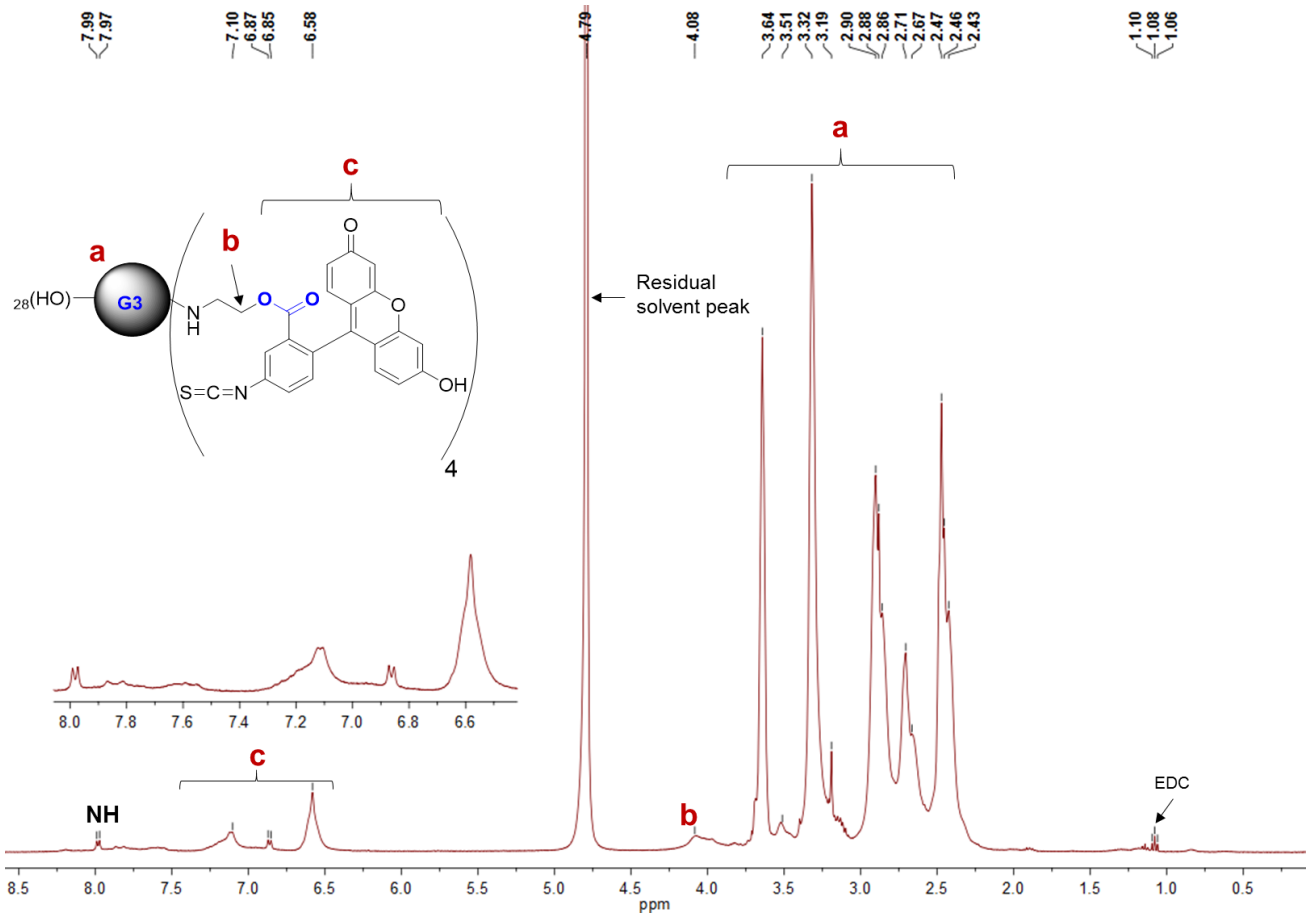

Figure 99 – The ^{1}H NMR spectrum of the FITC-G3PAMAM-OH conjugate in D_2O (at 400 MHz).

According to the data shown in the Figures 99 and 100, the distinct peak profile of the FITC aromatic protons (around δ = 6.58-7.10 ppm) and the appearance of a new peak at 4.08 ppm indicates the formation of the ester bond between the FITC and both PAMAM-OH dendrimers. Additionally, the shift of the aliphatic protons of the conjugated dendrimer in relation to the unconjugated counterpart (marked as “a”, see annexes sections A3 and A4) provided further evidences of the successful formation of a covalent bond between the FITC dye and the PAMAM-OH dendrimers.

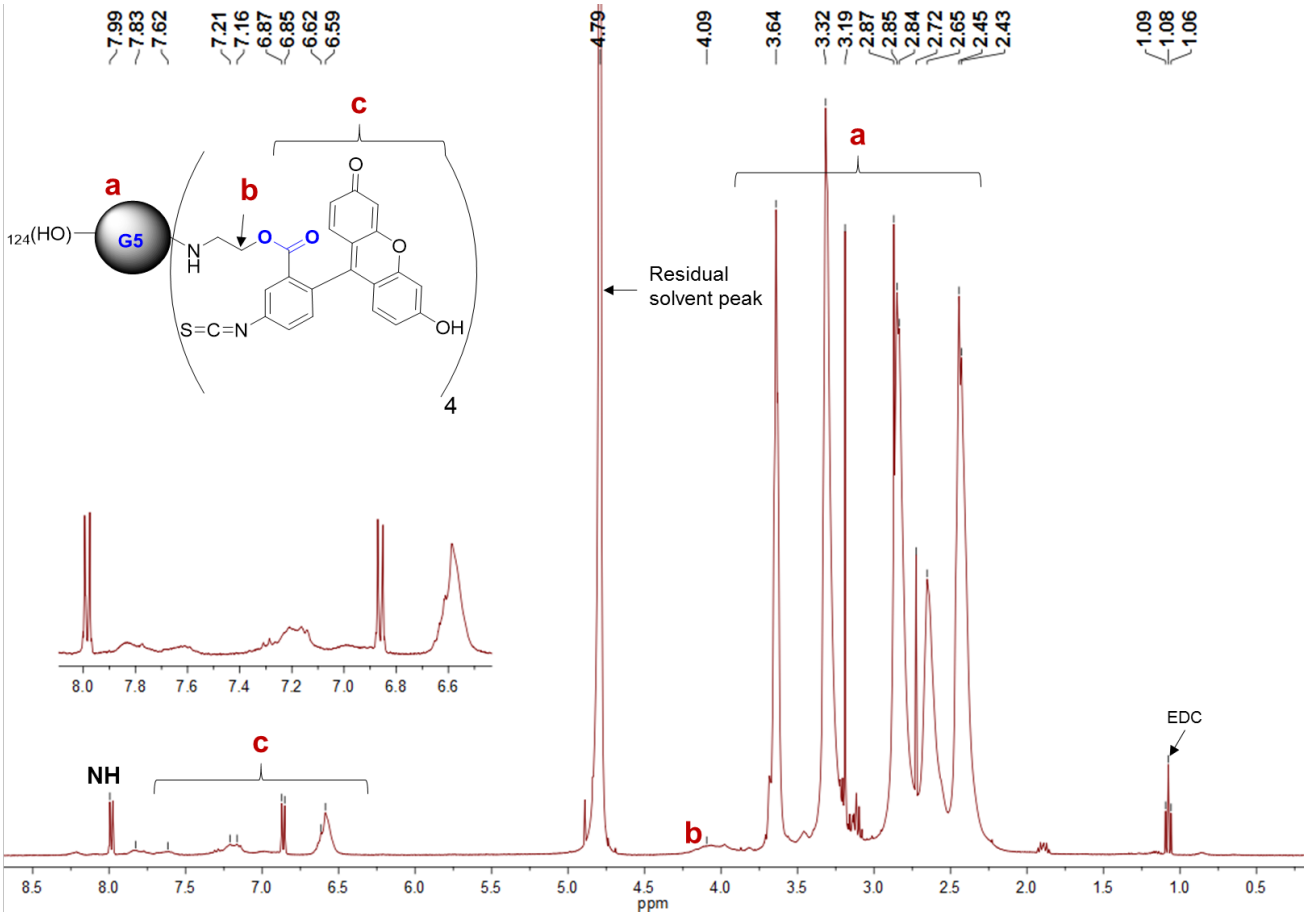

Figure 100 - The ^{1}H NMR spectrum of the FITC-G5PAMAM-OH conjugate in D_2O (at 400 MHz).

In the same way of the FITC-PAMAM-NH_2 conjugates, the number of FITC molecules per PAMAM-OH dendrimer was determined based on the data of the ^{1}H NMR spectra.

In the case of these FITC-PAMAM-OH conjugates, the conjugation efficiency was determined by doing the ratio of the integral values between the amidic protons of the PAMAM scaffold (δ = 7.97-7.99 ppm) and the aromatic protons of the FITC (δ = 6.59-7.21 ppm). Based on these calculations, for both dendrimer generations, an average of four FITC molecules were theoretically bond per PAMAM-OH scaffold. These results are similar to other reported values that applied the same calculations and conjugation conditions[235,257].

Again, in this case, we support that the possible back-folding of the G5 PAMAM-OH terminal groups may have limited the functionalization of additional terminal units. Also, it is important to highlight that the presented conjugation efficiency is only an average of the whole sample population[162].

In order to obtain additional information regarding the success of these reactions, both FITC-PAMAM-OH conjugates were also characterized by UV/Vis and FTIR. These spectra are shown in the Figures 101 and 102, respectively.

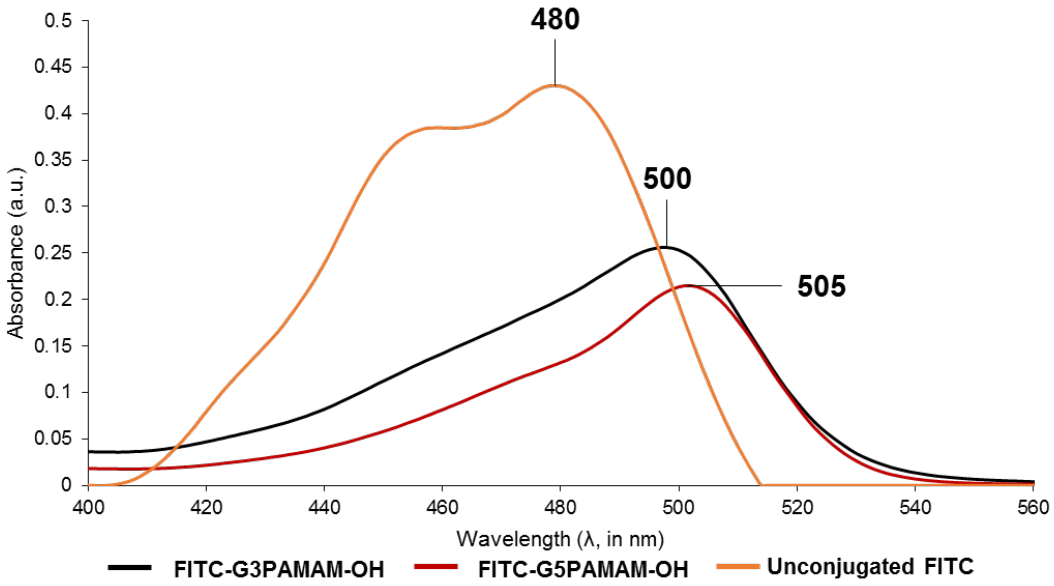

Figure 101 – UV/vis spectra of both FITC-PAMAM-OH conjugates (0.02 mg/mL) and FITC (0.01 mg/mL) in UP water.

In respect to the UV/vis spectra, in both conjugates, a red-shift of the FITC λ_{max} was observed (from 480 nm → 500 or 505 nm). Similarly to the FITC-PAMAM-NH_2 conjugates, in this case we support that the formation of the ester bond between the FITC and the PAMAM-OH dendrimers may have resulted in a slight change of the FITC electronic aromatic system (*e.g.* charge transfer events).

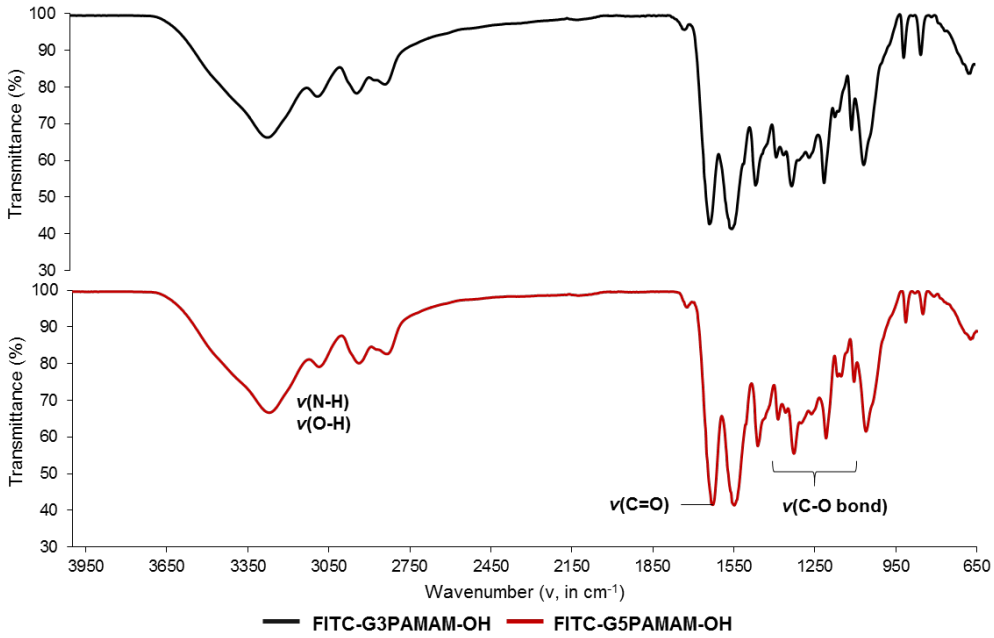

Figure 102 – FTIR spectra of the FITC-PAMAM-OH conjugates.

In combination with the ^{1}H NMR data, the appearance in both FTIR spectra of the peaks around 1300 – 1200 cm^{-1} may be associated with a vibrational mode of the newly formed ester bond (C-O). These results can further confirm the successful conjugation between the FITC dye and the PAMAM-OH dendrimers.

In order to determine the surface charge of the products, the zeta potential was measured in PBS at pH = 7.4. Given that at this pH, the hydroxyl surface groups of the PAMAM scaffold are weakly ionized, they mainly exhibit a surface charge that is close to zero. Our results are consistent with this statement, where the zeta potential observed for the G3 and G5 FITC-PAMAM-OH products were -6.10 and -5.05 mV respectively. These results are comparable to reported values at similar conditions[128,234]. The obtained zeta potential values show that no profound changes in the surface charge of the PAMAM-OH dendrimer occurred as a function of the conjugation reaction.

As shown along this section, the preparation of FITC-PAMAM-OH conjugates is far from being a facile and straightforward task. The stochastic method followed for the conjugation reactions does not allow a fine control of the functionalization degree and in which may produce heterogeneous samples with different types of FITC-PAMAM populations. Such variability increases the difficulty to purify the final products properly. Although not accomplished in this work, we recommend that the extent of unconjugated FITC should be investigated in order to predict its impact over the whole product (*e.g.* by HPLC). It is clear that the TLC analysis is not enough to accomplish such findings.

Furthermore, as referred at the end of the section 3.1, it is crucial to follow preparation methods (*e.g.* click chemistry) capable of producing homogenous PAMAM-dye conjugates that can be more easily purified and characterized. Additionally, the preparation of such homogenous samples facilitates the acquisition of more consistent and reproducible results during cell studies by allowing a feasible relationship between the biological activity and their molecular structure.

3.3. Synthesis and characterization of FITC-PAMAM-COOH conjugates

For the preparation of the FITC-PAMAM-COOH conjugates, we faced the similar issues of the previous compounds. Likewise, several attempts were accomplished based on the use of different reaction parameters (*i.e.* such as molar ratios, reaction times, pH) in order to fluorescently label the G2.5 and G4.5 PAMAM-COOH dendrimers. Nevertheless, as we will see in the next paragraphs, based on the conditions reported in this work we were unable to clearly characterize and confirm the conjugation between the FITC dye and the both generation PAMAM-COOH scaffolds.

Since that the purpose of the current work was to fluorescently label the PAMAM-COOH dendrimers with minimal surface modification, we avoided the conjugation methods involving the prior-modification of the carboxyl dendrimer surface for an improved bonding efficiency with the FITC (*e.g.* with EDA[128,277]). As a result, we decided to follow the previously reported one-step reaction

comprising the use of EDC and DMAP at alkaline conditions, without any prior modification of the PAMAM-COOH terminal groups[235,278].

The reactions applied in the current work relied on the previously reported observations where carbodiimides may be used for the preparation of acid anhydrides in the absence of other more reactive species like amines or alcohols[279–281]. For the best of our knowledge, since no reaction mechanisms have been proposed for the EDC/DMAP conjugation of FITC and PAMAM-COOH dendrimer, herein in the Figure 103, we show a general scheme that represents the possible reaction between them.

As shown in the Figure 103, the reaction proceeds in a similar way of the previous PAMAM-OH conjugates. However, in this case, the critical step for the formation of the anhydride bond depends on the absence of other stronger nucleophiles. If that is the case, the carboxyl terminated dendrimers can react with the “active” amide (intermediary formed by DMAP) and give rise to an anhydride. The reaction must occur at alkaline pH, since that at this pH most of the PAMAM carboxyl groups are in their reactive form (not protonated) and the activity of the EDC is also higher.

In this type of reactions, the presence of the DMAP is also crucial for the reaction to occur and avoid the formation of other side-products[279,281,282]. It is worth mentioning that according to previously reported conditions, parameters such as nature of the solvent or the carbodiimides may influence the fate and successfulness of these reactions[279].

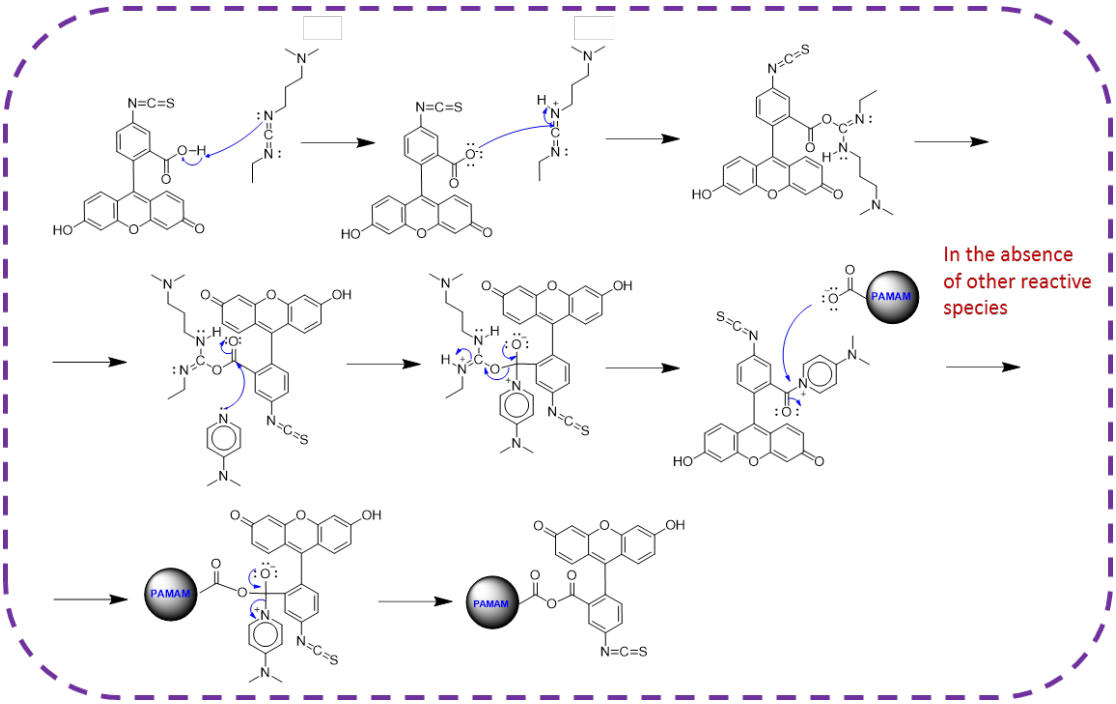

Figure 103 – Representation of the possible reaction between the carboxyl groups of PAMAM dendrimers and the carboxyl groups of the FITC through the EDC/DMAP chemistry.

Similarly to the previous cases, in order to assess the conjugation efficiency, the obtained compounds were fully characterized by ^{1}H NMR, UV/Vis, FITC and zeta potential. The unconjugated counterparts were also characterized by the same techniques, and their spectra can be found in the annexes, section A.

The ^{1}H NMR spectra of the both reaction products can be found in the Figures 104 and 105. However, since that we were unable to completely purify the final products, it is highly difficult to confirm the conjugation between the FITC and the PAMAM-COOH dendrimers solely based on the ^{1}H NMR data.

Additionally, given the ^{1}H NMR spectra complexity of the unconjugated counterparts (see annexes, section A5 and A6), it is difficult to assign any peaks associated with the successful formation of the conjugates. Besides that, since that no new peaks related with the protons near the anhydride bond can be clearly identified in the spectra, it make us to believe that the conjugation was not successful based on the conditions reported in this work. Also, the appearance in both spectra of unexpected peaks (1.06 - 2.00 pm) may indicate the existence of by-products or degradation products in the final materials.

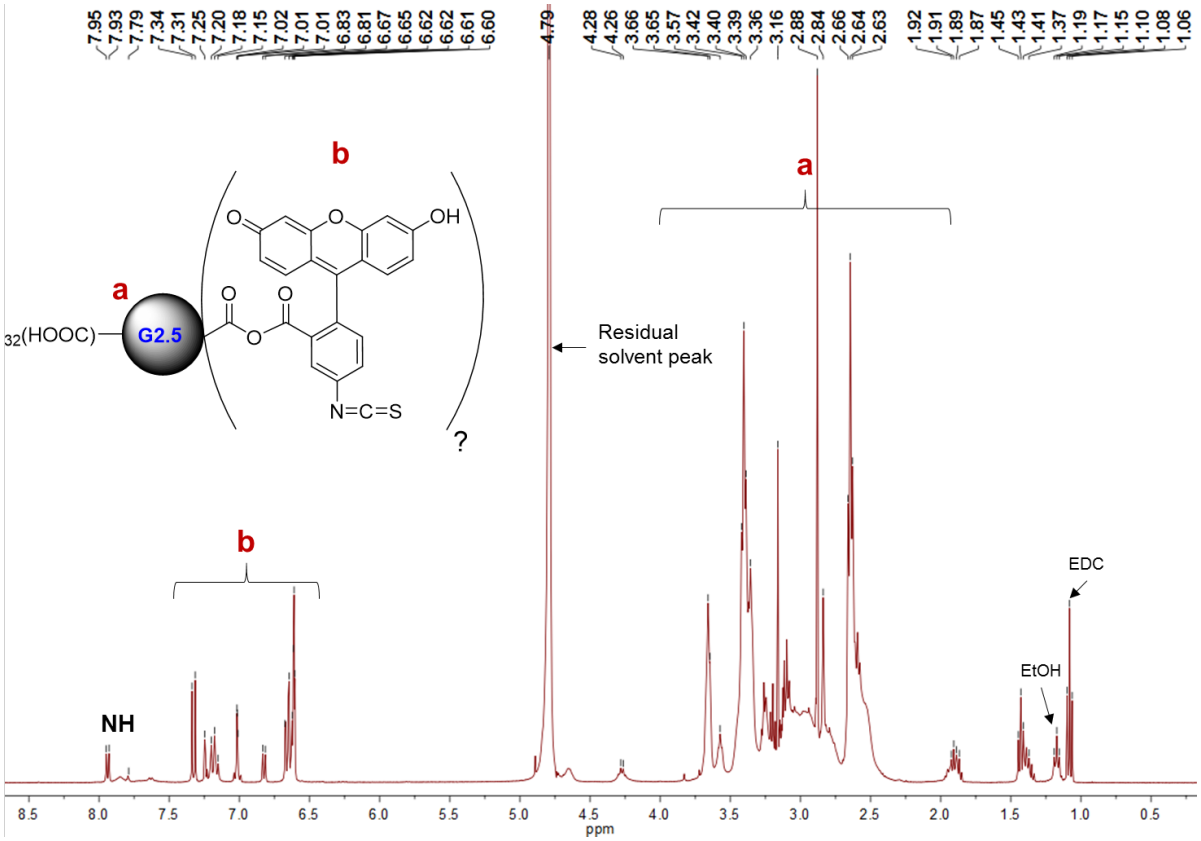

Figure 104 – ^{1}H NMR spectrum of the reaction product between the FITC and the G2.5 PAMAM-COOH in D_2O (at 400 MHz).

When comparing the ^{1}H NMR spectra of these conjugates with the ones of the previous sections, it is observable that the peak profile of the FITC aromatic protons is remarkably different. While in the case of the FITC-PAMAM-NH_2 and –OH conjugates the peak profile changes (marked as “b” in the spectra), in this case, the peak nature is highly similar to the unconjugated FITC (see annexes, section A). Although still unclear, the broadening of the FITC aromatic protons may be associated with an effect caused by the conjugation between the PAMAM dendrimer and the FITC. For example, in the case of a successful conjugation, the peak broadening of the FITC aromatic protons may be attributed to long-range coupling phenomenons or to distinct relaxation times[283]. As a result, the data provided by the ^{1}H NMR spectra of the FITC-PAMAM-COOH conjugation products may further indicate an unsuccessful conjugation.

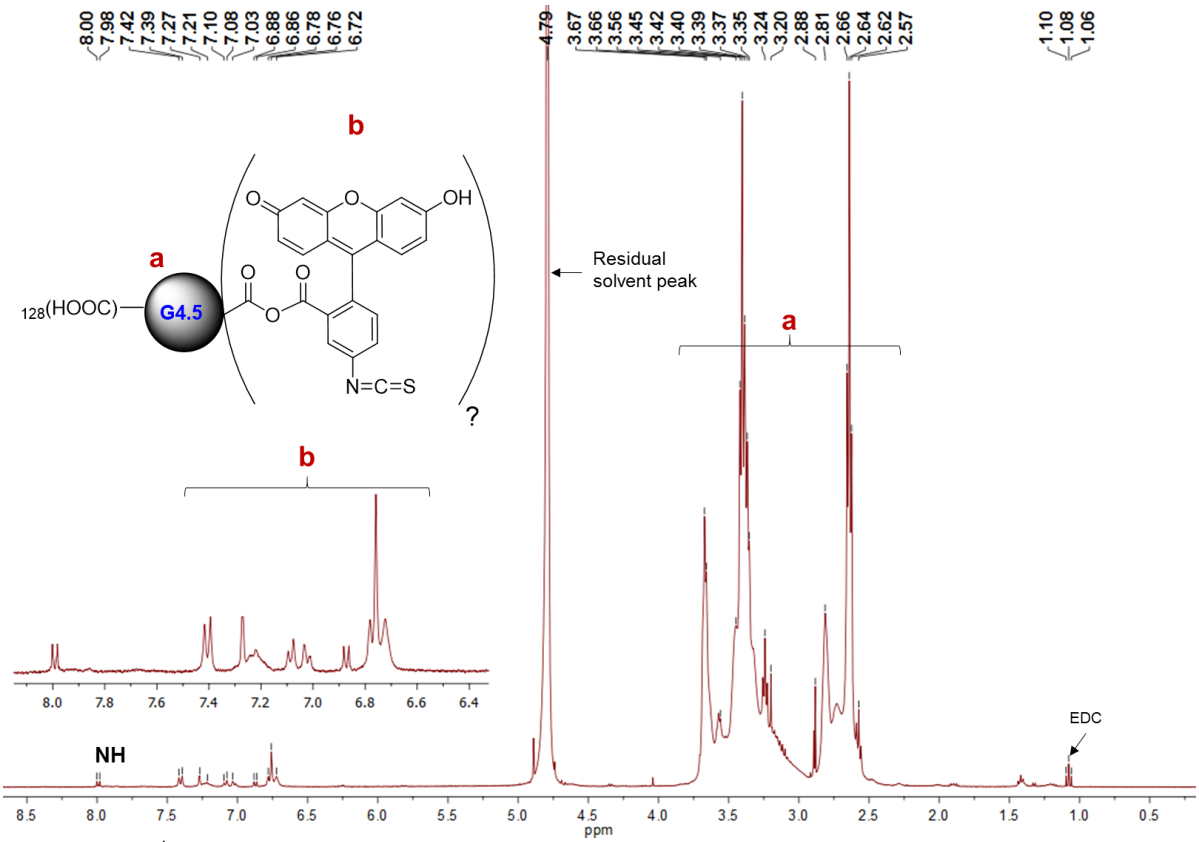

Figure 105 - ^{1}H NMR spectrum of the reaction product between the FITC and the G4.5 PAMAM-COOH in D_2O (at 400 MHz).

Similarly to the previous conjugates, we also proceeded with the UV/Vis characterization of both reaction products. The obtained UV/Vis spectra are shown in the Figure 106. Interestingly, in both products a red shift in the FITC λ_{max} was detected (480 → 490 and 502 nm). Although these λ_{max} shift may indicate some kind of alteration in the aromatic system of the FITC probe, no further conclusions can be taken since that the data provided by the other characterization techniques do not give enough evidences of a successful conjugation.

Similarly, the FTIR characterization of both reaction products does not provide enough data to confirm the successful conjugation (see Figure 107). Although the peaks around 1300 – 1000 cm^{-1} may be attributed to the different vibration modes of the bonds from the FITC molecules (see unconjugated FITC spectrum, annexes, section A), it is difficult to obtain any further conclusion due to the limited purity of the final products and uncertain data from the other characterization techniques.

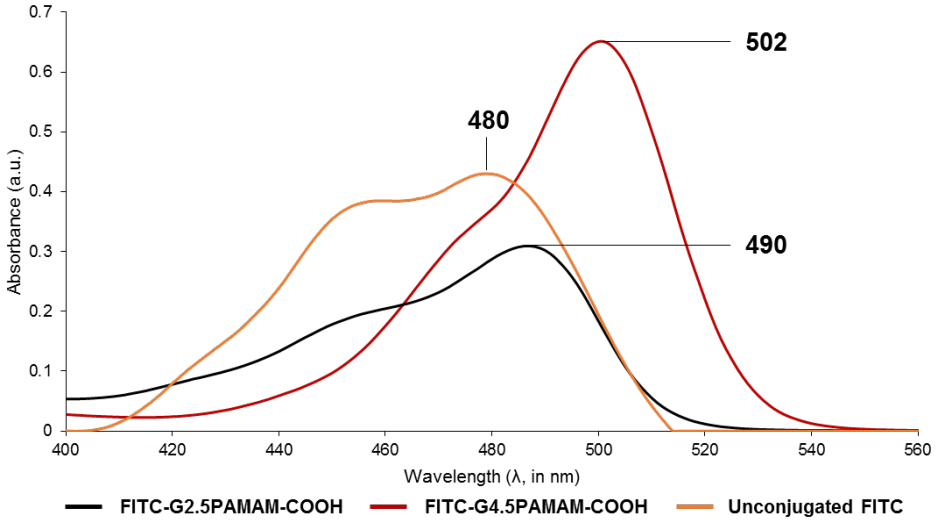

Figure 106 – UV/Vis spectra of the reaction products between the FITC and the G2.5 and G4.5 PAMAM-COOH (at 0.02 mg/mL) and FITC (0.01 mg/mL) in UP water.

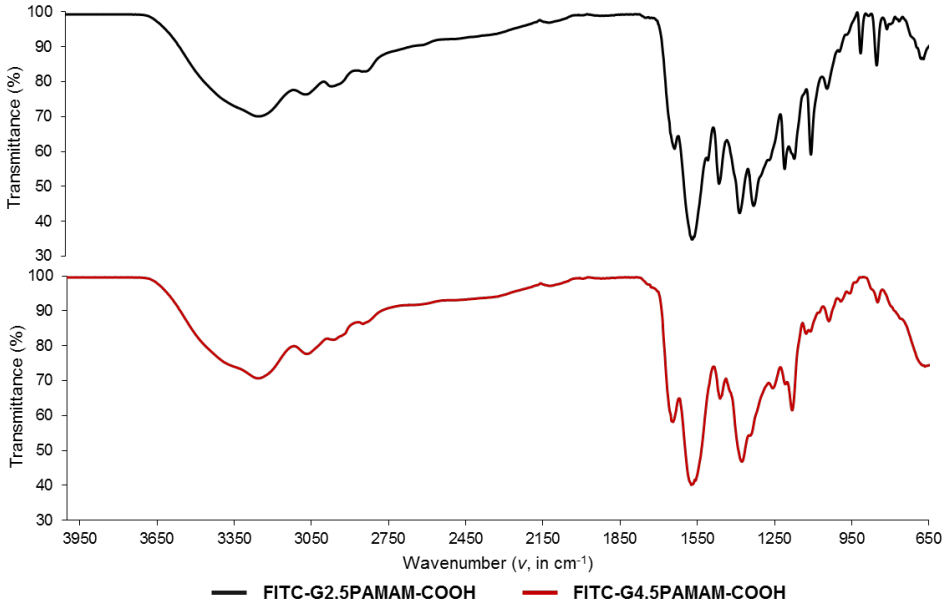

Figure 107 – FTIR spectra of the reaction products between the FITC and the G2.5 and G4.5 PAMAM-COOH.

Despite the unclear conjugation efficiency, we also proceeded with the zeta potential measurement of the obtained products. At pH 7.4 in PBS, the ξ values were -9.07 and -14.50 mV for

the G2.5 PAMAM-COOH and G4.5 PAMAM-COOH products respectively. These results are consistent with reported values for this type of carboxyl terminated PAMAM dendrimers[128,269]. In this case, at the pH 7.4, most of the carboxyl surface groups are deprotonated resulting in a more negative surface charge when compared with the hydroxyl terminated PAMAM dendrimers.

While the main reason for the ineffective conjugation remains elusive, we point out a few possible causes.

Firstly, the conditions followed in this work relied on the formation of an anhydride intermediary that is only stable for short periods of time, especially in the presence of strong nucleophiles[176]. It has been reported that the successful formation and stability of this type of anhydrides is equally dependent of the solvent polarity (*i.e.* higher polarity means less stability). As a result, it is known that although this type of intermediary anhydrides can be isolated, they cannot stored for future use due to their relatively low stability, especially in the conditions used for cell studies[284].

Additionally, the reaction lacks on specificity, which may result in low the conjugation efficiencies. In other words, this lack of specificity may allow the formation of FITC dimers (π-π interactions). This type dimers may then lead to some kind of steric hindrance that reduces the availability of the FITC molecules to the carboxyl surface groups of the PAMAM dendrimers[285].

In order to avoid this type of dimerization, we proceeded with the dropwise addition of the FITC dye (see section 2.1.4). Nevertheless, this approach did not result in the successful functionalization of the dendrimer scaffold.

Given the purification and characterization difficulties described along this section, we propose that the fluorescent labeling of the PAMAM-COOH dendrimer should follow other approaches than the ones presented here. If the stochastic conjugation is intended, an alternative method may rely on the conjugation of other fluorescein derivatives that exhibit an improved specificity to the carboxyl terminal groups of the PAMAM dendrimer. As shown in Figure 108, an alternative relies on the use of the 5-(aminomethyl)-fluorescein that along with EDC/NHS chemistry allows a successful fluorescent labelling of the carboxyl-terminal groups of the PAMAM scaffold as previously reported by Grainger *et al.*[269].

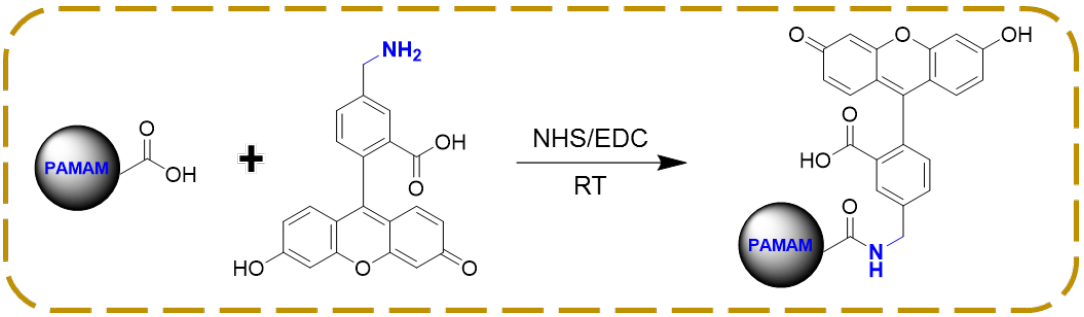

Figure 108 – An alternative stochastic approach for the conjugation of a fluorescein derivative to the carboxyl terminated PAMAM dendrimers (Figure adapted from Ref. 269).

Other very recent alternatives involve the surface labeling of the PAMAM dendrimers through a set of complementary chemical groups that allow the well-controlled functionalization based on “click” chemistry reactions. Some of the novel approaches rely on the use of very specific linkers that facilitate the controlled functionalization of the PAMAM dendrimers surface with several functional units[286,287].

3.4. Effect of pH on fluorescence intensity of FITC-PAMAM conjugates

The labelling of the PAMAM dendrimers with the FITC probe is a widely employed method to explore the cell internalization of these dendritic structures. As referred at the end of the section 1.7, the PAMAM dendrimers may be internalized by distinct endocytic routes. Most of the endocytic pathways involve the entrapment of the cargo in vesicles (*i.e.* endosomes and then lysosomes) where along the trafficking process the intravesicular pH drops from 6.5 to 4.0[288,289].

As shown in the Figure 109, the cell internalization of cargo through endocytosis usually involves a series of maturation and fusion events of the vesicles responsible for the intracellular trafficking. This process comprises a series of changes in the individual vesicles including the gradual reduction of the pH, the binding and unbinding of signaling proteins and the dynamic change in the cell membrane lipid composition. Additionally, the fate of the cargo relies on a series of signaling events associated with its internalization. While some materials are directed to the degradative pathway, others may be directed to specific cell compartments or be recycled again to the plasma membrane[288,289].

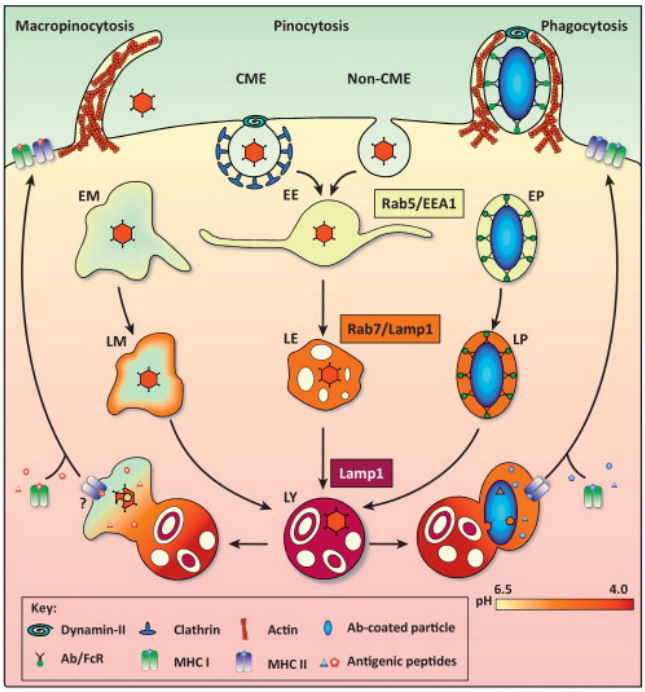

Figure 109 – The trafficking of cargo inside the cells and the associated fusion/maturation events. (Figure adapted from Ref. 269).

Since the FITC has been widely used in the literature to explore the cell internalization of the PAMAM dendrimers, we wanted to investigate their performance during the possible endosomal/lysosomal maturation events. For this purpose, the higher generation PAMAM conjugates were dispersed in PBS under distinct concentrations (0 – 4 μg/mL), and pH values (4.0 – 7.4).

The Figure 110 shows the impact of the pH over the fluorescence intensity of the higher generation conjugation products. It is worth mentioning that the much lower fluorescence intensity in the case of the FITC-G5PAMAM-NH_2 conjugate may be associated with the increased quenching effects caused by the PAMAM scaffold and due to possible electrostatic interactions between the cationic -NH_2 end groups and the anionic FITC dye. However, the clear explanation of such behavior remains elusive.

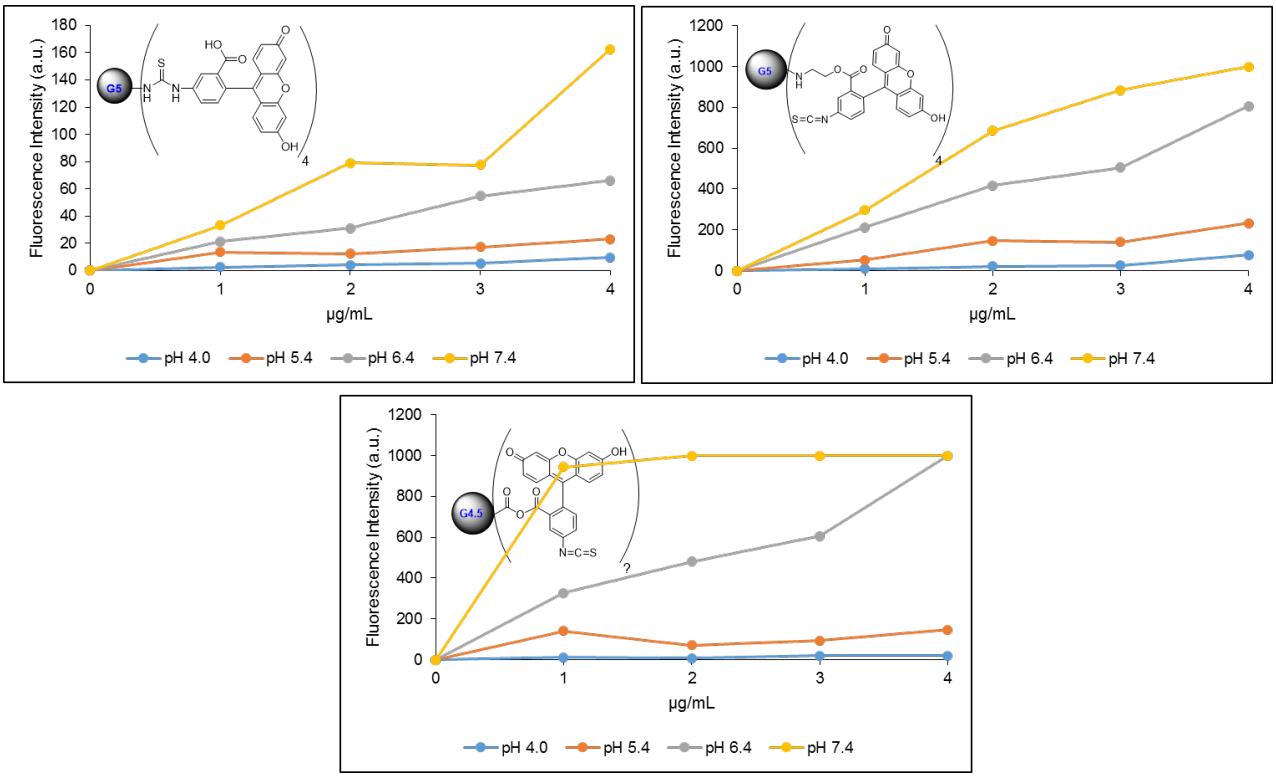

Figure 110 – The preliminary study of the pH effect over the fluorescence intensity of the prepared FITC-PAMAM conjugates. Note that the fluorescence intensity saturation level of the equipment is 1000. The fluorescent intensity is presented as arbitrary units (a.u.).

Before relating the influence of the pH over the FITC fluorescence intensity it is important to understand the origin of the fluorescence emission in this molecule.

The FITC is a fluorescein derivate based on the xanthene dye system and that has been widely applied as a fluorescent probe due to the high quantum yield, molar absorptivity, well-characterized behavior in solution and the ability to conjugate with other molecules. Many well-characterized

fluorescein derivatives exist for several purposes, including: for improved conjugation with molecules of interest; greater solubility in specific solvents or enhanced stability[165,271].

In the case of the FITC, the fluorescent emission arises due to the existence of a conjugated polycyclic system. As shown in the Figure 111, the existence of the oxygen bridge between the two phenyl rings provides a rigid aromatic system that forces the structure into a planar shape. Such architecture results in the fluorescent emission when subjected to incident radiations at specific wavelengths (see section 1.4.4). The nature of this planar structure allows the photons to be reemitted due to the reduced number of electron-related secondary relaxation processes[176,290–292a].

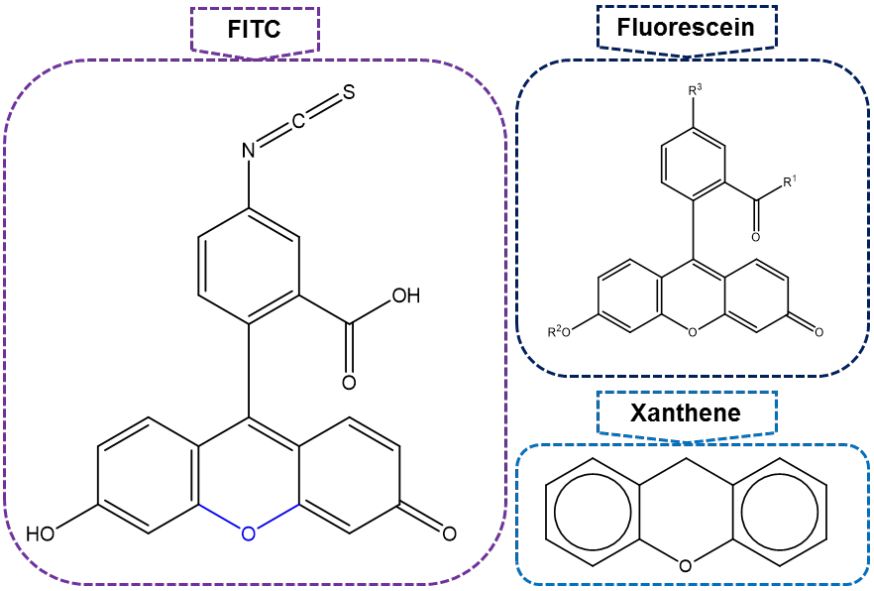

Figure 111 – The fluorescein derivative, FITC, containing the oxygen bridge that allows the characteristic fluorescent emission.

It has been widely reported that the photophysical properties of the fluorescein derivatives are strongly dependent of the environmental conditions. As a result, depending on the pH and solvent polarity, different forms of fluorescein may exist in solution resulting in discrete fluorescence spectra, quantum yields and fluorescence lifetimes at specific excitation wavelengths. For example, depending on the solvent nature, the existence of non-covalent interactions between the fluorescent dye and the solvent molecules may decrease the rotational freedom of the dye and result in fluorescence quenching[176,290,291,293,294].

When in aqueous solution, the fluorescein derivatives may exist in different monomeric forms over the whole pH range, where each form has its own pK_a value. As shown in the Figure 112, while that at highly acidic solutions (pH < 2) the cationic form prevails, the fluorescein derivatives become neutral between pH 2 and 4. Until pH 5, the fluorescein molecules are mainly in monoanionic form while that at pH above 7 the monoanion becomes a dianion[263].

At the pH range explored in the current work and according to the data shown in the previous figure, it is expected that different forms of the FITC were present in the samples.

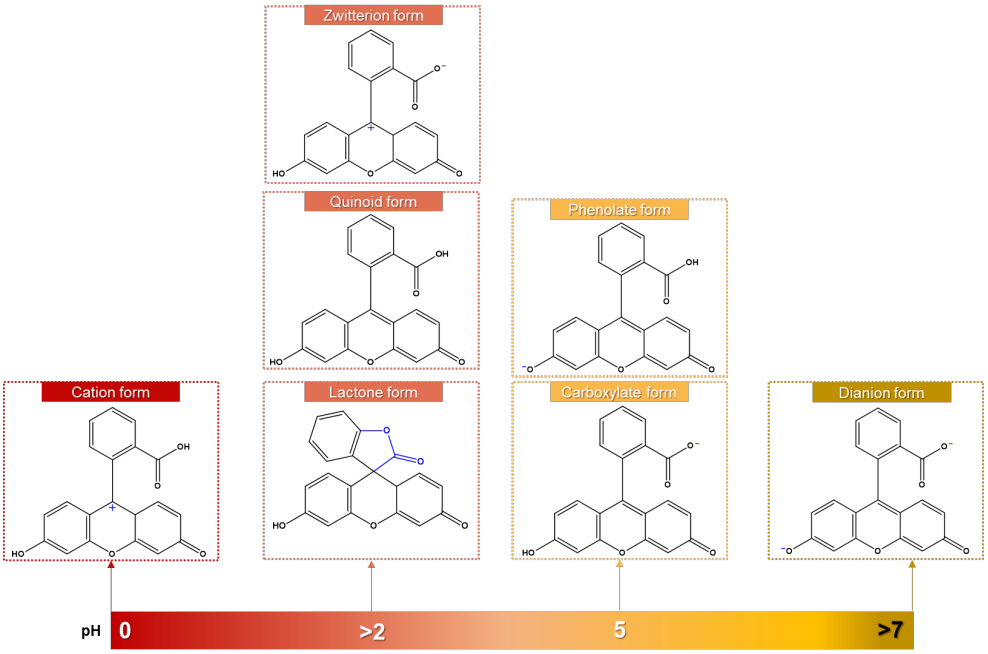

Figure 112 – The forms of the fluorescein at distinct pH conditions. All the forms exist in equilibrium at specific pH values. It is important to note that the polarity of the solvent also affects the form of the fluorescein. At neutral pH: in polar solvents the fluorescein is usually as a dianion, while that in nonpolar solvents the lactone form prevails (Figure adapted from Refs. 263,290 and 291).

As a result, at pH 4.0 the neutral FITC structures prevailed, resulting in distinct quantum yields and emission spectra. It has been reported that the fluorescein-based structures at this pH present a QY ~ 0.18. Since that the neutral FITC structures do not contribute for any significant fluorescence, it is known that the fluorescent emission only occurs by the conversion of these structures, in the excited state, into the anionic forms. Since that at pH 4, the quinoid structure usually prevails in solution, the conversion into the anionic form occurs by the extremely rapid transfer of the proton from the carboxyl groups to the solvent molecules. For these reasons, the fluorescein structures at acidic pH (4-5) usually exhibit shorter fluorescence lifetimes and weaker intensities when compared with the “true” anionic forms. Additionally, the low fluorescence of the neutral species may also be attributed to internal conversion or intersystem crossing processes that compete with the fluorescent emission (see section 1.4.4)[290,291,293].

On the other hand, at the pH intervals between 5.4 and 6.4, both anionic forms of the FITC prevail which have contributed for the characteristic fluorescence emission and quantum yields shown in the Figure 110. It has been reported that the anion and dianion forms of the FITC and fluorescein derivatives are the only ones that truly contribute for the fluorescence emission. It is known that at the pH range of 5.4 – 6.4, the prevailing FITC structures present a QY of ~ 0.37. By further increasing the

pH towards the physiological values, the dianion starts to dominate resulting in one of the most brightly fluorescent low-molecular weight compounds known today, possessing a QY around 0.93*. However, as already referred, even in this form, the presence of the PAMAM dendrimers in the sample may have surely contributed for the fluorescence quenching of this FITC form[291,292a].

It is worth mentioning that in the case of the FITC, the existence of the isothiocyanate group is not enough to cause deep changes in the pK_a value when compared with unsubstituted fluorescein molecule. It has been reported that substitutions on the phthalein ring have little effect on the pK_a due to the remote distance in relation to the xanthene group. Usually the phthalein ring is twisted out of the plane from the xanthene rigid structure and as a result, the substitution on the phthalein part has little effect in the fluorescence output along the pH†. By this way, the behavior observed for the fluorescein molecule at different pH values can also be related for the FITC[292a].

Besides of the aforementioned changes in the FITC structure, it is important to have in mind that depending on the buffering capacity of the surrounding conditions, the PAMAM scaffold may also undergo in structural changes as a function of the pH (see section 1.2, Figure 14). As a result, depending on the degree of compaction such structural changes may also affect the fluorescence emission of the FITC through secondary absorption effects.

With the results reported along this section, it is clear that the FITC labelling of the PAMAM dendrimers for cell colocalization studies can be limited.

According to the data shown in the Figures 109 and 110, while that at neutral pH conditions (cytoplasm), the signal of the conjugated FITC may be detected, its internalization into vesicular structures (*i.e.* lysosomes, LYs) by endocytosis may result in a marked decrease of the fluorescent emission. This statement is in agreement with previous reported observations for other fluorescein based probes[292b,c].

It is important to have in mind that the LYs are functional cell organelles that contain an high proton concentration along with more than 50 distinct hydrolases‡ that may participate in the cell's degradative pathway. As shown in the Figure 113, the biological membrane of the lysosomes has several integral proteins that are responsible to define the charge gradient inside these vesicles[295]. For this reason, the blackout of the fluorescence emission from the PAMAM-FITC may occur due to the characteristic decrease in the lysosomal pH during the endocytic trafficking.

With the results reported in the Figure 110, it is expected that during the endosomal/lysosomal maturation events, the neutral FITC forms (pH ~ 4) will prevail resulting in a very low QY. Although

*The improved fluorescence of the fluorescein anion and dianion forms are mainly associated with the increased QYs and fluorescence lifetimes provided by the characteristic electron system at the referred pH range.
†On the other hand, the introduction of substituents on the xanthene rings may be explored to change the behavior of the fluorescein derivatives at distinct pH. While that, electron withdrawing groups lower the pK_a, the electron donating groups increase this parameter.
‡The hydrolases are digestive enzymes produced in the endoplasmatic reticulum and that migrate to the lysosomes to participate in the degradative pathway. This diversity of these enzymes is so great that almost any type of organic molecules may be degraded inside the lysosomes.

such behavior may not be useful for quantitative cell colocalization studies, the FITC may be explored for the preparation of biosensors as a function of the vesicular pH during endocytic trafficking[296].

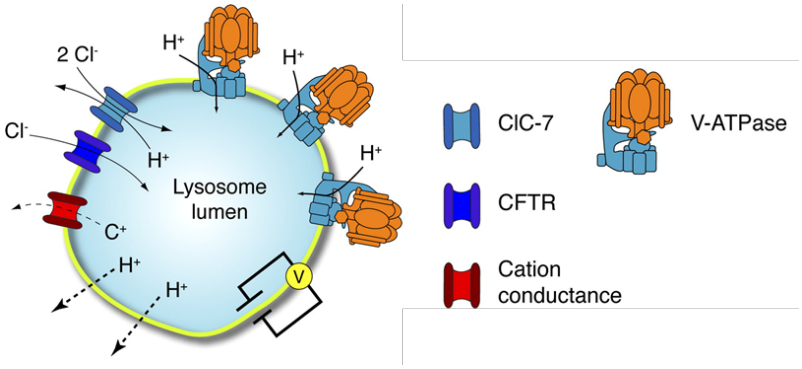

Figure 113 – The elements that are responsible to define the lysosomal pH. The lysosomal pH is defined by V-ATPase activity that is responsible to control the H^+ gradient based on the ATP hydrolysis. The pH level is also regulated by other elements that promote the influx of anions (*e.g.* like the chloride proton antiporter (CIC-7) and cystic fibrosis transmembrane-conductance regulator (CFTR)) (Figure adapted from Ref. 296).

3.5. Preliminary cytotoxicity studies of FITC-PAMAM conjugates

The Figure 114 shows the preliminary results regarding the cytotoxic behavior of the higher generation FITC labeled products on the mouse embryonic fibroblast cell line NIH 3T3. Each dataset was plotted based on the mean and the corresponding RSD of a single independent study with six replicates for each concentration. All data sets were plotted in relation to the negative control.

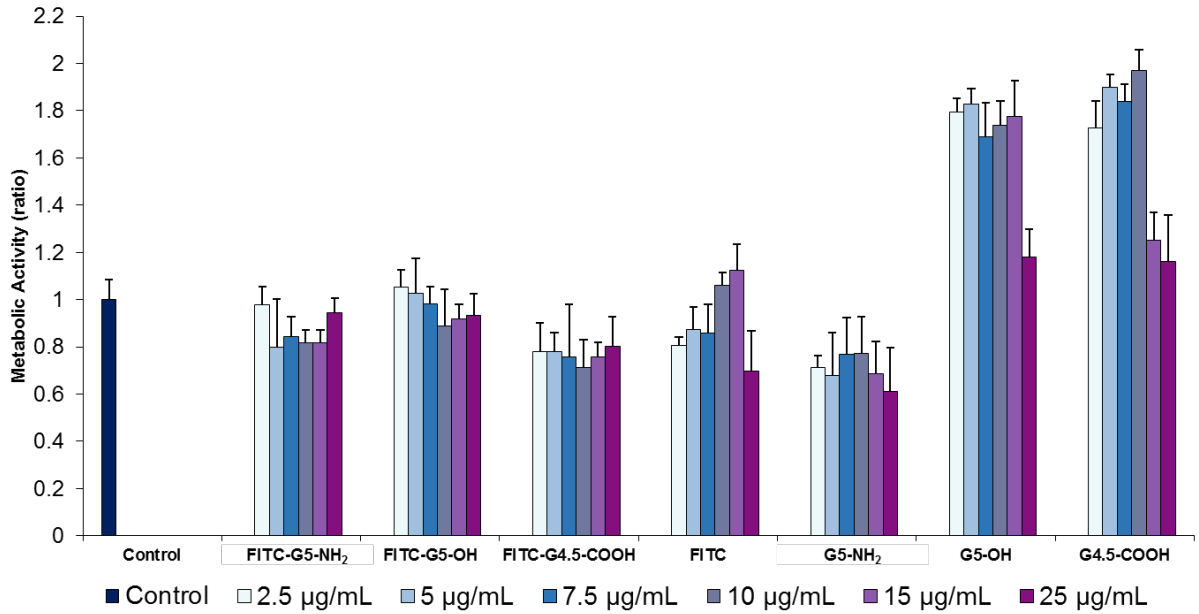

Figure 114 - Cytotoxicity evaluation of FITC-functionalized PAMAM dendrimers and free FITC on the mouse embryonic fibroblast cell line NIH 3T3.

The results presented in the Figure 114 are in terms of metabolic activity since that the cytotoxic behavior of the compounds was assessed through the resazurin reduction assay. This method relies on the ability of the metabolically active cells to convert a redox non-fluorescent dye (resazurin) into the fluorescent product (resorufin). Since that both, the resazurin and resorufin are permeable through the cell membrane, the resazurin has the ability to enter the cells and be reduced, while on the other hand, the resulting metabolic product, resorufin, can pass through the plasma membrane and accumulate in the cell medium. As a result, this assay relies on the fact that nonviable cells are metabolically inactive and cannot convert the resazurin into resorufin. As a result, after exposing the cells to the compounds of interest, the resazurin reagent is added to cell medium and left to incubate. After the incubation time, the fluorescence signal of the medium is monitored through a microplate-reading fluorometer or by the spectrofluorometer[297-299].

The results shown in the Figure 114 indicate that no profound cytotoxic behavior of the conjugation products could be observed on the NIH 3T3 cells at the studied concentrations and incubation times (3 h). For all conjugation products, the metabolic activity indicates that none of the concentrations induced alterations below 0.7.

Interestingly, the lower effect of FITC-G5PAMAM-NH_2 conjugate in the cell metabolic activity suggests that the conjugation of the FITC molecule shielded the surface charge of the dendrimer. Consequently, this shielding resulted in a lower cytotoxic behavior when compared with the non-conjugated PAMAM-NH_2 dendrimer[300]. On the other hand, the reduced effect of the FITC-PAMAM-COOH and –OH conjugates is in agreement with the reported observations referred in the section 1.7 due their characteristic charge and reduced interactions with the plasma membrane at physiological pH.

In the cases where the metabolic activity was greater than 1 in relation to the control (*i.e.* non-conjugated PAMAM-COOH and –OH dendrimers) may be associated with the upregulation of the metabolic conversion of resazurin due to the presence of these exogenous molecules.

The results presented in the section show that the prepared FITC-PAMAM conjugated do not induce deep alterations in the cell metabolic activity. This data indicates that the prepared compounds do not exhibit a noticeable cytotoxicity behavior at the concentrations and incubation time explored in the current work. Nevertheless, since that the results reported in this section are only preliminary we recommend the further optimization of described conditions along with the use of complementary cytotoxicity assays (*e.g.* LDH, ATP or total DNA assays) in order to provide a better understanding of the biological interaction of the prepared FITC-PAMAM conjugates.

Part 4. Conclusions and outlook

Contents

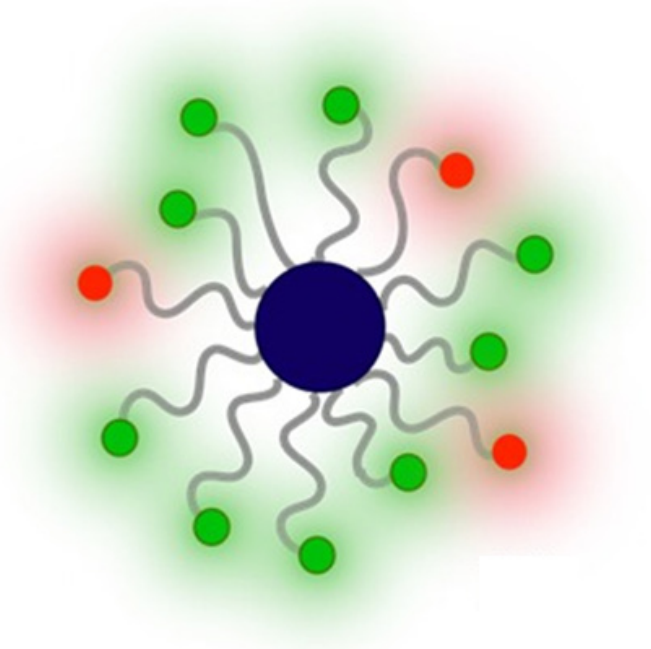

Dendrimers as a platform for fluorescent indicators. Figure taken from: Albertazzi, L.; Brondi, M.; Pavan, G. M.; Sato, S. S.; Signore, G.; Storti, B.; Ratto, G. M.; Beltram, F. Dendrimer-Based Fluorescent Indicators : In Vitro and In Vivo Applications. PLoS ONE **2011**, *6*, e284506.

4. Conclusions and outlook

With the advent of the synthetic perpetual hyperbranched polymers, a great diversity of dendritic structures with unique chemical functionalities and physicochemical properties started to emerge.

Thanks to the development of the synthetic routes and characterization methods, it is currently possible to prepare almost an unlimited number of dendrimers containing a discrete chemical nature along with a will-defined size, shape and surface chemistry.

As shown in the early sections of this thesis, the current diversity of the dendrimer chemistry is huge and many different types of applications have been hypothesized for this type of structures. As an example, many properties of the dendrimers have been exploited in order to be specifically applied for the biomedical field. Some biomedical applications include for drug delivery, gene therapy, biosensors or as imaging agents. Although several dendrimer families have been explored for these purposes, the PAMAM dendrimers remain the most widely studied dendritic scaffolds. They are the most well-characterized dendrimer family and were the first to become commercially available with a great diversity of functional units at high generations.

Some of the most attractive properties of the PAMAM dendrimers are associated with its multifunctional surface and hydrophobic interior. The almost unlimited functionality of the surface allows the conjugation with a great diversity of molecules including drugs, proteins or fluorescent dyes.

Although in the last twenty years many research groups have explored the characteristics of the PAMAM dendrimers for biomedical applications, many of these works have overlooked the importance of the endocytic routes for the biological effect of these dendrimers. Nevertheless, with the recent discoveries associated with the endocytic processes, many works started to explore the importance of the endocytosis over the internalization and fate of the PAMAM dendrimers when exposed in the biological conditions.

Some of the recent approaches to study the cell internalization of the PAMAM dendrimers involve the functionalization of the dendrimer surface with fluorescent dye for colocalization studies during endocytic trafficking. The stochastic functionalization with the FITC fluorescent dye, has been one of the most widely used approaches for being cost-effective and thanks to the high QY, fluorescence lifetimes and diversity chemical functionalities of this fluorescent molecule.

Given the wide use of these FITC-PAMAM conjugates for cell internalization studies of the PAMAM dendrimers, in the current thesis, the goal was to explore the conjugation efficacy between the FITC and the PAMAM scaffold containing distinct surface groups (-NH_2; -OH and –COOH) and generations (G2.5 → G5).

As result, here we have explored the effect of different conjugation chemistries and reaction parameters in order to verify their successfulness for the FITC labelling of the PAMAM dendrimers with distinct terminal groups.

Firstly, in the case of the FITC-PAMAM-NH_2 functionalization the well-known reactivity between isothiocyanate groups of the FITC and the primary amines of the PAMAM dendrimer terminal groups was explored. Based on this approach, we were able to identify the successful functionalization of both generation PAMAM dendrimers with the FITC dye. However, the complete purification of the final products could not be accomplished based on the methods applied in this work (*i.e.* dialysis, PD-10 columns).

For the fluorescent labelling of the PAMAM-OH dendrimers, it was followed the EDC/DMAP chemistry for the carboxyl group activation of the FITC molecules and improved conjugation with the hydroxyl terminal groups of the dendrimer scaffold. Despite the possible existence of unconjugated fluorescent dye, the characterization data indicated the successful conjugation of the FITC with the G3 and G5 PAMAM-OH dendrimers.

Regarding the FITC labelling of the carboxyl terminated PAMAM dendrimers, we have employed a previously reported method that relied on the formation of an anhydride bond through the EDC/DMAP chemistry. In this work and regardless the presented optimization attempts, the successful conjugation could not be clearly determined.

Since that all the conjugation reactions were accomplished based on a stochastic method, we acknowledge the possible existence of heterogeneous PAMAM-FITC populations among the different samples. This heterogeneous nature may have increased the difficulty to achieve a better purity level through the followed methods. Additionally, we support that the further optimization of the presented reaction and purification conditions may provide better results in future attempts.

Additionally, by exploring the fluorescence intensity of the FITC-PAMAM conjugation products at different pH conditions, we were able to analyze the applicability of the FITC probe for cell internalization studies. Based on the results reported in this work, we were able to confirm that the FITC molecules are highly sensitive to the environmental pH conditions. Based on spectrofluorometric studies, we have concluded that, while at physiological pH the prevailing FITC species exhibit a high QY, at lysosomal pH values, the dominant FITC species show a poor fluorescent performance. Although this sensitivity of the FITC may not be useful to study the endocytic trafficking of the PAMAM dendrimers, it may be explored as an intracellular biosensor that is sensitive to the environmental pH.

The preliminary cytotoxicity studies on the NIH 3T3 cells (through resazurin assay) of the higher generation FITC-PAMAM conjugates have indicated that no profound cytotoxic behavior is observed between the concentrations of 0-25 μg/mL and 3 hours of incubation time. Our introductory results indicate that these type of conjugates may be further used for other type cell studies at described concentrations since that no significant changes on the cell metabolic activity was observed. Nevertheless, the further analysis of the biological interaction of these conjugates is recommended based on the optimization of the presented conditions and by the additional use of other cytotoxicity assays (*e.g.* LDH, ATP or total DNA assays) and parameters (*e.g.* other cell types and incubation times).

The results presented along this thesis may provide new insights regarding the synthesis and applicability of FITC-PAMAM conjugates for biological studies. It is therefore clear that the development of more efficient preparation, purification and characterization methods regarding the fluorescent labelling of the PAMAM dendrimers may provide useful tools to understand the pathways involved in their interaction with biological interface. For example, the development of such systems will help to understand the effect of the PAMAM surface functionalities over their cellular uptake and fate. This type of studies may aid in the development of novel PAMAM dendrimer-based drug/gene carriers with enhanced delivery efficiency across physiological barriers.

References

Contents

References

(1) Campagna, S.; Ceroni, P.; Puntoriero, F. (editors). *Designing Dendrimers*; Wiley: USA, 2011; Chapters 1-3.

(2) Tomalia, D. A.; Christensen, J. B.; Boas, U. (editors). *Dendrimers, Dendrons, and Dendritic Polymers: Discovery, Applications, and the Future*; Cambridge University Press: UK, 2012; Chapters 1-4 and 7.

(3) Fréchet, J. M. J.; Tomalia, D. A. (editors). *Dendrimers and Other Dendritic Polymers*; Wiley series in polymer science; Wiley: USA, 2001; Chapters 1-4, 10-14 and 18.

(4) Boas, U.; Christensen, J. B.; Heegaard, P. M. H.; Peng, L. (editors). *Dendrimers in Medicine and Biotechnology*; The Royal Society of Chemistry: UK, 2006; pp. 1-89.

(5) Pictures Database. URL: <http://www.picturesdatabase.net/tree-above-and-below-ground/> (accessed on Dec 30th, 2014).

(6) Buhleier, E.; Wehner, W.; Vogtle, F. Cascade-Chain-like and Nonskid-Chain-like Syntheses of Molecular Cavity Topologies. *Synthesis-Stuttgart* **1978**, *2,* pp. 155–158.

(7) Tomalia, D. A.; Baker, H.; Dewald, J.; Hall, M.; Kallos, G.; Martin, S.; Roeck, J.; Ryder, J.; Smith, P. A New Class of Polymers: Starburst-Dendritic Macromolecules. *Polym. J.* **1985**, *17*, 117–132.

(8) Newkome, G. R.; Yao, Z.; Baker, G. R.; Gupta, V. K. Micelles. Part 1. Cascade Molecules: A New Approach to Micelles. A [27]-Arborol. *J. Org. Chem.* **1985**, *50*, 2003–2004.

(9) Maciejewski, M. Concepts of Trapping Topologically by Shell Molecules. *J. Macromol. Sci.* **1982**, *17*, 689–703.

(10) De Gennes, P. G.; Hervet, H. Statistics of «starburst» Polymers. *J. Phys. Lettres* **1983**, *44*, 351–360.

(11) Flory, P. J. Molecular Size Distribution in Three Dimensional Polymers. VI. Branched Polymers Containing A-R-B_{f-1} Type Units. *J. Am. Chem. Soc.* **1952**, *74*, 2718–2723.

(12) Vögtle, F.; Richardt, G.; Werner, N.; Rackstraw, A. J. (editors). *Dendrimer Chemistry*; Wiley, USA, 2009; pp. 1-75 and 253-282.

(13) Mintzer, M. A.; Grinstaff, M. W. Biomedical Applications of Dendrimers: A Tutorial. *Chem. Soc. Rev.* **2011**, *40*, 173–190.

(14) Reinhoudt, D. N. (editors). *Supramolecular Materials and Technologies*; Perspectives in Supramolecular Chemistry Volume 4; Wiley, UK, 2008; pp. 1-47.

(15) Denkenwalter, R. G.; Kolc, J. F.; Lukasavage, W. J. Preparation of lysine based macromolecular highly branched homogeneous compound. US Pat. 4.360.646, 1982.

(16) Kesharwani, P.; Jain, K.; Jain, N. K. Dendrimer as Nanocarrier for Drug Delivery. *Prog. Polym. Sci.* **2014**, *39*, 268–307.

(17) Tomalia, D. A. Birth of a New Macromolecular Architecture: Dendrimers as Quantized Building Blocks for Nanoscale Synthetic Polymer Chemistry. *Prog. Polym. Sci.* **2005**, *30*, 294–324.

(18) Shcharbin, D.; Shakhbazau, A.; Bryszewska, M. Poly (amidoamine) Dendrimer Complexes as a Platform for Gene Delivery. *Expert Opin. Drug Deliv.* **2013**, *10*, 1687–1698.

(19) Emrick, T.; Fréchet, J. M. J. Self-Assembly of Dendritic Structures. *Curr. Opin. Colloid Interface Sci.* **1999**, *4*, 15–23.

(20) ISI Web of Science. URL: <http://apps.webofknowledge.com/>, (accessed on Dec 30th, 2014).

(21) Espacenet Patent Search. URL: <http://worldwide.espacenet.com/?locale=en_EP>, (accessed on Dec 30th, 2014).

(22) IDS8 - 8th International Dendrimer Simposyum. URL: <http://www.ids-8.com/>, (accessed on Dec 30th, 2014).

(23) Highlights of the 8th International Dendrimer Symposium. URL: <http://is.gd/IITUdg>, (accessed on Dec 30th, 2014).

(24) Biodendrimers 2014. URL: <http://www.biodendrimer2014.supsi.ch/>, (accessed on Dec 30th, 2014).

(25) Kumbar, S.; Laurencin, C.; Deng, M. (editors). *Natural and Synthetic Biomedical Polymers,* 1st Edition; Elsevier Science: USA, 2014; p. 243.

(26) Hecht, S.; Fréchet, J. M. J. Dendritic Encapsulation of Function: Applying Nature's Site Isolation Principle from Biomimetics to Materials Science. *Angew. Chemie Int. Ed.* **2001**, *40*, 74–91.
(27) Huang, B.; Tomalia, D. A. Dendronization of Gold and CdSe/cdS (core–shell) Quantum Dots with Tomalia Type, Thiol Core, Functionalized Poly (amidoamine)(PAMAM) Dendrons. *J. Lumin.* **2005**, *111*, 215–223.
(28) Turnbull, W. B.; Stoddart, J. F. Design and Synthesis of Glycodendrimers. *Rev. Mol. Biotechnol.* **2002**, *90*, 231–255.
(29) Zhou, T.; Wang, Y.; Dong, Y.; Chen, C.; Liu, D.; Yang, Z. Tetrahedron DNA Dendrimers and Their Encapsulation of Gold Nanoparticles. *Bioorg. Med. Chem.* **2014**, *22*, 4391-4394.
(30) Tan, H.; Li, X.; Liao, S.; Yu, R.; Wu, Z. Highly-Sensitive Liquid Crystal Biosensor Based on DNA Dendrimers-Mediated Optical Reorientation. *Biosens. Bioelectron.* **2014**, *62*, 84–89.
(31) Haridas, V.; Sharma, Y. K.; Sahu, S.; Verma, R. P.; Sadanandan, S.; Kacheshwar, B. G. Designer Peptide Dendrimers Using Click Reaction. *Tetrahedron* **2011**, *67*, 1873–1884.
(32) Hudak, J. E.; Bertozzi, C. R. Glycotherapy: New Advances Inspire a Reemergence of Glycans in Medicine. *Chem. Biol.* **2014**, *21*, 16–37.
(33) García-Vallejo, J. J.; Ambrosini, M.; Overbeek, A.; van Riel, W. E.; Bloem, K.; Unger, W. W. J.; Chiodo, F.; Bolscher, J. G.; Nazmi, K.; Kalay, H. Multivalent Glycopeptide Dendrimers for the Targeted Delivery of Antigens to Dendritic Cells. *Mol. Immunol.* **2013**, *53*, 387–397.
(34) Zhou, T.; Chen, P.; Niu, L.; Jin, J.; Liang, D.; Li, Z.; Yang, Z.; Liu, D. pH-Responsive Size-Tunable Self-Assembled DNA Dendrimers. *Angew. Chemie* **2012**, *124*, 11433–11436.
(35) Torres, Á.; Albericio, F.; Royo, M. Polyproline–OEG Co-Oligomeric Dendrimers: A Family of Highly Branched Polyproline Macromolecules. *European J. Org. Chem.* **2013**, *2013*, 8279-8287.
(36) Maiti, P. K.; Çağın, T.; Lin, S. T.; Goddard, W. A. Effect of Solvent and pH on the Structure of PAMAM Dendrimers. *Macromolecules* **2005**, *38*, 979–991.
(37) Lee, I.; Athey, B. D.; Wetzel, A. W.; Meixner, W.; Baker, J. R. Structural Molecular Dynamics Studies on Polyamidoamine Dendrimers for a Therapeutic Application: Effects of pH and Generation. *Macromolecules* **2002**, *35*, 4510–4520.
(38) Rietveld, I. B.; Bouwman, W. G.; Baars, M. W. P. L.; Heenan, R. K. Location of the Outer Shell and Influence of pH on Carboxylic Acid-Functionalized Poly(propyleneimine) Dendrimers. *Macromolecules* **2001**, *34*, 8380–8383.
(39) D'Emanuele, A.; Attwood, D. Dendrimer–drug Interactions. *Adv. Drug Deliv. Rev.* **2005**, *57*, 2147–2162.
(40) Dendritech. URL: <http://www.dendritech.com/pamam.html>, (accessed on Dec 30th, 2014).
(41) Maiti, P. K.; Çağın, T.; Wang, G.; Goddard, W. A. Structure of PAMAM Dendrimers: Generations 1 through 11. *Macromolecules* **2004**, *37*, 6236–6254.
(42) Astruc, D.; Boisselier, E.; Ornelas, C. Dendrimers Designed for Functions: From Physical, Photophysical, and Supramolecular Properties to Applications in Sensing, Catalysis, Molecular Electronics, Photonics, and Nanomedicine. *Chem. Rev.* **2010**, *110*, 1857–1959.
(43) Jevprasesphant, R.; Penny, J.; Jalal, R.; Attwood, D.; McKeown, N. B.; D'Emanuele, A. The Influence of Surface Modification on the Cytotoxicity of PAMAM Dendrimers. *Int. J. Pharm.* **2003**, *252*, 263–266.
(44) Govender, P.; Therrien, B.; Smith, G. S. Bio-Metallodendrimers–Emerging Strategies in Metal-Based Drug Design. *Eur. J. Inorg. Chem.* **2012**, *2012*, 2853–2862.
(45) Gasser, G. *Inorganic Chemical Biology: Principles, Techniques and Applications*; Wiley:USA, 2014, Chapter 11.
(46) El Kazzouli, S.; El Brahmi, N.; Mignani, S.; Bousmina, M.; Zablocka, M.; P Majoral, J. From Metallodrugs to Metallodendrimers for Nanotherapy in Oncology: A Concise Overview. *Curr. Med. Chem.* **2012**, *19*, 4995–5010.
(47) Xu, L.; Chen, L. J.; Yang, H. B. Recent Progress in the Construction of Cavity-Cored Supramolecular Metallodendrimers via Coordination-Driven Self-Assembly. *Chem. Commun.* **2014**, *50*, 5156–5170.

(48) Rodrigues, J.; Jardim, M. G.; Figueira, J.; Gouveia, M.; Tomas, H.; Rissanen, K. Poly(alkylidenamines) Dendrimers as Scaffolds for the Preparation of Low-Generation Ruthenium Based Metallodendrimers. *New J. Chem.* **2011**, *35*, 1938–1943.
(49) Astruc, D.; Ruiz, J. The Redox Functions of Metallodendrimers. *J. Inorg. Organomet. Polym. Mater.* **2014**, 1–10.
(50) Astruc, D.; Rapakousiou, A.; Wang, Y.; Djeda, R.; Diallo, A.; Ruiz, J.; Ornelas, C. Review: Mixed-Valent Metallodendrimers: Design and Functions. *J. Coord. Chem.* **2014**, *67*, 3809–3821.
(51) Wang, Y.; Salmon, L.; Ruiz, J.; Astruc, D. Metallodendrimers in Three Oxidation States with Electronically Interacting Metals and Stabilization of Size-Selected Gold Nanoparticles. *Nat Commun* **2014**, *5*, 908–911.
(52) Menjoge, A. R.; Kannan, R. M.; Tomalia, D. A. Dendrimer-Based Drug and Imaging Conjugates: Design Considerations for Nanomedical Applications. *Drug Discov. Today* **2010**, *15*, 171–185.
(53) Moeller, M.; Matyjaszewski, K. (editors). *Polymer Science: A Comprehensive Reference*, 10 Volume Set, Elsevier: USA, 2012, Volume 6, pp. 113-176.
(54) Dong, R.; Zhou, Y.; Zhu, X. Supramolecular Dendritic Polymers: From Synthesis to Applications. *Acc. Chem. Res.* **2014**, *47*, 2006–2016.
(55) Chatani, S.; Podgórski, M.; Wang, C.; Bowman, C. N. Facile and Efficient Synthesis of Dendrimers and One-Pot Preparation of Dendritic–Linear Polymer Conjugates via a Single Chemistry: Utilization of Kinetically Selective Thiol–Michael Addition Reactions. *Macromolecules* **2014**, *47*, 4894–4900.
(56) Gao, C.; Liu, M.; Lü, S.; Zhang, X.; Chen, Y. Synthesis and Self-Assembly of PAMAM/PAA Janus Dendrimers. *Mater. Res. Express* **2014**, *1*, 15005.
(57) Wang, L.; Kiemle, D. J.; Boyle, C. J.; Connors, E. L.; Gitsov, I. “Click” Synthesis of Intrinsically Hydrophilic Dendrons and Dendrimers Containing Metal Binding Moieties at Each Branching Unit. *Macromolecules* **2014**, *47*, 2199–2213.
(58) Kannan, R. M.; Nance, E.; Kannan, S.; Tomalia, D. A. Emerging Concepts in Dendrimer-based Nanomedicine: From Design Principles to Clinical Applications. *J. Intern. Med.* **2014**, *276*, 579–617.
(59) Abbasi, E.; Aval, S. F.; Akbarzadeh, A.; Milani, M.; Nasrabadi, H. T.; Hanifepour, Y.; Nejati-Koshki, K.; Pashaei-Asl, R. Dendrimers: Synthesis, Applications, and Properties. *Nanoscale Res. Lett.* **2014**, *9*, 247-257.
(60) Kottari, N.; Chabre, Y. M.; Shiao, T. C.; Rej, R.; Roy, R. Efficient and Accelerated Growth of Multifunctional Dendrimers Using Orthogonal Thiol–ene and SN2 Reactions. *Chem. Commun.* **2014**, *50*, 1983–1985.
(61) Gonzaga, F.; Sadowski, L. P.; Rambarran, T.; Grande, J.; Adronov, A.; Brook, M. A. Highly Efficient Divergent Synthesis of Dendrimers via Metal-Free “click” Chemistry. *J. Polym. Sci. Part A Polym. Chem.* **2013**, *51*, 1272–1277.
(62) Caminade, A. M.; Turrin, C. O.; Laurent, R.; Ouali, A.; Delavaux-Nicot, B. (editors). *Dendrimers: Towards Catalytic, Material and Biomedical Uses*; Wiley: USA, 2011; Chapters 1,2,16 and 18.
(63) Sowinska, M.; Urbanczyk-Lipkowska, Z. Advances in the Chemistry of Dendrimers. *New J. Chem.* **2014**, *38*, 2168–2203.
(64) Walter, M. V.; Malkoch, M. Simplifying the Synthesis of Dendrimers: Accelerated Approaches. *Chem. Soc. Rev.* **2012**, *41*, 4593–4609.
(65) Nair, D. P.; Podgórski, M.; Chatani, S.; Gong, T.; Xi, W.; Fenoli, C. R.; Bowman, C. N. The Thiol-Michael Addition Click Reaction: A Powerful and Widely Used Tool in Materials Chemistry. *Chem. Mater.* **2013**, *26*, 724–744.
(66) Hawker, C. J.; Frechet, J. M. J. Preparation of Polymers with Controlled Molecular Architecture. A New Convergent Approach to Dendritic Macromolecules. *J. Am. Chem. Soc.* **1990**, *112*, 7638–7647.
(67) Xi, W.; Scott, T. F.; Kloxin, C. J.; Bowman, C. N. Click Chemistry in Materials Science. *Adv. Funct. Mater.* **2014**, *24*, 2572–2590.

(68) Pittelkow, M.; Christensen, J. B. Convergent Synthesis of Internally Branched PAMAM Dendrimers. *Org. Lett.* **2005**, *7*, 1295–1298.
(69) Enciso, A. E.; Abid, Z. M.; Simanek, E. E. Rapid, Semi-Automated Convergent Synthesis of Low Generation Triazine Dendrimers Using Microwave Assisted Reactions. *Polym. Chem.* **2014**, *5*, 4635-4640.
(70) Thirunarayanan, A.; Raja, S.; Mohanraj, G.; Rajakumar, P. Synthesis of Chiral Core Based Triazole Dendrimers with M-Terphenyl Surface Unit and Their Antibacterial Studies. *RSC Adv.* **2014**, *4*, 41778–41783.
(71) Ornelas, C.; Pennell, R.; Liebes, L. F.; Weck, M. Construction of a Well-Defined Multifunctional Dendrimer for Theranostics. *Org. Lett.* **2011**, *13*, 976–979.
(72) Kalhapure, R. S.; Kathiravan, M. K.; Akamanchi, K. G.; Govender, T. Dendrimers-from Organic Synthesis to Pharmaceutical Applications: An Update. *Pharm. Dev. Technol.* **2013**, (Note: [Epub. ahead of print]).
(73) Tuuttila, T.; Lipsonen, J.; Lahtinen, M.; Huuskonen, J.; Rissanen, K. Synthesis and Characterization of Chiral Azobenzene Dye Functionalized Janus Dendrimers. *Tetrahedron* **2008**, *64*, 10590–10597.
(74) Kumar, P. D.; Kumar, P. V.; Saravanan, G. Strategies in Dendritic Architecture for Drug delivery–An over Review. *Indian J. Res. Pharm. Biotechnol.* **2013**, *6*, 922-934.
(75) Wooley, K. L.; Hawker, C. J.; Frechet, J. M. J. Hyperbranched Macromolecules via a Novel Double-Stage Convergent Growth Approach. *J. Am. Chem. Soc.* **1991**, *113*, 4252–4261.
(76) Hadad, C.; García-Martínez, J. C.; Rodríguez-López, J. Layer-Block Dendrimers with Alternating Thienylenevinylene and Phenylenevinylene Units. *J. Org. Chem.* **2012**, *77*, 6223-6230.
(77) Wang, X.; Yang, Y.; Gao, P.; Li, D.; Yang, F.; Shen, H.; Guo, H.; Xu, F.; Wu, D. POSS Dendrimers Constructed from a 1 → 7 Branching Monomer. *Chem. Commun.* **2014**, *50*, 6126-6129.
(78) Tiwari, A.; Demir, M. M. (editors). *Advanced Sensor and Detection Materials*; John Wiley & Sons: USA, **2014**; Chapter 11.
(79) Carlmark, A.; Malmström, E.; Malkoch, M. Dendritic Architectures Based on Bis-MPA: Functional Polymeric Scaffolds for Application-Driven Research. *Chem. Soc. Rev.* **2013**, *42*, 5858–5879.
(80) Ihre, H.; Hult, A.; Fréchet, J. M. J.; Gitsov, I. Double-Stage Convergent Approach for the Synthesis of Functionalized Dendritic Aliphatic Polyesters Based on 2, 2-Bis (hydroxymethyl) Propionic Acid. *Macromolecules* **1998**, *31*, 4061–4068.
(81) Spindler, R.; Fréchet, J. M. J. Two-Step Approach towards the Accelerated Synthesis of Dendritic Macromolecules. *J. Chem. Soc. Perkin Trans. 1* **1993**, 913–918.
(82) Zeng, F.; Zimmerman, S. C. Rapid Synthesis of Dendrimers by an Orthogonal Coupling Strategy. *J. Am. Chem. Soc.* **1996**, *118*, 5326–5327.
(83) Xu, X.; Jian, Y.; Li, Y.; Zhang, X.; Tu, Z.; Gu, Z. Bio-Inspired Supramolecular Hybrid Dendrimers Self-Assembled from Low-Generation Peptide Dendrons for Highly Efficient Gene Delivery and Biological Tracking. *ACS Nano* **2014**, *8*, 9255–9264.
(84) Sebestik, J.; Niederhafner, P.; Jezek, J. Peptide and Glycopeptide Dendrimers and Analogous Dendrimeric Structures and Their Biomedical Applications. *Amino Acids* **2011**, *40*, 301–370.
(85) Maraval, V.; Pyzowski, J.; Caminade, A.-M.; Majoral, J.-P. “Lego” Chemistry for the Straightforward Synthesis of Dendrimers. *J. Org. Chem.* **2003**, *68*, 6043–6046.
(86) Sebestik, J.; Reinis, M.; Jezek, J. *Biomedical Applications of Peptide-, Glyco- and Glycopeptide Dendrimers, and Analogous Dendrimeric Structures*; Springer: USA, 2012; pp. 55-70.
(87) Caminade, A. M.; Laurent, R.; Majoral, J. P. Characterization of Dendrimers. *Adv. Drug Deliv. Rev.* **2005**, *57*, 2130–2146.
(88) Mullen, D. G.; Desai, A.; van Dongen, M. A.; Barash, M.; Baker Jr, J. R.; Banaszak Holl, M. M. Best Practices for Purification and Characterization of PAMAM Dendrimer. *Macromolecules* **2012**, *45*, 5316–5320.
(89) Young, J. K.; Baker, G. R.; Newkome, G. R.; Morris, K. F.; Johnson Jr, C. S. “Smart” Cascade Polymers. Modular Syntheses of Four-Directional Dendritic Macromolecules with Acidic,

Neutral, or Basic Terminal Groups and the Effect of pH Changes on Their Hydrodynamic Radii. *Macromolecules* **1994**, *27*, 3464–3471.
(90) Meltzer, A. D.; Tirrell, D. A.; Jones, A. A.; Inglefield, P. T.; Hedstrand, D. M.; Tomalia, D. A. Chain Dynamics in Poly (amidoamine) Dendrimers: A Study of Carbon-13 NMR Relaxation Parameters. *Macromolecules* **1992**, *25*, 4541–4548.
(91) Skoog, D.; West, D.; Holler, F.; Crouch, S. *Fundamentals of Analytical Chemistry*; 9th Edition; Cengage Learning: USA, 2013; pp. 649-760.
(92) Basic UV/Visible Spectrophotometry. URL: <http://is.gd/lUhB6J> (accessed on Dec 30th, 2014).
(93) Deloncle, R.; Caminade, A.-M. Stimuli-Responsive Dendritic Structures: The Case of Light-Driven Azobenzene-Containing Dendrimers and Dendrons. *J. Photochem. Photobiol. C Photochem. Rev.* **2010**, *11*, 25–45.
(94) Ornelas, C.; Ruiz, J.; Belin, C.; Astruc, D. Giant Dendritic Molecular Electrochrome Batteries with Ferrocenyl and Pentamethylferrocenyl Termini. *J. Am. Chem. Soc.* **2008**, *131*, 590–601.
(95) Liu, H.; Sun, K.; Zhao, J.; Guo, R.; Shen, M.; Cao, X.; Zhang, G.; Shi, X. Dendrimer-Mediated Synthesis and Shape Evolution of Gold–silver Alloy Nanoparticles. *Colloids Surf., A* **2012**, *405*, 22–29.
(96) Liu, H.; Shen, M.; Zhao, J.; Guo, R.; Cao, X.; Zhang, G.; Shi, X. Tunable Synthesis and Acetylation of Dendrimer-Entrapped or Dendrimer-Stabilized Gold–silver Alloy Nanoparticles. *Colloids Surf., B* **2012**, *94*, 58–67.
(97) Hawker, C. J.; Wooley, K. L.; Frechet, J. M. J. Solvatochromism as a Probe of the Microenvironment in Dendritic Polyethers: Transition from an Extended to a Globular Structure. *J. Am. Chem. Soc.* **1993**, *115*, 4375–4376.
(98) Majoros, I. J.; Myc, A.; Thomas, T.; Mehta, C. B.; Baker, J. R. PAMAM Dendrimer-Based Multifunctional Conjugate for Cancer Therapy: Synthesis, Characterization, and Functionality. *Biomacromolecules* **2006**, *7*, 572–579.
(99) Wells, M.; Crooks, R. M. Interactions between Organized, Surface-Confined Monolayers and Vapor-Phase Probe Molecules. 10. Preparation and Properties of Chemically Sensitive Dendrimer Surfaces. *J. Am. Chem. Soc.* **1996**, *118*, 3988–3989.
(100) Furer, V. L.; Majoral, J. P.; Caminade, A. M.; Kovalenko, V. I. Elementoorganic Dendrimer Characterization by Raman Spectroscopy. *Polymer* **2004**, *45*, 5889–5895.
(101) Specac. Reflectance Spectroscopy. URL: <http://is.gd/eQV8nq> (accessed on Dec 30th, 2014).
(102) Dhanikula, R. S.; Hildgen, P. Synthesis and Evaluation of Novel Dendrimers with a Hydrophilic Interior as Nanocarriers for Drug Delivery. *Bioconjug. Chem.* **2005**, *17*, 29–41.
(103) Devarakonda, B.; Otto, D. P.; Judefeind, A.; Hill, R. A.; de Villiers, M. M. Effect of pH on the Solubility and Release of Furosemide from Polyamidoamine (PAMAM) Dendrimer Complexes. *Int. J. Pharm.* **2007**, *345*, 142–153.
(104) Kolhe, P.; Misra, E.; Kannan, R. M.; Kannan, S.; Lieh-Lai, M. Drug Complexation, in Vitro Release and Cellular Entry of Dendrimers and Hyperbranched Polymers. *Int. J. Pharm.* **2003**, *259*, 143–160.
(105) Markatou, E.; Gionis, V.; Chryssikos, G. D.; Hatziantoniou, S.; Georgopoulos, A.; Demetzos, C. Molecular Interactions between Dimethoxycurcumin and PAMAM Dendrimer Carriers. *Int. J. Pharm.* **2007**, *339*, 231–236.
(106) Nigam, S.; Chandra, S.; Newgreen, D. F.; Bahadur, D.; Chen, Q. Poly(ethylene glycol)-Modified PAMAM-Fe_3O_4-Doxorubicin Triads with the Potential for Improved Therapeutic Efficacy: Generation-Dependent Increased Drug Loading and Retention at Neutral pH and Increased Release at Acidic pH. *Langmuir* **2014**, *30*, 1004-1011.
(107) Zhao, H.; Gu, W.; Ye, L.; Yang, H. Biodistribution of PAMAM Dendrimer Conjugated Magnetic Nanoparticles in Mice. *J. Mater. Sci. Mater. Med.* **2014**, *25*, 769–776.
(108) Cao, Q.; Liu, Y.; Wang, C.; Cheng, J. Phosphorus-Modified Poly(styrene-Co-divinylbenzene)-PAMAM Chelating Resin for the Adsorption of uranium(VI) in Aqueous. *J. Hazard. Mater.* **2013**, *263,* 311–321.
(109) Ji, Y.; Yang, X.; Qian, Y. Poly-Amidoamine Structure Characterization: Amide Resonance Structure of Imidic Acid (HO-C=N) and Tertiary Ammonium. *RSC Adv.* **2014**, *4*, 49535–49540.

(110) Kubitscheck, U. (editor). *Fluorescence Microscopy: From Principles to Biological Applications*; Wiley: USA, 2013; Chapters 2-4.
(111) Staneva, D.; Bosch, P.; Asiri, A. M.; Taib, L. A.; Grabchev, I. Studying pH Dependence of the Photophysical Properties of a Blue Emitting Fluorescent PAMAM Dendrimer and Evaluation of Its Sensor Potential. *Dye. Pigment.* **2014**, *105*, 114–120.
(112) Chen, M.; Yin, M. Design and Development of Fluorescent Nanostructures for Bioimaging. *Prog. Polym. Sci.* **2014**, *39*, 365–395.
(113) Georgiev, N. I.; Asiri, A. M.; Qusti, A. H.; Alamry, K. A.; Bojinov, V. B. Design and Synthesis of pH-Selective Fluorescence Sensing PAMAM Light-Harvesting Dendrons Based on 1,8-Naphthalimides. *Sensors Actuators B Chem.* **2014**, *190*, 185–198.
(114) Sharma, A.; Mejia, D.; Maysinger, D.; Kakkar, A. Design and Synthesis of Multifunctional Traceable Dendrimers for Visualizing Drug Delivery. *RSC Adv.* **2014**, *4*, 19242–19245.
(115) Denora, N.; Laquintana, V.; Lopalco, A.; Iacobazzi, R. M.; Lopedota, A.; Cutrignelli, A.; Iacobellis, G.; Annese, C.; Cascione, M.; Leporatti, S. *In Vitro* Targeting and Imaging the Translocator Protein TSPO 18-kDa through G(4)-PAMAM–FITC Labeled Dendrimer. *J. Controlled Release* **2013**, *172*, 1111–1125.
(116) Salgado, A. J.; Oliveira, J. M.; Pirraco, R. P.; Pereira, V. H.; Fraga, J. S.; Marques, A. P.; Neves, N. M.; Mano, J. F.; Reis, R. L.; Sousa, N. Carboxymethylchitosan/Poly (amidoamine) Dendrimer Nanoparticles in Central Nervous Systems-Regenerative Medicine: Effects on Neuron/Glial Cell Viability and Internalization Efficiency. *Macromol. Biosci.* **2010**, *10*, 1130-1140.
(117) Ciepluch, K.; Ionov, M.; Majoral, J.-P.; Muñoz-Fernández, M. A.; Bryszewska, M. Interaction of Phosphorus Dendrimers with HIV peptides - Fluorescence Studies of Nano-Complexes Formation. *J. Lumin.* **2014**, *148*, 364–369.
(118) Shen, D.; Zhou, F.; Xu, Z.; He, B.; Li, M.; Shen, J.; Yin, M.; An, C. Systemically Interfering with Immune Response by a Fluorescent Cationic Dendrimer Delivered Gene Suppression. *J. Mater. Chem. B* **2014**, *2*, 4653–4659.
(119) Gonçalves, M.; Maciel, D.; Capelo, D.; Xiao, S.; Sun, W.; Shi, X.; Rodrigues, J.; Tomás, H.; Li, Y. Dendrimer-Assisted Formation of Fluorescent Nanogels for Drug Delivery and Intracellular Imaging. *Biomacromolecules* **2014**, *15*, 492–499.
(120) Li, X.; Takashima, M.; Yuba, E.; Harada, A.; Kono, K. PEGylated PAMAM Dendrimer-doxorubicin Conjugate-Hybridized Gold Nanorod for Combined Photothermal-Chemotherapy. *Biomaterials* **2014**, *35*, 6576–6584.
(121) Wang, S.; Li, Y.; Fan, J.; Wang, Z.; Zeng, X.; Sun, Y.; Song, P.; Ju, D. The Role of Autophagy in the Neurotoxicity of Cationic PAMAM Dendrimers. *Biomaterials* **2014**, *35*, 7588–7597.
(122) Wang, D.; Imae, T.; Miki, M. Fluorescence Emission from PAMAM and PPI Dendrimers. *J. Colloid Interface Sci.* **2007**, *306*, 222–227.
(123) Jia, D.; Cao, L.; Wang, D.; Guo, X.; Liang, H.; Zhao, F.; Gu, Y.; Wang, D. Uncovering a Broad Class of Fluorescent Amine-Containing Compounds by Heat Treatment. *Chem. Commun.* **2014**, *50*, 11488–11491.
(124) Hornyak, G. L. (editor). *Introduction to Nanoscience*; CRC Press: USA, 2008; pp. 318–322.
(125) McNeil, S. E. (editor). *Characterization of Nanoparticles Intended for Drug Delivery*, Humana Press: USA, 2010; pp. 63–70.
(126) Malvern. Zetasizer Nano User Manual (English). URL: <http://is.gd/jzz3BQ> (accessed on Dec 30th, 2014).
(127) NanoSight. Zetapotential Analysis. URL:<http://is.gd/oIpXLx> (accessed Dec 30th, 2014).
(128) Venuganti, V. V.; Sahdev, P.; Hildreth, M.; Guan, X.; Perumal, O. Structure-Skin Permeability Relationship of Dendrimers. *Pharm. Res.* **2011**, *28*, 2246–2260.
(129) Chen, W.; Tomalia, D. A.; Thomas, J. L. Unusual pH-Dependent Polarity Changes in PAMAM Dendrimers: Evidence for pH-Responsive Conformational Changes. *Macromolecules* **2000**, *33*, 9169–9172.
(130) Shi, X.; Majoros, I. J.; Baker, J. R. Capillary Electrophoresis of Poly(amidoamine) Dendrimers: From Simple Derivatives to Complex Multifunctional Medical Nanodevices. *Mol. Pharm.* **2005**, *2*, 278–294.

(131) Ertürk, A. S.; Tülü, M.; Bozdoğan, A. E.; Parali, T. Microwave Assisted Synthesis of Jeffamine Cored PAMAM Dendrimers. *Eur. Polym. J.* **2014**, *52*, 218–226.
(132) Van Dongen, M. A.; Desai, A.; Orr, B. G.; Baker Jr, J. R.; Banaszak Holl, M. M. Quantitative Analysis of Generation and Branch Defects in G5 Poly (amidoamine) Dendrimer. *Polymer* **2013**, *54*, 4126–4133.
(133) Kolhatkar, R. B.; Kitchens, K. M.; Swaan, P. W.; Ghandehari, H. Surface Acetylation of Polyamidoamine (PAMAM) Dendrimers Decreases Cytotoxicity While Maintaining Membrane Permeability. *Bioconjug. Chem.* **2007**, *18*, 2054–2060.
(134) Kumar, P. D.; Kumar, P. V.; Selvam, T. P.; Rao, K. R. S. S. PEG Conjugated PAMAM Dendrimers with a Anti-HIV Drug Stavudine for Prolong Release. *Res. Biotechnol.* **2013**, *4*.
(135) Son, S. J.; Yu, G. S.; Choe, Y. H.; Kim, Y.-J.; Lee, E.; Park, J.-S.; Choi, J. S. PAMAM Dendrimers Conjugated with L-Arginine and γ-Aminobutyric Acid as Novel Polymeric Gene Delivery Carriers. *Bull. Korean Chem. Soc.* **2013**, *34*, 579–584.
(136) Zhu, J.; Zheng, L.; Wen, S.; Tang, Y.; Shen, M.; Zhang, G.; Shi, X. Targeted Cancer Theranostics Using Alpha-Tocopheryl Succinate-Conjugated Multifunctional Dendrimer-Entrapped Gold Nanoparticles. *Biomaterials* **2014**, *35*, 7635–7646.
(137) Burgess, R. R.; Deutscher, M. P. (editors). *Guide to Protein Purification*; Methods in enzymology; Elsevier Science: UK, 2009; pp. 104–107.
(138) Wixom, R. L.; Gehrke, C. W. (editors). *Chromatography: A Science of Discovery*; Wiley: USA, 2011; Chapters 1 and 2.
(139) Wu, C. S. *Handbook Of Size Exclusion Chromatography And Related Techniques: Revised And Expanded*; Chromatographic science series; Taylor & Francis: USA, 2003; Chapter 1.
(140) Heftmann, E. *Chromatography: Fundamentals and Applications of Chromatography and Related Differential Migration Methods - Part A: Fundamentals and Techniques*, 6th Edition; Elsevier Science: Netherlands, 2004; pp. 1-88.
(141) Ulaszewska, M. M.; Hernando, M. D.; Moreno, A. U.; García, A. V.; Calvo, E. G.; Fernández, A. R. Identification and Quantification of Poly(amidoamine) PAMAM Dendrimers of Generations 0 to 3 by Liquid Chromatography/hybrid Quadrupole Time-of-Flight Mass Spectrometry in Aqueous Medium. *Rapid Commun. Mass Spectrom.* **2013**, *27*, 747–762.
(142) Park, E. J.; Cho, H.; Kim, S. W.; Na, D. H. Chromatographic Methods for Characterization of Poly(ethylene Glycol)-Modified Polyamidoamine Dendrimers. *Anal. Biochem.* **2014**, *449*, 42-44.
(143) Uclés, A.; Martínez Bueno, M. J.; Ulaszewska, M. M.; Hernando, M. D.; Ferrer, C.; Fernández-Alba, A. R. Quantitative Determination of Poly(amidoamine) Dendrimers in Urine by Liquid Chromatography/electrospray Ionization Hybrid Quadrupole Linear Ion Trap Mass Spectrometry. *Rapid Commun. Mass Spectrom.* **2013**, *27*, 2519–2529.
(144) Studzińska, S.; Rola, R.; Buszewski, B. Determination of Nucleotides in Infant Milk Formulas Using Novel Dendrimer Ion-Exchangers. *J. Chromatogr. B* **2014**, *949–950*, 87–93.
(145) Hubbard, D.; Ghandehari, H.; Brayden, D. J. Transepithelial Transport of PAMAM Dendrimers across Isolated Rat Jejunal Mucosae in Ussing Chambers. *Biomacromolecules* **2014**, *15*, 2889–2895.
(146) Van Dongen, M. A.; Silpe, J. E.; Dougherty, C. A.; Kanduluru, A. K.; Choi, S. K.; Orr, B. G.; Low, P. S.; Banaszak Holl, M. M. Avidity Mechanism of Dendrimer–Folic Acid Conjugates. *Mol. Pharm.* **2014**, *11*, 1696–1706.
(147) Noriega-Luna, B.; Godínez, L. A.; Rodríguez, F. J.; Rodríguez, A.; Zaldívar-Lelo de Larrea, G.; Sosa-Ferreyra, C. F.; Mercado-Curiel, R. F.; Manríquez, J.; Bustos, E. Applications of Dendrimers in Drug Delivery Agents, Diagnosis, Therapy, and Detection. *J. Nanomater.* **2014**, *2014*, 1-19.
(148) Mignani, S.; Kazzouli, S. El; Bousmina, M.; Majoral, J.-P. Dendrimer Space Concept for Innovative Nanomedicine: A Futuristic Vision for Medicinal Chemistry. *Prog. Polym. Sci.* **2013**, *38*, 993–1008.
(149) Mignani, S.; El Kazzouli, S.; Bousmina, M.; Majoral, J.-P. Expand Classical Drug Administration Ways by Emerging Routes Using Dendrimer Drug Delivery Systems: A Concise Overview. *Adv. Drug Deliv. Rev.* **2013**, *65*, 1316–1330.

(150) Longmire, M. R.; Ogawa, M.; Choyke, P. L.; Kobayashi, H. Dendrimers as High Relaxivity MR Contrast Agents. *Wiley Interdiscip. Rev.: Nanomed. Nanobiotechnol.* **2014**, *6*, 155–162.
(151) Wu, D.; Yang, J.; Li, J.; Chen, L.; Tang, B.; Chen, X.; Wu, W.; Li, J. Hydroxyapatite-Anchored Dendrimer for in Situ Remineralization of Human Tooth Enamel. *Biomaterials* **2013**, *34*, 5036–5047.
(152) Qi, R.; Gao, Y.; Tang, Y.; He, R.-R.; Liu, T.-L.; He, Y.; Sun, S.; Li, B.-Y.; Li, Y.-B.; Liu, G. PEG-Conjugated PAMAM Dendrimers Mediate Efficient Intramuscular Gene Expression. *AAPS J.* **2009**, *11*, 395–405.
(153) Labieniec, M.; Watala, C. PAMAM Dendrimers-diverse Biomedical Applications. Facts and Unresolved Questions. *Cent. Eur. J. Biol.* **2009**, *4*, 434–451.
(154) Calabretta, M. K.; Kumar, A.; McDermott, A. M.; Cai, C. Antibacterial Activities of Poly(amidoamine) Dendrimers Terminated with Amino and Poly(ethylene Glycol) Groups. *Biomacromolecules* **2007**, *8*, 1807–1811.
(155) Thomas, T. P.; Choi, S. K.; Li, M.-H.; Kotlyar, A.; Baker Jr., J. R. Design of Riboflavin-Presenting PAMAM Dendrimers as a New Nanoplatform for Cancer-Targeted Delivery. *Bioorg. Med. Chem. Lett.* **2010**, *20*, 5191–5194.
(156) Peng, J.; Qi, X.; Chen, Y.; Ma, N.; Zhang, Z.; Xing, J.; Zhu, X.; Li, Z.; Wu, Z. Octreotide-Conjugated PAMAM for Targeted Delivery to Somatostatin Receptors Over-Expressed Tumor Cells. *J. Drug Targeting* **2014**, *22*, 428–438.
(157) Bugaj, A. M. Targeted Photodynamic Therapy–a Promising Strategy of Tumor Treatment. *Photochem. Photobiol. Sci.* **2011**, *10*, 1097–1109.
(158) Chaplot, S. P.; Rupenthal, I. D. Dendrimers for Gene Delivery–a Potential Approach for Ocular Therapy? *J. Pharmacol. Pharmacother.* **2014**, *66*, 542–556.
(159) Lee, J.; Jung, J.; Kim, Y.-J.; Lee, E.; Choi, J. S. Gene Delivery of PAMAM Dendrimer Conjugated with the Nuclear Localization Signal Peptide Originated from Fibroblast Growth Factor 3. *Int. J. Pharm.* **2014**, *459*, 10–18.
(160) Wängler, C.; Moldenhauer, G.; Saffrich, R.; Knapp, E.; Beijer, B.; Schnçlzer, M.; Wängler, B.; Eisenhut, M.; Haberkorn, U.; Mier, W. PAMAM Structure-Based Multifunctional Fluorescent Conjugates for Improved Fluorescent Labelling of Biomacromolecules. *Chemistry* **2008**, *27*, 8116–8130.
(161) a) Shen, M.; Shi, X. Dendrimer-Based Organic/inorganic Hybrid Nanoparticles in Biomedical Applications. *Nanoscale* **2010**, *2*, 1596–1610. b) Majoros, I.; Baker, J. R. (editors) *Dendrimer-Based Nanomedicine*; Pan Stanford: Singapore, 2008; Chapters 1,3, 7-9 and 11.
(162) Mullen, D. G.; Fang, M.; Desai, A.; Baker, J. R.; Orr, B. G.; Banaszak Holl, M. M. A Quantitative Assessment of Nanoparticle−Ligand Distributions: Implications for Targeted Drug and Imaging Delivery in Dendrimer Conjugates. *ACS Nano* **2010**, *4*, 657–670.
(163) Zhu, J.; Shi, X. Dendrimer-Based Nanodevices for Targeted Drug Delivery Applications. *J. Mater. Chem. B* **2013**, *1*, 4199–4211.
(164) Chen, Q.; Li, K.; Wen, S.; Liu, H.; Peng, C.; Cai, H.; Shen, M.; Zhang, G.; Shi, X. Targeted CT/MR Dual Mode Imaging of Tumors Using Multifunctional Dendrimer-Entrapped Gold Nanoparticles. *Biomaterials* **2013**, *34*, 5200–5209.
(165) Osma, J. F.; Stoytcheva, M. (editors). *Biosensors: Recent Advances and Mathematical Challenges*; Omniascience: Mexico, 2014; Chapter 6.
(166) Miodek, A.; Castillo, G.; Hianik, T.; Korri-Youssoufi, H. Electrochemical Aptasensor of Cellular Prion Protein Based on Modified Polypyrrole with Redox Dendrimers. *Biosens. Bioelectron.* **2014**, *56*, 104–111.
(167) Hasanzadeh, M.; Shadjou, N.; Eskandani, M.; Soleymani, J.; Jafari, F.; de la Guardia, M. Dendrimer-Encapsulated and Cored Metal Nanoparticles for Electrochemical Nanobiosensing. *TrAC, Trends Anal. Chem.* **2014**, *53*, 137–149.
(168) Jie, G.; Zhang, J.; Jie, G.; Wang, L. A Novel Quantum Dot Nanocluster as Versatile Probe for Electrochemiluminescence and Electrochemical Assays of DNA and Cancer Cells. *Biosens. Bioelectron.* **2014**, *52*, 69–75.
(169) Araque, E.; Villalonga, R.; Gamella, M.; Martínez-Ruiz, P.; Sánchez, A.; García-Baonza, V.; Pingarrón, J. M. Water-Soluble Reduced Graphene Oxide–Carboxymethylcellulose Hybrid Nanomaterial for Electrochemical Biosensor Design. *ChemPlusChem* **2014**, *79*, 1334–1341.

(170) Kavosi, B.; Salimi, A.; Hallaj, R.; Amani, K. A Highly Sensitive Prostate-Specific Antigen Immunosensor Based on Gold nanoparticles/PAMAM Dendrimer Loaded on MWCNTS/chitosan/ionic Liquid Nanocomposite. *Biosens. Bioelectron.* **2014**, *52*, 20–28.
(171) Xu, W.; Wu, Y.; Yi, H.; Bai, L.; Chai, Y.; Yuan, R. Porous Platinum Nanotubes Modified with Dendrimers as Nanocarriers and Electrocatalysts for Sensitive Electrochemical Aptasensors Based on Enzymatic Signal Amplification. *Chem. Commun.* **2014**, *50*, 1451–1453.
(172) Kavosi, B.; Hallaj, R.; Teymourian, H.; Salimi, A. Au nanoparticles/PAMAM Dendrimer Functionalized Wired Ethyleneamine–viologen as Highly Efficient Interface for Ultra-Sensitive A-Fetoprotein Electrochemical Immunosensor. *Biosens. Bioelectron.* **2014**, *59*, 389–396.
(173) Krishnakumar, B.; Imae, T. Chemically Modified Novel PAMAM-ZnO Nanocomposite: Synthesis, Characterization and Photocatalytic Activity. *Appl. Catal., A* **2014**, *486*, 170–175.
(174) Niu, Y.; Qu, R.; Chen, H.; Mu, L.; Liu, X.; Wang, T.; Zhang, Y.; Sun, C. Synthesis of Silica Gel Supported Salicylaldehyde Modified PAMAM Dendrimers for the Effective Removal of Hg(II) from Aqueous Solution. *J. Hazard. Mater.* **2014**, *278*, 267–278.
(175) Cardoso, F. P.; Aquino Neto, S.; Fenga, P. G.; Ciancaglini, P.; De andrade, A. R. Electrochemical Characterization of methanol/O2 Biofuel Cell: Use of Laccase Biocathode Immobilized with Polypyrrole Film and PAMAM Dendrimers. *Electrochim. Acta* **2013**, *90*, 90-94.
(176) Hermanson, G. T. (editors) *Bioconjugate Techniques*; Elsevier Science: UK, 2013, Chapters 3, 8 and 10.
(177) Narain, R. *Chemistry of Bioconjugates: Synthesis, Characterization, and Biomedical Applications,* 1st Edition; Wiley: USA, 2013. Chapter 5.
(178) Zong, H.; Thomas, T. P.; Lee, K. H.; Desai, A. M.; Li, M.; Kotlyar, A.; Zhang, Y.; Leroueil, P. R.; Gam, J. J.; Banaszak Holl, M. M.; Baker, J. R. Bifunctional PAMAM Dendrimer Conjugates of Folic Acid and Methotrexate with Defined Ratio. *Biomacromolecules* **2012**, *13*, 982–991.
(179) Yu, S.; Larson, R. G. Monte-Carlo Simulations of PAMAM Dendrimer-DNA Interactions. *Soft Matter* **2014**, *10*, 5325–5336.
(180) Cao, L.; Yang, W.; Yang, J.; Wang, C.; Fu, S. Hyperbranched Poly (amidoamine)-Modified Multi-Walled Carbon Nanotubes via Grafting-from Method. *Chem. Lett.* **2004**, *33*, 490–491.
(181) Marangoni, V. S.; Paino, I. M.; Zucolotto, V. Synthesis and Characterization of Jacalin-Gold Nanoparticles Conjugates as Specific Markers for Cancer Cells. *Colloids Surf., B* **2013**, *112*, 380–386.
(182) Yeo, Y. (editor). *Nanoparticulate Drug Delivery Systems: Strategies, Technologies, and Applications*; Wiley: USA, 2013; Chapters 6 and 7.
(183) Karp, G. (editor). *Cell and Molecular Biology: Concepts and Experiments*; 7th Edition; John Wiley & Sons: USA, 2013; Chapter 4.
(184) Alberts, B. (editor). *Molecular Biology of the Cell*, Reference Edition Volume 1, 5th Edition; Garland Science, 2008; Chapters 10 and 11.
(185) Lodish, H.; Berk, A.; Kaiser, C. A.; Krieger, M.; Bretscher, A.; Ploegh, H.; Amon, A.; Scott, M. P. (editors). *Molecular Cell Biology*, 7th Edition; W. H. Freeman: USA, 2012; Chapters 10 and 11.
(186) Cooper, G. M.; Hausman, R. E. (editors). *The Cell: A Molecular Approach*, 6th Edition; ASM Press: USA, 2013; Chapter 13.
(187) Yameen, B.; Choi, W. Il; Vilos, C.; Swami, A.; Shi, J.; Farokhzad, O. C. Insight into Nanoparticle Cellular Uptake and Intracellular Targeting. *J. Controlled Release* **2014**, *190*, 485–499.
(188) CK-12. Cell Transport and Homeostasis. URL: <http://www.ck12.org/book/CK-12-Biology/section/3.3/> (accessed on Dec 30th, 2014).
(189) Xu, S.; Olenyuk, B. Z.; Okamoto, C. T.; Hamm-Alvarez, S. F. Targeting Receptor-Mediated Endocytotic Pathways with Nanoparticles: Rationale and Advances. *Adv. Drug Deliv. Rev.* **2013**, *65*, 121–138.
(190) Shang, L.; Nienhaus, K.; Nienhaus, G. U. Engineered Nanoparticles Interacting with Cells: Size Matters. *J. Nanobiotechnology* **2014**, *12*, 5-16.
(191) Rajendran, L.; Knölker, H.-J.; Simons, K. Subcellular Targeting Strategies for Drug Design and Delivery. *Nat. Rev. Drug Discov.* **2010**, *9*, 29–42.
(192) Mayor, S.; Parton, R. G.; Donaldson, J. G. Clathrin-Independent Pathways of Endocytosis. *Cold Spring Harbor Perspect. Biol.* **2014**, *6*, a016758.

(193) Mayor, S.; Pagano, R. E. Pathways of Clathrin-Independent Endocytosis. *Nat. Rev. Mol. Cell Biol.* **2007**, *8*, 603–612.
(194) Bitsikas, V.; Corrêa, I. R.; Nichols, B. J. Clathrin-Independent Pathways Do Not Contribute Significantly to Endocytic Flux. *Elife* **2014**, *3*, e03970.
(195) Canton, I.; Battaglia, G. Endocytosis at the Nanoscale. *Chem. Soc. Rev.* **2012**, *41*, 2718–2739.
(196) Venkatachalam, K.; Wong, C.-O.; Zhu, M. X. The Role of TRPMLs in Endolysosomal Trafficking and Function. *Cell Calcium*. **2014** (Note: In Press, Corrected Proof).
(197) Duncan, R.; Richardson, S. C. W. Endocytosis and Intracellular Trafficking as Gateways for Nanomedicine Delivery: Opportunities and Challenges. *Mol. Pharm.* **2012**, *9*, 2380–2402.
(198) Kou, L.; Sun, J.; Zhai, Y.; He, Z. The Endocytosis and Intracellular Fate of Nanomedicines: Implication for Rational Design. *Asian J. Pharm. Sci.* **2013**, *8*, 1–10.
(199) Kettiger, H.; Schipanski, A.; Wick, P.; Huwyler, J. Engineered Nanomaterial Uptake and Tissue Distribution: From Cell to Organism. *Int. J. Nanomed.* **2013**, *8*, 3255-3269.
(200) Xu, S.; Olenyuk, B. Z.; Okamoto, C. T.; Hamm-Alvarez, S. F. Targeting Receptor-Mediated Endocytotic Pathways with Nanoparticles: Rationale and Advances. *Adv. Drug Deliv. Rev.* **2013**, *65*, 121–138.
(201) McMahon, H. T.; Boucrot, E. Molecular Mechanism and Physiological Functions of Clathrin-Mediated Endocytosis. *Nat. Rev. Mol. Cell Biol.* **2011**, *12*, 517–533.
(202) Zhu, S.; Hong, M.; Zhang, L.; Tang, G.; Jiang, Y.; Pei, Y. PEGylated PAMAM Dendrimer-Doxorubicin Conjugates: In Vitro Evaluation and In Vivo Tumor Accumulation. *Pharm. Res.* **2010**, *27*, 161–174.
(203) Shen, W.; van Dongen, M. A.; Han, Y.; Yu, M.; Li, Y.; Liu, G.; Banaszak Holl, M. M.; Qi, R. The Role of Caveolin-1 and Syndecan-4 in the Internalization of PEGylated PAMAM Dendrimer Polyplexes into Myoblast and Hepatic Cells. *Eur. J. Pharm. Biopharm.* **2014**, *88*, 658-663.
(204) Zwicke, G. L.; Mansoori, G. A.; Jeffery, C. J. Utilizing the Folate Receptor for Active Targeting of Cancer Nanotherapeutics. *Nano Rev.* **2012**, *3*, 1-11.
(205) Schütze, S.; Tchikov, V.; Schneider-Brachert, W. Regulation of TNFR1 and CD95 Signalling by Receptor Compartmentalization. *Nat. Rev. Mol. Cell Biol.* **2008**, *9*, 655–662.
(206) Albertazzi, L.; Serresi, M.; Albanese, A.; Beltram, F. Dendrimer Internalization and Intracellular Trafficking in Living Cells. *Mol. Pharm.* **2010**, *7*, 680–688.
(207) Albertazzi, L.; Fernandez-Villamarin, M.; Riguera, R.; Fernandez-Megia, E. Peripheral Functionalization of Dendrimers Regulates Internalization and Intracellular Trafficking in Living Cells. *Bioconjug. Chem.* **2012**, *23*, 1059–1068.
(208) Kaksonen, M.; Toret, C. P.; Drubin, D. G. Harnessing Actin Dynamics for Clathrin-Mediated Endocytosis. *Nat. Rev. Mol. Cell Biol.* **2006**, *7*, 404–414.
(209) Mercer, J.; Helenius, A. Virus Entry by Macropinocytosis. *Nat. Cell Biol.* **2009**, *11*, 510–520.
(210) Mooren, O. L.; Galletta, B. J.; Cooper, J. A. Roles for Actin Assembly in Endocytosis. *Annu. Rev. Biochem.* **2012**, *81*, 661–686.
(211) Lunov, O.; Syrovets, T.; Loos, C.; Beil, J.; Delacher, M.; Tron, K.; Nienhaus, G. U.; Musyanovych, A.; Mailänder, V.; Landfester, K.; Simmet, T. Differential Uptake of Functionalized Polystyrene Nanoparticles by Human Macrophages and a Monocytic Cell Line. *ACS Nano* **2011**, *5*, 1657–1669.
(212) Oh, N.; Park, J. H. Endocytosis and Exocytosis of Nanoparticles in Mammalian Cells. *Int. J. Nanomed.* **2014**, *9*, 51-63.
(213) Nel, A. E.; Mädler, L.; Velegol, D.; Xia, T.; Hoek, E. M. V; Somasundaran, P.; Klaessig, F.; Castranova, V.; Thompson, M. Understanding Biophysicochemical Interactions at the Nano-Bio Interface. *Nat. Mater.* **2009**, *8*, 543–557.
(214) Albanese, A.; Tang, P. S.; Chan, W. C. W. The Effect of Nanoparticle Size, Shape, and Surface Chemistry on Biological Systems. *Annu. Rev. Biomed. Eng.* **2012**, *14*, 1–16.
(215) Verma, A.; Stellacci, F. Effect of Surface Properties on Nanoparticle–cell Interactions. *Small* **2010**, *6*, 12–21.
(216) Pack, D. W.; Hoffman, A. S.; Pun, S.; Stayton, P. S. Design and Development of Polymers for Gene Delivery. *Nat. Rev. Drug Discov.* **2005**, *4*, 581–593.
(217) Akinc, A.; Battaglia, G. Exploiting Endocytosis for Nanomedicines. *Cold Spring Harbor Perspect. Biol.* **2013**, *5*, a016980.

(218) Sahay, G.; Alakhova, D. Y.; Kabanov, A. V. Endocytosis of Nanomedicines. *J. Controlled Release* **2010**, *145*, 182–195.
(219) Wang, Z.; Chen, C.; Liu, R.; Fan, A.; Kong, D.; Zhao, Y. Two Birds with One Stone: Dendrimer Surface Engineering Enables Tunable Periphery Hydrophobicity and Rapid Endosomal Escape. *Chem. Commun.* **2014**, *50*, 14025–14028.
(220) Lucien, F.; Harper, K.; Pelletier, P.-P.; Volkov, L.; Dubois, C. M. Simultaneous pH Measurement in Endocytic and Cytosolic Compartments in Living Cells Using Confocal Microscopy. *Journal Vis. Exp.* **2014**, e51395–e51395.
(221) Duke, E. M. H.; Razi, M.; Weston, A.; Guttmann, P.; Werner, S.; Henzler, K.; Schneider, G.; Tooze, S. A.; Collinson, L. M. Imaging Endosomes and Autophagosomes in Whole Mammalian Cells Using Correlative Cryo-Fluorescence and Cryo-Soft X-Ray Microscopy (cryo-CLXM). *Ultramicroscopy* **2014**, *143*, 77–87.
(222) Idrissi, F.-Z.; Geli, M. I. Zooming in on the Molecular Mechanisms of Endocytic Budding by Time-Resolved Electron Microscopy. *Cell. Mol. Life Sci.* **2014**, *71*, 641–657.
(223) Peckys, D. B.; de Jonge, N. Gold Nanoparticle Uptake in Whole Cells in Liquid Examined by Environmental Scanning Electron Microscopy. *Microsc. Microanal.* **2014**, *20*, 189–197.
(224) Liang, K.; Gunawan, S. T.; Richardson, J. J.; Such, G. K.; Cui, J.; Caruso, F. Endocytic Capsule Sensors for Probing Cellular Internalization. *Adv. Healthc. Mater.* **2014**, *10*, 1551-1554.
(225) Liang, K.; Such, G. K.; Johnston, A. P. R.; Zhu, Z.; Ejima, H.; Richardson, J. J.; Cui, J.; Caruso, F. Endocytic pH-Triggered Degradation of Nanoengineered Multilayer Capsules. *Adv. Mater.* **2014**, *26*, 1901–1905.
(226) Bourgaux, C.; Couvreur, P. Interactions of Anticancer Drugs with Biomembranes: What Can We Learn from Model Membranes? *J. Controlled Release* **2014**, *190*, 127-138.
(227) Whited, A. M.; Park, P. S. H. Atomic Force Microscopy: A Multifaceted Tool to Study Membrane Proteins and Their Interactions with Ligands. *Biochim. Biophys. Acta (BBA)-Biomembranes* **2014**, *1838*, 56–68.
(228) Vasir, J. K.; Labhasetwar, V. Quantification of the Force of Nanoparticle-Cell Membrane Interactions and Its Influence on Intracellular Trafficking of Nanoparticles. *Biomaterials* **2008**, *29*, 4244–4252.
(229) Ivanov, A. I. Pharmacological Inhibition of Endocytic Pathways: Is It Specific Enough to Be Useful? In *Exocytosis and Endocytosis*; Springer, 2008; pp. 15–33.
(230) Luo, D.; Carter, K. A.; Lovell, J. F. Nanomedical Engineering: Shaping Future Nanomedicines. *Wiley Interdiscip. Rev.: Nanomed. Nanobiotechnol.* **2014** (Note: [Epub. ahead of print]).
(231) a) Arteta, M. Y.; Ainalem, M. L.; Porcar, L.; Martel, A.; Coker, H.; Lundberg, D.; Chang, D. P.; Soltwedel, O.; Barker, R.; Nylander, T. Interactions of PAMAM Dendrimers with Negatively Charged Model Biomembranes. *J. Phys. Chem. B* **2014**, *118*, 12892–12906. b) Duncan, R.; Izzo, L. Dendrimer Biocompatibility and Toxicity. *Adv. Drug Deliv. Rev.* **2005**, *57*, 2215–2237; c) Monticelli, G. R. and L. Modeling the Effect of Nano-Sized Polymer Particles on the Properties of Lipid Membranes. *J. Phys. Condens. Matter* **2014**, *26*, 503101-503112. d) Smith, P.; Brender, J. R.; Dürr, U. H. N.; Xu, J.; Mullen, D. G.; Banaszak Holl, M. M.; Ramamoorthy, A. Solid-State NMR Reveals the Hydrophobic-Core Location of Poly(amidoamine) Dendrimers in Biomembranes. *J. Am. Chem. Soc.* **2010**, *132*, 8087–8097. e) Lee, H. Self-Assembly of Mixtures of a Dendrimer and Lipids: Effects of Hydrophobicity and Electrostatics. *Mol. Simul.* **2011**, *38*, 534–539; f) Kelly, C. V; Liroff, M. G.; Triplett, L. D.; Leroueil, P. R.; Mullen, D. G.; Wallace, J. M.; Meshinchi, S.; Baker, J. R.; Orr, B. G.; Banaszak Holl, M. M. Stoichiometry and Structure of Poly(amidoamine) Dendrimer−Lipid Complexes. *ACS Nano* **2009**, *3*, 1886–1896.
(232) Hong, S.; Leroueil, P. R.; Janus, E. K.; Peters, J. L.; Kober, M.-M.; Islam, M. T.; Orr, B. G.; Baker, J. R.; Banaszak Holl, M. M. Interaction of Polycationic Polymers with Supported Lipid Bilayers and Cells: Nanoscale Hole Formation and Enhanced Membrane Permeability. *Bioconjug. Chem.* **2006**, *17*, 728–734.
(233) Sweet, D. M.; Kolhatkar, R. B.; Ray, A.; Swaan, P.; Ghandehari, H. Transepithelial Transport of PEGylated Anionic Poly(amidoamine) Dendrimers: Implications for Oral Drug Delivery. *J. Controlled Release* **2009**, *138*, 78–85.

(234) Kitchens, K. M.; Kolhatkar, R. B.; Swaan, P. W.; Eddington, N. D.; Ghandehari, H. Transport of Poly (amidoamine) Dendrimers across Caco-2 Cell Monolayers: Influence of Size, Charge and Fluorescent Labeling. *Pharm. Res.* **2006**, *23*, 2818–2826.
(235) Perumal, O. P.; Inapagolla, R.; Kannan, S.; Kannan, R. M. The Effect of Surface Functionality on Cellular Trafficking of Dendrimers. *Biomaterials* **2008**, *29*, 3469–3476.
(236) Goncalves, M.; Castro, R.; Rodrigues, J.; Tomas, H. The Effect of PAMAM Dendrimers on Mesenchymal Stem Cell Viability and Differentiation. *Curr. Med. Chem.* **2012**, *19*, 4969–4975.
(237) Tiriveedhi, V.; Kitchens, K. M.; Nevels, K. J.; Ghandehari, H.; Butko, P. Kinetic Analysis of the Interaction between Poly(amidoamine) Dendrimers and Model Lipid Membranes. *Biochim. Biophys. Acta - Biomembr.* **2011**, *1808*, 209–218.
(238) Avaritt, B.; Swaan, P. Intracellular Ca^{2+} Release Mediates Cationic but Not Anionic Poly(amidoamine) (PAMAM) Dendrimer-Induced Tight Junction Modulation. *Pharm. Res.* **2014**, *31*, 2429–2438.
(239) Mukherjee, S. P.; Byrne, H. J. Polyamidoamine Dendrimer Nanoparticle Cytotoxicity, Oxidative Stress, Caspase Activation and Inflammatory Response: Experimental Observation and Numerical Simulation. *Nanomedicine Nanotechnology, Biol. Med.* **2013**, *9*, 202–211.
(240) Wang, W.; Xiong, W.; Wan, J.; Sun, X.; Xu, H.; Yang, X. The Decrease of PAMAM Dendrimer-Induced Cytotoxicity by PEGylation via Attenuation of Oxidative Stress. *Nanotechnology* **2009**, *20*, 105103-105110.
(241) Li, X.; Haba, Y.; Ochi, K.; Yuba, E.; Harada, A.; Kono, K. PAMAM Dendrimers with an Oxyethylene Unit-Enriched Surface as Biocompatible Temperature-Sensitive Dendrimers. *Bioconjug. Chem.* **2013**, *24*, 282–290.
(242) Nam, H. Y.; Nam, K.; Hahn, H. J.; Kim, B. H.; Lim, H. J.; Kim, H. J.; Choi, J. S.; Park, J.-S. Biodegradable PAMAM Ester for Enhanced Transfection Efficiency with Low Cytotoxicity. *Biomaterials* **2009**, *30*, 665–673.
(243) Seib, F. P.; Jones, A. T.; Duncan, R. Comparison of the Endocytic Properties of Linear and Branched PEIs, and Cationic PAMAM Dendrimers in B16f10 Melanoma Cells. *J. Controlled Release* **2007**, *117*, 291–300.
(244) Goldberg, D. S.; Ghandehari, H.; Swaan, P. W. Cellular Entry of G3.5 Poly (amido Amine) Dendrimers by Clathrin-and Dynamin-Dependent Endocytosis Promotes Tight Junctional Opening in Intestinal Epithelia. *Pharm. Res.* **2010**, *27*, 1547–1557.
(245) Saovapakhiran, A.; D'Emanuele, A.; Attwood, D.; Penny, J. Surface Modification of PAMAM Dendrimers Modulates the Mechanism of Cellular Internalization. *Bioconjug. Chem.* **2009**, *20*, 693–701.
(246) Huang, R.; Ke, W.; Han, L.; Liu, Y.; Shao, K.; Ye, L.; Lou, J.; Jiang, C.; Pei, Y. Brain-Targeting Mechanisms of Lactoferrin-Modified DNA-Loaded Nanoparticles. *J. Cereb. Blood Flow Metab.* **2009**, *29*, 1914–1923.
(247) Huang, H.; Cao, D.; Qin, L.; Tian, S.; Liang, Y.; Pan, S.; Feng, M. Dilution-Stable PAMAM G1-Grafted Polyrotaxane Supermolecules Deliver Gene into Cells through a Caveolae-Dependent Pathway. *Mol. Pharm.* **2014**, *11*, 2323–2333.
(248) Oddone, N.; Zambrana, A. I.; Tassano, M.; Porcal, W.; Cabral, P.; Benech, J. C. Cell Uptake Mechanisms of PAMAM G4-FITC Dendrimer in Human Myometrial Cells. *J. Nanoparticle Res.* **2013**, *15*, 1776–1790.
(249) Liu, X.; Liu, C.; Laurini, E.; Posocco, P.; Pricl, S.; Qu, F.; Rocchi, P.; Peng, L. Efficient Delivery of Sticky siRNA and Potent Gene Silencing in a Prostate Cancer Model Using a Generation 5 Triethanolamine-Core PAMAM Dendrimer. *Mol. Pharm.* **2012**, *9*, 470–481.
(250) Perez, A. P.; Cosaka, M. L.; Romero, E. L.; Morilla, M. J. Uptake and Intracellular Traffic of siRNA Dendriplexes in Glioblastoma Cells and Macrophages. *Int. J. Nanomed.* **2011**, *6*, 2715-2728.
(251) Qi, R.; Mullen, D. G.; Baker Jr, J. R.; Banaszak Holl, M. M. The Mechanism of Polyplex Internalization into Cells: Testing the GM1/caveolin-1 Lipid Raft Mediated Endocytosis Pathway. *Mol. Pharm.* **2010**, *7*, 267–279.
(252) Imamura, M.; Kodama, Y.; Higuchi, N.; Kanda, K.; Nakagawa, H.; Muro, T.; Nakamura, T.; Kitahara, T.; Sasaki, H. Ternary Complex of Plasmid DNA Electrostatically Assembled with

Polyamidoamine Dendrimer and Chondroitin Sulfate for Effective and Secure Gene Delivery. *Biol. Pharm. Bull.* **2014**, *37*, 552–559.
(253) Pan, S.; Cao, D.; Fang, R.; Yi, W.; Huang, H.; Tian, S.; Feng, M. Cellular Uptake and Transfection Activity of DNA Complexes Based on Poly (ethylene Glycol)-Poly (l-Glutamine) Copolymer with PAMAM G2. *J. Mater. Chem. B* **2013**, *1*, 5114–5127.
(254) Han, M.; Lv, Q.; Tang, X.-J.; Hu, Y. L.; Xu, D. H.; Li, F. Z.; Liang, W. Q.; Gao, J. Q. Overcoming Drug Resistance of MCF-7/ADR Cells by Altering Intracellular Distribution of Doxorubicin via MVP Knockdown with a Novel siRNA Polyamidoamine-Hyaluronic Acid Complex. *J. Controlled Release* **2012**, *163*, 136–144.
(255) El-Sayed, M.; Kiani, M. F.; Naimark, M. D.; Hikal, a H.; Ghandehari, H. Extravasation of Poly(amidoamine) (PAMAM) Dendrimers across Microvascular Network Endothelium. *Pharm. Res.* **2001**, *18*, 23–28.
(256) Jevprasesphant, R.; Penny, J.; Attwood, D.; McKeown, N. B.; D'Emanuele, A. Engineering of Dendrimer Surfaces to Enhance Transepithelial Transport and Reduce Cytotoxicity. *Pharm. Res.* **2003**, *20*, 1543–1550.
(257) Dai, H.; Navath, R. S.; Balakrishnan, B.; Guru, B. R.; Mishra, M. K.; Romero, R.; Kannan, R. M.; Kannan, S. Intrinsic Targeting of Inflammatory Cells in the Brain by Polyamidoamine Dendrimers upon Subarachnoid Administration. *Nanomedicine* **2010**, *5*, 1317–1329.
(258) Kitchens, K.; Foraker, A.; Kolhatkar, R.; Swaan, P.; Ghandehari, H. Endocytosis and Interaction of Poly (Amidoamine) Dendrimers with Caco-2 Cells. *Pharm. Res.* **2007**, *24*, 2138–2145.
(259) Maddani, M. R.; Prabhu, K. R. A Concise Synthesis of Substituted Thiourea Derivatives in Aqueous Medium. *J. Org. Chem.* **2010**, *75*, 2327–2332.
(260) Devillanova, F. A. *Handbook of Chalcogen Chemistry: New Perspectives in Sulfur, Selenium and Tellurium*; RSC Publishing: UK, 2007; Chapter 2.
(261) Klugerman, M. R. Chemical and Physical Variables Affecting the Properties of Fluorescein Isothiocyanate and Its Protein Conjugates. *J. Immunol.* **1965**, *95*, 1165–1173.
(262) McClatchey, K. D. (editor). *Clinical Laboratory Medicine*; LWW Doody's all reviewed collection; Lippincott Wiliams & Wilkins: USA, 2002; p. 1374.
(263) Romanchuk, K. G. Fluorescein. Physicochemical Factors Affecting Its Fluorescence. *Surv. Ophthalmol.* **1982**, *26*, 269–283.
(264) Yellepeddi, V. K.; Kumar, A.; Palakurthi, S. Biotinylated Poly (amido) Amine (PAMAM) Dendrimers as Carriers for Drug Delivery to Ovarian Cancer Cells in Vitro. *Anticancer Res.* **2009**, *29*, 2933–2943.
(265) Pisal, D. S.; Yellepeddi, V. K.; Kumar, A.; Kaushik, R. S.; Hildreth, M. B.; Guan, X.; Palakurthi, S. Permeability of Surface-Modified Polyamidoamine (PAMAM) Dendrimers across Caco-2 Cell Monolayers. *Int. J. Pharm.* **2008**, *350*, 113–121.
(266) Do, J. H.; An, J.; Joun, Y. S.; Chung, D. J.; Kim, J. H. Cellular-Uptake Behavior of Polymer Nanoparticles into Consideration of Biosafety. *Macromol. Res.* **2008**, *16*, 695–703.
(267) Thomas, T. P.; Majoros, I. J.; Kotlyar, A.; Kukowska-Latallo, J. F.; Bielinska, A.; Myc, A.; Baker, J. R. Targeting and Inhibition of Cell Growth by an Engineered Dendritic Nanodevice. *J. Med. Chem.* **2005**, *48*, 3729–3735.
(268) Choi, Y.; Thomas, T.; Kotlyar, A.; Islam, M. T.; Baker, J. R.; Arbor, A. Synthesis and Functional Evaluation of DNA-Assembled Polyamidoamine Dendrimer Clusters for Cancer Cell-Specific Targeting. *Chem. Biol.* **2005**, *12*, 35–43.
(269) Jones, C. F.; Campbell, R. A.; Franks, Z.; Gibson, C. C.; Thiagarajan, G.; Vieira-de-Abreu, A.; Sukavaneshvar, S.; Mohammad, S. F.; Li, D. Y.; Ghandehari, H.; Weyrich, A.S; Brooks, B. D.; Grainger, D. W. Cationic PAMAM Dendrimers Disrupt Key Platelet Functions. *Mol. Pharm.* **2012**, *9*, 1599–1611.
(270) Mukherjee, S. P.; Davoren, M.; Byrne, H. J. In Vitro Mammalian Cytotoxicological Study of PAMAM Dendrimers – Towards Quantitative Structure Activity Relationships. *Toxicol. In Vitro* **2010**, *24*, 169–177.
(271) Neises, B.; Steglich, W. Simple Method for the Esterification of Carboxylic Acids. *Angew. Chem., Int. Ed. Engl.* **1978**, *17*, 522–524.

(272) Evans, D. A.; Barrow, J. C.; Leighton, J. L.; Robichaud, A. J.; Sefkow, M. Asymmetric Synthesis of the Squalene Synthase Inhibitor Zaragozic Acid C. *J. Am. Chem. Soc.* **1994**, *116*, 12111–12112.
(273) Ghosh, A. K.; Liu, C. Total Synthesis of Antitumor Depsipeptide (−)-Doliculide. *Org. Lett.* **2001**, *3*, 635–638.
(274) Organic Chemistry Portal. URL: <http://www.organic-chemistry.org/namedreactions/steglich-esterification.shtm> (accessed on Dec 30th, 2014).
(275) Wang, Z. (editor). *Comprehensive Organic Name Reactions and Reagents*, Volume 3; Wiley: USA, 2009; pp. 2656–2658.
(276) a) Jolly, A. M.; Bonizzoni, M. Intermolecular Forces Driving Encapsulation of Small Molecules by PAMAM Dendrimers in Water. *Macromolecules* **2014**, *47*, 6281–6288. b) Kline, K. K.; Morgan, E. J.; Norton, L. K.; Tucker, S. A. Encapsulation and Quantification of Multiple Dye Guests in Unmodified Poly(amidoamine) Dendrimers as a Function of Generation. *Talanta* **2009**, *78*, 1489–1491. c) Nagatani, H.; Sakamoto, T.; Torikai, T.; Sagara, T. Encapsulation of Anilinonaphthalenesulfonates in Carboxylate-Terminated PAMAM Dendrimer at the Polarized Water|1,2-Dichloroethane Interface. *Langmuir* **2010**, *26*, 17686–17694. d) Teow, H. S. An Investigation of The Use of Dendrimer-Based Carrier to Cross Cellular Barrier. 2011, PhD Thesis. University of Central Lancashire.
(277) Wang, B.; Navath, R. S.; Romero, R.; Kannan, S.; Kannan, R. Anti-Inflammatory and Anti-Oxidant Activity of Anionic dendrimer–N-Acetyl Cysteine Conjugates in Activated Microglial Cells. *Int. J. Pharm.* **2009**, *377*, 159–168.
(278) Inapagolla, R. (editor). *Dendrimer Based Delivery of Therapeutic Agents for Thrombolysis and Asthma*; Wayne State University, 2007; pp. 28-30.
(279) Selinger, Z.; Lapidot, Y. Synthesis of Fatty Acid Anhydrides by Reaction with Dicyclohexylcarbodiimide. *J. Lipid Res.* **1966**, *7* , 174–175.
(280) Gurdag, S.; Khandare, J.; Stapels, S.; Matherly, L. H.; Kannan, R. M. Activity of Dendrimer−Methotrexate Conjugates on Methotrexate-Sensitive and -Resistant Cell Lines. *Bioconjug. Chem.* **2006**, *17*, 275–283.
(281) Iwasawa, T.; Wash, P.; Gibson, C.; Rebek Jr, J. Reaction of an Introverted Carboxylic Acid with Carbodiimide. *Tetrahedron* **2007**, *63*, 6506–6511.
(282) Nakajima, N.; Ikada, Y. Mechanism of Amide Formation by Carbodiimide for Bioconjugation in Aqueous Media. *Bioconjug. Chem.* **1995**, *6*, 123–130.
(283) a) Pavia, D.; Lampman, G.; Kriz, G.; Vyvyan, J. *Introduction to Spectroscopy*; Cengage Learning, 2014; pp. 360–363; b) Relaxation in NMR spectroscopy. URL: <http://www.chem.wisc.edu/areas/reich/nmr/08-tech-01-relax.htm> (accessed on Dec 30th, 2014).
(284) El-Faham, A.; Albericio, F. Peptide Coupling Reagents, More than a Letter Soup. *Chem. Rev.* **2011**, *111*, 6557–6602.
(285) Casalini, T.; Salvalaglio, M.; Perale, G.; Masi, M.; Cavallotti, C. Diffusion and Aggregation of Sodium Fluorescein in Aqueous Solutions. *J. Phys. Chem. B* **2011**, *115*, 12896–12904.
(286) Zong, H.; Goonewardena, S. N.; Chang, H.-N.; Otis, J. B.; Baker Jr., J. R. Sequential and Parallel Dual Labeling of Nanoparticles Using Click Chemistry. *Bioorg. Med. Chem.* **2014**, *22*, 6288–6296.
(287) Huang, B.; Kukowska-Latallo, J. F.; Tang, S.; Zong, H.; Johnson, K. B.; Desai, A.; Gordon, C. L.; Leroueil, P. R.; Baker Jr, J. R. The Facile Synthesis of Multifunctional PAMAM Dendrimer Conjugates through Copper-Free Click Chemistry. *Bioorg. Med. Chem. Lett.* **2012**, *22*, 3152-3156.
(288) Sorkin, A.; von Zastrow, M. Signal Transduction and Endocytosis: Close Encounters of Many Kinds. *Nat. Rev. Mol. Cell Biol.* **2002**, *3*, 600–614.
(289) Mercer, J.; Greber, U. F. Virus Interactions with Endocytic Pathways in Macrophages and Dendritic Cells. *Trends Microbiol.* **2013**, *21*, 380–388.
(290) Song, A.; Zhang, J.; Zhang, M.; Shen, T.; Tang, J. Spectral Properties and Structure of Fluorescein and Its Alkyl Derivatives in Micelles. *Colloids Surf., A* **2000**, *167*, 253–262.
(291) Sjöback, R.; Nygren, J.; Kubista, M. Absorption and Fluorescence Properties of Fluorescein. *Spectrochim. Acta Part A Mol. Biomol. Spectrosc.* **1995**, *51*, L7–L21.

(292) a) Taylor, D. L.; Wang, Y. (editors) *Methods In Cell Biology.* Fluorescence Microscopy of Living Cells in Culture Part B, Volume 30; Academic Press: USA, 1989; pp. 133-135; b) Seib, F. P.; Jones, A. T.; Duncan, R. Comparison of the Endocytic Properties of Linear and Branched PEIs, and Cationic PAMAM Dendrimers in B16f10 Melanoma Cells. *J. Control. release* **2007**, *117*, 291–300; c) Massou, S.; Albigot, R.; Prats, M. Carboxyfluorescein Fluorescence Experiments. *Biochem. Educ.* **2000**, *28*, 171–173.
(293) Martin, M. M.; Lindqvist, L. The pH Dependence of Fluorescein Fluorescence. *J. Lumin.* **1975**, *10*, 381–390.
(294) Cole, L.; Coleman, J.; Evans, D.; Hawes, C. Internalisation of Fluorescein Isothiocyanate and Fluorescein Isothiocyanatedextran by Suspension-Cultured Plant Cells. *J. Cell Sci.* **1990**, *96*, 721–730.
(295) Saftig, P. (editors) *Lysosomes*; Medical Intelligence Unit, Landes Bioscience and Spinger: USA, 2007; Chapter 1.
(296) DiCiccio, J. E.; Steinberg, B. E. Lysosomal pH and Analysis of the Counter Ion Pathways That Support Acidification. *J. Gen. Physiol.* **2011**, *137* , 385–390.
(297) Celis, J. E.; Carter, N.; Simons, K.; Small, J. V; Hunter, T.; Shotton, D. *Cell Biology, Four-Volume Set: A Laboratory Handbook*; Elsevier Science: UK, 2005; pp. 29–31.
(298) Wu, G. (editors). *Assay Development: Fundamentals and Practices*; Wiley: USA, 2010; Chapter 1.
(299) Stoddart, M. J. (editors) *Mammalian Cell Viability: Methods and Protocols*; Methods in Molecular Biology; Humana Press: UK, 2011; Chapter 1.
(300) Lai, P. S.; Shieh, M. J.; Pai, C. L.; Wang, C. Y.; Lou, P. J. Studies on the Intracellular Trafficking of PAMAM Dendrimer. In *NSTI Nanotech* **2005**, *1*, 232–235.

Annexes

Contents

A. Supplementary data regarding the characterization of FITC-PAMAM conjugates

A1. Supplementary characterization data of FITC-G3PAMAM-NH₂ conjugate

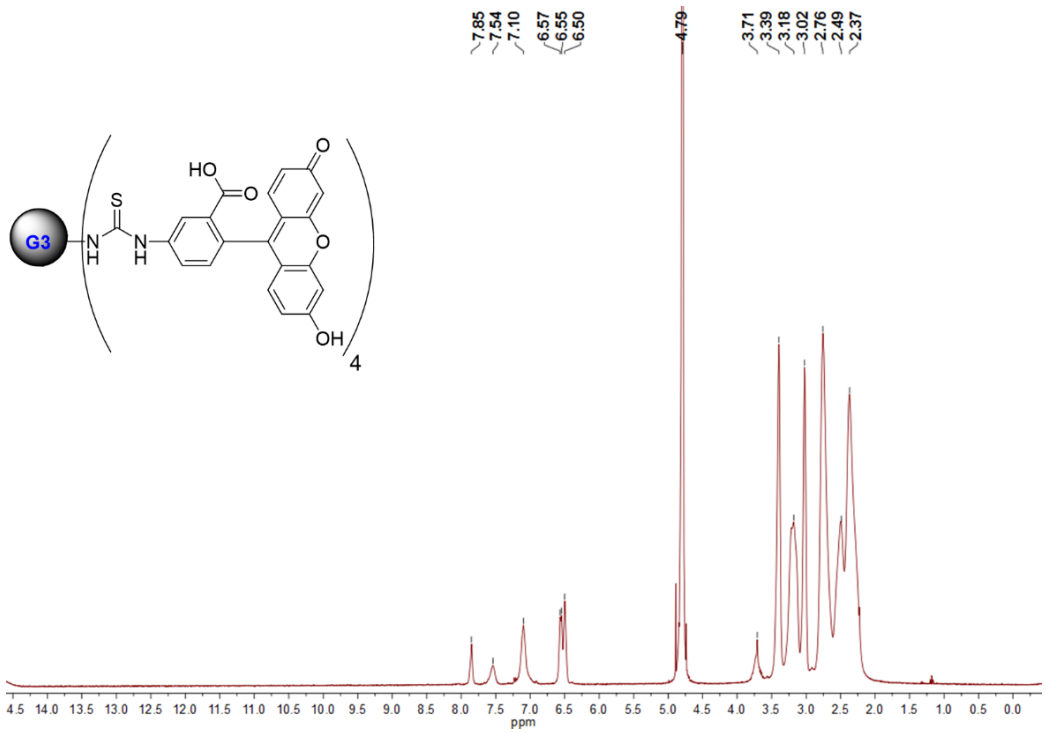

Figure A - I – Complete ^{1}H NMR spectrum of the FITC-G3PAMAM-NH_2 conjugate in D_2O at 400 MHz.

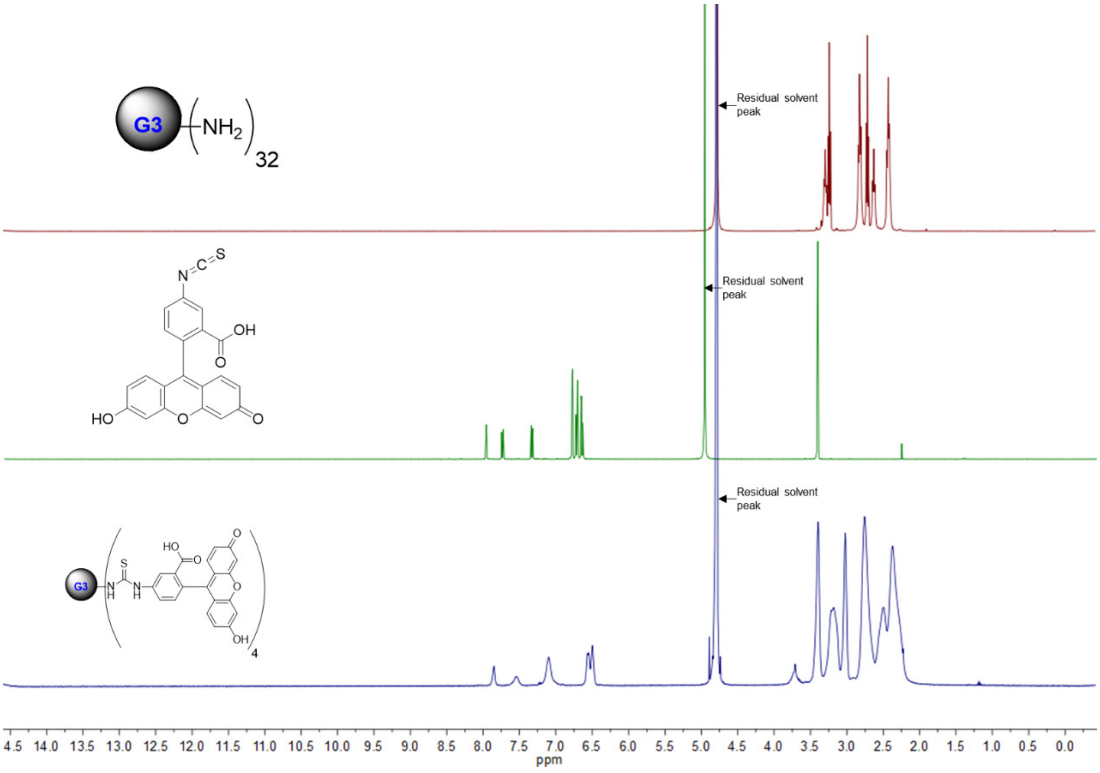

Figure A - II - ^{1}H NMR spectra of the G3PAMAM-NH_2 dendrimer (in D_2O, top); unconjugated FITC (MeOD, middle) and; FITC-G3PAMAM-NH_2 conjugate (in D_2O, bottom) at 400 MHz.

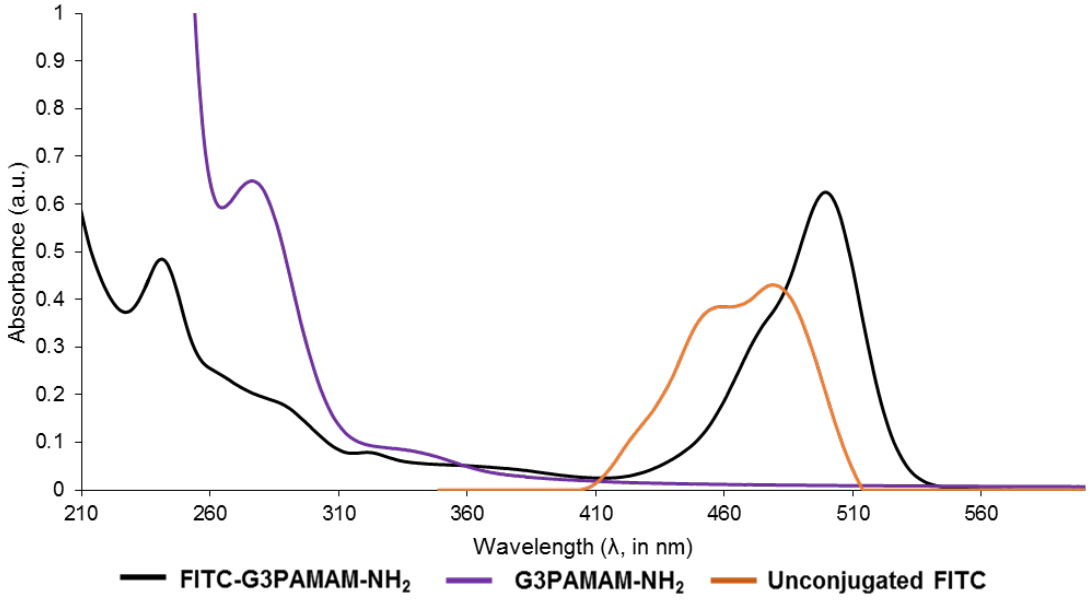

Figure A - III – UV spectra of G3PAMAM-NH_2 (in UP water at 16 mg/mL, purple line); unconjugated FITC (in UP water, normalized, orange line) and; FITC-G3PAMAM-NH_2 conjugate (in UP water at 0.02 mg/mL, black line).

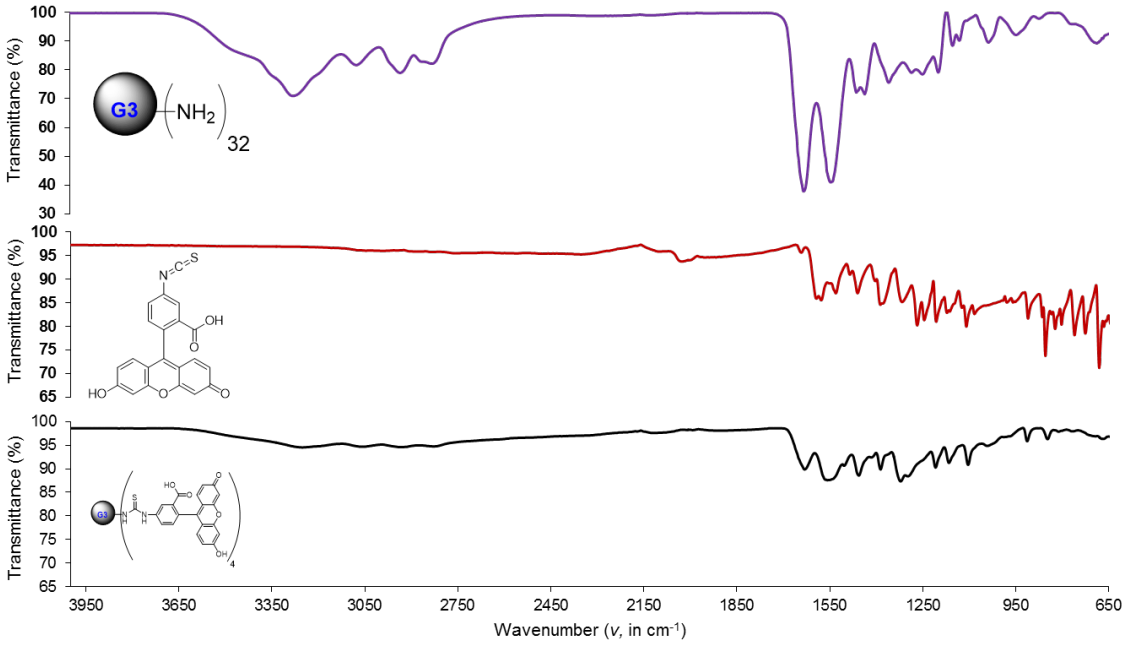

Figure A - IV – FTIR-ATR spectra of G3PAMAM-NH_2 (top); unconjugated FITC (middle) and; FITC-G3PAMAM-NH_2 conjugate (bottom).

A2. Supplementary characterization data of FITC-G5PAMAM-NH$_2$ conjugate

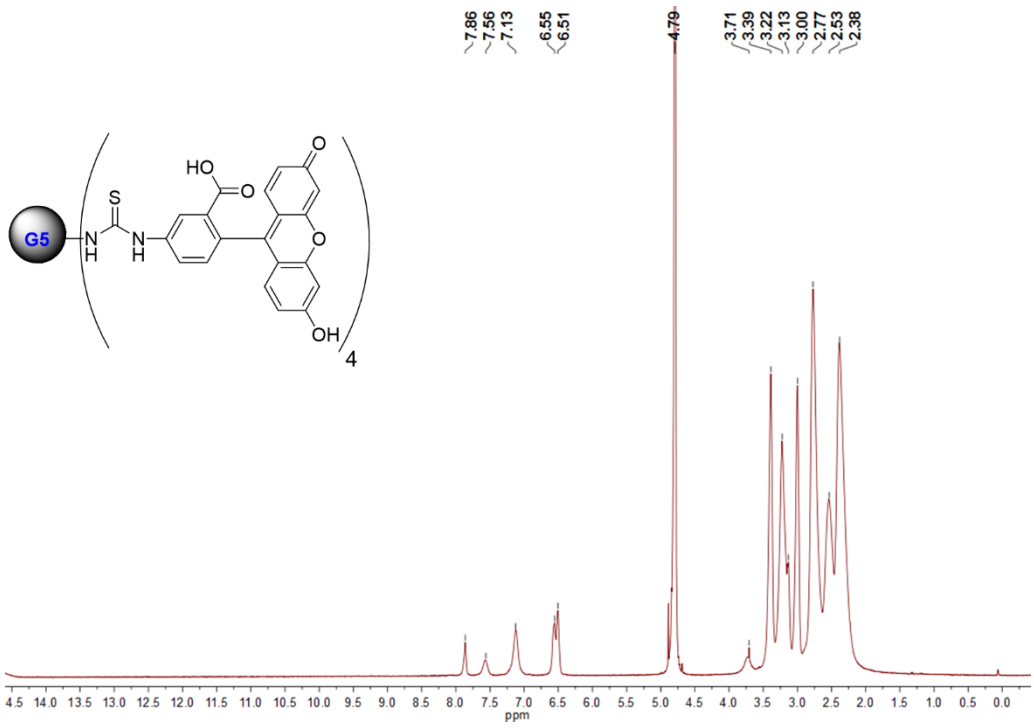

Figure A - V - Complete ^{1}H NMR spectrum of the FITC-G5PAMAM-NH$_2$ conjugate in D$_2$O at 400 MHz.

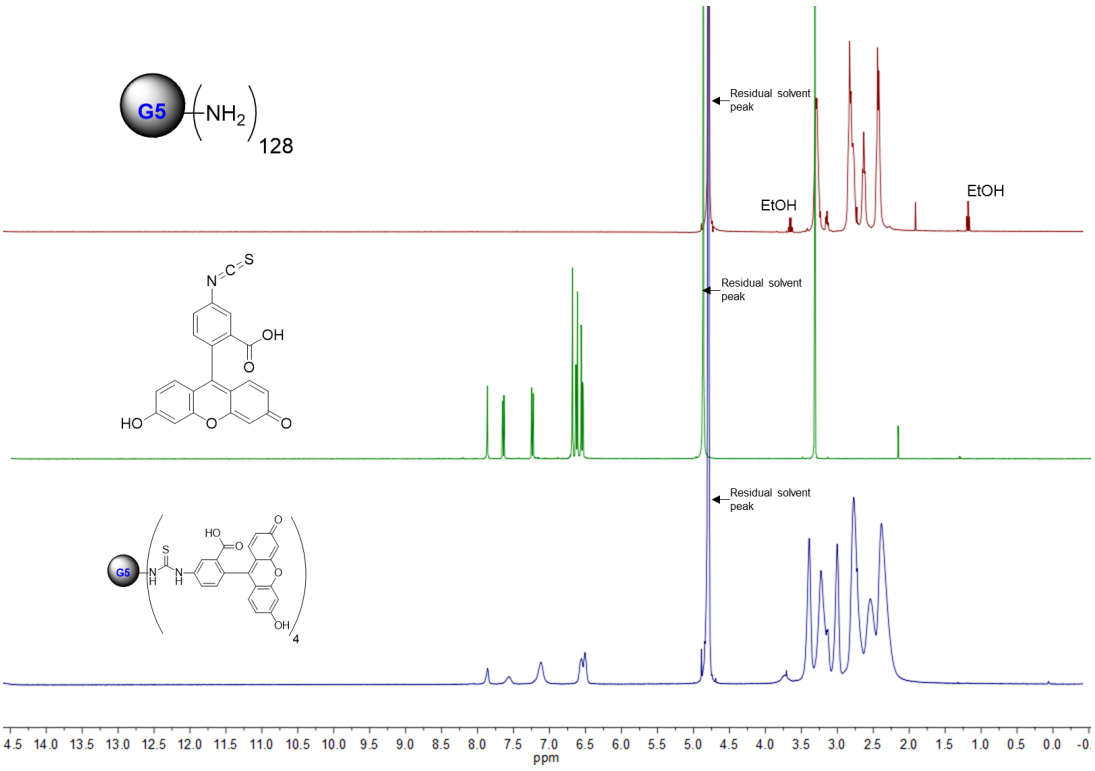

Figure A - VI - ^{1}H NMR spectra of the G5PAMAM-NH$_2$ dendrimer (in D$_2$O, top); unconjugated FITC (MeOD, middle) and; FITC-G5PAMAM-NH$_2$ conjugate (in D$_2$O, bottom) at 400 MHz.

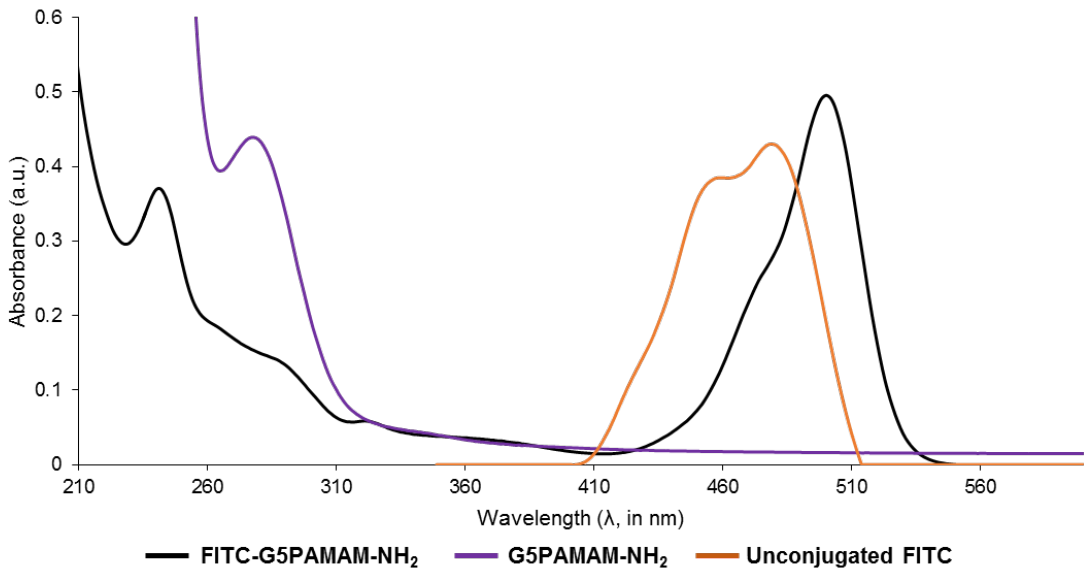

Figure A - VII - UV spectra of G5PAMAM-NH_2 (in UP water at 13.75 mg/mL, purple line); unconjugated FITC (in UP water, normalized, orange line) and; FITC-G5PAMAM-NH_2 conjugate (in UP water at 0.02 mg/mL, black line).

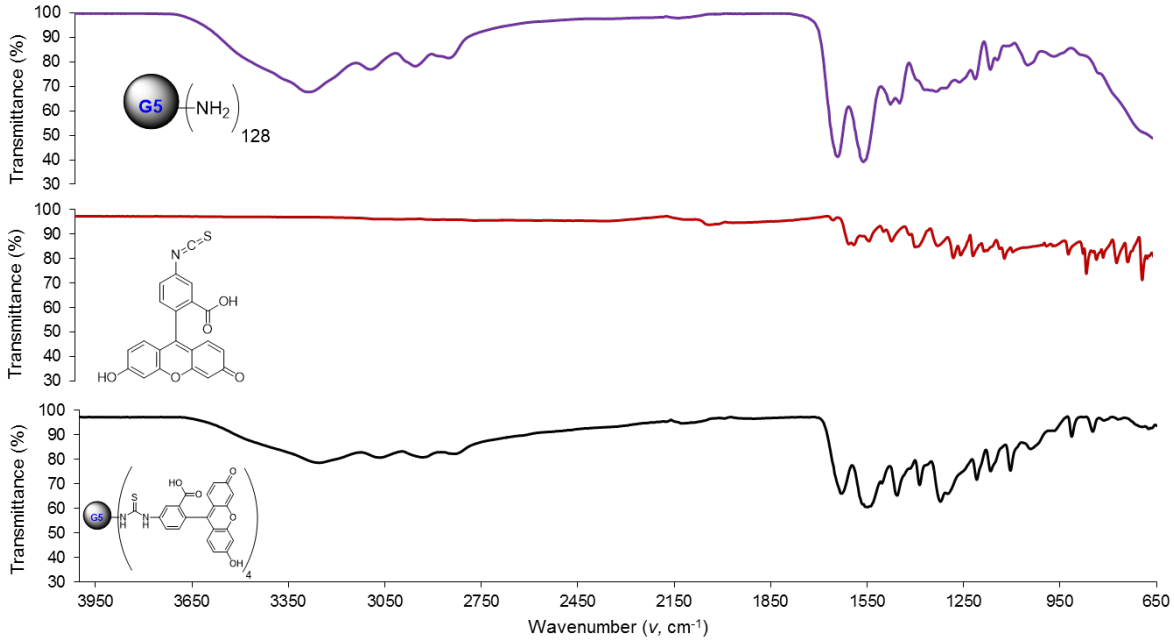

Figure A - VIII - FTIR-ATR spectra of G5PAMAM-NH_2 (top); unconjugated FITC (middle) and; FITC-G5PAMAM-NH_2 conjugate (bottom).

A3. Supplementary characterization data of FITC-G3PAMAM-OH conjugate

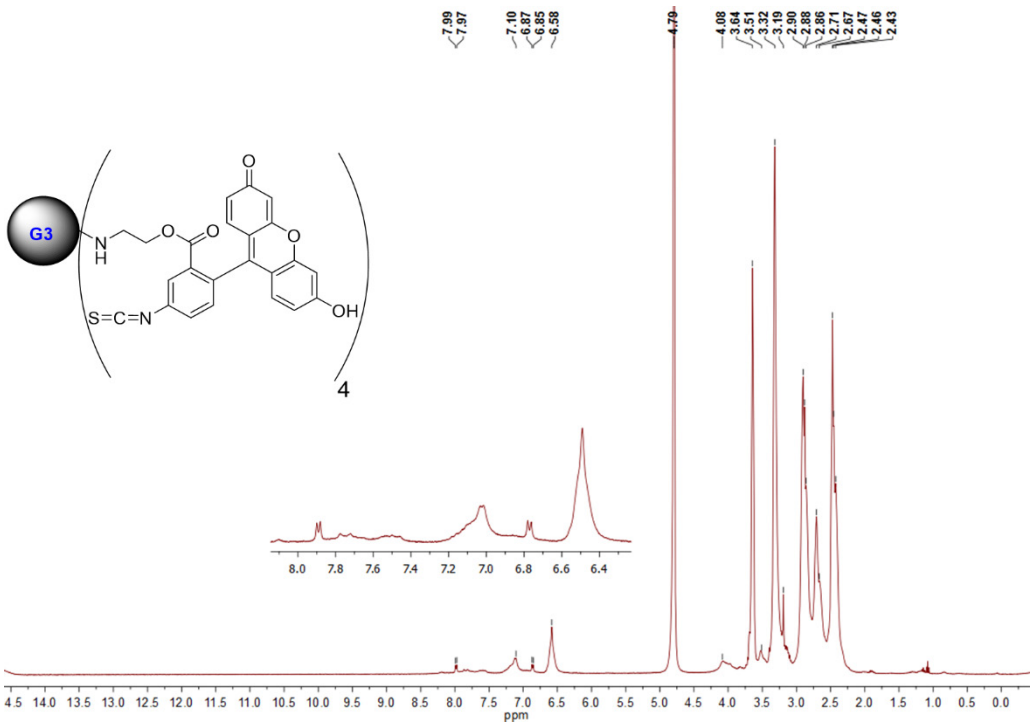

Figure A - IX - Complete ^{1}H NMR spectrum of the FITC-G3PAMAM-OH conjugate in D_2O at 400 MHz.

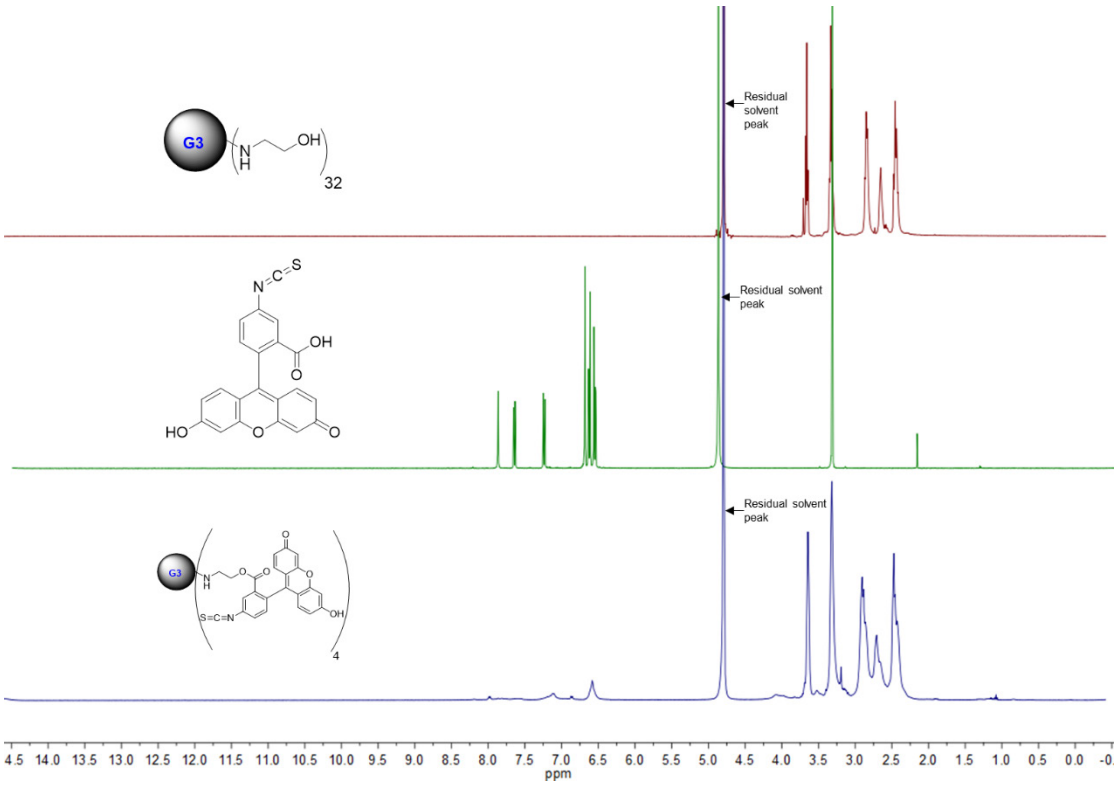

Figure A - X - ^{1}H NMR spectra of the G3PAMAM-OH dendrimer (in D_2O, top); unconjugated FITC (MeOD, middle) and; FITC-G3PAMAM-OH conjugate (in D_2O, bottom) at 400 MHz.

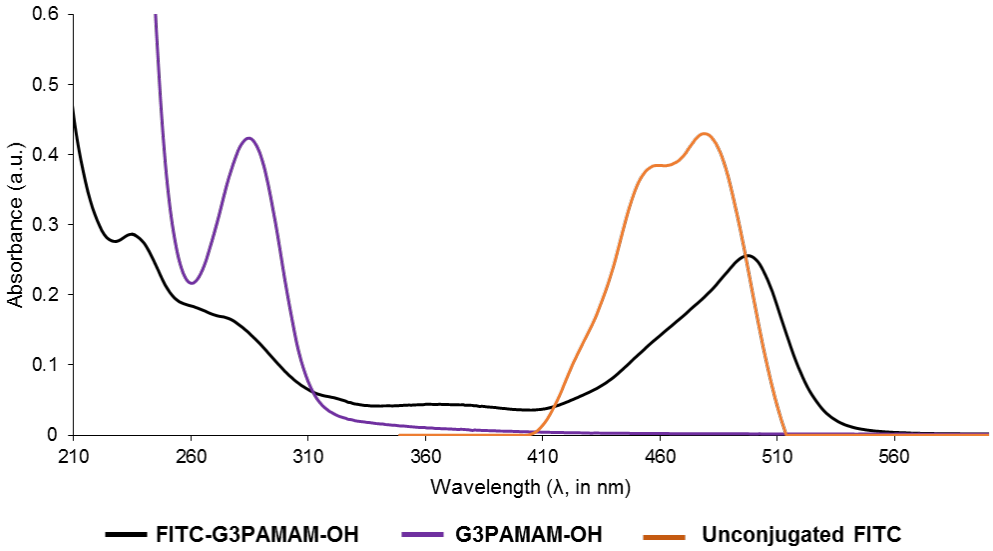

Figure A - XI - UV spectra of G3PAMAM-OH (in UP water at 3.53 mg/mL, purple line); unconjugated FITC (in methanol, normalized, orange line) and; FITC-G3PAMAM-OH conjugate (in UP water at 0.02 mg/mL, black line).

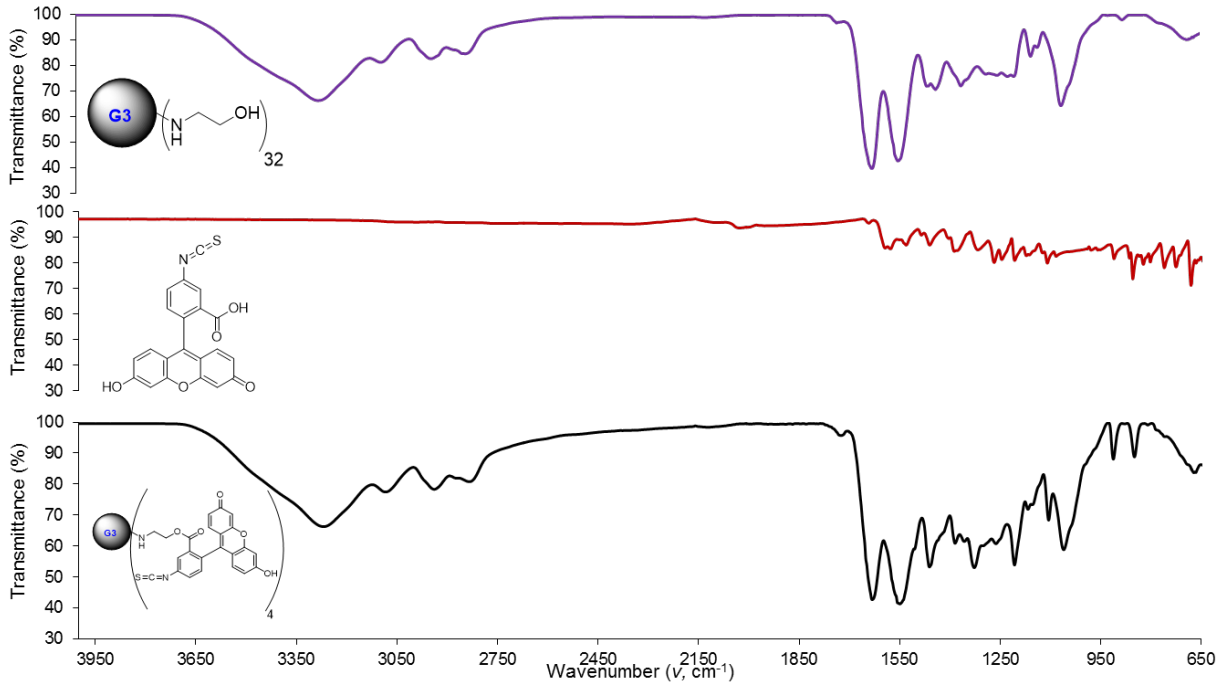

Figure A - XII - FTIR-ATR spectra of G3PAMAM-OH (top); unconjugated FITC (middle) and; FITC-G3PAMAM-OH conjugate (bottom).

A4. Supplementary characterization data of FITC-G5PAMAM-OH conjugate

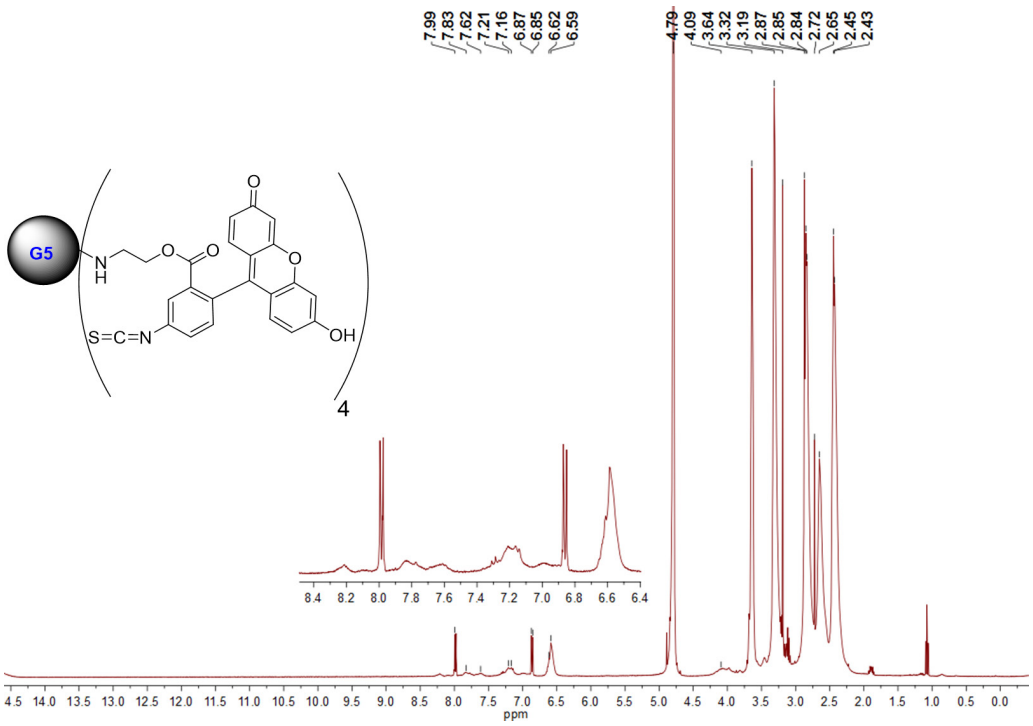

Figure A - XIII - Complete ^{1}H NMR spectrum of the FITC-G5PAMAM-OH conjugate in D_2O at 400 MHz.

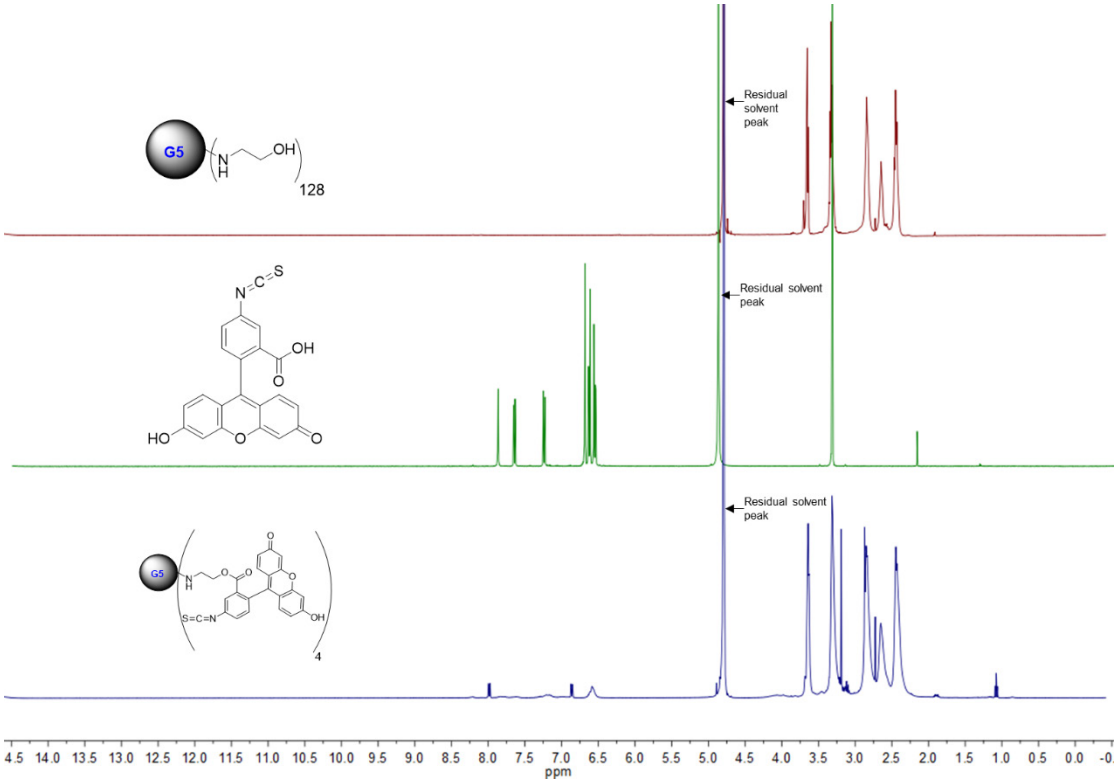

Figure A - XIV - ^{1}H NMR spectra of the G5PAMAM-OH dendrimer (in D_2O, top); unconjugated FITC (MeOD, middle) and; FITC-G5PAMAM-OH conjugate (in D_2O, bottom) at 400 MHz.

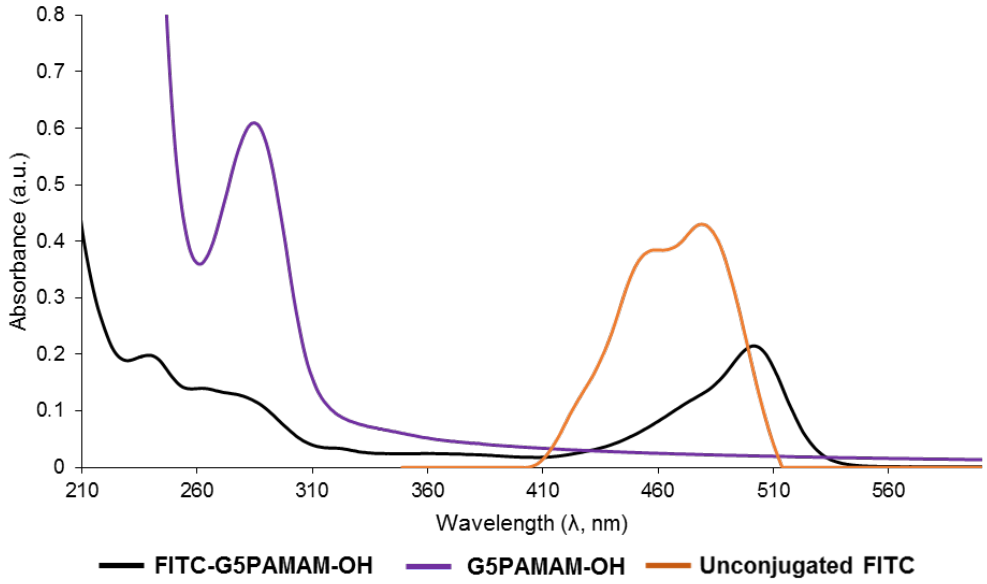

Figure A - XV - UV spectra of G5PAMAM-OH (in UP water at 3.53 mg/mL, purple line); unconjugated FITC (in UP water, normalized, orange line) and; FITC-G5PAMAM-OH conjugate (in UP water at 0.02 mg/mL, black line).

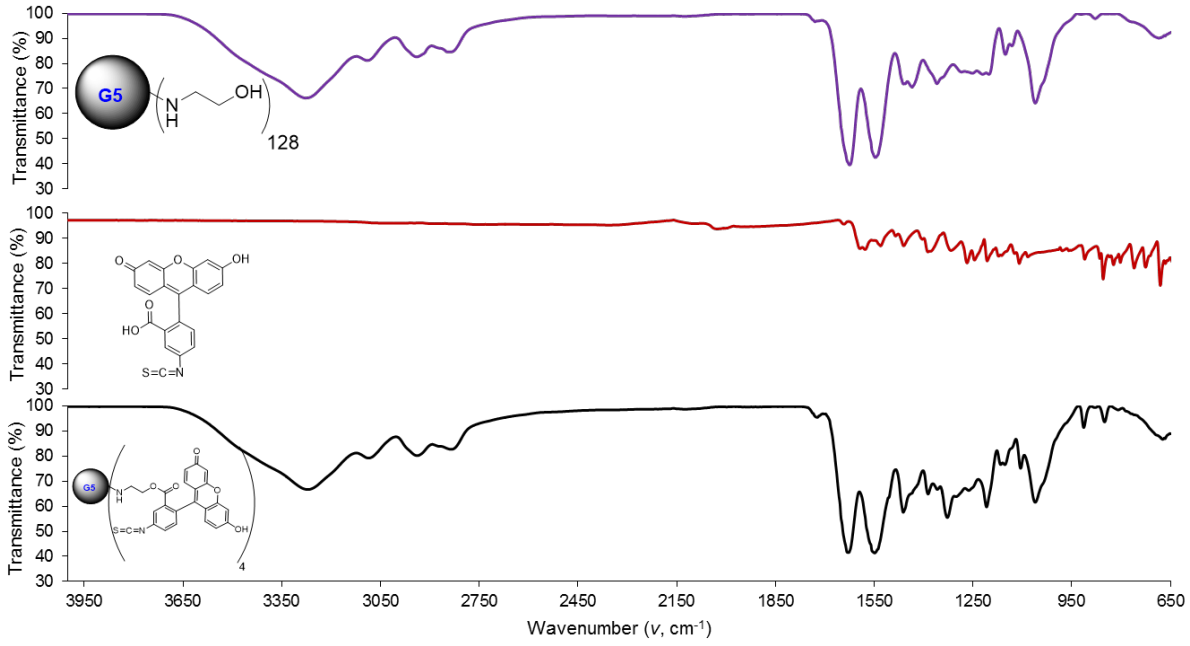

Figure A - XVI - FTIR-ATR spectra of G5PAMAM-OH (top); unconjugated FITC (middle) and; FITC-G5PAMAM-OH conjugate (bottom).

A5. Supplementary characterization data of FITC-G2.5PAMAM-COOH conjugate

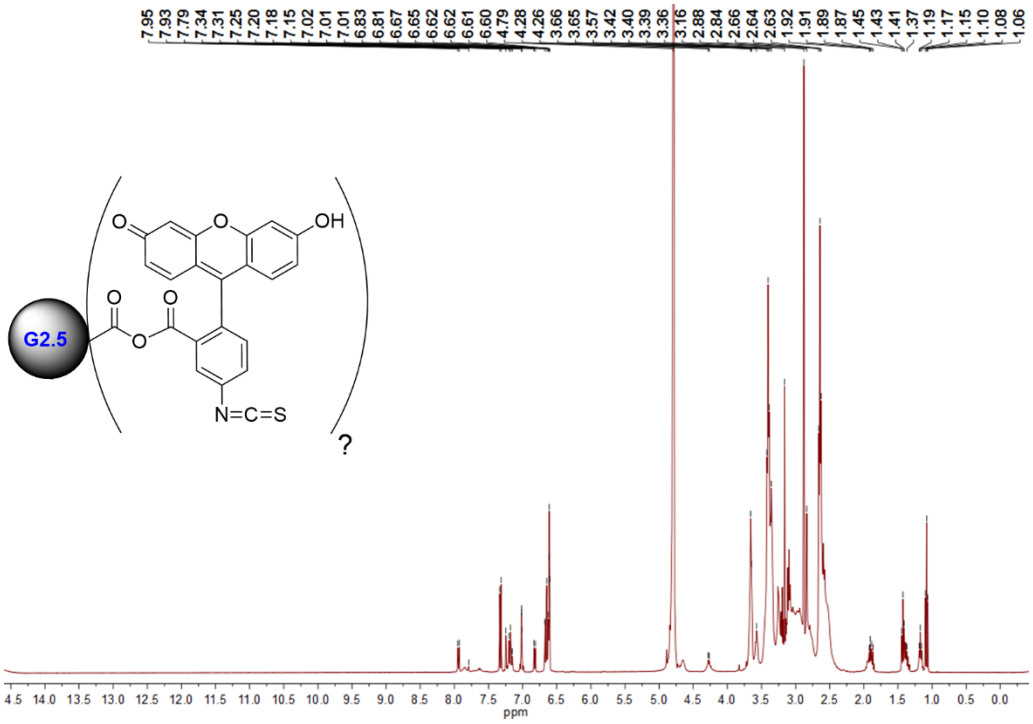

Figure A - XVII - Complete ^{1}H NMR spectrum of the FITC-G2.5PAMAM-COOH conjugation products in D_2O at 400 MHz.

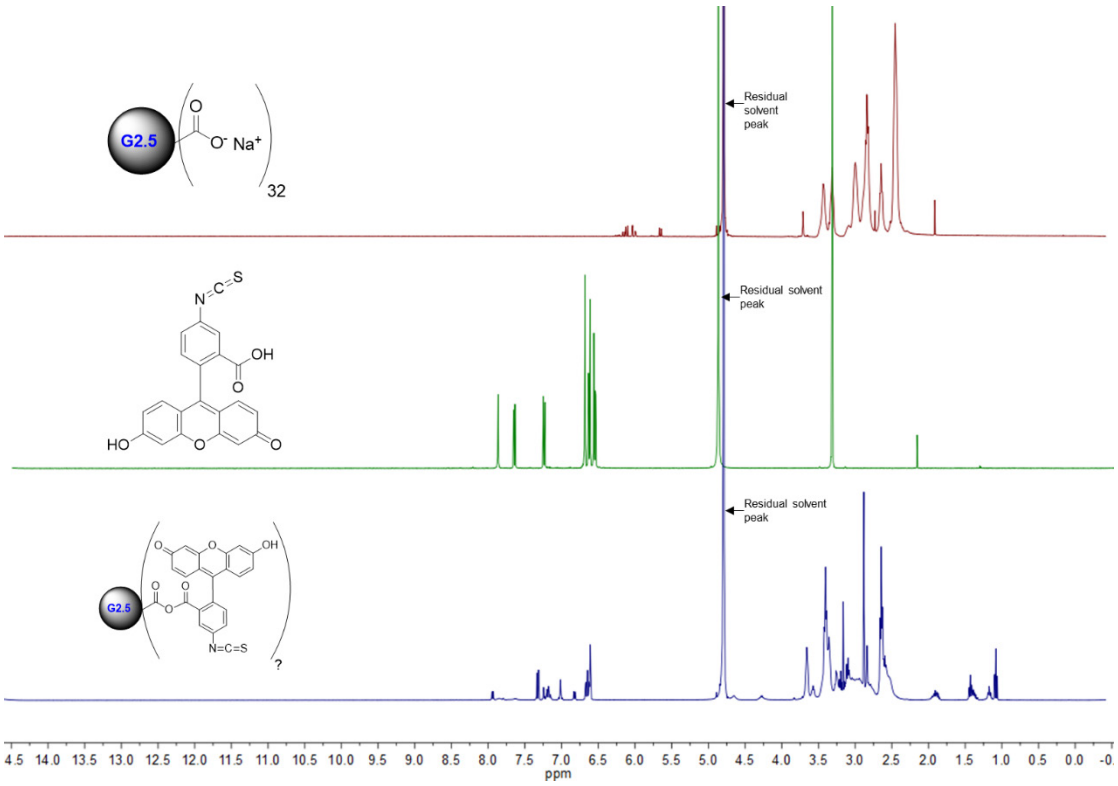

Figure A - XVIII - ^{1}H NMR spectra of the G2.5PAMAM-COOH dendrimer (in D_2O, top); unconjugated FITC (MeOD, middle) and; FITC-G2.5PAMAM-COOH conjugation products (in D_2O, bottom), at 400 MHz.

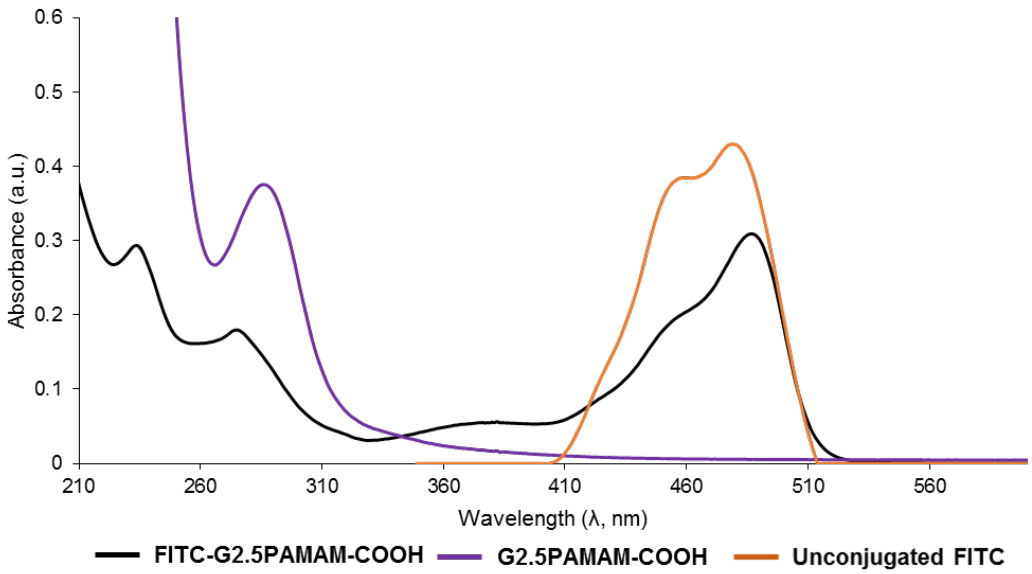

Figure A - XIX - UV spectra of G2.5PAMAM-COOH (in UP water at 3.1 mg/mL, purple line); unconjugated FITC (in UP water, normalized, orange line) and; FITC-G2.5PAMAM-COOH conjugation products (in UP water at 0.02 mg/mL, black line).

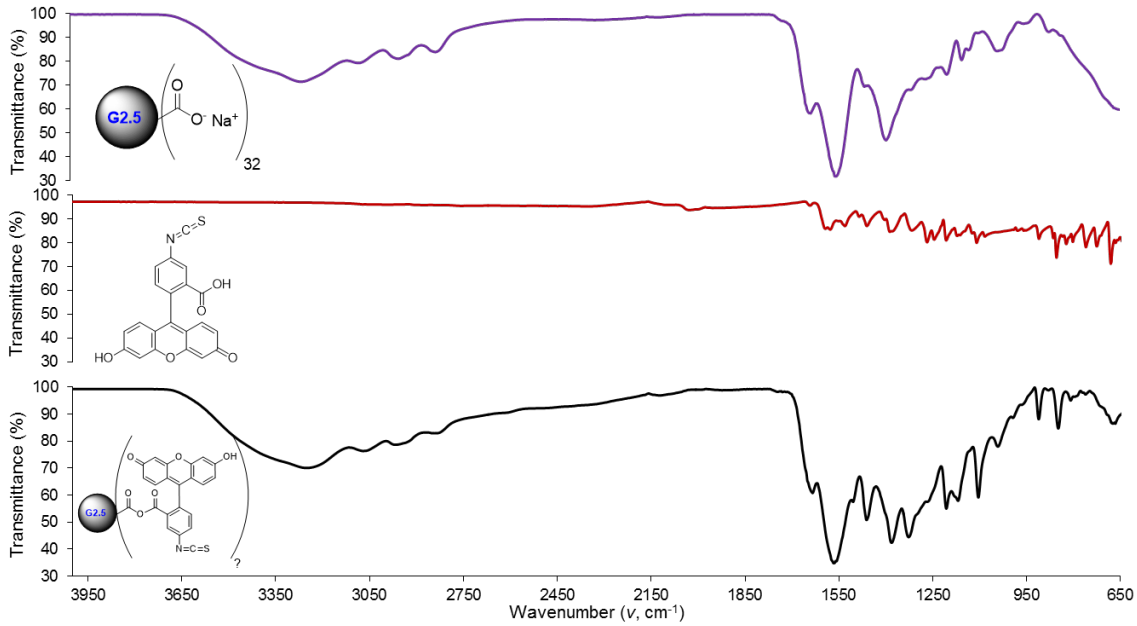

Figure A - XX - FTIR-ATR spectra of G2.5PAMAM-COOH (top); unconjugated FITC (middle) and; FITC-G2.5PAMAM-COOH conjugation products (bottom).

A6. Supplementary characterization data of FITC-G4.5PAMAM-COOH conjugate

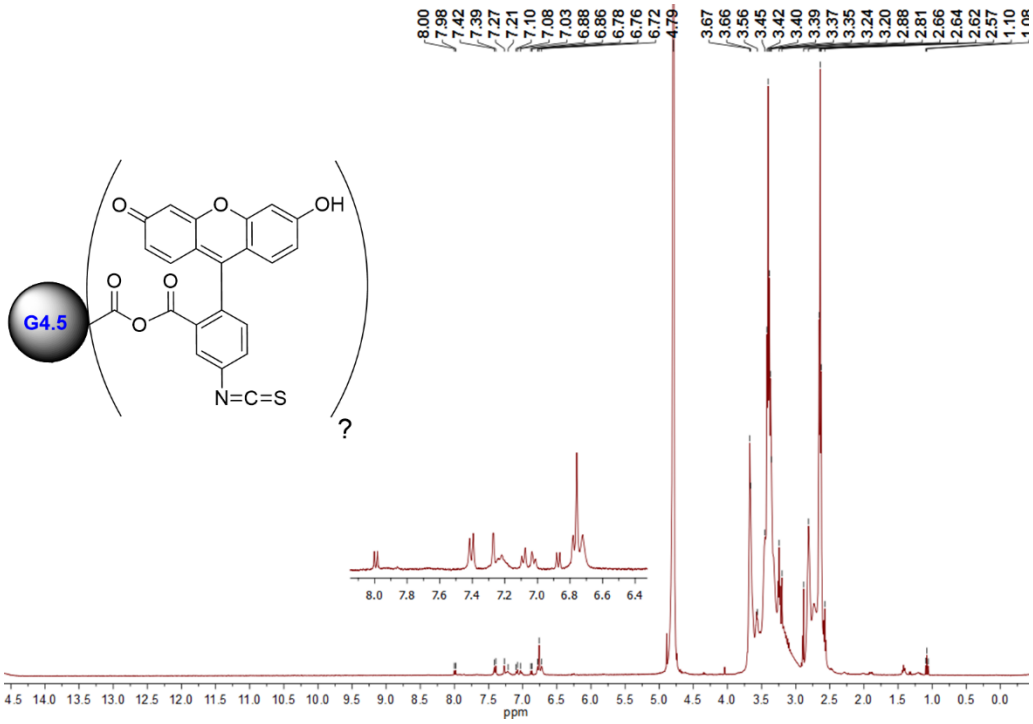

Figure A - XXI - Complete ^{1}H NMR spectrum of the FITC-G4.5PAMAM-COOH conjugation products in D_2O at 400 MHz.

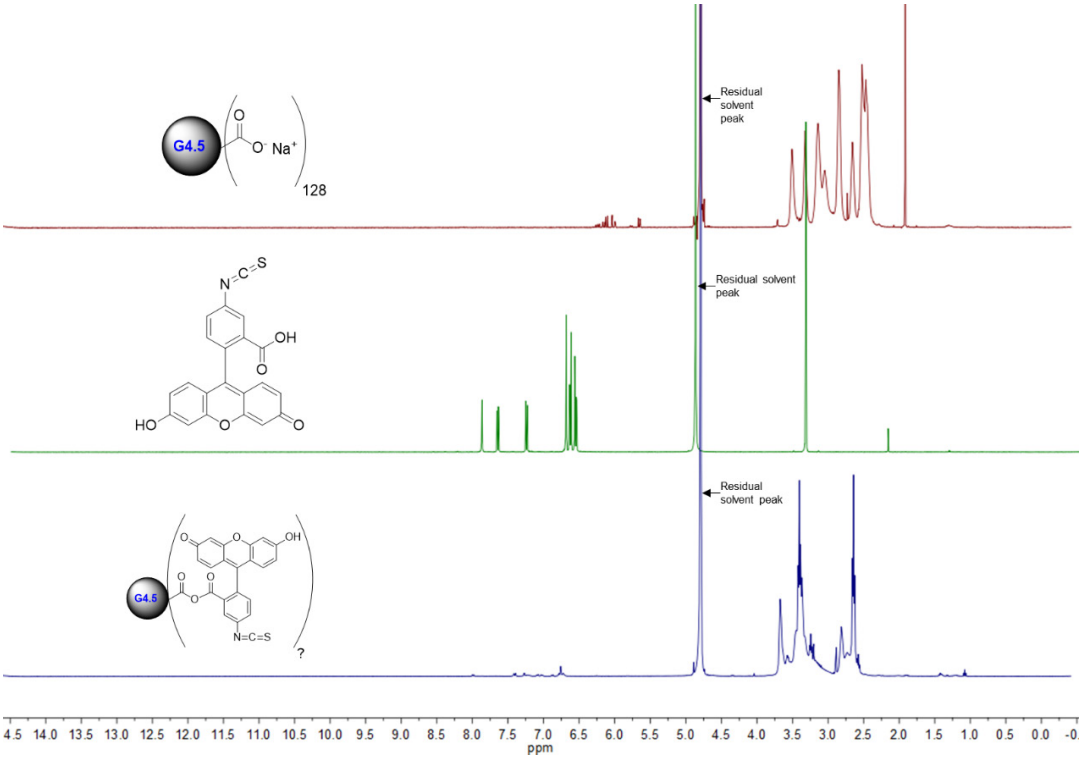

Figure A - XXII - ^{1}H NMR spectra of the G4.5PAMAM-COOH dendrimer (in D_2O, top); unconjugated FITC (MeOD, middle) and; FITC-G4.5PAMAM-COOH conjugation products (in D_2O, bottom), at 400 MHz.

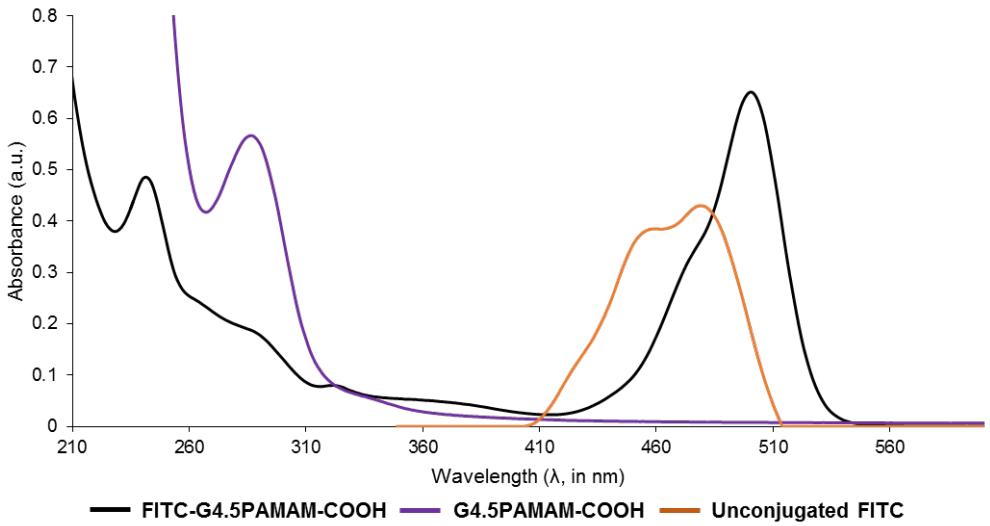

Figure A - XXIII - UV spectra of G4.5PAMAM-COOH (in UP water at 3.1 mg/mL, purple line); unconjugated FITC (in UP water, normalized, orange line) and; FITC-G4.5PAMAM-COOH conjugation products (in UP water at 0.02 mg/mL, black line).

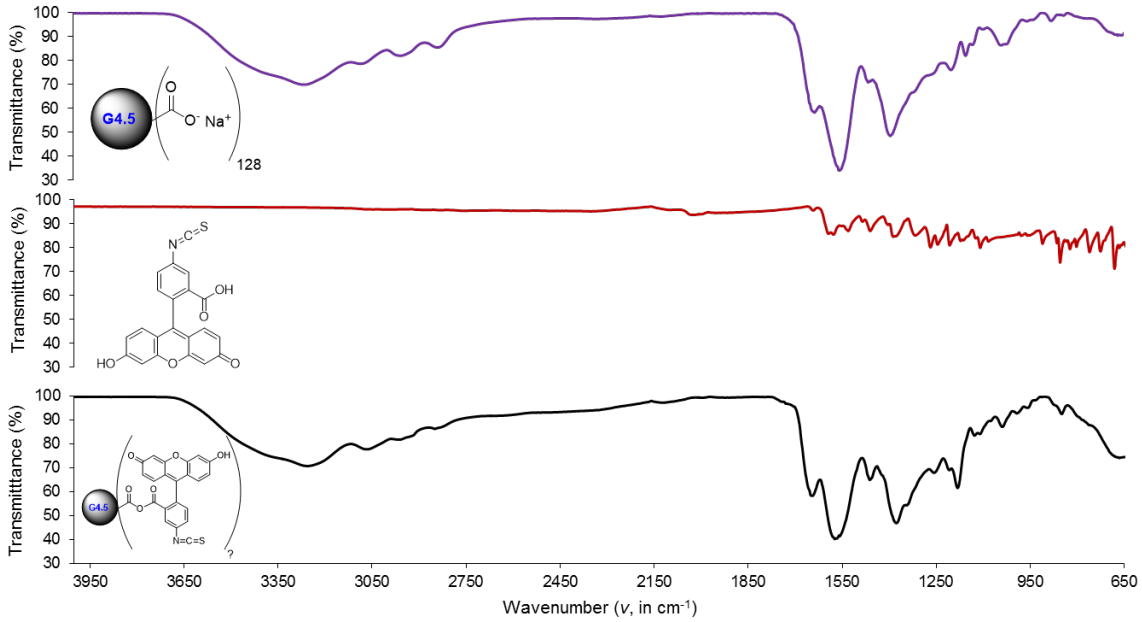

Figure A - XXIV - FTIR-ATR spectra of G4.5PAMAM-COOH (top); unconjugated FITC (middle) and; FITC-G4.5PAMAM-COOH conjugation products (bottom).

A7. General data related with the characterization of FITC-PAMAM conjugates

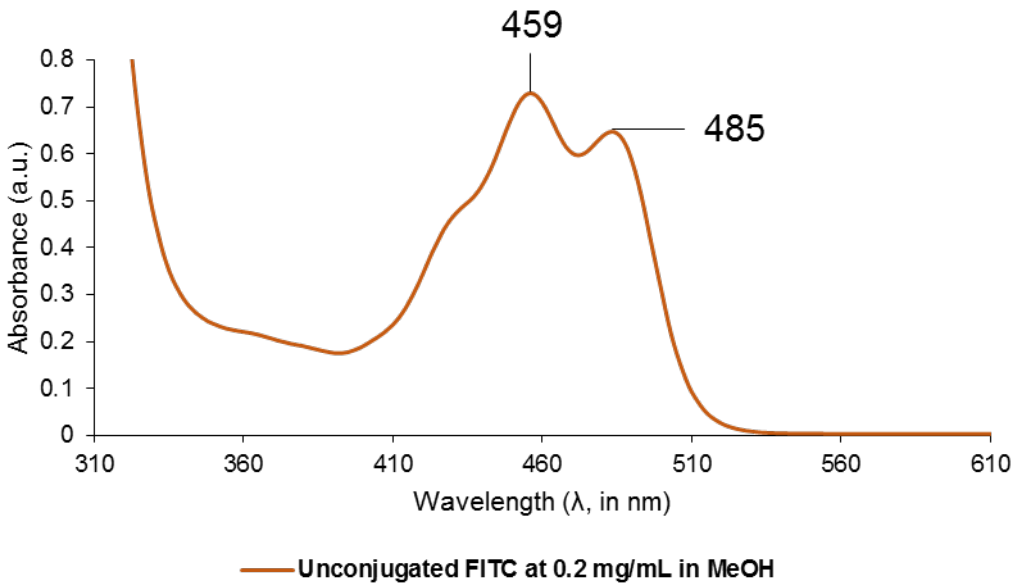

Figure A - XXV – UV-Vis spectrum of unconjugated FITC (in MeOH at 0.2 mg/mL; no adjustments were done).

Please note that in the previous sections, the appearance of the dendrimer peak in the UV region (around 250 nm) arises from the tertiary amines of the dendrimer interior. These results follow previously reported observations (Pande, S.; Crooks, R. M. Analysis of Poly (amidoamine) Dendrimer Structure by UV–Vis Spectroscopy. *Langmuir* **2011**, *27*, 9609–9613).

Table A1 – Reported zeta potential values for the higher generation PAMAM dendrimers with distinct terminal groups. Please note that the dispersing medium and its pH have a strong impact over the net-charge of the PAMAM dendrimers.

Dendrimer	ξ (in mv)	Dispersing medium	pH	Reference
G5PAMAM-NH_2	**25**	PBS	7.5	A1
G5PAMAM-OH	**1.69**	Distilled Water	n/a	A2
G4.5PAMAM-COOH	**-18**	PBS	n/a	A3

(A1) Liu, K. C.; Yeo, Y. Zwitterionic Chitosan–Polyamidoamine Dendrimer Complex Nanoparticles as a pH-Sensitive Drug Carrier. *Mol. Pharm.* **2013**, *10*, 1695–1704.

(A2) Sadekar, S.; Ray, A.; Janat-Amsbury, M.; Peterson, C. M.; Ghandehari, H. Comparative Biodistribution of PAMAM Dendrimers and HPMA Copolymers in Ovarian-Tumor-Bearing Mice. *Biomacromolecules* **2010**, *12*, 88–96.

(A3) Shcharbin, D.; Mazur, J.; Szwedzka, M.; Wasiak, M.; Palecz, B.; Przybyszewska, M.; Zaborski, M.; Bryszewska, M. Interaction between PAMAM 4.5 Dendrimer, Cadmium and Bovine Serum Albumin: A Study Using Equilibrium Dialysis, Isothermal Titration Calorimetry, Zeta Potential and Fluorescence. *Colloids Surfaces B Biointerfaces* **2007**, *58*, 286–289.

B. Supplementary experimental data related with the preparation of FITC-PAMAM conjugates

B1. TLCs

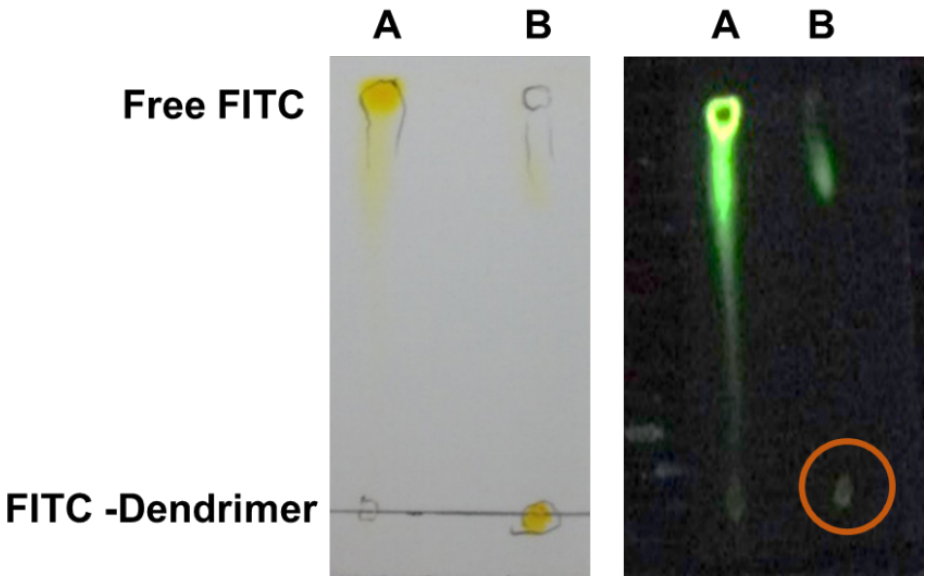

Figure B - I - TLC separation of the FITC-G3PAMAM-NH_2 conjugate after dialysis. *Left:* TLC analysis of unconjugated FITC (A) and FITC-G3PAMAM-NH_2 conjugate (B); *Right:* UV revelation of the same TLC plate at λ=366 nm.

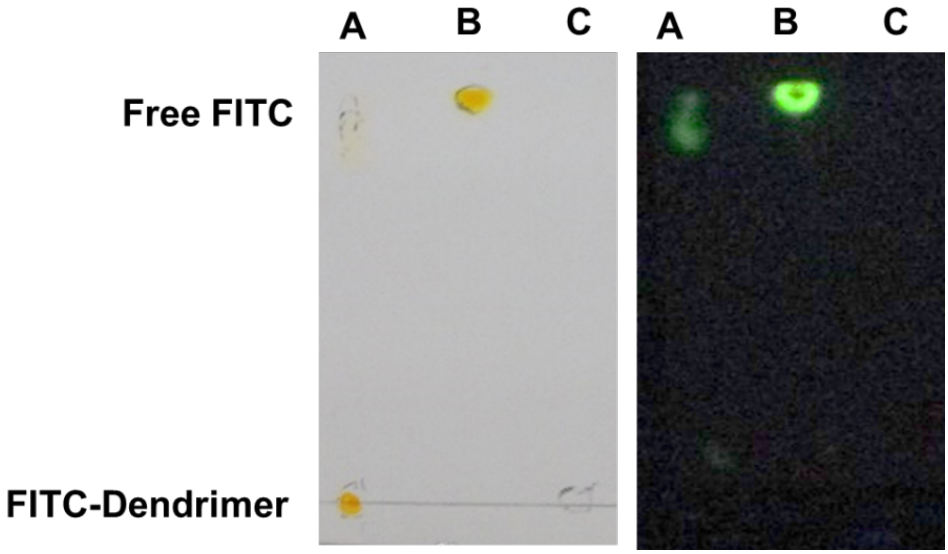

Figure B - II - TLC separation of the same FITC-G3PAMAM-NH_2 conjugate after extended dialysis. *Left:* TLC analysis of the FITC-G3PAMAM-NH_2 (A); unconjugated FITC standard in MeOH (B); G3PAMAM-NH_2 in PBS (C). *Right:* UV revelation of the same TLC plate at λ=366 nm.

Figure B - III - TLC separation of the FITC-G5PAMAM-NH_2 conjugate after dialysis and: Before passing the sample through PD-10 column (A); after passing the sample through PD-10 column (B).

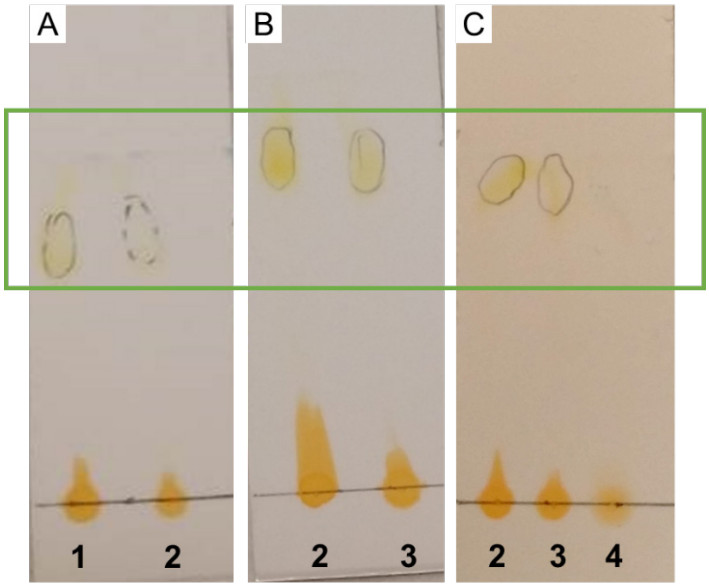

Figure B - IV – TLC separation of the FITC-G5PAMAM-OH sample after dialysis, precipitation and passing the sample through the PD-10 desalting columns, where: A) 1st PD-10 purification; B) 2nd PD-10 purification; C) 3rd PD-10 purification; and 1) Before PD-10 purification; 2) After the 1st PD-10 purification; 3) After the 2nd PD-10 purification; 4) After the 3rd PD-10 purification. Note that the spots of free FITC in (A) are not in the same place as in (B) or (C) since that the pictures taken are not in the same proportion. Although not clearly visible, in C) the spot of free FITC in (4) was also present (much lower intensity).

Note that the TLC separation for other samples was also accomplished but they are not shown in here. Just a few examples are described based on the conditions reported along the thesis.

Based on the reported solvent system, the Rf values obtained were: $Rf_{FITC\text{-}PAMAM} = 0$; $Rf_{unconjugated\ FITC} = 0.9$.

UNIVERSIDADE da MADEIRA

CQM CENTRO DE QUÍMICA DA MADEIRA

FCT Fundação para a Ciência e a Tecnologia

MINISTÉRIO DA EDUCAÇÃO E CIÊNCIA

Molecular Materials® RESEARCH GROUP MADEIRA ISLAND · PORTUGAL

RNE

PTNMR

Portugal סרגר Portuguese Nanotechnology Network

VIDAMAR RESORTS ★★★★★ MADEIRA

UNIÃO EUROPEIA

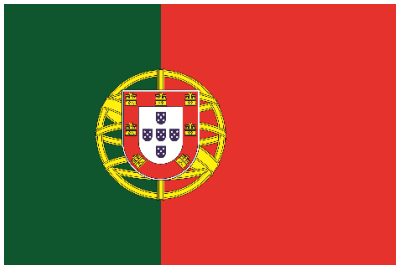

GOVERNO DA REPÚBLICA PORTUGUESA

REGIÃO AUTÓNOMA DA MADEIRA

A Nossa Universidade

Colégio dos Jesuítas
Rua dos Ferreiros - 9000-082, Funchal

Tel: +351 291 209400
Fax: +351 291 209410
Email: gabinetedareitoria@uma.pt